Development of a Stand-Pipe Lysimeter for Unsaturated Waste Rock

A Thesis Submitted to the College of
Graduate Studies and Research
in Partial Fulfillment of the Requirements
for the Degree of Master of Science
in the Department of Civil Engineering
University of Saskatchewan
Saskatoon, CANADA

By
Dwayne K. Rowlett
Spring 2000

Permission to use

In presenting this thesis in partial fulfillment of the requirements for a postgraduate degree from the University of Saskatchewan, I agree that the Libraries of this University may make it freely available for inspection. I further agree that permission for copying of this thesis in any manner, in whole or in part, for scholarly purposes may be granted by the professor or professors who supervised my thesis work or, in their absence, by the Head of the Department or the Dean of the College in which my thesis work was done. It is understood that any copying or publication or use of this thesis or parts thereof for financial gain shall not be allowed without my written permission. It is also understood that due recognition shall be given to me and to the University of Saskatchewan in any scholarly use which may be made of any material in my thesis.

Requests for permission to copy or to make other use of material in this thesis in whole or part should be addressed to:

Head of the Department of Civil Engineering
University of Saskatchewan
Saskatoon, Saskatchewan
S7N 0W0
CANADA

Abstract

A concern of the mining industry is the release of contaminants from waste rock piles into the environment. The current method of monitoring waste rock piles is to install piezometers below the water table in the soils underlying the unsaturated waste rock piles and collect a sample of water for chemical analysis. However, once a problem is detected it may be too late to initiate effective remedial measures because the contaminants are already in the local groundwater system. Therefore, it would be desirable to have an instrument that could serve as a piezometer, but be located in the unsaturated waste rock well above the local groundwater table.

A stand-pipe lysimeter designed to measure suction and collect pore water samples from unsaturated waste rock piles has been developed and verified in a large-scale laboratory test. The laboratory testing of the prototype lysimeter involved the building of two large-scale test columns, each of which was 0.56 m in diameter and 3.6 m in height. The gradations of the test columns (coarse and fine) bracket the range of grainsize curves for waste rock as found in the literature and as measured in a number of research programs at the University of Saskatchewan. Applying different infiltration rates to the top of the column varied the suction profiles within the waste rock column. For each infiltration rate the suction profile of the columns was measured using both tensiometers and the lysimeters. The suction measurements were then compared and evaluated. Pore water samples were collected from the lysimeter by draining the base of the lysimeter. The volume of water and the time required to collect a pore water sample was measured.

The results of column testing verified that the lysimeter could be used to measure the suction within the waste rock columns. The lysimeter measurement of suction was found to be slightly lower than the suction obtained with tensiometers, with an error of less than 1 kPa at suctions less than 10 kPa and an error of less than 2 kPa for suctions between 10 and 20 kPa. The pore fluid collection rates for the lysimeter, expressed as a ratio of the applied flux increased as the applied flux decreased. This was found to be a result of the lysimeter backfill becoming the preferential flowpath at low flux rates.

Dedication

This thesis is dedicated to my grandparents, Percy Rowlett and Gosta and Elsie Wallster. They taught me more about life than they ever realized.

Acknowledgments

I would like to express my sincere appreciation to Dr. S.L. Barbour for his enthusiasm, guidance, and suggestions during the course of my research program. Dr. Barbour is a first class researcher who has a unique and insightful way of looking at data from a number of different perspectives. Dr. Barbour's commanding grasp of engineering principles is foreshadowed only by his enthusiasm for the work that he does. I would also like to express my appreciation to Dr. M.D. Haug for encouraging me to enter the graduate program. Dr. Haug has served as a first rate mentor throughout my studies. I would also like to extend my thanks to all the other professors in the Department of Civil Engineering at the university for their encouragement and willingness to help me with my project.

A special thank you is reserved for Mr. Alex Kozlow, Mr. Dale Pavier and Mr. Curtis Kelln. The help of these individuals was invaluable during my testing program. I would also like to thank Mr. Henry Berg and all the staff of engineering shops for helping me build the lysimeter prototype. Mr. Berg's extensive knowledge of machining and materials was invaluable during the construction of the prototypes.

I would like to thank all of my fellow graduate students. They provided the friendship and encouragement to make the writing of this thesis a pleasurable experience.

I would like to thank my parents, Roy & Carol Rowlett, for instilling in me the drive, ambition and determination to complete this project. My deepest gratitude and appreciation is extended to my wife Betty and my children, Thomas and April for their patience, love, encouragement and support. Betty held our home together during the countless hours I spent preparing this thesis.

Table of Contents

List of Figures

List of Tables

List of Appendices

CHAPTER 1 INTRODUCTION

1.1 Background

The mining of ore bodies includes the removal of the rock surrounding or above the ore bearing rock. This rock, known as waste rock, is removed from the mine and placed in large piles at on the surface. Due to the coarse nature of waste rock, waste rock piles tend to be well drained, which creates unsaturated conditions within the waste rock piles. As a result, oxygen and other gases can readily enter and circulate within the waste rock pile. This provides conditions that promote the rapid weathering of the minerals within the waste rock pile. The weathering of minerals combined with the flow of water through the pile may cause the release of potentially toxic contaminants from waste rock piles into the environment.

The current method of monitoring waste rock piles is to install piezometers below the water table in the soils underlying the unsaturated waste rock piles and collect a sample of water for chemical analysis. However, once a problem is detected it may be too late to initiate effective remedial measures because the contaminants are already in the local groundwater system.

A more effective approach to monitoring waste rock piles would be to analyze the water chemistry of the effluent produced from within the pile. This would allow for quantitative estimates of the rate of weathering of the minerals and the release of contaminants within the waste rock pile. If this data were then combined with an understanding of the flow of water within the waste rock pile it would be possible to predict the effects of the waste rock pile on the environment. This knowledge would be especially useful in the design of effective long term decommissioning alternatives for the waste rock piles.

To characterize the geochemistry of a waste rock pile with time requires that a sample of water be drawn from within the waste rock pile at discrete time intervals. Due in part to the unsaturated nature of waste rock pile there is no currently accepted method for performing this function. To characterize the flow of water within the waste rock pile the material properties of the waste rock and the hydraulic heads within the pile must be known. The material properties of the waste rock can be characterized using standard unsaturated geotechnical tests. The hydraulic heads within the waste rock pile would have to be measured. Due to problems associated with the coarse nature of waste rock, there is not currently a device that can be reliably used to measure the hydraulic head.

A specially designed stand-pipe lysimeter has been proposed to perform the above functions.

1.2 Objective

The objective of this research program was to design a stand-pipe lysimeter capable of measuring soil suction and collecting a pore water sample from within unsaturated waste rock.

1.3 Scope

The scope of this thesis shall be limited to the design and construction of a prototype lysimeter to verify the operating theory of the lysimeter.

1.4 Organization of Thesis

This thesis has been organized into sections which have contributed to the development and construction of a standpipe lysimeter to measure suction and collect a pore water sample. Chapter 2 provides a literature review of the information required to characterize the geochemistry and flow within waste rock piles and a review of previous work performed on lysimeters. Chapter 2 also includes with a review of current unsaturated zone soil suction measuring devices and pore water samplers. Chapter 3 discusses the basic theoretical aspects related to the lysimeter design. Chapter 4 presents the results of a preliminary modelling program used to identify key elements of the

standpipe lysimeter design. Chapter 5 presents the test methods used in the laboratory program and the prototype lysimeter testing program, while Chapter 6 presents and discusses the results of these tests. Chapter 7 provides an analysis of the data collected from the prototype lysimeter testing program. Chapter 8 presents the conclusions that could be made from this work

CHAPTER 2 BACKGROUND & LITERATURE REVIEW

2.1 Introduction

This chapter will review background literature that is relevant to the development of the standpipe lysimeter. The hydrogeologic characterization of waste rock piles will be discussed. This is followed by a brief discussion on the origin and description of different types of lysimeters. Aspects of lysimeter design as it pertains to the development of the standpipe lysimeter are then discussed. The chapter concludes with a review of current unsaturated zone suction measuring and sampling devices.

2.2 Hydrogeologic Characterization of Waste Rock Piles

The Nevada Division of Water Planning (1998) defines hydrogeology as:

"*the part of geology concerned with the functions of water in modifying the earth, especially by erosion and deposition; geology of ground water, with particular emphasis on the chemistry and movement of water.*"

Therefore, a proper characterization of the hydrogeology of a waste rock pile requires a study of both the hydrology and geochemistry. The following subsections define both hydrology and geochemistry as it relates to this thesis. The last subsection presents a brief review of previous hydrogeologic studies on waste rock piles

2.2.1 The Hydrologic Cycle

The flow of water within waste rock piles can be described using the same guidelines established to describe water flow through other geologic materials. The flow of water in any system can be described using the hydrologic cycle. Freeze and Cherry (1979)

describe the hydrologic cycle as the endless circulation of water between the ocean, atmosphere and land. Figure 2.1 shows a diagram of the hydrologic cycle. This figure displays most of the components required to characterize the hydrology of any site. These components include climate, topography, geology (stratigraphy, lithology and structural features) and hydraulics (hydraulic heads and material properties).

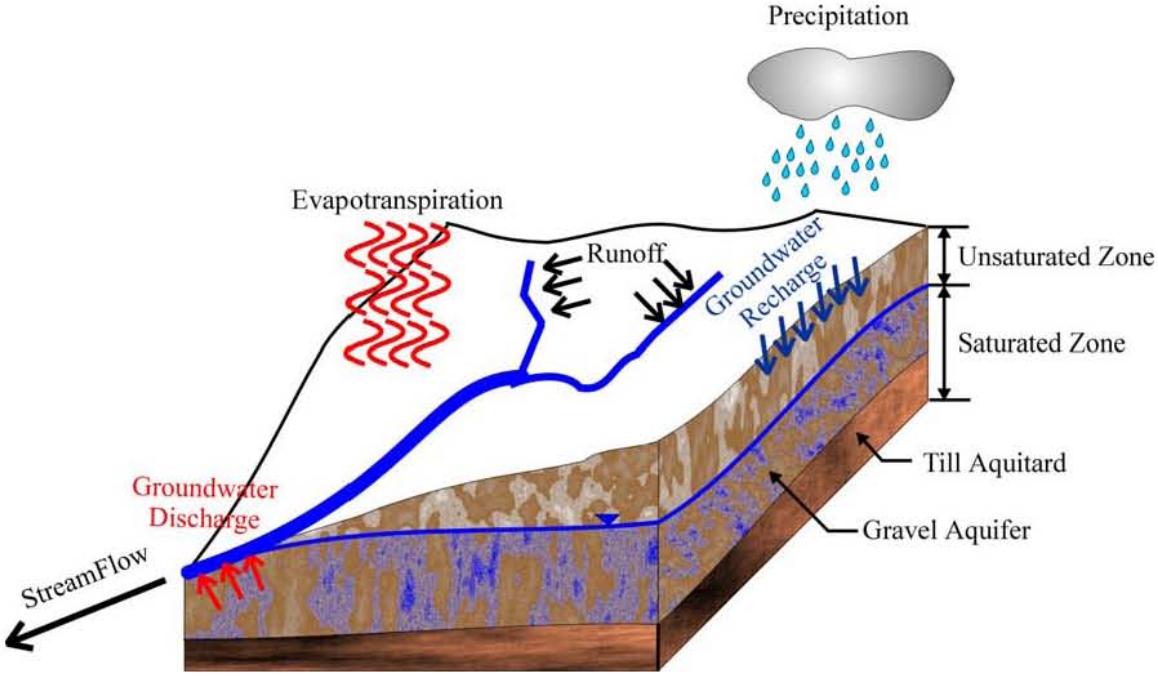

Figure 2.1 - The hydrologic cycle (after Freeze and Cherry, 1979)

2.2.2 Geochemistry

Geochemistry can be defined as the chemical interactions between the minerals, pore water and dissolved gases in the pore water coupled with the effects of microorganisms. A detailed development of the principles of geochemistry is beyond the scope of this thesis. The reader is referred to Freeze and Cherry (1979) for an overview of geochemistry and Stumm and Morgan (1981) for a more detailed description of geochemical processes.

The primary geochemical concern as it relates to waste rock lies in the products of the geochemical reactions that take place within the pile following placement. When waste rock is removed from the ground its environment is changed from that of a reducing environment to that of an oxidizing environment. For each mineral within the waste rock

pile an analysis could be performed to determine the effect of changing the environment of the waste rock from a premining condition to the conditions that exist within the waste rock pile. The production of acid from sulfur bearing waste rock (known as acid mine drainage) is a classic example of the effect of changing the environment of the waste rock. O'Kane (1995) reviewed the kinetics of the acid producing geochemical reactions

Characterization of the geochemistry of any waste rock pile requires knowledge of the distribution of mineral phases and the pore water chemistry within the waste rock piles. Monitoring the changes in pore water chemistry with time would allow for a quantitative estimate on the rate of weathering of the mineral phases and whether the resulting pore water poses a threat to the environment.

2.2.3 Previous Hydrogeological Studies of Waste Rock Piles

In this section, the results from previous studies on the hydrogeology of waste rock piles are reviewed. To understand the flow of water within waste rock piles it has become convenient to discuss the factors that affect waste rock pile hydrology. Whiting (1985) characterized the factors that affect the hydrology of a waste rock dump as a function of their origin as shown in Table 2.1. A few researchers (Herasymiak (1996) and Saretzky (1998)) have used Whiting's (1985) factors to review hydrogeologic studies on waste rock. However, these factors are subgroups related to the classical hydrologic format outlined by Freeze and Cherry (1979) in Section 2.2.1. Some of Whiting's (1985) factors shall be cross-referenced as they are encountered during this classical review of waste rock hydrogeology

Table 2.1 - Factors affecting waste rock pile hydrology (after Whiting, 1985)

Physical	Chemical	Others
Stratification	pH	Precipitation
Channeling	Precipitation/Hydrolysis	Evaporation
Sorption	Temperature	Sublimation
Foundation	Weathering	Evapotranspiration
Hydraulic Conductivity		
Construction		

2.2.3.1 Climate

Climate is a major component in defining the hydrogeology of any site. Climate can be related directly or indirectly to precipitation, evaporation, sublimation and evapotranspiration. Whiting (1985) cites these factors as being important factors in waste rock pile hydrology. Measurements of climate data can be collected using weather stations.

2.2.3.2 Topography

Topography is important from a hydrologic point of view because elevation represents one of the components of hydraulic head. The topography defines the original energy state of a single drop of rain as it lands on the surface of the earth.

The topography of waste rock piles is strongly dependant on the topography of the site prior to the waste rock pile being built and the method of construction of the pile (Couzens, 1985). Taylor et al. (1985) classified waste rock piles according to how they have been placed in accordance with their original surroundings. The classification described by Taylor et al. (1985) is presented in Figure 2.2.

The topography of waste rock piles can generally be established from an as-built survey of the mine site. However, the local topography around the waste rock pile should also be examined using topographic maps to establish potential recharge and discharge areas.

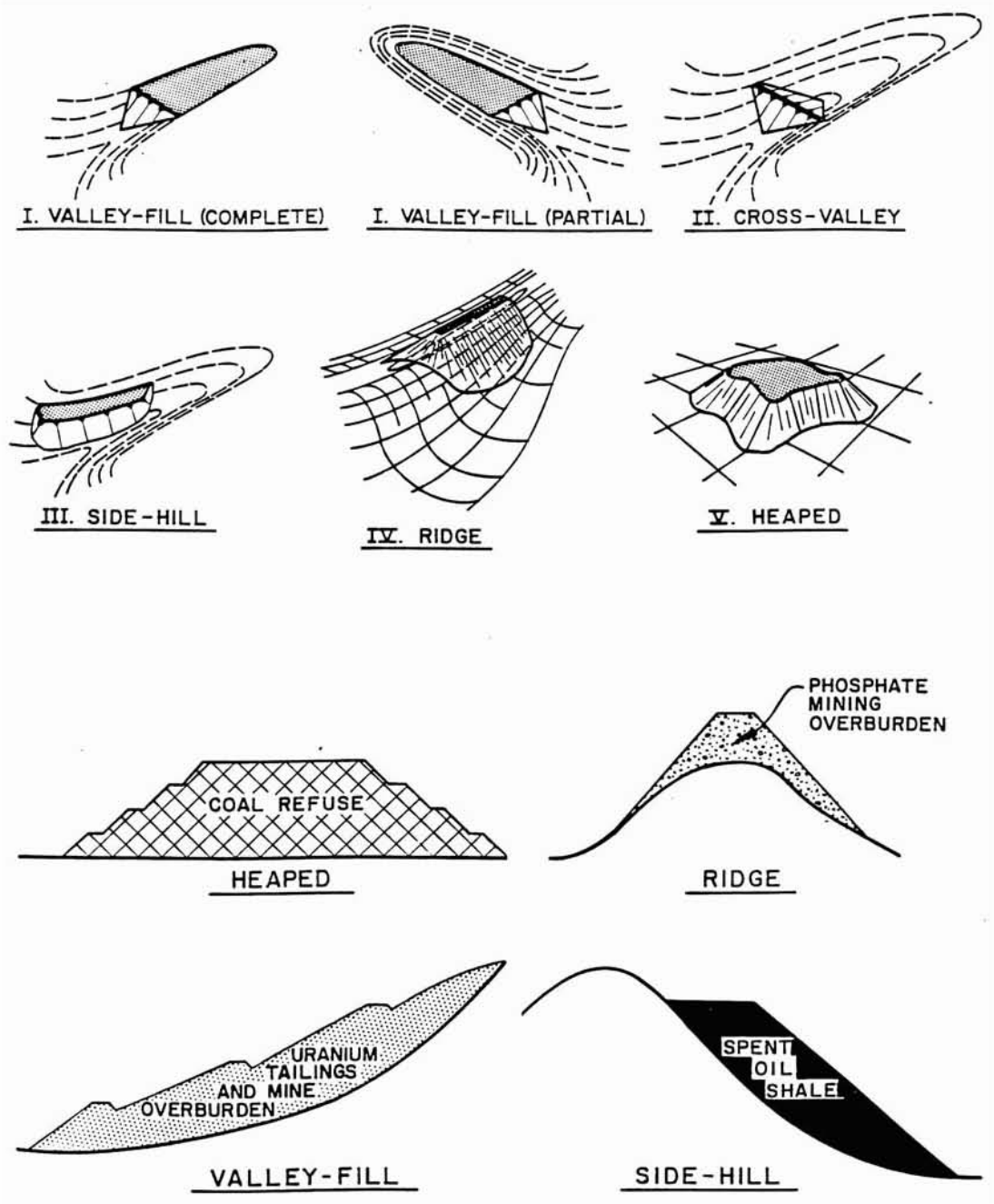

Figure 2.2 - Classification of waste rock piles (Taylor, 1985)

2.2.3.3 Geology

Freeze and Cherry (1979) describe geology as being derived from three main components. The first is stratigraphy, which describes the geometry and age relationships between different layers. The second is lithology, which describes the physical makeup of individual layers and includes mineral composition, grainsize and

grain packing. The third component is comprised of structural features that describe the geometric properties produced by deformation after deposition.

The classical subgroups of geology as defined by Freeze and Cherry (1979) can be used to characterize the framework within which the regional groundwater must flow. This framework is important because it defines the geologic pathways for flow either around or through the waste rock pile. When combined with knowledge of the hydraulics of the system, it can be used to characterize the foundation condition described by Whiting (1985). Whiting (1985) explained that the foundation condition was important in determining the elevation of the water table within the waste rock pile.

The classical subgroups of geology, as they relate to hydrology, can also be used to characterize the framework within which the porewater in the waste rock piles flows. However, there must be some minor modifications to the definition of structural features. The classical definition of structural features is related to deformation of geologic materials with time. In waste rock piles the deformation of the geologic materials is related to the manner in which the pile was constructed. The following paragraphs discuss structural features as they relate to waste rock piles.

The single most important geologic feature of waste rock piles are structural features. These structural features are the direct result of the method of construction of the dump. Smith et al. (1995) identified two different types of waste rock piles; segregated and non-segregated. Herasymiak (1996) investigated the internal structure of a segregated waste rock dump. The waste rock pile construction procedure consisted of end dumping successive layers of material in lifts. The end dumping led to the segregation of fine and coarse materials resulting in layers of alternating fine and coarse materials. These layers had a dip of approximately 40º. End dumping off the edge of the pile led to a coarse rubble zone at the bottom of the pile. As each lift was constructed, the movements of haul trucks on the surface resulted in thin compacted layers being formed between each lift. Figure 2.3 illustrates the structure described by Herasymiak (1996). It should be noted that differing construction procedures would produce different structural features.

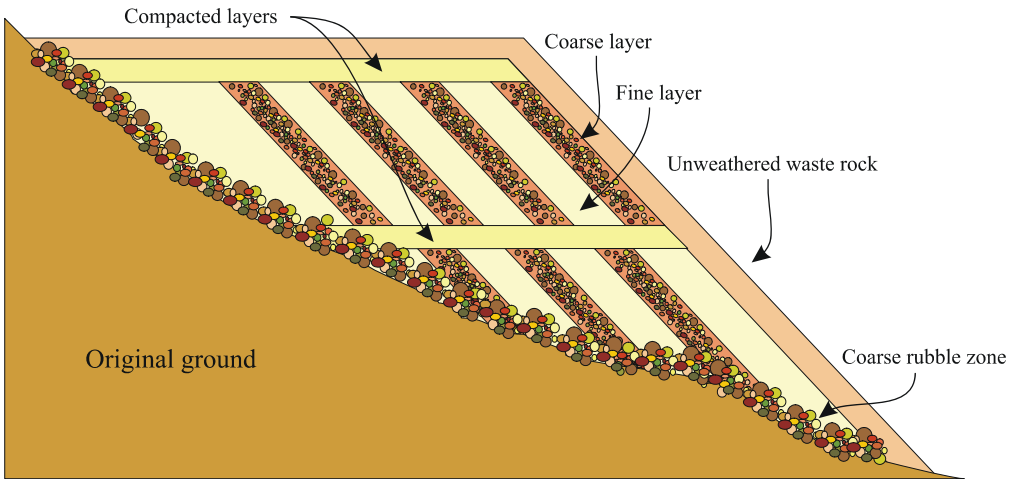

Figure 2.3 - Structure of a waste rock dump (after Herasymiak, 1996)

Whiting (1985) identified that the method of construction of the waste rock pile was important and affects stratification of the pile and channeling within the waste rock pile.

Many researchers (Whiting, 1985; Robertson and Barton Bridges, 1990) have discussed the effect of stratification on channelization through coarse waste rock layers due to the preferential water flow that develops in various layers as a result of construction practices. However, very little quantitative data exists to support these claims. Aside from Herasymiak (1996), most of the data has been obtained from drilling (Morin et al., 1994). Drilling would tend to mask the existence of stratified layers. Channelization will be discussed in more detail in the next section.

Lithology describes the physical make up and mineral composition of the different layers within the waste rock pile. As might be expected, lithology plays a considerable role in defining the geochemistry of waste rock piles. Whiting (1985) discussed factors such as pH, precipitation/hydrolysis reactions, weathering, sorption, and hydraulic conductivity. All of these are directly or indirectly related to lithology when it is assumed that the original mineralogy of the waste rock pile has a distinct effect on the geochemistry within the waste rock pile. The cumulative effects of these processes on the hydraulic conductivity of the waste rock pile will be examined in the next section. The grainsize of waste rock has been characterized from a number of mine sites and is

illustrated in Figure 2.4. Both Herasymiak (1996) and Smith (1995) noted that the coarse fraction could be under represented due to problems of proper sampling techniques on a large scale.

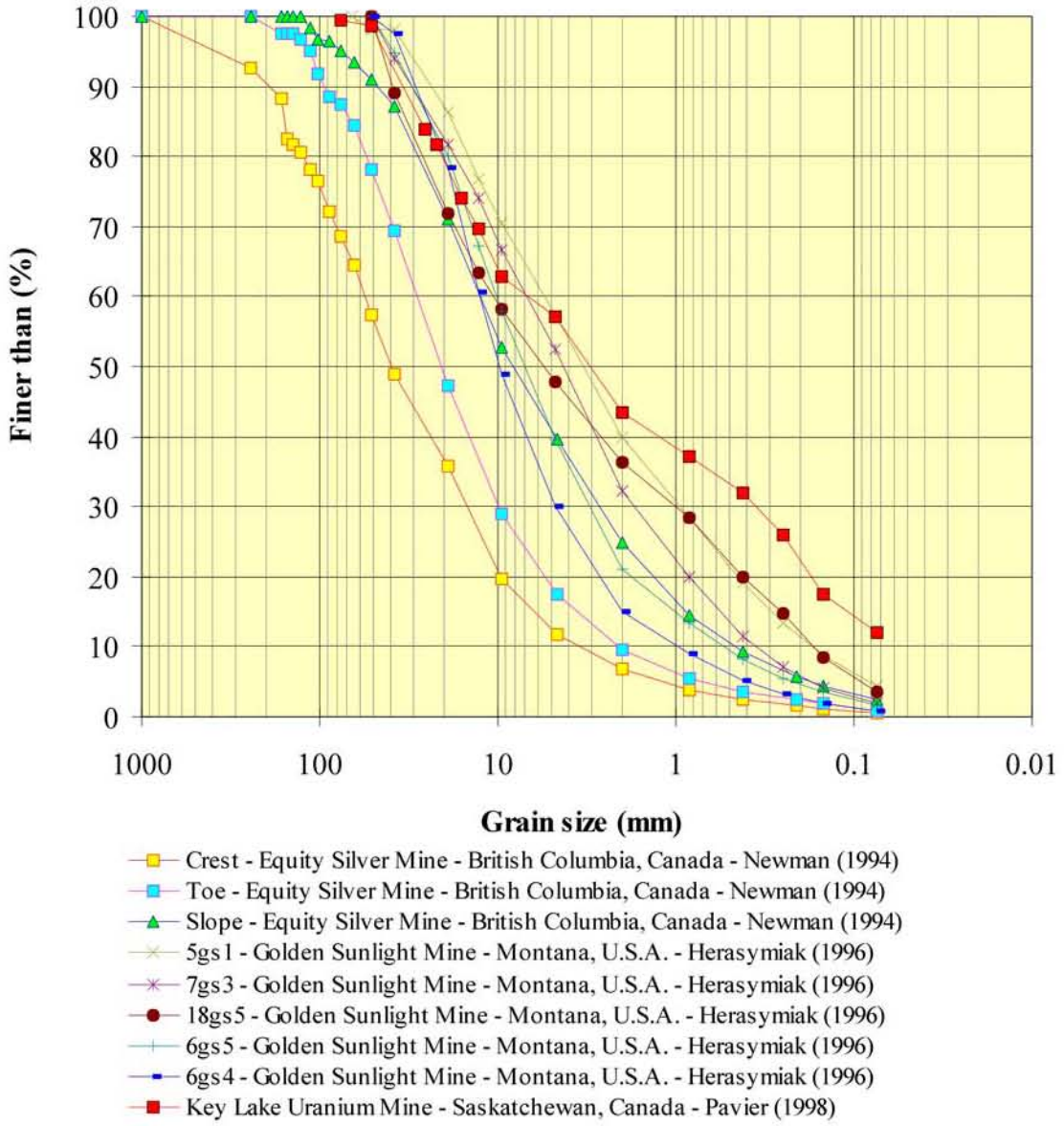

Figure 2.4 - Waste rock grainsize curves from selected mine sites

2.2.3.4 Hydraulics

The previous three subsections provide most of the necessary information to describe the hydrology of a waste rock pile. The climate section provides information on the water being supplied to the system. The topography section provides preliminary information on hydraulic heads at the surface boundary. The geology section provides the framework within which the water must flow. This section completes the characterization of the hydrologic cycle by describing the flow of water through the soil with respect to hydraulic conductivity and hydraulic heads.

The hydraulic conductivity defines the ability of a soil to transmit water under an applied gradient. The saturated hydraulic conductivity of waste rock has been measured by a number of researchers. Smith (1995) tabulated the results of several researchers and found that the range of hydraulic conductivities of waste rock materials ranged from 1E-2 cm/s to 1E-7 cm/s. The saturated hydraulic conductivity of a material can be lowered with time due to physical and chemical weathering processes. When the soil is unsaturated, the hydraulic conductivity can be orders of magnitude lower than the saturated hydraulic conductivity. The decrease in hydraulic conductivity as the soil becomes unsaturated is described in detail in the theory section.

The movement of water in waste rock piles often occurs under unsaturated conditions. As a result, the hydraulic conductivity of the waste rock pile is a function of the suction within the waste rock. The alternating layers of coarse and fine materials, as described by Herasymiak (1996), will provide a preferential flow path through one of the materials. The preferential flow path can be developed through either of the layers dependent on the total flux through the system and the hydraulic conductivity of the layers (Newman, 1999).

Herasymiak (1996) noted that the characterization of the soil-water characteristic curve for unsaturated waste rock is an area that is absent from the literature. As a result, the only reference including soil-water characteristic curves is Herasymiak (1996). The results of Herasymiak (1996) work on soil-water characteristic curves of waste rock

revealed that waste rock can be classified as ‘soil like’ or ‘rock like’ or as a transition material with a behavior between that of soil or rock.

Herasymiak (1996) chose to differentiate between the different classes based on the ability of the waste rock to retain water under an applied matric suction and the amount of material passing the 4.75 mm and 2 mm sieves. Table 2.2 displays a summary of Herasymiak’s classification system.

Table 2.2 - Classification of waste rock on the basis of air entry value (after Herasymiak, 1996)

Passing 4.75 mm Sieve (%)	Passing 2 mm Sieve (%)	Air Entry Value (kPa)	Herasymiak's Classification
>50	> 20	3.5 - 5	Soil like
40 - 49	> 20	3.5 - 5	Soil like
30 - 39	20	< 0.1	Transition
20 - 29	< 20	<< 0.1	Rock like

Herasymiak (1996) describes the soil like behavior as being dominated by the fine grained waste rock. In this classification, the coarse particles are suspended in a fine matrix. The coarse particles may or may not be touching, but all of the interparticle space is infilled with the fine matrix. As a result, the samples have a soil-water characteristic curve that is similar to that of the fine material.

As the volume of fines decrease, as in the range of 30 to 39% passing the 4.75 mm sieve, a point is reached that where the amount of fines is no longer adequate to fill the spaces between the coarse materials. Herasymiak (1996) classifies this type of material as transition. The soil-water characteristic curve displays an initial drop in volumetric water content as the empty spaces drain quickly at low suctions, however, as drainage continues the curve more closely resembles that of the fine grained samples. The soil like and transition classifications have comparable residual water content and suctions.

The rock like classification is characterized by a very low air entry value followed by residual volumetric water contents at suctions less than 1 kPa. Herasymiak (1996) describes this material as no longer containing enough fine grained material to be considered a fine grained dominated matrix. In other words, the majority of the water drains from the large pores under low applied suctions and the fines do not have enough physical mass to have an effect on the overall volumetric water content of the sample. As a result, the sample behaves as a rock like material. Soil-water characteristic curves and hydraulic conductivity functions for these types of materials are shown in Figure 2.5

Many researchers have noted evidence of the flow of water through coarse channels. The theory of flow in unsaturated soils would suggest that the majority of the water should be transmitted through the fine material during unsaturated conditions. Smith (1995) suggested one flow mechanism for non-segregated waste rock piles and two possible flow mechanisms for segregated waste rock piles. In non-segregated waste rock piles, flow would travel through the soil matrix as described by unsaturated flow theory. In segregated waste rock there are two scenarios; Flow can occur either through the fine layers or the coarse layers. Newman (1999) discusses the conditions under which preferential flow will occur in each material.

The driving force for water flow is the gradient of hydraulic head. Hydraulic head can be defined as the energy state of water as defined by its elevation (as referenced from a common datum) and pressure head. Elevation heads can be obtained by simply knowing the elevation above a datum. The pressure head can be calculated knowing the soil suction present in the waste rock pile. Very few researchers have tried to measure the pressure head in waste rock piles. Herasymiak (1996) in his investigation of the Golden Sunlight Mine attempted to measure suction using a tensiometer. Herasymiak (1996) was not successful due to problems with establishing a hydraulic connection between the soil and the ceramic tip of the tensiometer. Smith (1995) measured suctions in waste rock piles using thermal conductivity sensors. Smith (1995) found that these sensors could be used in areas of waste rock piles that do not generate significant amounts of heat and are not frozen. Smith (1995) explained that heat produced from acid rock

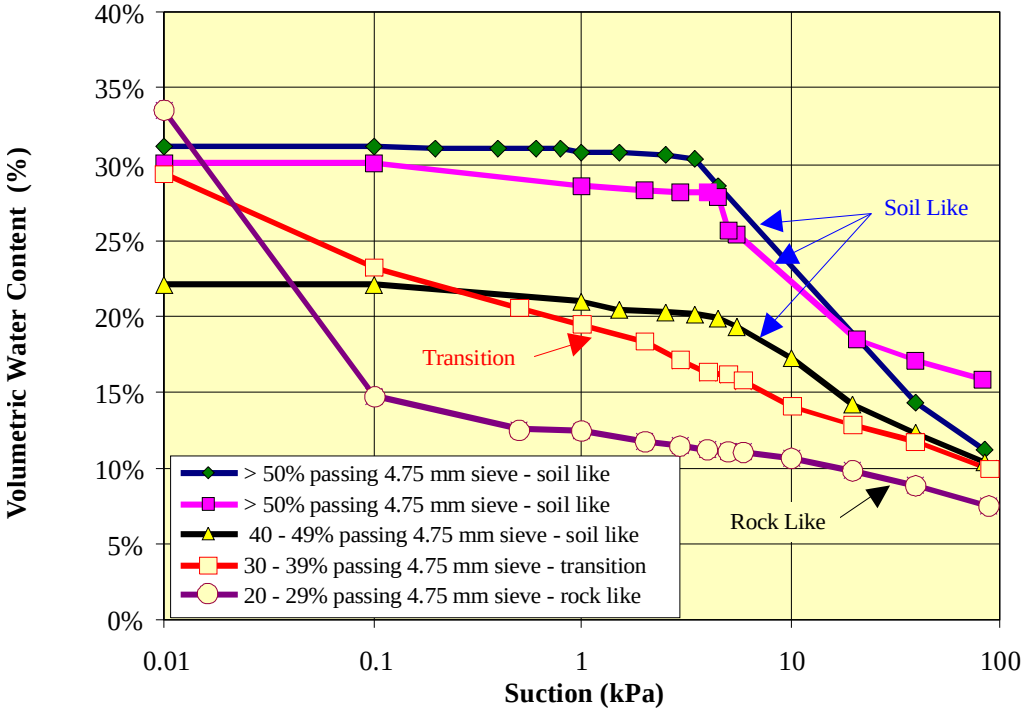

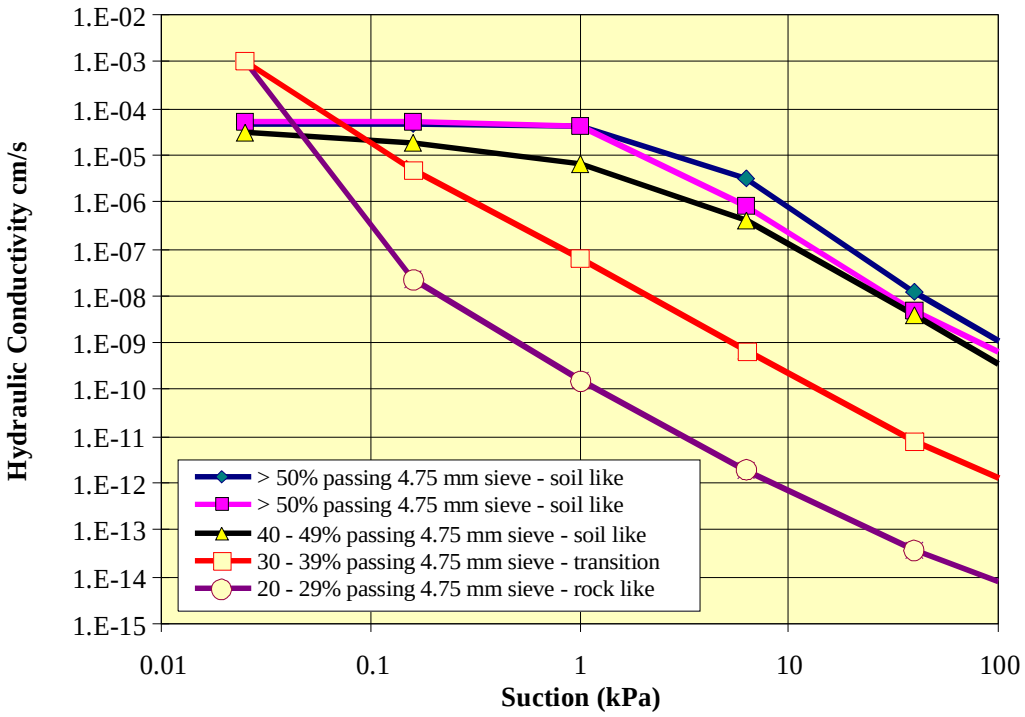

Figure 2.5 - Soil-water characteristic curves and hydraulic conductivity functions corresponding to Herasymiak's (1996) classification system

drainage interfered with the thermal conductivity sensors. In areas of the pile that were frozen, the heat generated by the sensor melted the ice around the sensor. This caused increased water contents in the sensor and subsequently the sensor recorded decreased matric potentials. Smith (1995) concluded that using the thermal conductivity sensors did not provide a clear indication of infiltration.

Measurements of gravimetric water contents have been performed on some waste rock piles, thus providing a qualitative indication of the pressure head profile within the pile when referenced to a soil-water characteristic curve. Herasymiak (1996) found that Golden Sunlight Mine in Montana was wetter at the top of the waste rock pile and very dry near the bottom of the waste rock pile. Herasymiak (1996) concluded that the wet zone at the top of the pile corresponded to the wetting front gradually making its way down into the pile. Smith (1995) showed the same trends for several different mine sites. Smith concluded that the higher water contents in the upper part of the pile corresponded to end dumping practices that cause the fine material to stay near the top of the waste rock pile. The fine material has a greater ability to retain water than the coarse material located lower in the pile.

Aside from water flow, the heat produced in exothermic reactions can cause significant vapor flow within waste rock piles. Many researchers (Herasymiak 1996, Smith 1995 and Whiting 1985) site examples of active vents. Vents are a term to describe the upward movement of steam through coarse waste rock. Herasymiak (1996) stated that this might be a possible reason for the elevated water contents observed near the top of the pile. Steam generated at depth within the pile would rise to condense in the colder upper portions of the pile.

2.3 Lysimeters

The word lysimeter is derived from the two Greek words “lysis” which means dissolution or movement and “metron” which means to measure (Aboukhaled, 1982). Webster’s New Collegiate Dictionary defines a lysimeter *as a device for measuring the*

percolation of water through soils and for determining the soluble constituents removed in drainage.

There is a lot of literature available on lysimeters, unfortunately, little of it is directly applicable to the development of a standpipe lysimeter. This is due in part, to the indistinct meaning of the word lysimeter. The following sections will provide a description of the lysimeter used in this thesis and a discussion of some of the major lysimeter designs from the literature. The last section shall deal with lysimeter design criteria as it applies to this thesis.

2.3.1 Development and Types of Lysimeters

Kohnke et al. (1940) attributed the first recorded use of a lysimeter to the Frenchman De la Hire in the late 17th century. De la Hire was interested in the infiltration of water into the ground. To measure the infiltration rate he buried several large pots in the ground. At a later time, he dug out the pots to see how much water had collected in them over the elapsed time.

Since De la Hire, lysimeters have been used by many different disciplines of science with an interest in collecting or measuring the properties of water in the soil. In agriculture and soil sciences the interest is in two areas, the first being the measurement of the chemistry of pore water and the second being the measurement of moisture fluxes across the soil surface. In civil engineering, the primary interest is in the measurement of infiltration into soil. As a result of varying applications, lysimeters have made an appearance in many different forms over the years. Some of the more predominant lysimeter types are as follows:

- Pan (Ebermayer) Lysimeter
- Weighing Lysimeter
- Vacuum Lysimeter
- Gravity Lysimeters

2.3.1.1 Pan Lysimeters

Pan or Ebermayer lysimeters represent one of the largest groups of lysimeters found in the literature. This type of lysimeter has been used extensively for the collection of water for chemical analysis. The pan lysimeter consists of a shallow pan to collect water. The method of installation is to excavate a tunnel beside where the pan lysimeter is to be installed. The lysimeter is then placed into a hole excavated into the tunnel wall and is then wedged up against the soil. The pan is allowed to stay in place and collect the water that is percolating through the soil. (Tyler, 1977; Jemison, 1992)

Researchers from as early as the 1940's (Colman, 1947) realized that this type of lysimeter has a basic design flaw. In unsaturated soils, soil suction will cause most of the water to be diverted around the pan. Water that cannot be diverted around the pan (due to the low hydraulic conductivity of unsaturated material) will cause a water table to develop above the pan. Once a water table has been established the pan lysimeter will collect water. Even in this case; however, the flow of water in the soil is disturbed by the presence of the lysimeter and the amount of water that is collected in the pan does not reflect the actual amount of water passing through the soil.

Despite this basic design flaw this type of lysimeter has continued to be used for research. Some researchers (Jordan, 1966) have tried to improve the basic version by adding a fiberglass screen to the top of the pan and suspending glass wool rods inside the pan to allow the water drops to enter the pan more readily. This has become known as a zero tension pan lysimeter.

2.3.1.2 Weighing Lysimeters

Weighing lysimeters have been used in research to study evapotranspiration (Howell et al., 1991) and to study the vertical movement of water through soils. A weighing lysimeter is constructed by mounting a large size container on a weigh scale. The lysimeter and weigh scale are buried in the ground such that the edges are mounted flush with the surrounding ground. The lysimeter is then backfilled with material that is similar to the soil adjacent to it. A tunnel is also constructed to allow access to the

bottom of the lysimeter to allow for readings to be taken. In addition to weighing the lysimeter to measure the movement of water, these lysimeters have been instrumented with tensiometers and other devices to measure soil responses. The basic premise of this design is that by mounting the device flush with the ground surface, any infiltration or evapotranspiration that occurs in the soils should also occur in the lysimeter. Water movement across the surface boundary can be calculated from the total weight of the lysimeter.

Weighing lysimeters can be classified into various subgroups with respect to how the sample is placed in the lysimeter. In a reconstructed soils lysimeter the soil layers are manually reconstructed. In a monolithic lysimeter a monolithic block of soil is carefully excavated out and placed in the lysimeter. Another variation on this theme is the microlysimeter. The word micro does not apply to the lysimeter itself, but stands for microenvironment. In this type of lysimeter a monolithic block of soil is placed into a weighing lysimeter located at a laboratory where the environment of the entire lysimeter can be controlled thus creating a microenvironment.

2.3.1.3 Vacuum (Tension) Lysimeters

Vacuum or tension lysimeters are used to sample the porewater of unsaturated soils. The basic operating principle of vacuum lysimeters is that suction is applied to the soil so that water flows into the lysimeter. Vacuum lysimeters vary depending on the method used to apply the suction, the material used at the lysimeter-soil interface, the lysimeter geometry and the method in which the water sample is removed from the lysimeter.

The method of applying suction to the soil usually consists of applying a vacuum (negative air pressure) within the lysimeter. To use the vacuum method a material with a high air entry value must be used as the contact between the lysimeter and the soil. This allows for a continuous water phase between the water within the lysimeter and the soil while under suction.

Materials used in the construction of the lysimeters vary. The body of the lysimeter can consist of anything that is capable of holding both water and pressure and is often fabricated out of plastic. The materials used at the soil interface consist of high air entry disks made of porous ceramics, aluminum oxide disks, etc. with the most common being porous ceramics. The geometry of the lysimeter can vary from round and square plates to round and square tubes in a different shapes and sizes.

Figure 2.6 displays two different methods of removing a water sample from a vacuum lysimeter. The ceramic lysimeter uses the body of the lysimeter to store the vacuum. Once a sample has been collected the sample is removed through the access tubes. In the fritted glass lysimeter a vacuum hose is brought to the surface and the sample is collected above ground. In addition to these two types of collection methods there are many other schemes which are used to remove the water sample from the lysimeter. As can be seen in the preceeding discussion there are many types of vacuum lysimeters. The common feature of all these designs is the application of a vacuum or a tension to the soil to collect a water sample. The most common variety of vacuum lysimeter is the ceramic lysimeter shown in Figure 2.6.

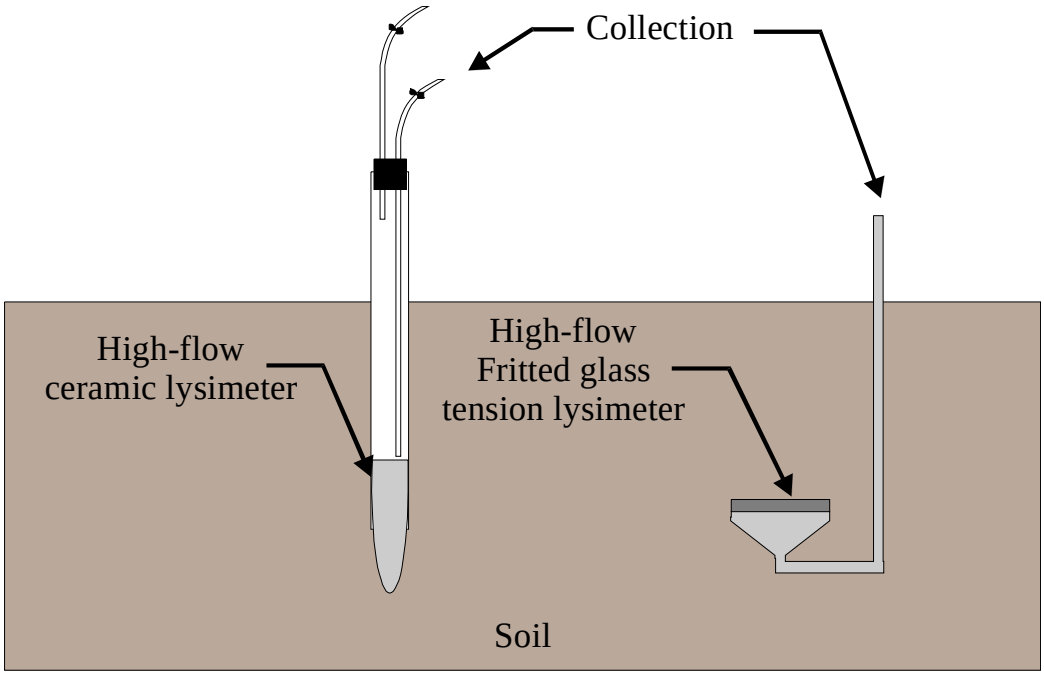

Figure 2.6 - Examples of vacuum lysimeters (revised after Krejsl et al., 1994)

2.3.1.4 Gravity Lysimeters

Gravity lysimeters represent a class of lysimeters that attempt to assess the flux across a given area by collecting the water flowing in that area. The method of collecting the water is to allow gravity to draw the water into a sample collection system. This type of lysimeter is used by civil engineers to measure the net flux through a liner or cover system. The lysimeter featured in this thesis is a variation of a gravity lysimeter.

Gravity lysimeters generally consist of a collection vessel or a flexible liner backfilled with soil. The water is collected at the base of the lysimeter. The amount of water that has entered the lysimeter is measured by determining the height of the water table within the lysimeter or collecting the water from the base of the lysimeter. Figure 2.7 displays a gravity type of lysimeter. Gravity lysimeter have the same design flaw as pan lysimeters in unsaturated soils. Fortunately, these problems can be mitigated through proper design practices. The design problems associated with gravity lysimeters shall be examined in detail in the next section.

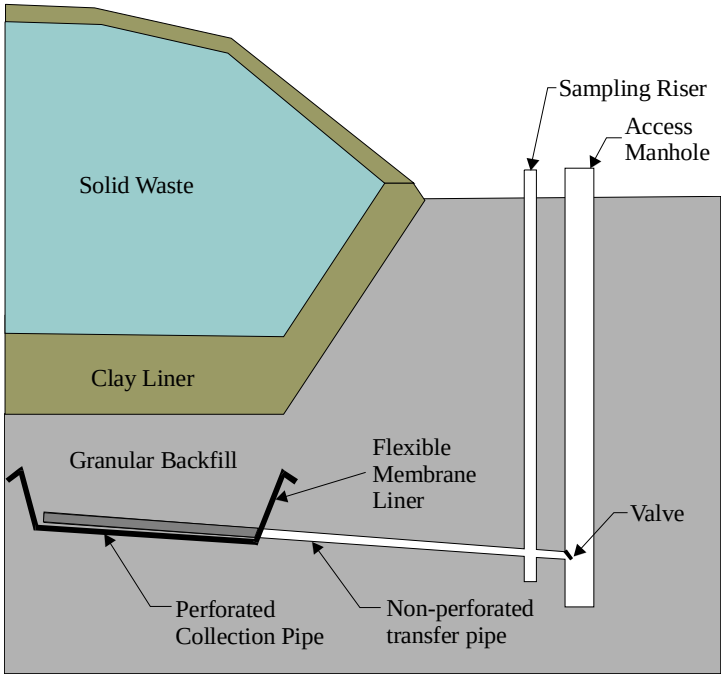

Figure 2.7 - Gravity lysimeter (revised after Gordon et al. , 1989)

2.3.2 Lysimeter Design Criteria

The design of pan lysimeters was investigated by Bews et al. (1997a and 1997b) during the design of lysimeters for a low flux cover system. Bews (1997b) used the two-dimensional finite element seepage model Seep/W (Geoslope Int. 1999) to identify key lysimeter design parameters. These key design parameters were:

- Height of Lysimeter Walls
- Lysimeter Backfill Material
- Width of Lysimeter

2.3.2.1 Height of Lysimeter Walls

To understand the following discussion it is essential that the reader have some understanding of the pressure profiles that develop in unsaturated soils under steady state conditions with downward flow. Figure 2.8 displays a pressure profile that can develop in unsaturated soils. The bottom of the chart corresponds to the location of the water table at a suction of 0 kPa. Above the water table the suction increases hydrostatically at a maximum slope of approximately 1 m of elevation per 10 kPa of suction. The limiting suction is a function of the applied flux. Different flux rates will produce different limiting suctions. This concept is more fully developed in the theory section of this thesis.

One of the most important design considerations identified by Bews (1997b) was the height of the lysimeter walls. If the wall height is too low, water will flow into the lysimeter only to be drawn out of the lysimeter by lower suctions in the soil surrounding the lysimeter. Figure 2.9(a) shows a poorly designed lysimeter and the effect of having lysimeter walls that are too short. In comparison, Figure 2.9(b) shows a properly functioning lysimeter with proper wall heights. Bews (1997b) determined that proper wall height was a function of two key parameters. The first parameter is the anticipated range of soil suctions. The range of expected soil suctions can be estimated from the anticipated infiltration rates and the hydraulic conductivity function. The second key

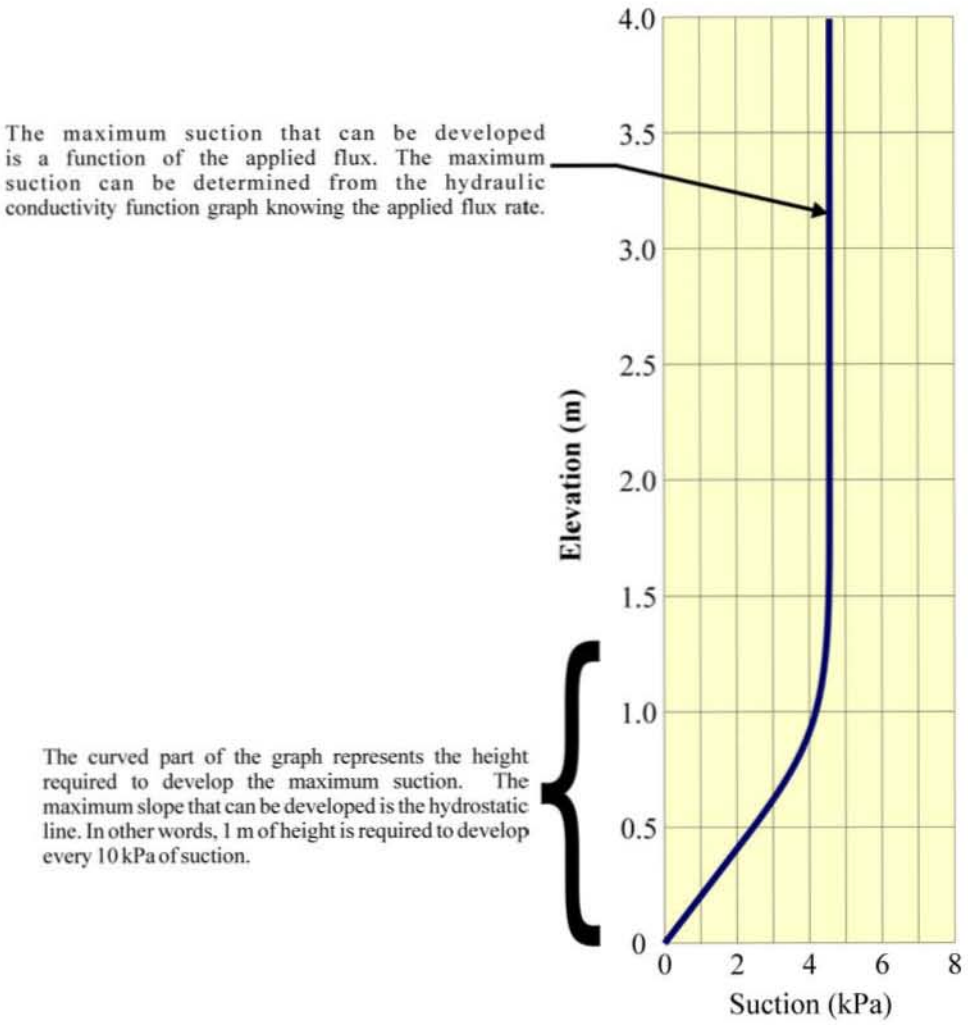

Figure 2.8 - Pressure profiles in unsaturated soils

parameter is the height required to develop the expected soil suction above the artificial water table in the lysimeter.

Bews (1997b) was able to estimate the infiltration rates into the low flux cover system using a range of flux values generated from the one-dimensional heat and mass transfer program, SoilCover (MEND 1993). The hydraulic conductivity of the soil must be equal to the applied infiltration rate in the constant pressure interval shown in Figure 2.8. Bews (1997b) was then able to pick values of soil suction off a hydraulic conductivity versus suction graph as estimated from the soil-water characteristic curve (these terms are explained fully in the Theory Section of this thesis). Bews (1997b) describes the maximum suction that can be developed as the "break point" and is the one that controls the height of the lysimeter walls as will be explained in the next paragraph.

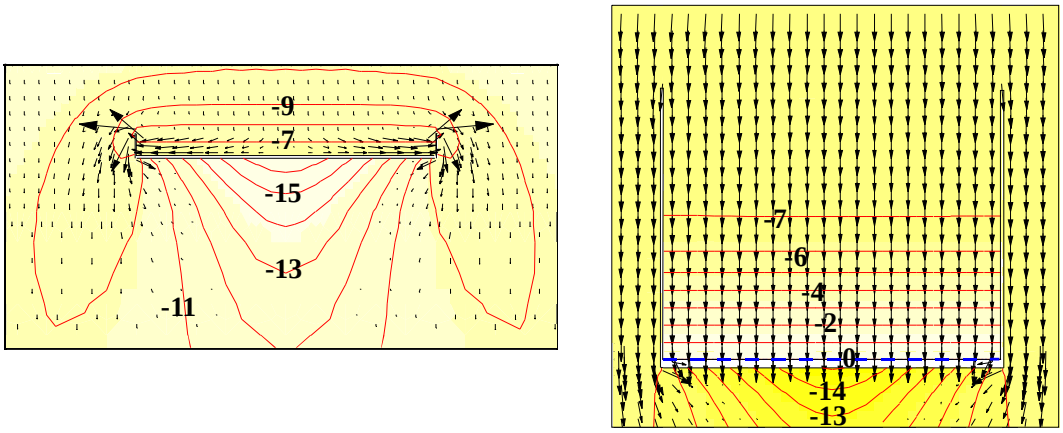

(a) pan (0.15m wall height) (b) 1.5 m wall height

Figure 2.9 - Effect of wall height on flow paths (Bews, 1997b)

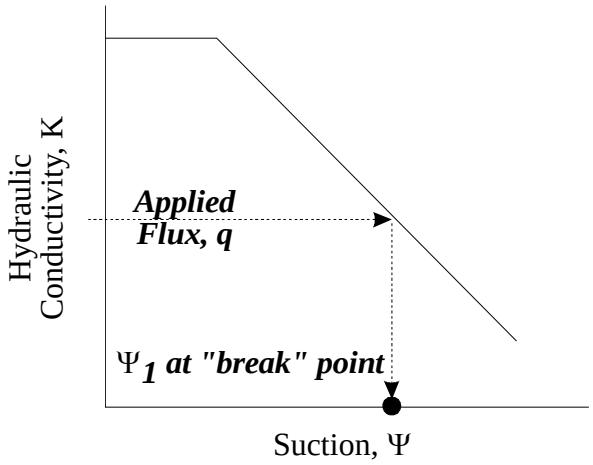

Figure 2.10 - Hydraulic conductivity versus suction (Bews, 1997b)

In order for the lysimeter not to affect the flow regime in the surrounding area, the soil suction at the top of the lysimeter must be equal to the soil suction in the surrounding waste rock. Bews (1997b) found that for steady state conditions that suctions increased hydrostatically above the water table to a specific elevation as shown in Figure 2.11. Using this criterion, choosing the correct minimum wall height is a matter of converting the maximum expected suction in kilopascals to an equivalent head of water. For example 10 kPa soil suction requires a minimum wall height of 1.02 m.

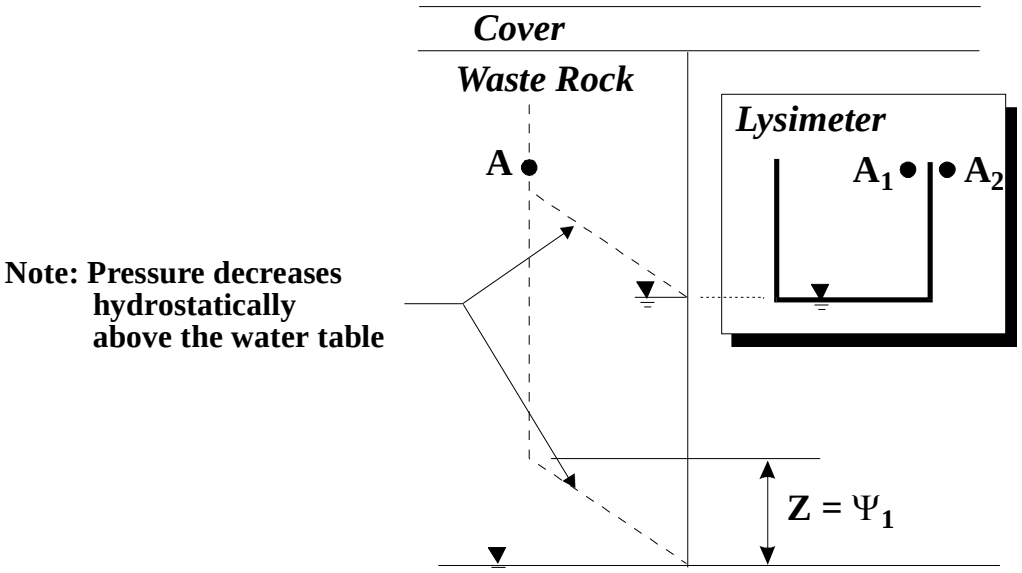

Figure 2.11 - Determination of minimum wall height (after Bews, 1997b)

2.3.2.2 Lysimeter Backfill Material

Wickland (1998) studied the effects of using different backfills in a lysimeter. At low flux rates Wickland (1998) observed that if the material used in the lysimeter is finer than the surrounding material it will act as a preferential flow path collecting more water than is actually flowing in the surrounding waste rock. When the lysimeter backfill was changed to a coarser material than the surrounding material, at low flux rates the surrounding material acted as the preferential flowpath and the flux into the lysimeter decreases. Wickland (1998) concluded that for low flux rates, the best lysimeter backfill is one that most closely resembles the material being monitored.

Bews (1997b) also noted that the choice of lysimeter backfill material was important. However, Bews (1997b) also realized that to effectively monitor a lysimeter, the materials at the base of the lysimeter must have well defined geotechnical properties. As a result, Bews (1997b) modelled a two layer system within the lysimeter. The upper layer corresponded to a material that had similar characteristics toe the material being monitored. The lower layer was a sand layer placed at the base of the lysimeter. Bews discovered that the layered system would work as long as the lysimeter was of sufficient depth.

2.3.2.3 Size of Lysimeter

Bews (1997b) also modelled the effect of the diameter of the body of the lysimeter, and discovered that if the lysimeter was built to the proper height and contained an appropriate backfill, that the diameter of the lysimeter was not a critical design factor. The size of the lysimeter only becomes a critical design factor if the gradients inside and out of the lysimeter are not equal (this is known as edge effects). In this scenario, a wider lysimeter will reduce the overall impacts of edge effects. Thus, lysimeters to measure infiltration should be built as large as possible to reduce any potential errors due to edge effects.

2.4 Unsaturated Zone Measuring Devices

The following subsections review the literature as it pertains to unsaturated zone suction measuring devices and pore water samplers. The method of operation and the advantages and disadvantages of each type of device with respect to installation in an unsaturated waste rock pile shall be investigated.

2.4.1 Suction Measurement Devices

The following discussion of suction measurement devices is largely condensed from the book *Soil Mechanics for Unsaturated Soils* authored by Fredlund and Rahardjo (1993). These authors discuss the following unsaturated zone soil suction measuring devices:

- Psychrometer
- Filter Paper
- Tensiometer
- Thermal Conductivity Sensors

2.4.1.1 Psychrometer

Thermocouple psychrometers can be used to measure the total suction of a soil by measuring the relative humidity in the air phase of the soil pores. Fredlund & Rahardjo (1993) showed that soil suction can be calculated from relative humidity using the following equation:

$$\psi = -\frac{RT}{\upsilon_{wo}\omega_{\upsilon}} \ln\left(\frac{\overline{u}_{\upsilon}}{\overline{u}_{\upsilon o}}\right) \quad \text{..... Eq. 2-1}$$

Where: ψ = Soil Suction (kPa)

R = Universal Molar Gas Constant (J/(mol K^o))

T = Absolute Temperature (^{o}K)

υ_{wo} = Specific Volume of Water (m^3/kg)

ω_{υ} = Molecular Mass of Water (kg/kmol)

$\overline{u}_{\upsilon}$ = Partial Pressure of Pore Water vapour (kPa)

$\overline{u}_{\upsilon o}$ = Saturated vapor pressure (kPa)

Psychrometers measure the relative humidity in the air phase using the Peltier and Seebeck effects. Peltier discovered that by passing a current through a circuit of two different metals one of the junctions becomes warmer while the other junction becomes cooler. In a psychrometer, this effect is used to cool the junction such that a drop of water condenses. Once a water droplet is formed the current is shut off. Seebeck discovered that electromotive force could be produced in a circuit of two different metals at different temperatures. In the psychrometer, as the water droplet evaporates it cools one of the junctions. The rate of evaporation is a function of the relative humidity of the air near the junctions. If the relative humidity is low the water drop will evaporate quickly, conversely if the relative humidity is high the drop of water will evaporate more slowly. The temperature difference between the two junctions can be measured as a voltage. The maximum voltage measured can be related to the soil suction. Figure 2.12 graphically shows this method and the accompanying output.

Psychrometers are extremely sensitive to changes in the temperature of the sample as indicated by the operating principle and the equation describing the relationship between relative humidity and soil suction. Fredlund and Rahardjo (1993) estimated that an accuracy of ± 10 kPa can attained if the temperature of the sample is controlled to within 0.001 degrees Celcius. In a field situation this would be difficult to maintain. As a

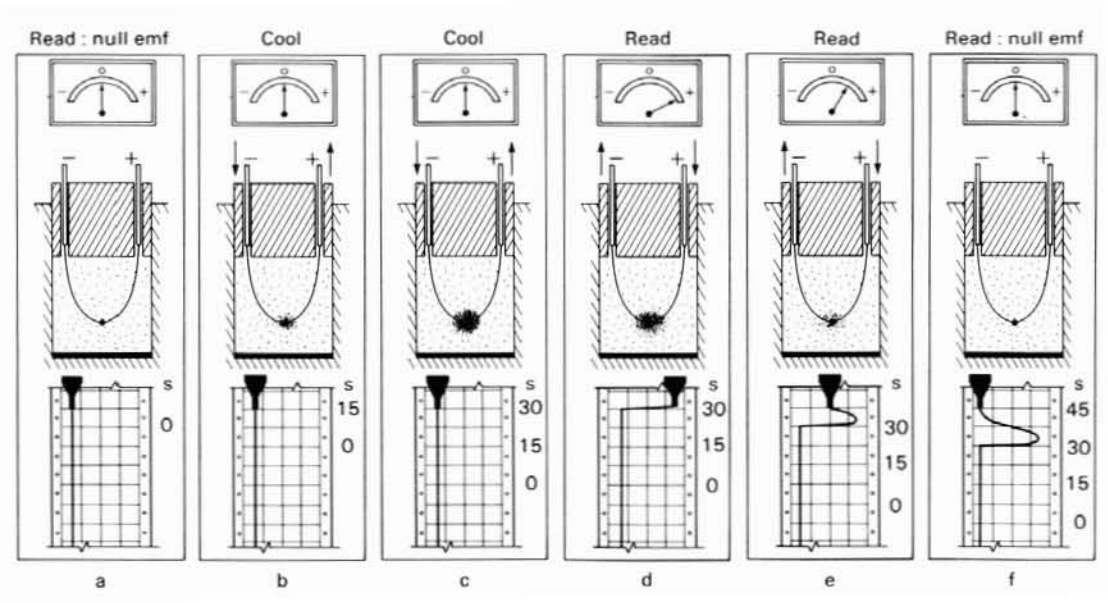

Figure 2.12 - Operational procedure of a psychrometer (Fredlund and Rahardjo, 1993)

result, Fredlund and Rahardjo (1993) do not recommend the use of psychrometers in the field.

2.4.1.2 Filter Paper

The filter paper method is an indirect method of measuring either total suction or matric suction. Fredlund and Rahardjo (1993) describe how the moisture in the filter paper comes into equilibrium with the moisture in the soil that it is placed on or near the filter paper. If the filter paper is placed in contact with the soil or near the soil, water or water vapour will flow into the filter paper. The water content of the filter paper can by determined by weighing. The moisture retention curve for the filter paper can then be used to determine the suction in the soil.

Fredlund and Rahardjo (1993) state that either matric or total suction can be measured, depending on the type of contact of the filter paper with the soil. If the filter paper is suspended above the soil it measures the combined effects of matric and osmotic suction (total suction). If the filter paper is in direct contact with the soil, the matric suction is measured because the water that enters the filter paper would have the same osmotic potential as the water in the soil. Thus, the osmotic potential would not be measured.

Fredlund and Rahardjo (1993) caution that the measurement of matric suction is highly dependent on the degree of contact between the soil and the filter paper.

The filter paper method has been used successfully in a number of field installations. However, due to the requirement of physically weighing the sample, most applications have been near surface installations. The applicability of the filter paper method for deep applications would be questionable due to the requirements of removing the sample. This would require an access tunnel, which in itself, may distort the flow regime in the area trying to be measured.

2.4.1.3 Tensiometer

A tensiometer is a device that directly measures the negative pore-water pressures in a soil. Fredlund and Rahardjo (1993) describe the device as consisting of a high air entry porous ceramic cup connected to a pressure measuring device through a small bore tube. The tube and cup are filled with de-aired water. Figure 2.13 displays a typical tensiometer manufactured by the Soilmoisture Equipment Corporation. The method of operation is to place the cup in direct contact with the soil. Soil suction draws water through the porous ceramic cup. As a consequence negative pore-water pressures build up in the tube. Once equilibrium has been attained the negative-pore water pressures can be measured using a pressure measuring device. Measurements of pressure by use of a tensiometer are limited to less than 100 kPa. This is due to that fact that water cavitates at suction values of 100 kPa.

Fredlund and Rahardjo (1993) note that tensiometers have been used on a number of occasions to measure soil suctions at field sites. As with the filter paper method, there are concerns about the applicability of tensiometer testing for deep applications. The foundation of these concerns is twofold. The first concern is due to the fact that tensiometers require periodic maintenance to remove air bubbles from the small bore tube. Fredlund and Rahardjo (1993) explained that over time air bubbles would develop in the small bore tube as a result of air diffusing through the porous ceramic. Air bubbles can cause the tensiometer to respond slowly to changes in suction. A second

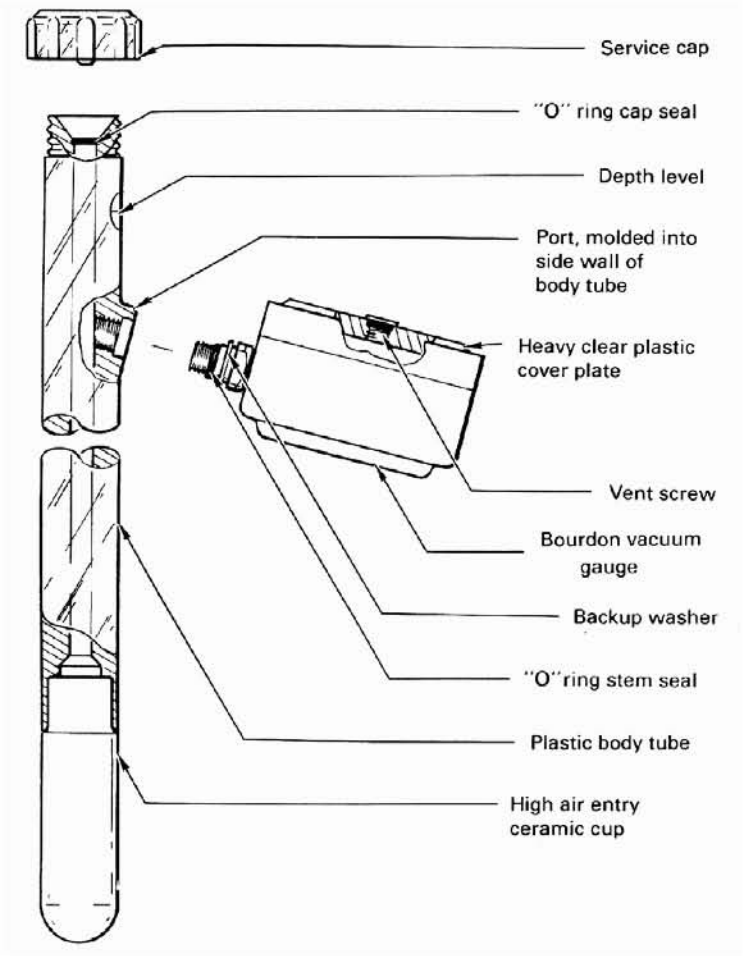

Figure 2.13 - Conventional tensiometer from Soilmoisture Equipment Corp. (Fredlund and Rahardjo, 1993)

concern is the access tunnel that would be required to maintain and read the tensiometers. The access tunnel itself would disrupt the flow regime in the area of interest. Figure 2.14 displays an access shaft that was used for insitu tensiometer measurements.

Bond (1985) describes the use of a vacuum lysimeter (same basic design as a tensiometer) in monitoring the effluent chemistry at heap leach and tailings sites. The installation procedure involves installing the tensiometer in a drill hole as shown in Figure 2.15. In coarse soils, Bond (1985) recommended the use of silica flour to ensure

contact between the soil and the ceramic cup. For deep applications, Bond recommends the use of internal check valves to remove the sample. Theoretically, a tensiometer could be used to measure soil suctions for moderately deep installations within a waste rock pile with some minor changes to the way the tensiometer is installed, and modifications to the basic tensiometer such that air bubbles could be periodically flushed. The depth of the lysimeter would have to be limited such that the suction at the recording end of the tensiometer was less than 100kPa, so that the water would not cavitate. In waste rock piles, this might require that the outlet end be placed at ground elevation on the outside of the pile.

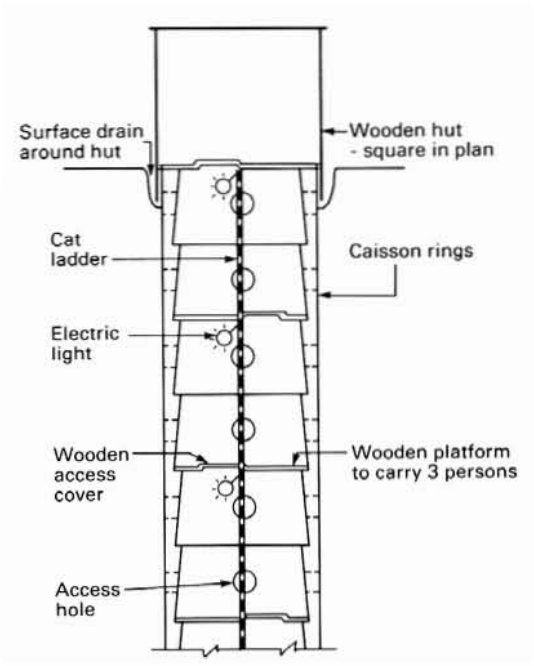

Figure 2.14 - Access tunnel for tensiometer measurements (Fredlund and Rahardjo, 1993)

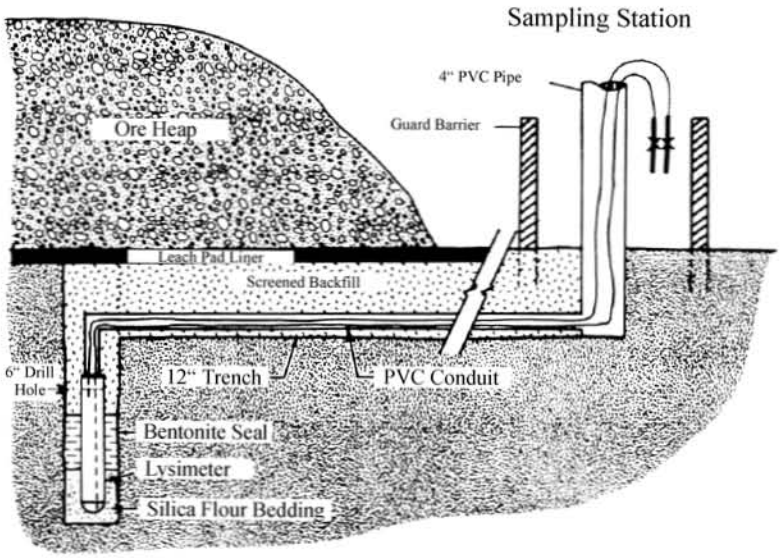

Figure 2.15 - Potential tensiometer installation technique (after Bond, 1985)

2.4.1.4 Thermal Conductivity Sensors

Fredlund and Rahardjo (1993) describe the thermal conductivity sensor as consisting of a porous ceramic block containing a temperature sensing element and a miniature heater. Figure 2.16 displays a cross section through a thermal conductivity sensor. The method of operation of this sensor as described by Fredlund and Rahardjo (1993) is that the thermal conductivity of the porous block is a function of the water content of the porous block. Thus, when the block is in contact with the soil, water can enter or leave the block until equilibrium is established. Once at equilibrium the thermal conductivity of the block can be measured. With calibration the measured thermal conductivity can be related to soil suction.

Thermal conductivity sensors have been used at numerous field sites, and have shown consistent, reproducible readings with time. However, Fredlund and Rahardjo (1993) caution that failures of these sensors have been experienced. These failures can be attributed to two main causes. Fredlund and Rahardjo (1993) note that these sensors have a continual problem with the porous blocks being too fragile. The second cause of failure is due to the failure of the electronics, especially when subjected to positive pore

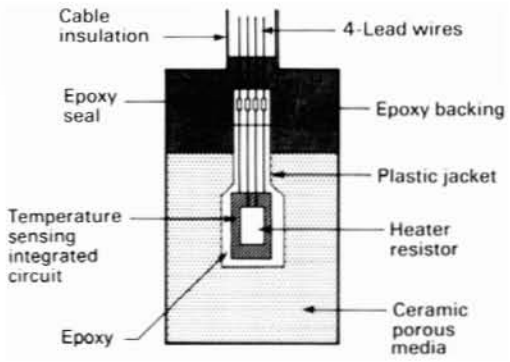

Figure 2.16 - Cross section of a thermal conductivity sensor (Fredlund and Rahardjo, 1993)

water pressures. Therefore, while the thermal conductivity sensor could be used to monitor waste rock piles, the longevity of these sensors would be questionable.

2.4.2 Pore Water Samplers

The following discussion of pore water samplers has been limited to include only the most common pore water samplers. Destructive testing techniques such as pore fluid squeezers or centrifuging have not been investigated, and do not offer a method of continually monitoring pore water samples. The following unsaturated pore water samplers have been considered in this section:

- Pan Lysimeters
- Vacuum Lysimeters
- Gravity Lysimeters

2.4.2.1 Pan Lysimeters

Pan lysimeters represent one of the most often used methods in agricultural applications of collecting a pore water sample. Unfortunately, as discussed in previous sections this type of lysimeter has a basic design flaw. The use of pan lysimeters distorts the flow path by creating an artificial water table above the lysimeter. For deep applications in waste rock piles this method would not be considered viable, due to the requirement of having an access tunnel to monitor and collect samples from the pan lysimeter. The requirement of the access tunnel for installation would also further disrupt the flow path.

2.4.2.2 Vacuum Lysimeters

Vacuum lysimeters have the same basic design as tensiometers. Instead of measuring suction, an air vacuum is applied to the small bore tube described by Fredlund and Rahardjo (1993). This creates a gradient towards the vacuum lysimeters causing pore water to flow through the porous section media and into the vacuum lysimeter. Wilson (1994) performed a review of in-situ pore liquid samplers used to characterize the unsaturated zone. This review demonstrated that vacuum lysimeters could be installed at depth to sample pore fluids. Wilson also addressed the concerns of using different types of porous media as the interface with the soils.

Wilson (1994) identified three different vacuum lysimeter designs. The designs are different with respect to the "plumbing" that is required to bring a pore water sample to the surface. Figure 2.17 displays the three different types of vacuum lysimeters.

The depth of the installation for the single chamber vacuum lysimeter (shown in Figure 2.17 a) is limited to either the air entry value of the porous media or the maximum suction that can be applied before water begins to cavitate. If the vacuum applied to the lysimeter exceeds the air entry value of the porous media, air will enter the body of the lysimeter and release the vacuum, thus a pore water sample cannot be collected.

In the single chamber pressure vacuum lysimeter (shown in Figure 2.17 b) the depth of installation is limited only by the air entry value of the porous media. In this system, the pore water sample is forced out of the lysimeter by means of air pressure. Once the air entry value of the porous media is exceeded by the pressure applied to remove the sample, the sample is forced out of the porous media. Therefore, it becomes difficult if not impossible to collect a sample.

An improvement on the single chamber pressure vacuum lysimeter is the dual chamber pressure vacuum lysimeter. This system isolates the porous media from the pressure applied to remove the sample by means of a one way flow valve. Theoretically, this

system could be used at any depth. Figure 2.17 shows the internal details of the dual chamber lysimeter.

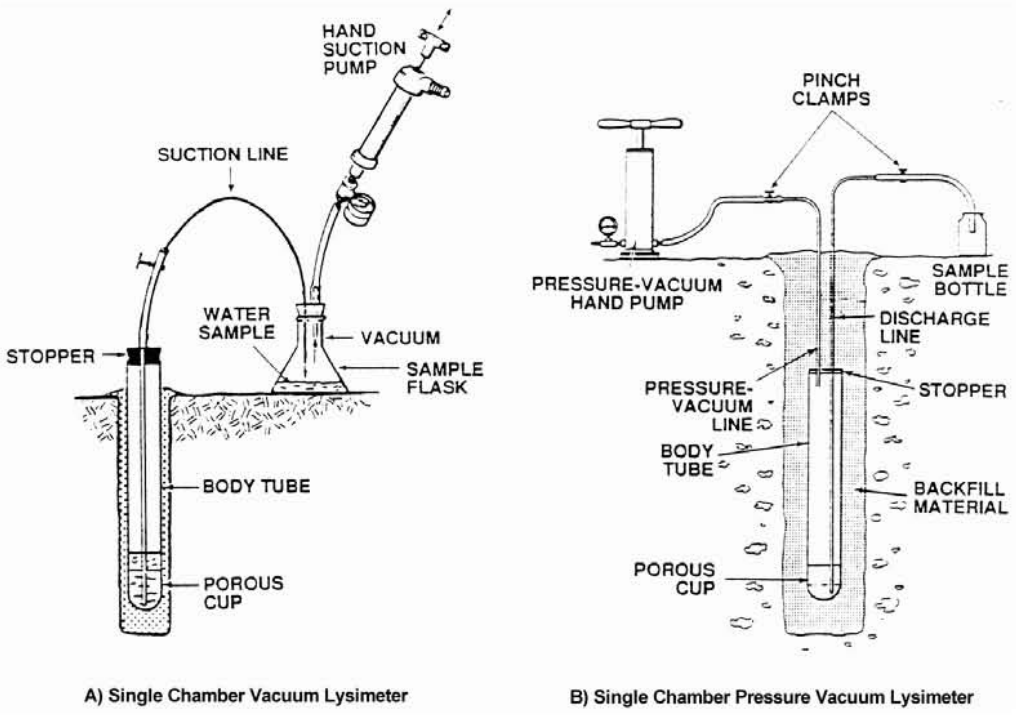

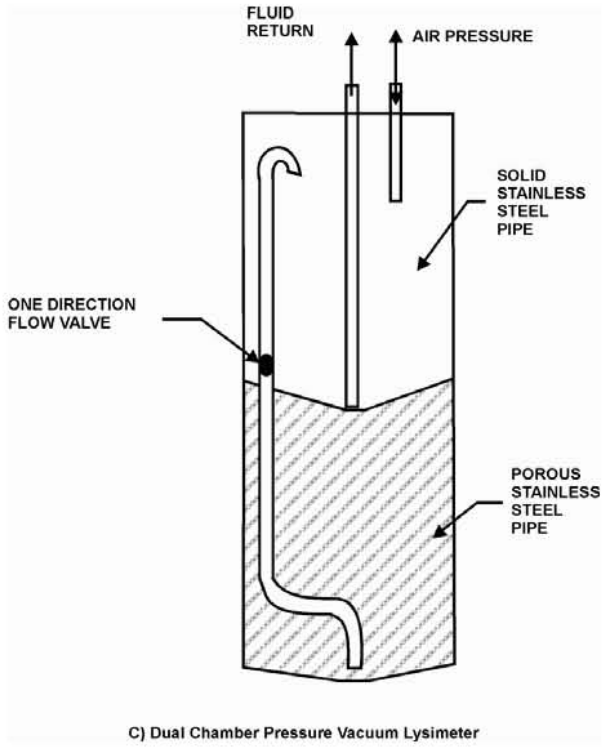

Figure 2.17 - Different types of vacuum lysimeter ((a) Wilson, 1994; (b)Wilson, 1994; (c) After Wilson, 1994)

Wilson (1994) compiled the maximum operating depths of the three different vacuum lysimeters for different types of porous media. The results of this compilation are shown in Table 2.3. From this table it can be seen that the maximum depths for the single chamber units are largely a function their respective air entry values.

Table 2.3 - Maximum sampling depths (After Wilson 1994)

Sampler Type	Porous Section Material	Maximum Pore Diameter (μm)	Air Entry Value (kPa)	HB HL	Operational Suction Range (kPa)	Maximum Recommended Depth (m)
Single Chamber Vacuum Lysimeters	Ceramic	1.1 - 2.1	>100	HL	< 60 - 80	< 2
	PTFE	25 - 35	7 - 20	HB	< 7 - 20	< 2
	Stainless Steel	6 - 14	20 - 50	HL	< 20 - 50	< 2
	Quartz	6 - 7	40 - 50	HL	< 40 - 50	< 2
Single Chamber Pressure Vacuum Lysimeter	Ceramic	1.1 - 2.1	>100	HL	< 60 - 80	< 15
	PTFE	25 - 35	7 - 20	HB	< 7 - 20	< 2
	Stainless Steel	6 - 14	20 - 50	HL	< 20 - 50	< 15
	Quartz	6 - 7	40 - 50	HL	< 40 - 50	< 15
Dual Chamber Pressure Vacuum Lysimeters	Ceramic	1.1 - 2.1	>100	HL	< 60 - 80	Unlimited
	PTFE	25 - 35	7 - 20	HB	< 7 - 20	Unlimited
	Stainless Steel	6 - 14	20 - 50	HL	< 20 - 50	Unlimited
	Quartz	6 - 7	40 - 50	HL	< 40 - 50	Unlimited

Notes: HB = Hydrophobic PTFE = Polytetrafluoroethylene
HL = Hydrophillic

Wilson (1994) also addressed a large concern of many people who use vacuum lysimeters. What is the effect of passing the sample through the porous media? Wilson (1994) explained that the choice of porous media should be a function of the expected contaminants to be measured. For metal analysis, McGuire et al. (1992) concluded that the general pattern of metal adsorption onto samplers generally followed the following pattern:

Ceramic > Stainless Steel >> Fritted Glass = Polytetrafluoroethylene (PTFE)

Wilson (1994) compiled the results of numerous studies as shown in Table 2.4 that describe the interactions of porous materials with various metals and compounds. Wilson (1994) cautions that this is far from a complete compilation, but represents

research that has been undertaken to date for porous materials. The numbers in parenthesis in the table refer to the particular study that made the recommendation. Please see the Handbook of Vadose Zone Characterization & Monitoring (Wilson 1994) for further information regarding these references.

2.4.2.3 Gravity Lysimeters

Gravity lysimeters have occasionally been used to collect pore water samples. These lysimeters generally try to measure infiltration. To correctly measure the infiltration rate it is desirable to collect a sample at a rate equal to the flux of the system. For very high fluxes a pore water sample can be collected, however, at low fluxes it may take years to collect a pore water sample. As a result of slow collection rates, gravity lysimeters have not traditionally been used to collect pore water samples.

Table 2.4 - Porous material interactions (after Wilson, 1994)

	Material Absorbs Species	Material Desorbs or Releases Species	Material Screens Species	No Significant Interaction	No Interaction
Al		C(2,30)		C(16,27)	
Alkalinity				SF(11)	
Ca	C(20,28)	C(1,2,18) PTFE (26)		C(3,6,10,11,25) PTFE (3) FG(18,22)	PTFE(13)
C		FG(22)			
CO_3		C(2)			
HCO_3		C(2)			
Cd	C(9,11,29) SS(29) SF(29)			C(3) PTFE(3,29)	
Cl				C(11,25) SF(11)	PTFE(13)
Co	C(29) SS(29) PTFE (29) FG(29) SF(29)				
Cr	C(19) SS(29) PTFE (29) FG(29) SF(29)	C(3) PTFE (3)			
Cu	C(9,11)	C(3) PTFE(3)			
Fe	C(11)	PTFE(3,26)		C(3,25)	PTFE(13)
H				SF(11)	
K	C(5,6,15,28)	C(18)		C(1,25) FG(18,22)	
Mg	C(6,28)	C(2,3,11,18) PTFE(26)		C(10,25) PTFE(3) FG(18,22)	PTFE(13)
Mn	C(11)			C(3,9) PTFE(3)	PTFE(13)
Na	C(6,20)	C(2,18,28) FG(18,22) PTFE(26)		C(1,11,25)	PTFE(13)
NH_4	C(4,12,15)			PTFE(4)	
N		FG(22)			
NO_2				C(4,5) PTFE(4)	
$(NO_2 + NO_3)$–N				C(5)	
P	C(1,5,8, 15,18)			FG(18)	

Table 2.4 - Porous material interactions (after Wilson, 1994) cont…

	Material Absorbs Species	Material Desorbs or Releases Species	Material Screens Species	No Significant Interaction	No Interaction
PO_4	C(4,5,7)			PTFE(4)	
PO_4-P				C(10)	
Pb	C(9)				PTFE(13)
SiO_2		C(2)			
Si		PTFE(26)		C(4) PTFE(4)	
SO_4				C(11)	
Sr		C(11)			
Zn	C(9)	C(11,29) SS(29) FG(29) SF(29)		PTFE(29)	PTFE(13)
High Molecular Weight Compounds			C(17,21)		
4-Nitro-phenol	PTFE (23)				
Chlorinated Hydrocarbons	PTFE(23,24)				
Diethyl-phthalate					PTFE(23)
Naphthalene	PTFE(23)				
Acenaphthene	PTFE(23)				
BTX	PTFE(30)				SS(30)
Bacteria	C(31)				
Virus	C(32)				SS(32)

[a]Comparisons of materials based on this table should be made cautiously. Differing experimental techniques should be considered as a source of differing conclusions. Undocumented factors often include material age and sampling history.
[b]Valence states are often not reported in studies.
[c]Abbreviations:
1. C = porous ceramic
2. PTFE = porous PTFE
3. FG = fritted glass
4. SS = porous stainless steel
5. SF = silica flour

[d]Numbers in parentheses refer to references in Table 26.4.

CHAPTER 3 THEORY

3.1 Introduction

This chapter presents the theory that is essential to an understanding of the design and operation of the prototype lysimeter. The chapter begins by discussing the nature of flow processes in soils. This is followed by a discussion of soil-water characteristic curves and hydraulic conductivity functions as they relate to unsaturated soils. A review of suction profiles that develop in unsaturated soils is then presented. Finally, preferential flow in unsaturated soils is discussed. A detailed development of soil suction in unsaturated soil mechanics is available in Fredlund and Rahardjo (1993)

3.2 Liquid Water Flow Through Porous Media - Darcy's Law

Darcy's Law is named after the French engineer who discovered the relationship between hydraulic gradient and flowrate. Freeze and Cherry (1979) expressed this relationship as:

$$Q = -k\frac{dh}{dl}A \quad \text{..... Eq. 3-1}$$

Where: Q = discharge (m^3/s)

k = hydraulic conductivity (m/s)

$\frac{dh}{dl}$ = hydraulic gradient (unitless)

h = hydraulic head (m)

l = sample length (m)

A = cross sectional area (m^2)

This equation holds true for both saturated and unsaturated soil. In saturated soils the hydraulic conductivity is a constant value which is dependent primarily on the void ratio of the soil (Fredlund and Rahardjo, 1993). However, in unsaturated soils the hydraulic conductivity (k) is not a constant, but a nonlinear function that is dependant on both void ratio and the degree of saturation (Fredlund and Rahardjo, 1993). Given that the void ratio of a given soil is relatively constant, the hydraulic conductivity of unsaturated soils thus becomes a function of the degree of saturation.

It is common to express the volume of water stored in an unsaturated soil in terms of the volumetric water content. The relationship between the degree of saturation and volumetric water content is as follows:

$$\theta_w = Sn \quad \text{..... Eq. 3-2}$$

Where: θ_w = volumetric water content

S = degree of saturation

n = porosity

The relationship between volumetric water content (degree of saturation) and hydraulic conductivity will be explored in more detail in the next section.

3.3 Soil-Water Characteristic Curves and Hydraulic Conductivity Functions

As noted in the previous section the hydraulic conductivity of an unsaturated soil is related to its volumetric water content. This phenomenon can be explained using two fundamental graphs, the soil-water characteristic curve and the hydraulic conductivity function.

3.3.1 Soil-Water Characteristic Curves

The soil-water characteristic curve can be defined as the relationship between the volumetric water content of the soil and soil suction. Stoicescu (1997) also notes that the curve may be defined as a storage function. Figure 3.1 shows a typical soil-water characteristic curve.

Figure 3.1 - A soil-water characteristic curve (after Stoicescu, 1997)

From this graphical representation of a soil-water characteristic curve it can be seen that there are three distinct stages. They are the pre-air entry stage, the transition stage, and the residual stage. It should also be noted that there is hysteresis between the drying curve and the wetting curve. Most researchers almost exclusively use the drying curve. Stoicescu (1997) provides a more detailed description of the cause and effects of hysteresis. Figure 3.1 also illustrates a graphical method to determine two very important points on the soil-water characteristic curve (Fredlund and Xing, 1994); the air entry value and the residual water content.

The pre-air entry stage corresponds to soil suctions that are too small to overcome the capillary forces holding the water within the largest pores in the soil. As a result the soil does not drain, and the volumetric water content stays constant. As the suction approaches the air entry value, the largest pores begin to drain and air is allowed to enter the soil structure. During the transition phase, pores of decreasing size are drained, as the suction becomes greater than the capillary forces in the soil. Finally, the residual

stage is characterized by a very slow decrease in volumetric water content with increasing suctions as the water phase becomes discontinuous.

Figure 3.2 displays typical soil-water characteristic curves for a variety of soils. As might be expected, as the soil type becomes finer, the air entry value occurs at larger suction values.

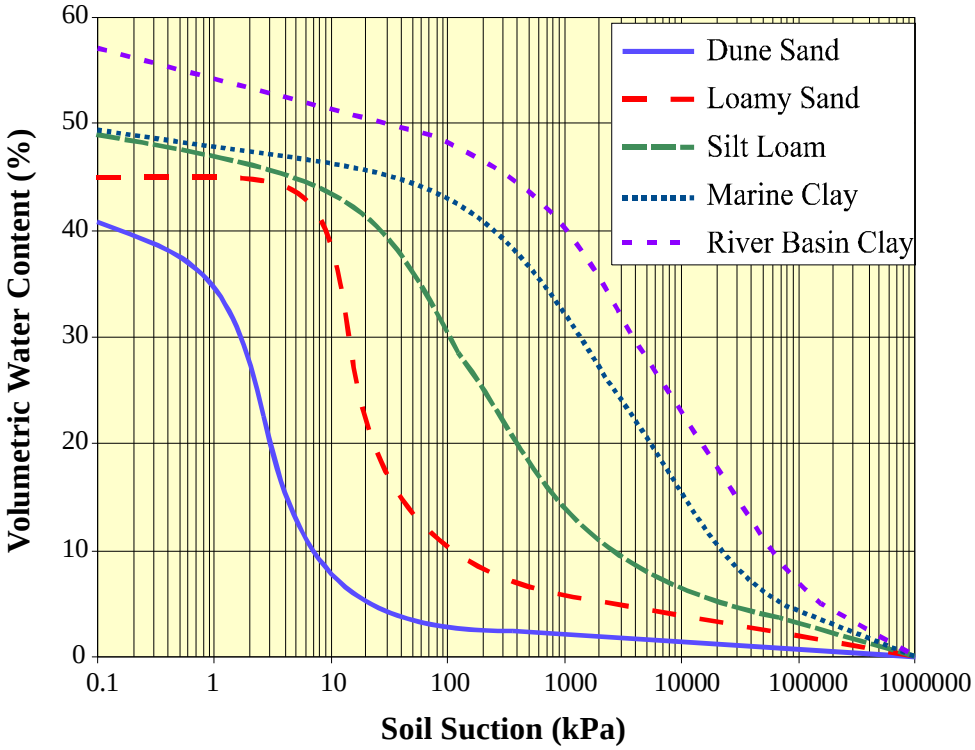

Figure 3.2 - Soil-water characteristic curves (after Koorevaar et al., 1983)

3.3.2 Hydraulic Conductivity Functions

As the soil desaturates the hydraulic conductivity of the soil also decreases. Fredlund and Rahardjo (1993) explain this decrease in hydraulic conductivity in the following quote:

"As a soil becomes unsaturated, air first replaces some of the water in the large pores, and this causes the water to flow through the smaller pores with an increased tortuosity to the flow path"

Figure 3.3 displays the effect of desaturation on the flowpaths available for flow. It can readily be seen that once the soil becomes unsaturated the area available for water flow is reduced. In addition the tortuosity of the flow path increases. These two effects combine to reduce the hydraulic conductivity of the soil as the level of saturation or volumetric water content decreases.

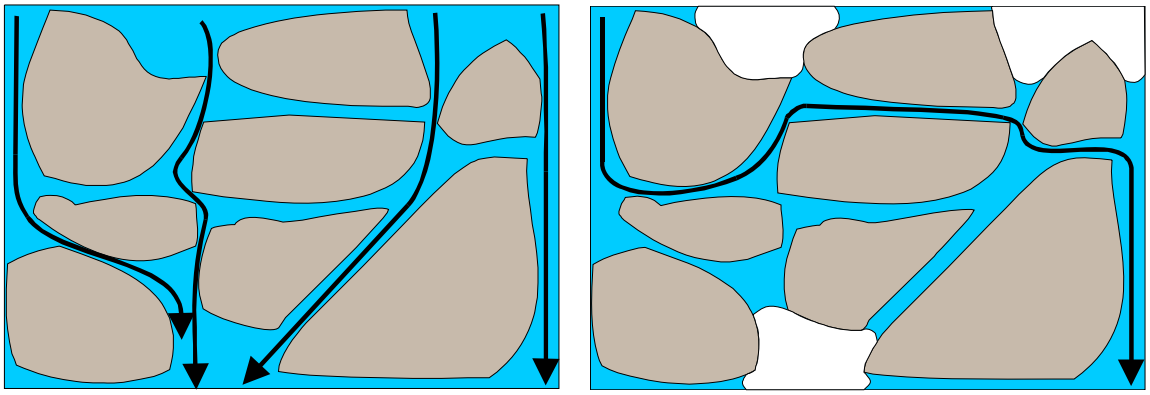

a) Flow paths in a Saturated Soil b) Flow paths in an Unsaturated Soil

Figure 3.3 - Effect of desaturation on hydraulic conductivity

Measurement of the hydraulic conductivity of an unsaturated soil is seldom performed because it requires a long time to perform the test. It is much more common to test the saturated hydraulic conductivity and estimate the unsaturated hydraulic conductivity using a formula that relies upon the shape of the soil-water characteristic curve.

The hydraulic conductivity remains at the saturated hydraulic conductivity during the pre air entry stage, as shown in Figure 3.4, as all of the water pathways remain saturated and are available for flow. In the transition stage the hydraulic conductivity drops rapidly as the soil becomes drier and the area available for flow decreases and the tortuosity increases. In the residual phase the hydraulic conductivity continues to decrease as the remaining flowpaths available slowly decrease.

There have been a number of formulas developed that are either theoretical in nature such as Fredlund and Xing (1994) or empirically based such as Brooks and Corey (1964) by which the unsaturated hydraulic conductivity curve can be estimated.

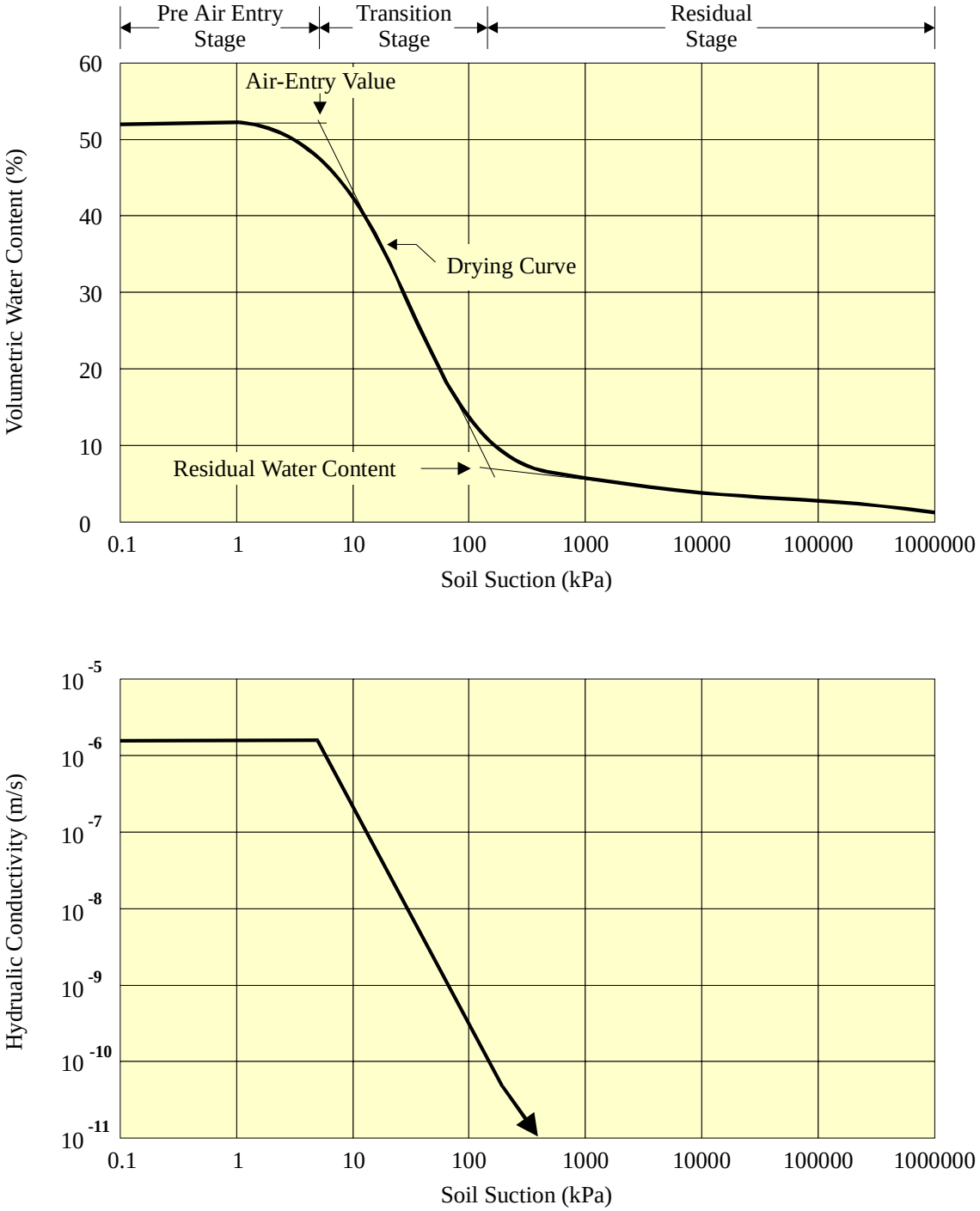

Figure 3.4 - Soil-water characteristic curve and hydraulic conductivity function

3.4 Pressure Profiles in Unsaturated Soils

In the late 1950's an Israeli researcher named Kisch (1959) proposed the following formulation to solve for the pressure profiles which might develop in unsaturated soils. This formulation assumed that Darcy's law is valid for both saturated and unsaturated soils and that the hydraulic conductivity is a function of volumetric water content or pressure head. Darcy's law can be written as shown below:

$$q = -k\frac{dh}{dz} \quad \text{.....Eq. 3-3}$$

Where: q = discharge per unit area (m^3/m^2s)

k = hydraulic conductivity (m/s)

h = hydraulic head (m)

z = elevation (m)

However, the hydraulic head can also be expressed as the sum of elevation head and pressure head as shown below:

$$h = p + z \quad \text{..... Eq. 3-4}$$

Where: h = Hydraulic Head (m)

p = Pressure Head (m)

z = Elevation head (m)

For steady state flow conditions, the above equations can be combined to form the following equation:

$$dz = \frac{dp}{\left(q/k + 1\right)} \quad \text{..... Eq. 3-5}$$

A pressure profile can then be calculated at a given flux (q) by starting at a known pressure and elevation (ie. water table, p = 0) and working upwards in small increments of pressure (dp). As mentioned previously, the hydraulic conductivity is a function of

volumetric water content (or suction). Therefore, this analysis requires that the hydraulic conductivity function for the given soil be known.

This formulation has proven effective for pressure profiles that remain at suctions less than the residual water content of the soil. However, as the suctions increase past the residual water content of the soil the suctions that are calculated may not be reflected in suctions measurements made in the soil. Barbour (1993) showed that tensiometers subjected to hydrostatic conditions greater than their residual suction moved very slowly towards the equilibrium condition. Barbour (1993) explained that this was due to the very low hydraulic conductivity of the material when near its residual value, preventing the drainage required to move the soil past the residual suction. Barbour also noted that this is not an equilibrium condition, but that these pressures may persist for long periods of time in the absence of other mechanisms of moisture movement such as vapour flow.

3.5 Preferential Flow in Unsaturated Soils

In saturated systems, it is intuitive that coarse soils allow higher flow rates. However, in unsaturated systems the opposite can be true, coarse soils can be a barrier to flow and fine soils become the conduit for flow. As described previously as soils desaturate their hydraulic conductivity decreases (See Figure 3.3).

This phenomenon can be explained using the hydraulic conductivity function for both coarse and fine materials as shown in Figure 3.5. At flux rates greater than 10^{-7} m/s the hydraulic conductivity of the coarse material remains high and the majority of the water will flow through coarse material. However, at a flux rate of 10^{-8} it can be seen that the hydraulic conductivity of the fine material is much greater than that of the coarse material. As a result, the majority of the flow would be directed through the fine soil layer.

Newman (1999) undertook a study of preferential flow within vertically layered unsaturated systems. The results of her testing showed that at flux rates slightly greater than the saturated hydraulic conductivity of the fine material, flow was shared between

the coarse and fine material. As flux rates were decreased below the saturated hydraulic conductivity of the fine material, the majority of the flow occurred in the fine material.

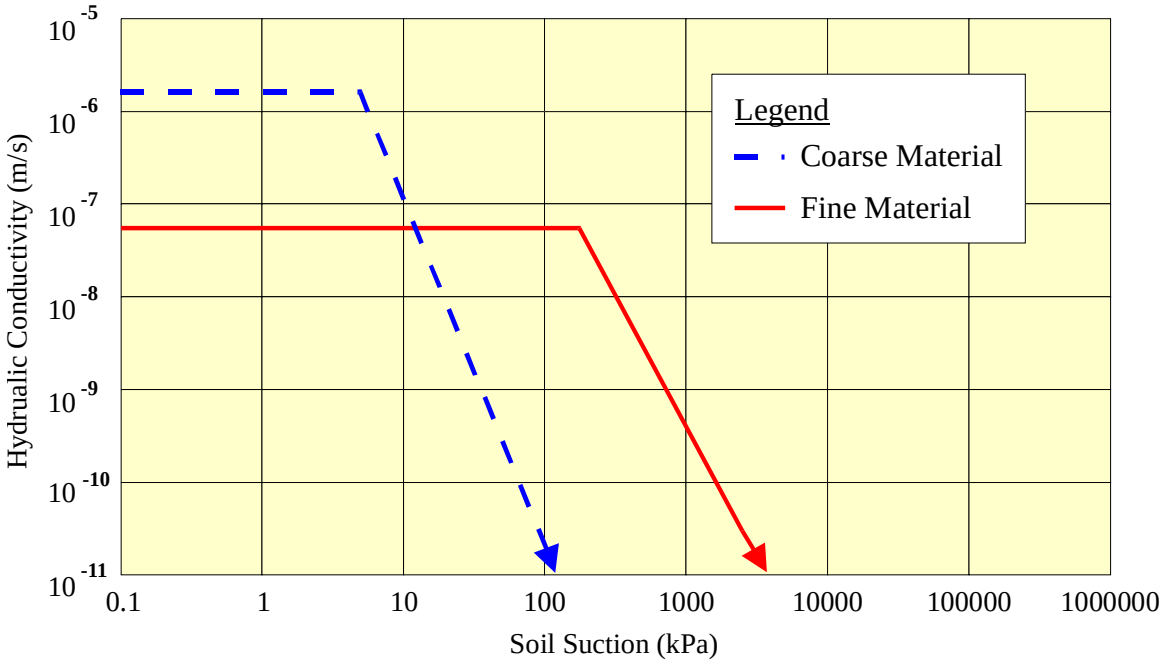

Figure 3.5 - Hydraulic conductivity functions for fine and coarse materials

CHAPTER 4 STANDPIPE LYSIMETER DESIGN

4.1 Introduction

The key design elements and assumptions considered in the design of the standpipe lysimeter to measure suction and collect a pore water sample are reviewed in this chapter. The chapter begins with a review of the operating principles and assumptions made in the preliminary design phase. The following section will deal with refinements to the design as a result of preliminary numerical modelling. The chapter concludes by presenting the final standpipe lysimeter design.

4.2 Operating Principles and Preliminary Lysimeter Design

The standpipe lysimeter has two principle functions; the first is to measure soil suction, the second is to collect a pore water sample. The operating procedures and design considerations relating to these functions will be discussed in the following subsections.

4.2.1 Soil Suction Measurement

The principle of operation of the lysimeter can be explained using a siphon hose as an analogy. Figure 4.1 illustrates the similarities between a siphon hose and the standpipe lysimeter. As can be seen in this illustration, the water within the barrel will drain until the hydraulic head within the barrel is equal to the hydraulic head of the outlet. In comparison, the water table within the lysimeter will also be drawn down to a level that corresponds to the hydraulic head in the surrounding soil, the difference is that the hose in the lysimeter is an interconnected water phase. The elevation head at the top of the lysimeter is the same as the elevation head of the surrounding waste rock. The drawdown in the lysimeter is a measure then of the negative water pressure (suction)

within the waste rock. If the pressure outside of the lysimeter increases, the interconnected water phase will draw water back into the lysimeter until the system comes into equilibrium. Therefore, the amount of drawdown in the lysimeter is a measure of the suction in the waste rock.

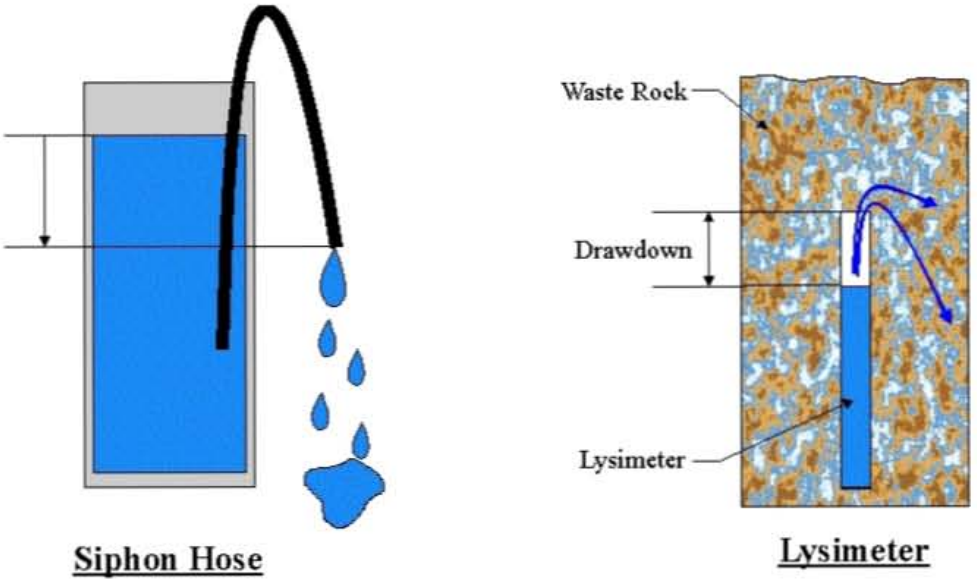

Figure 4.1 - Siphon hose analogy of standpipe lysimeter

Bews (1997b) showed that under steady state conditions (Figure 2.11), the suction within the saturated zone near the water table increases approximately hydrostatically. Therefore, the suction in the waste rock can be calculated by:

Suction (kPa) = Drawdown of the lysimeter (m) * 9.80 (kPa / m_$H_2$0)..... Eq. 4-1

In Section 3.4 of this thesis, it was noted that Barbour (1993) indicated that the hydrostatic condition was difficult to attain when the hydrostatic suctions required in the material are greater than the suction of the material at or near its residual water content. This is due to the very low hydraulic conductivity of the material, as it approaches its residual water content. As a result, the material chosen as the backfill material for the standpipe lysimeter should remain well above its residual water content.

The standpipe lysimeter operates in a manner similar to that of a gravity lysimeter, with a few notable exceptions. In a gravity lysimeter, the objective is to collect a representative flux rate from the system. In contrast, the standpipe lysimeter should maximize flow into the lysimeter and take advantage of the backfill material properties such that the water table within the lysimeter can change quickly. Wickland (1998) suggests that using a material that is finer than the surrounding waste rock will maximize the amount of water entering the lysimeter. The time for the water table to rise or fall can be minimized by using a material that has an air entry value that is higher than the expected range of soil suctions. In this manner, the water level within the standpipe lysimeter will change quickly, since only small volumes of water have to enter or leave the lysimeter to change the water level.

The height of the walls of the lysimeter must correspond to the design criteria as described in Section 2.3.2.1 of this thesis. The diameter of the lysimeter body should be as small as possible to increase edge effects as described in Section 2.3.2.3 of this thesis.

4.2.2 Collection of a Pore Water Sample

Once a water table condition has been established within the lysimeter, the process of collecting a pore water sample is as simple as lowering the water table in the lysimeter by draining the base. This creates a gradient towards the lysimeter and the surrounding pore water is drawn into the lysimeter. Figure 4.2 displays a representation of lysimeter drainage for a field installation along with the pressure contours generated by a numerical model.

To effectively collect a pore water sample at the low flux rates expected for waste rock piles in Northern Saskatchewan, typically 1E-8 to 1E-10 m/s, the lysimeter must be able to maximize flow into the lysimeter. This can be accomplished by choosing a backfill material that becomes a preferential flow path during the drainage phase. This can be accomplished by choosing a lysimeter backfill material that has a higher hydraulic conductivity than that of the waste rock over the given flux ranges. This implies that the backfill material should remain saturated over the entire range of anticipated suctions.

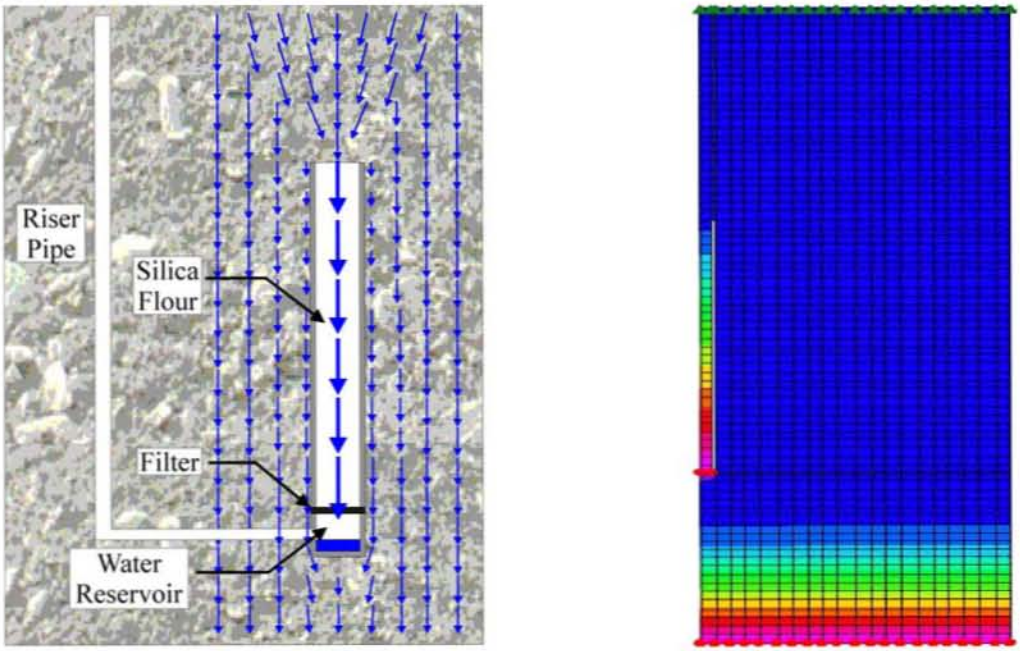

Figure 4.2 - Collection of a pore water sample by lysimeter drainage

Thus, the backfill material should have an air entry value higher than the expected suctions in the waste rock. Ideally, the backfill material should also have a high saturated hydraulic conductivity. Therefore, the design of the lysimeter backfill material lies in striking a balance between a high saturated hydraulic conductivity and a sufficiently high air entry value.

Another concern associated with the collection of a pore water sample is the length of time required to "flush" the lysimeter in order to collect a sample which reflects the water chemistry within the waste rock at the top of the lysimeter. Choosing a material that has a high hydraulic conductivity and a low void ratio can minimize the time required to collect a pore water sample. Again, this requirement must be balanced with the need for a high air entry value.

4.3 Preliminary Numerical Modelling

A numerical modelling study was undertaken to verify the key parameters in the design of the prototype lysimeter. This section will begin by introducing the numerical model and discussing the physical layout, grid spacing, material properties and boundary

conditions that were used in the simulations. A discussion of the results and a summary of the key findings of the numerical modelling will then follow.

4.3.1 Numerical Model

The computer software used was Seep/W ver. 4.05 produced by Geo-Slope International Ltd. Seep/W is a finite element groundwater model that is capable of handling seepage in both saturated and unsaturated soil . Seep/W is also capable of modelling both steady state and transient cases. The model was run as an axisymmetric analysis. An axisymmetric analysis can be used to simulate three-dimensional problems with symmetry about a vertical axis of rotation.

4.3.2 Layout and Modelling Considerations

The layout of the model consisted of a 4 m wide column of waste rock. Inspection of pressure contours generated by the model showed that at this width the pressure contours at the edge of the model opposite the lysimeter were unaffected by the presence of the lysimeter. The lysimeter was modelled at the center of the waste rock column. The thickness of the lysimeter walls in all simulations was 0.025 m. The lysimeters modelled were all 3.0 m in height, although some models had a 0.5 m extension of silica flour into the waste rock. The bottom of the lysimeter was placed 2 m above the bottom of the waste rock so that the flow around the lysimeter could be investigated and the pressure profile within the waste rock could be established. The top of the lysimeter was arbitrarily placed at 2.5 m below the ground surface. Figure 4.3 illustrates the dimensions of the numerical model.

The grid spacing for the model was set at a maximum of 0.1 m. The model was run at a number of different grid spacings to determine which was the most efficient spacing. The data from each run was compared. The results of the model were consistent for spacings of 0.1 m or less.

The convergence parameters for the model were set to produce consistent results in the steady state models in 200 to 300 iterations. The model convergence parameters were set as follows:

- Tolerance (%) = .001
- Hydraulic Conductivity Maximum Change = 1 Order of Magnitude
- Hydraulic Conductivity Rate of Change = 1.05 Order of Magnitude
- Hydraulic Conductivity Minimum Change = 1E-9 Order of Magnitude

4.3.3 Preliminary Modelling Program

The preliminary modelling program conducted as part of this thesis was an extension of work performed by Brenda Bews (1997) of the Unsaturated Soils Group at the University of Saskatchewan. The modelling program consisted of varying the following parameters:

- Fluxes on the system
- The inclusion or exclusion of a 0.5 m silica flour extension above the lysimeter into the waste rock
- The diameter of the lysimeter
- Widening the diameter of the lysimeter near the top of the lysimeter to increase its area of contact
- Changing the hydraulic conductivity of the waste rock and silica flour used in the simulations.

A number of different fluxes were applied to the top of the waste rock column. The fluxes investigated in the modelling program were: 1E-6 $m^3/m^2 \cdot s$, 1E-7 $m^3/m^2 \cdot s$, 1E-8 $m^3/m^2 \cdot s$, 1E-9 $m^3/m^2 \cdot s$ and 1E-10 $m^3/m^2 \cdot s$. By varying the applied flux, the suction within the waste rock column varied, thus the response of the lysimeter at different suction values could be investigated.

The standpipe lysimeter was designed to take advantage of preferential flow through the lysimeter backfill material at low fluxes. To increase the area of contact of the lysimeter

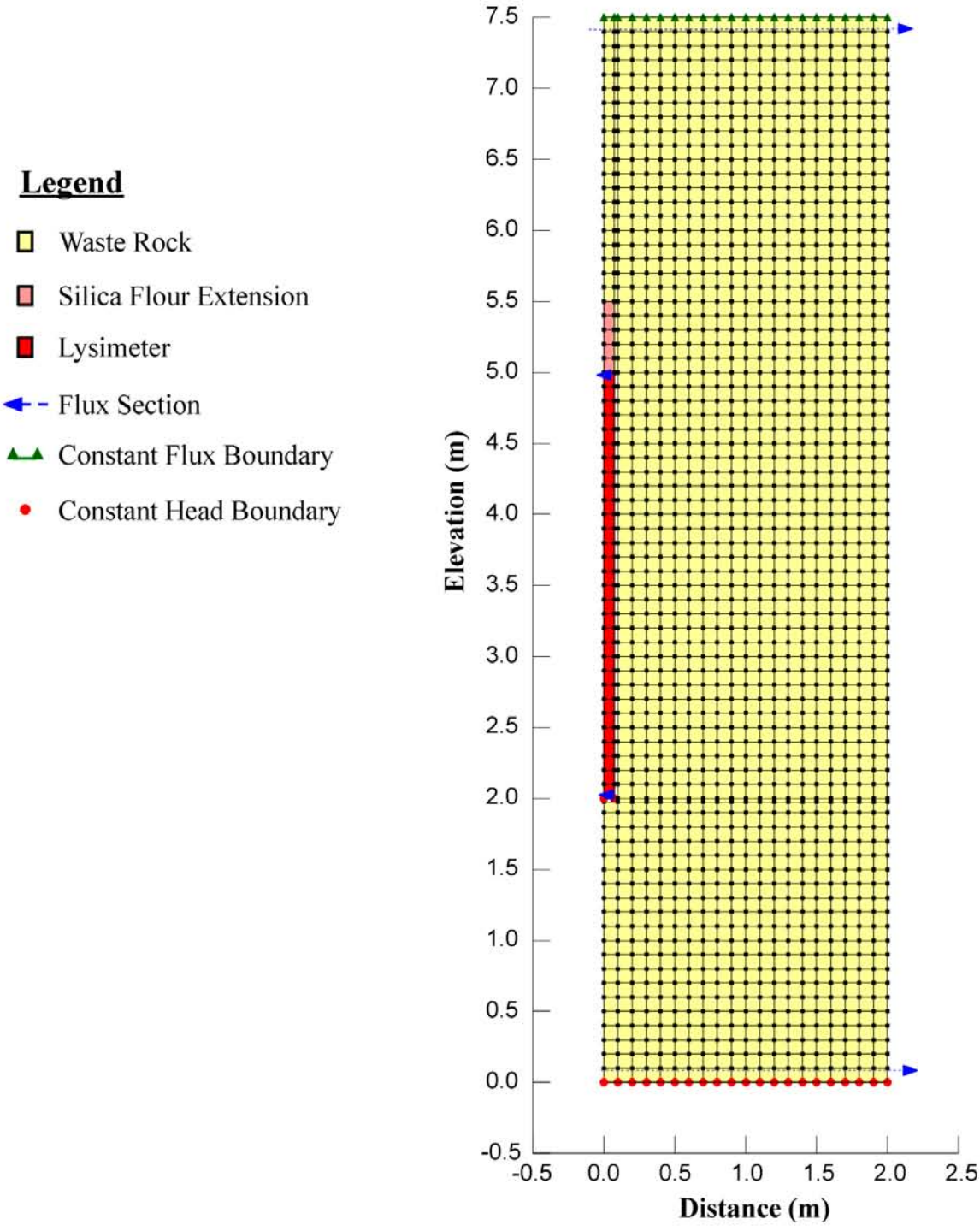

Figure 4.3 - Layout of numerical model

backfill and promote flow into the lysimeter, most of the models incorporated a 0.5 m extension of the silica flour above the lysimeter. The effect of removing the silica flour extension was also investigated.

A variety of different diameters of the lysimeter were modelled. The diameters chosen were 5 cm, 10 cm and 15 cm. These diameters were chosen because they represent readily available material sizes to construct the lysimeter body such that the lysimeter could be installed within a drill hole. The 15 cm diameter was considered the upper limit based on this latter restriction. Modelling of the diameter of the lysimeter allowed the response time of the lysimeter for different sizes to be investigated. Additionally, the time to collect a pore water sample with different diameter lysimeters could also be investigated.

The effect of using a "bell" shape near the top of the lysimeter was also modelled. This involved modelling of the 5 cm lysimeter with a 10 cm and 15 cm top. This modelling investigated the possibility of increasing the flux into the lysimeter by increasing the area at the top, while maintaining a small pore volume throughout the rest of the lysimeter. This could potentially decrease the amount of time required to flush the lysimeter.

The soil-water characteristic curve and hydraulic conductivity function for the materials used in the model are shown in Figure 4.4. The saturated hydraulic conductivity of the waste rock material was varied from 1E-3 m/s to 1E-6 m/s in order of magnitude intervals. This affects the waste rock material by shifting the hydraulic conductivity function vertically up or down. The saturated hydraulic conductivity of the silica flour was also varied from 1E-6 m/s to 1E-8 m/s in order of magnitude intervals. This property was modelled to examine the relationship between flux into the lysimeter as a function of the difference in hydraulic conductivities between the waste rock and the silica flour. The response of the lysimeter using different values of hydraulic conductivity for the saturated silica flour was also investigated to determine the sensitivity of the system to this parameter.

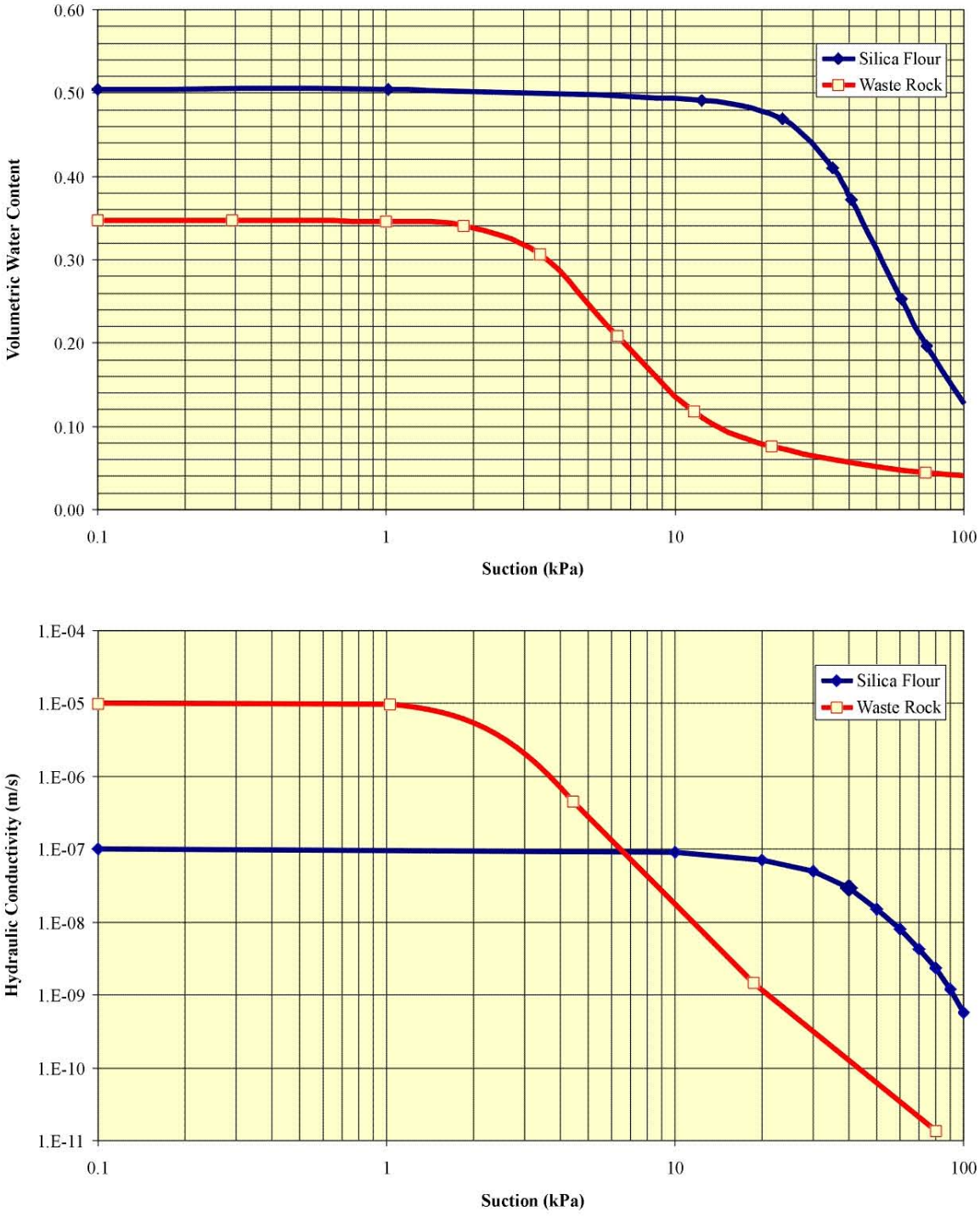

Figure 4.4 - Material properties used in preliminary modelling

Three different models were used to characterize the response of the system. The three different models are as follows:

- Steady State - Suction Measurement
- Steady State - Drainage
- Transient Modelling from Steady State - Drainage to Steady State - Suction Measurement

The steady state - suction measurement model utilized a constant flux boundary on the top of the waste rock and a constant head (H=0) boundary condition at the base of the waste rock column. The bottom of the lysimeter had a flux equals zero boundary condition. In this model, the location of the water table inside the lysimeter could be determined by recording the pressure head at the bottom of lysimeter. The suction within the waste rock outside the lysimeter was calculated based on the assumption of hydrostatic conditions within the silica flour using Equation 4.1. This suction value was then compared to soil suction calculated by the model at the outside edge of the waste rock column (at the same elevation as the top of the lysimeter). The suction error was calculated using the following formula:

$$\text{Suction Error (\%)} = \frac{S_{OC} - S_L}{S_{OC}} \text{ x } 100 \quad \text{..... Eq. 4-2}$$

Where: S_{OC} = Suction at the outside of the column (kPa)

S_L = Suction measured in the lysimeter (kPa)

The steady state - drainage model was identical to the steady state - suction measurement model with the exception that at the bottom of the lysimeter a constant head (H(P=0)) boundary was imposed. The flux into the lysimeter was obtained from a flux section drawn near the top of the lysimeter. A new term called the equivalent collection area ratio was defined to quantify the flow of water into the lysimeter as a function of the applied flux rate. Figure 4.5 displays the definition of the equivalent collection area ratio.

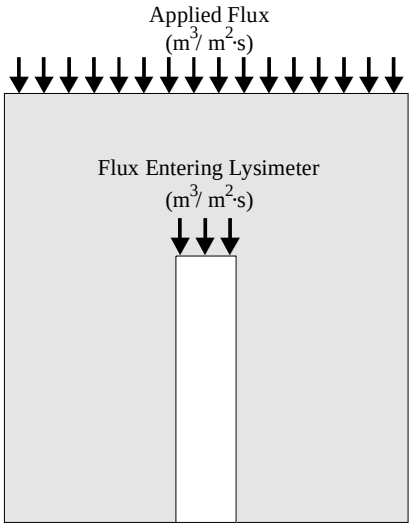

Definition of
Equivalent Collection Area Ratio (ECAR)

$$ECAR = \frac{\text{Flux Entering Lysimeter } (m^3/m^2 \cdot s)}{\text{Applied Flux } (m^3/m^2 \cdot s)}$$

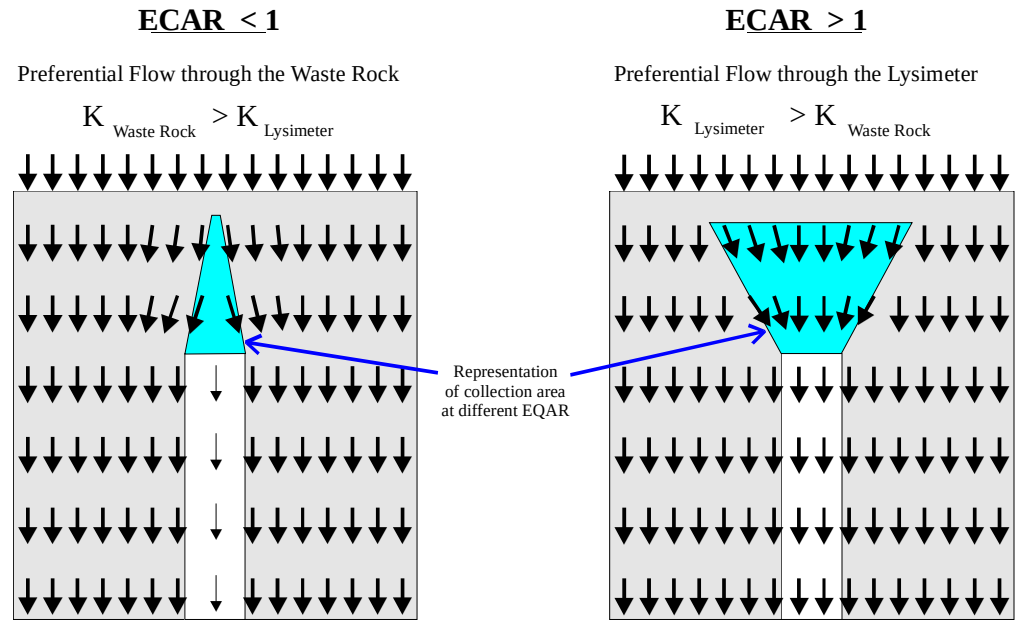

Figure 4.5 - Definition of equivalent collection area ratio

The equivalent collection area ratio was calculated from a steady state - drainage model. In addition, the amount of time required to flush the lysimeter was calculated based on the flux rate going into the lysimeter and the porosity of the lysimeter backfill. The porosity of the lysimeter backfill was assumed to be 0.45 for all cases.

The time for the transition from the steady state - drainage condition to the steady state - suction measurement condition was simulated using a transient model. In this model, the time required to fill the lysimeter until it registered the proper suction from the drained condition was examined. Theoretically, it takes an infinite amount of time to come to equilibrium. Therefore, in order to assess the response time of the lysimeter an equilibrium condition was defined. For this modelling program, the lysimeter was considered to be at equilibrium if the change in the height of the water table within the lysimeter was less than 5.0 mm/day. This value was chosen, because it represented the smallest change in the height of the water table that could reliably and readily be distinguished above small numerical fluctuations in the model. The method of assessing the equilibrium time was to collect the pressure head data at the bottom of lysimeter versus time from the model. The rate of change of the height of the water table with time was then calculated for each time interval. This data was then reviewed and the time interval between which the rate of change of the water table with time changed to the defined equilibrium condition was recorded.

4.4 Results of Preliminary Modelling

The following subsections present the results of the preliminary modelling program. Summary tables of the modelling simulations are available in Appendix A.

4.4.1 Varying Fluxes

This section will review the performance of the lysimeter under varying applied flux rates. Three different lysimeter diameters (5, 10 and 15 cm) were simulated. All of the lysimeters modelled included a 0.5 m silica flour extension into the waste rock.

Figure 4.6 displays the results of modelling performed to investigate the error associated with suction measurements in the lysimeter. It can be seen from this graph that as the diameter of the lysimeter increases the amount of error in the suction measurement also increases. This is due to a small amount of pressure that must be developed in the lysimeter backfill to push the water out of the silica flour and into the waste rock surrounding the lysimeter. As the diameter of the lysimeter and silica flour extension

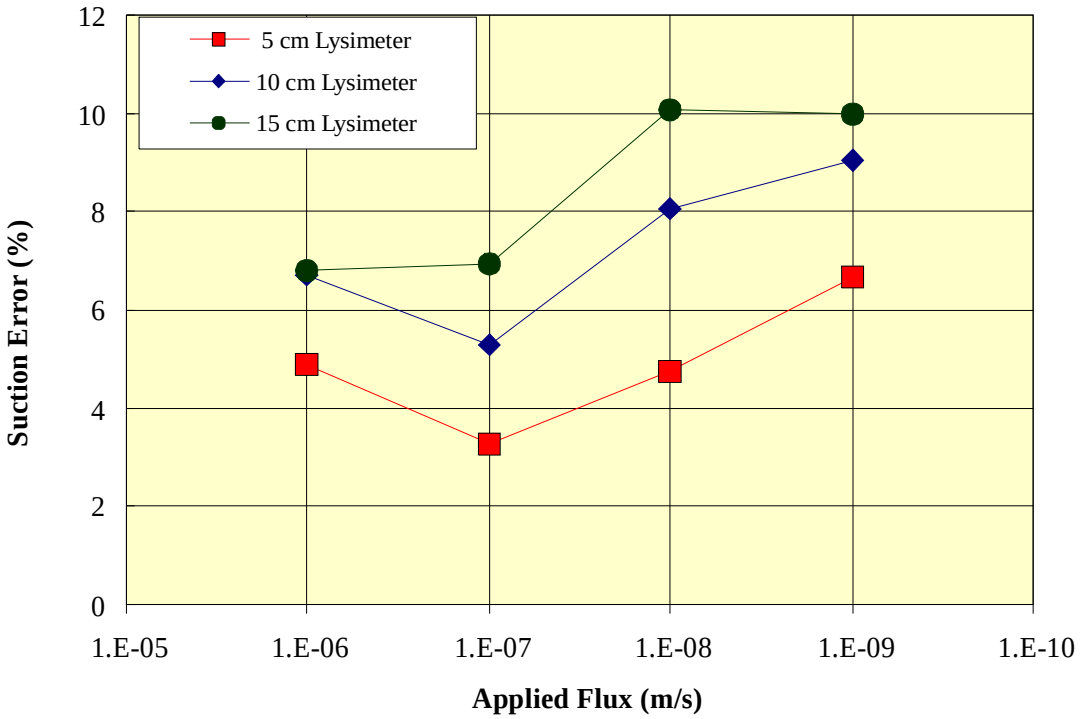

Figure 4.6 - Effect of varying the flux on suction measurement error

increases, the amount of pressure required to push the water out into the waste rock also increases. It should be noted that in all model runs, the lysimeter showed lower suctions than those seen at the outside edge of the column. The slope of the lines in Figure 4.6 change sign at a flux that is equal to the saturated hydraulic conductivity of the lysimeter backfill material. This indicates that the error is related to flow in the lysimeter backfill material.

The effect of varying the applied flux on the equivalent collection area ratio was also examined. These results are shown in Figure 4.7. All of the lysimeters showed an increase in the equivalent collection area ratio as the applied flux was reduced. This was expected as the hydraulic conductivity of the waste rock outside the lysimeter decreased with a decrease in the flux, the hydraulic conductivity of the lysimeter backfill stayed constant. At fluxes higher than the saturated hydraulic conductivity of the lysimeter backfill (1E-7 m/s) the equivalent collection area ratio is less than one, indicating that the waste rock is the preferential flow path. At fluxes lower than the saturated hydraulic conductivity of the lysimeter backfill the equivalent collection area ratio is greater than

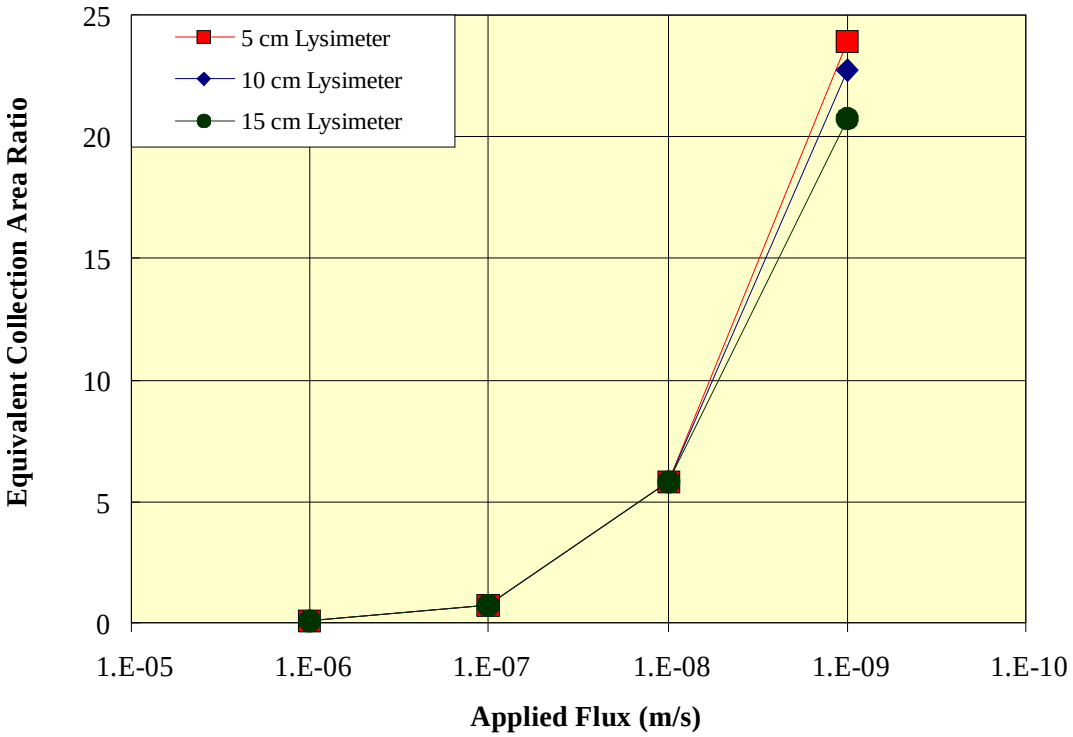

Figure 4.7 - Effect of varying the flux on the equivalent collection area ratio

one that indicates that the lysimeter backfill is the preferential flow path. At the lowest flux rate, the smallest diameter lysimeter had the largest equivalent collection area ratio. This is likely due to increased edge effects in the smaller lysimeter.

Figure 4.8 and Figure 4.9 illustrate the effect of varying the flux on the time to equilibrium and the time to flush the lysimeter respectively. Both of these properties are related to the magnitude of the flow into the lysimeter, and as a result, they resemble the results presented for the equivalent collection area ratio. As the flux decreases both the time to reach equilibrium increases, and the time required to flush the lysimeter also increase. As might be expected based on the equivalent collection area ratio graph, the smallest diameter lysimeter responds the fastest.

4.4.2 Inclusion \ Exclusion of Silica Flour Extension

The effect of including or excluding a 0.5 m silica flour extension into the waste rock is illustrated in the following analyses. The data provided in the previous section (includes a 0.5 m silica flour extension) will be compared against additional model runs that did not include the silica flour extension.

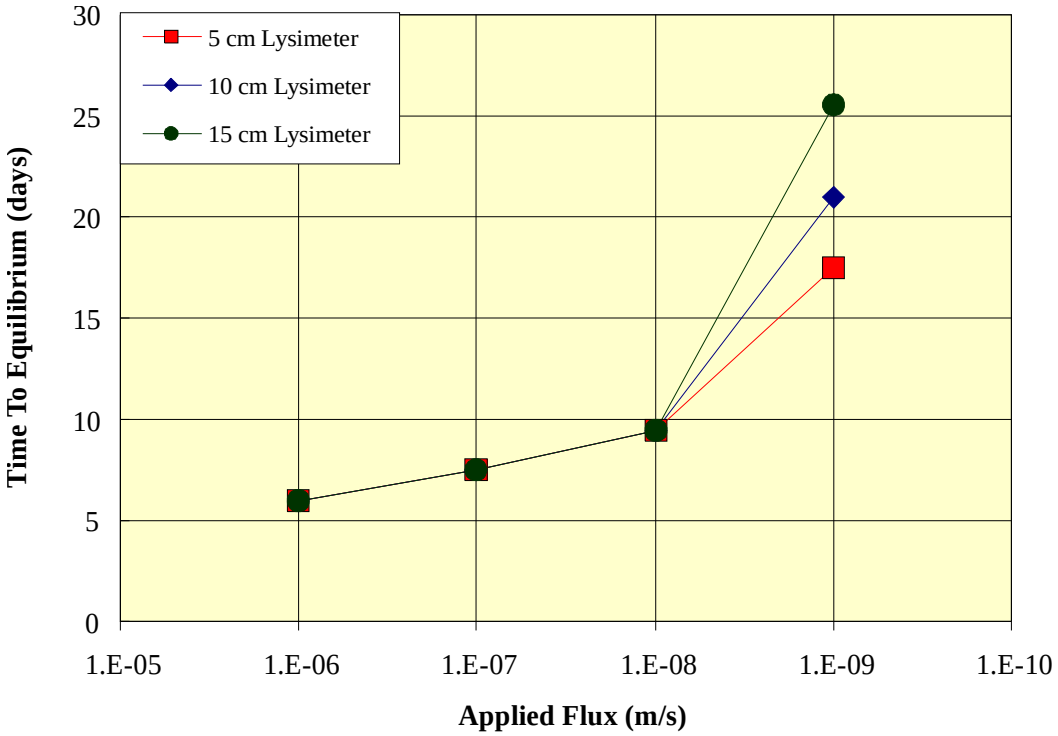

Figure 4.8 - Effect of varying the flux on the time to equilibrium

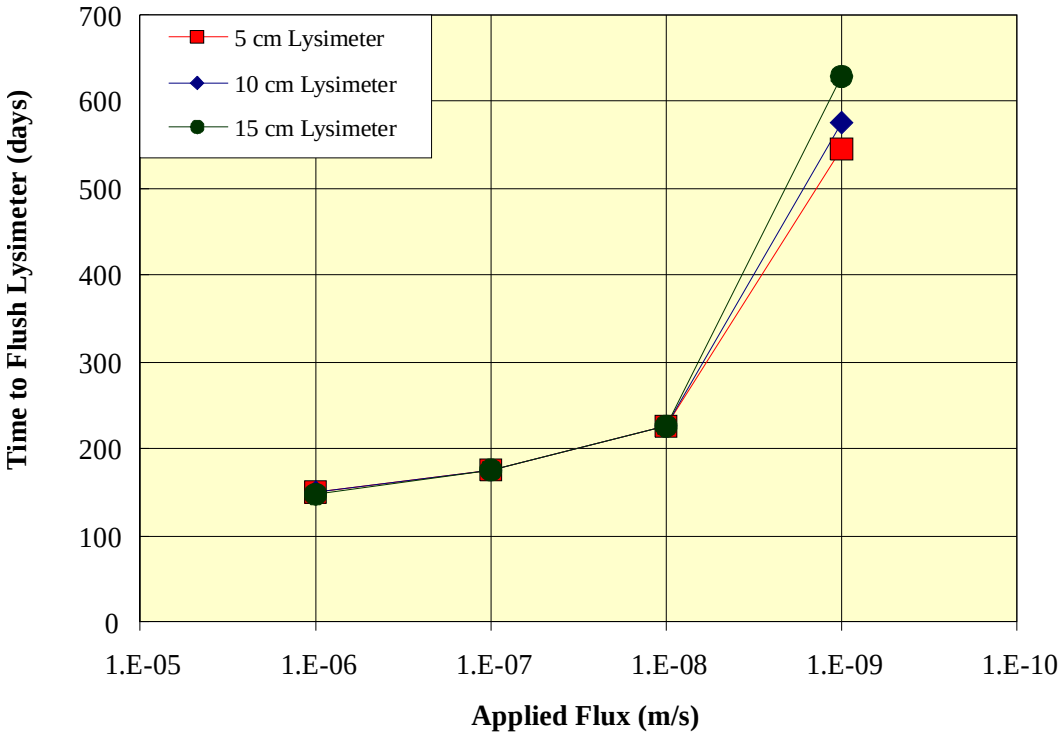

Figure 4.9 - Effect of varying the flux on time to flush lysimeter

Figure 4.10 displays the effect of the silica flour extension on the suction error. For lysimeters that do not use the silica flour extension, the error decreases with a decrease in applied flux. In comparison, lysimeters that include the silica flour extension showed a notable increase in error at fluxes lower than the saturated hydraulic conductivity of the lysimeter backfill. This suggests that the suction error is related to the flow into the extension above the top of the lysimeter. The inclusion of a silica flour extension increases the suction error. The smallest errors occurred in the smallest diameter lysimeters.

The equivalent collection area ratio was significantly affected by the inclusion or exclusion of the silica flour extension as shown in Figure 4.11. The exclusion of the silica flour extension decreased the equivalent collection area ratios. At a flux rate of 1E-9 m/s, the 5 cm diameter lysimeter experienced a 27% decrease in the equivalent

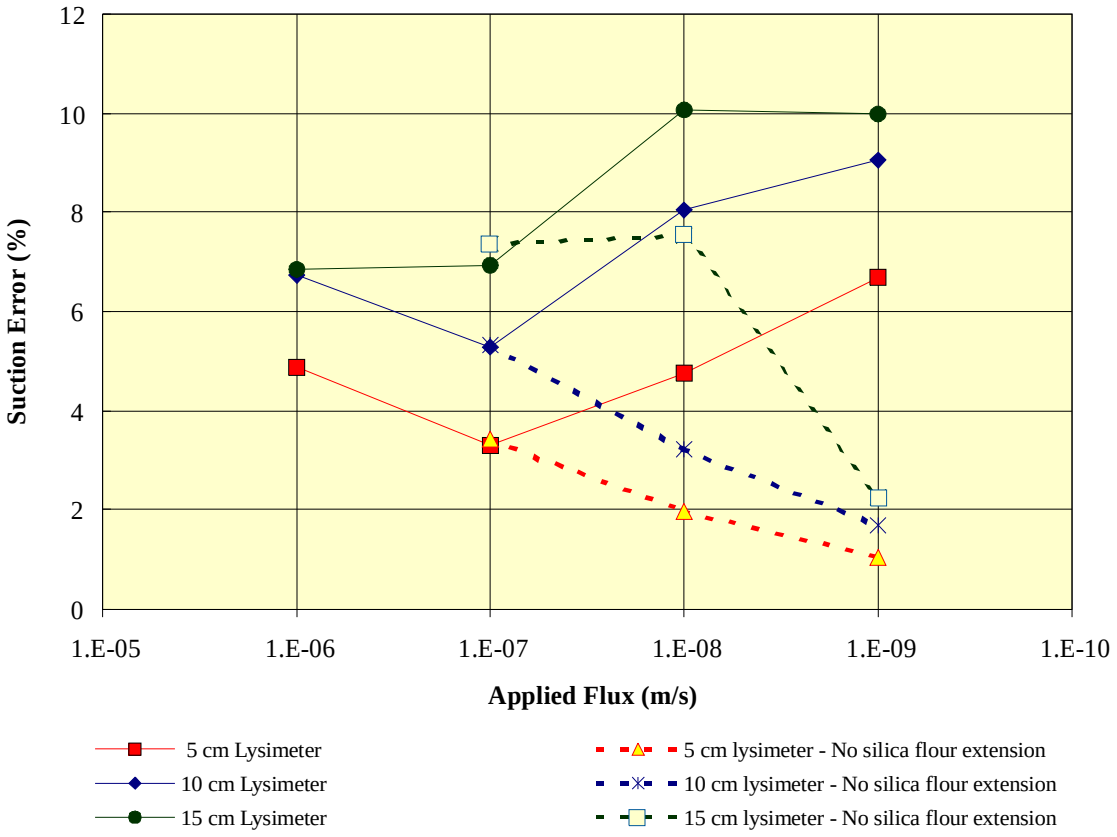

Figure 4.10 - Effect of silica flour extension on suction error

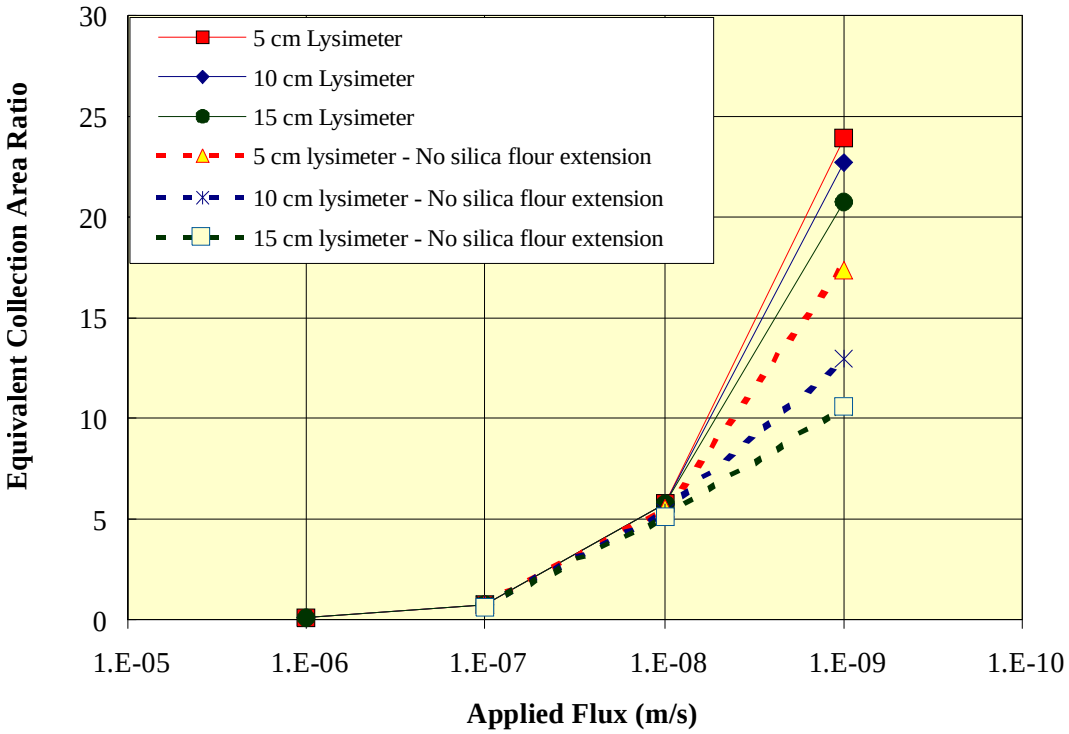

Figure 4.11 - Effect of silica flour extension on equivalent collection area ratios

collection area ratio due to the exclusion of the silica flour extension. Similarly, the 10 and 15 cm lysimeter experienced a 43% and 49% decrease in the equivalent collection area ratio respectively.

Figure 4.12 and Figure 4.13 display the effect of the silica flour extension on the time to equilibrium and the time required to flush the lysimeter. As might be expected, the decrease in the equivalent collection area ratio due to the exclusion of the silica flour extension dramatically increases the time required to come to equilibrium and flush the lysimeter. This effect is the most pronounced for the larger size lysimeters.

4.4.3 Bell Shaped Lysimeters

The following analysis compared two different bell shaped lysimeters to the 5 cm diameter lysimeter reviewed in Section 4.4.1. The bell shaped lysimeters consisted of increasing the diameter of the lysimeter from 5 - 10 cm and 5 - 15 cm at a distance of 0.1 m from the top of the lysimeter.

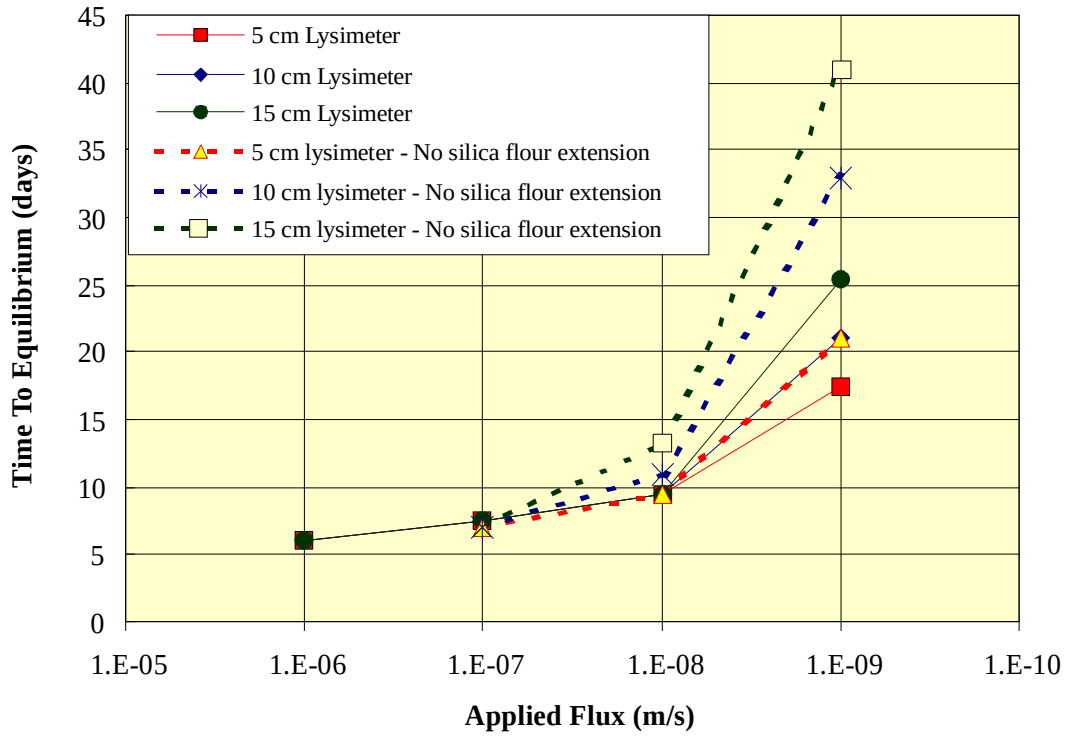

Figure 4.12 - Effect of silica flour extension on time to equilibrium

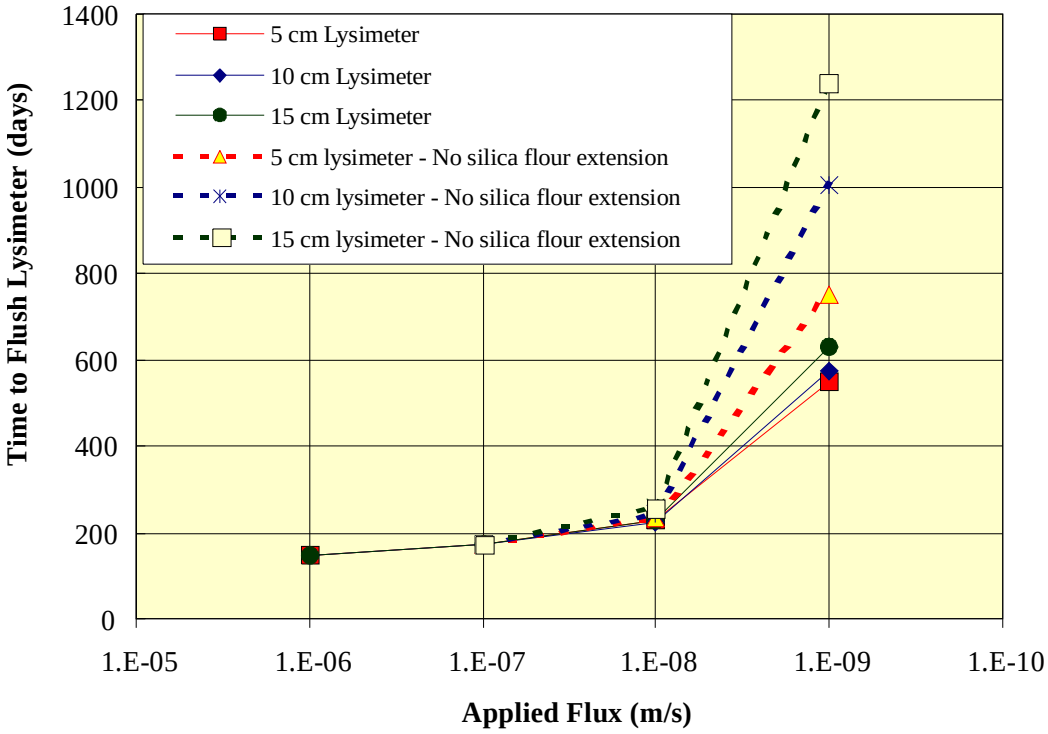

Figure 4.13 - Effect of silica flour extension on time to flush lysimeter

Figure 4.14 illustrates the effects of bell shapes on the suction error. From this graph it is apparent that as the diameter of the bell shape increases, the error increases. When compared to Figure 4.6 it is noted that the error associated with the 10 cm and 15 cm lysimeters are almost identical to the 5 - 10 cm lysimeter and 5 - 15 cm lysimeter respectively. This is most likely due to the comparable size of the silica flour extension above the lysimeter.

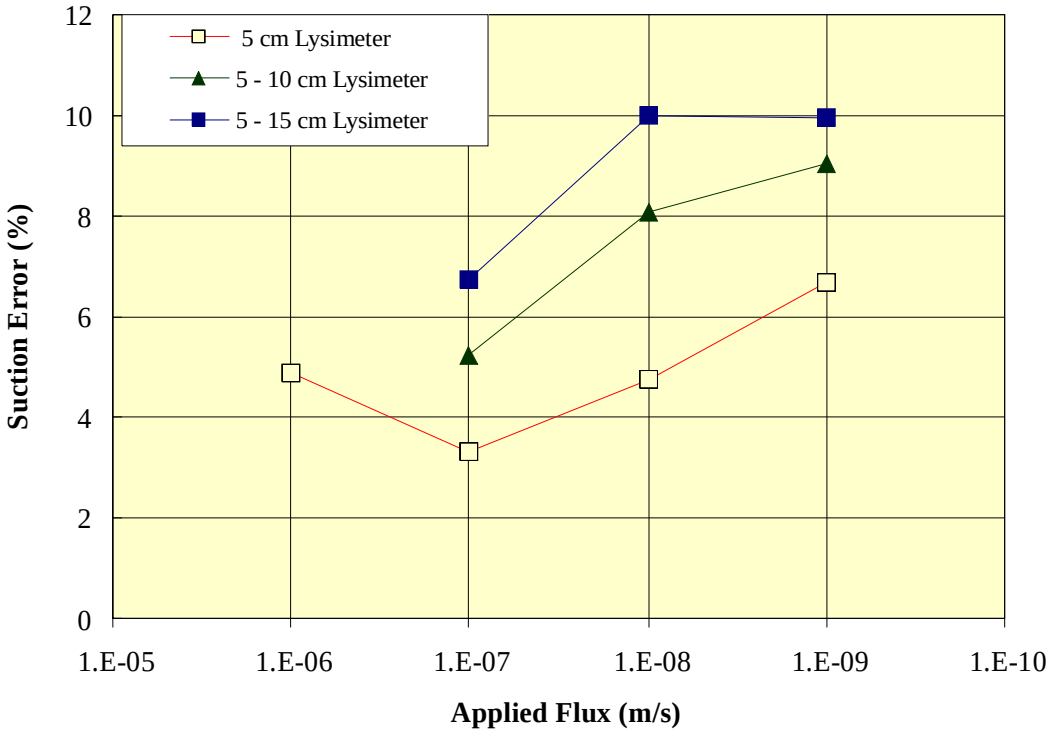

Figure 4.14 - The effect of bell shapes on suction measurement error

Figure 4.15 displays the increase in the equivalent collection area ratios for the two bell shaped lysimeters that were considered. While the area at the top of the lysimeter was increased by factors of 4 (in the 5 - 10 cm lysimeter) and 9 (in the 5 -15 cm lysimeter) the equivalent collection area ratio did not increase proportionally. In fact at a flux rate of 1E-9 m/s, the equivalent collection area ratio only showed increases of 18% and 23 % for the 5 - 10 and 5 - 15 cm lysimeters respectively. This also demonstrates that as the bell shape becomes larger it becomes less efficient at transmitting water to the lysimeter.

Figure 4.16 and Figure 4.17 illustrate the effect of bell shapes on the time to equilibrium and the time required to flush the lysimeter. As with the previous models, the increase in the equivalent collection area ratio due to the bell shape is reflected in decreases in the time required for the lysimeter to come to equilibrium and to flush the lysimeter. This effect is much less pronounced as the ratio of the diameters of the bell shape increases.

4.4.4 Varying the Saturated Hydraulic Conductivity of Materials in the Model

The effect of varying the saturated hydraulic conductivity of both the waste rock and the silica flour was investigated to determine if there was a link between saturated hydraulic conductivity and lysimeter performance. The model runs that involved varying the saturated hydraulic conductivity of the waste rock were difficult to interpret and have not been documented in this section (these model runs have been included in Appendix A). This was due to the fact, that as the hydraulic conductivity of the waste rock changed, different suctions were produced at the same flux rate. As a result, it was difficult to compare lysimeter response at different suctions and flux rates.

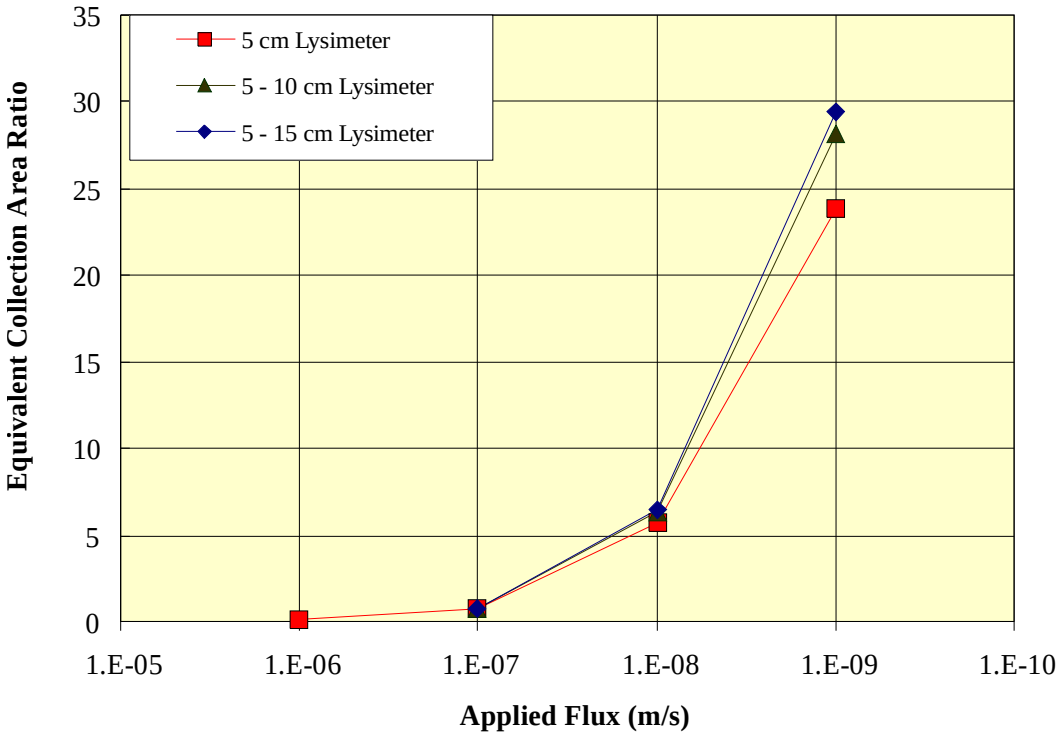

Figure 4.15 - The effect of bell shapes on the equivalent collection area ratio

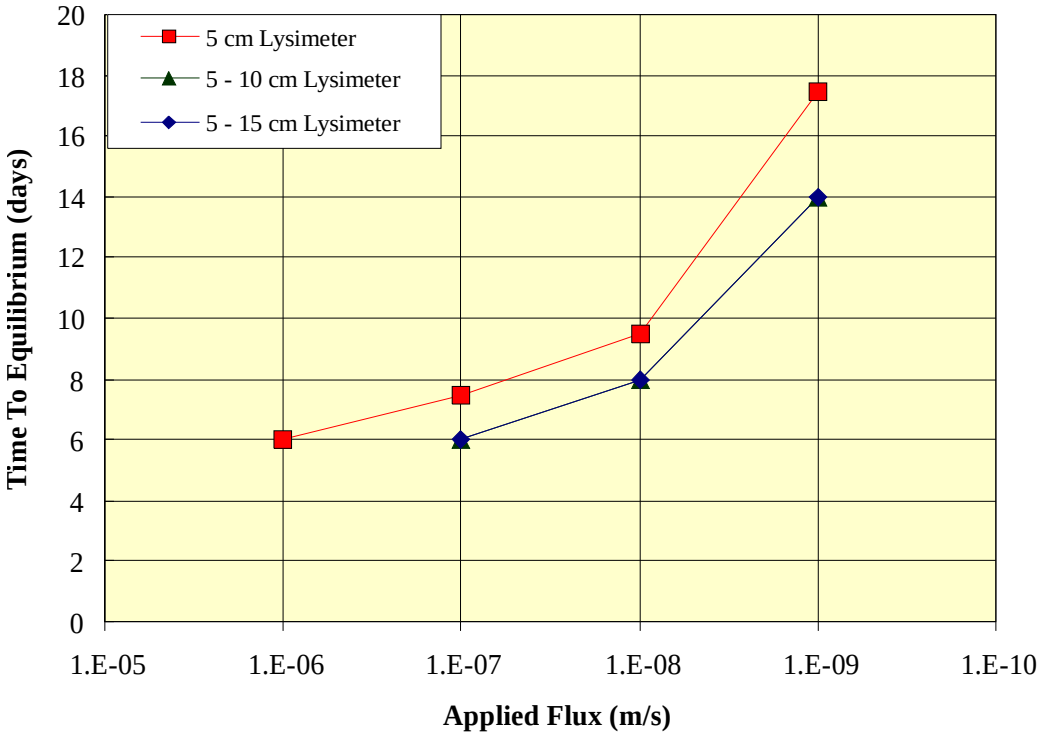

Figure 4.16 - Effect of bell shapes on the time to equilibrium

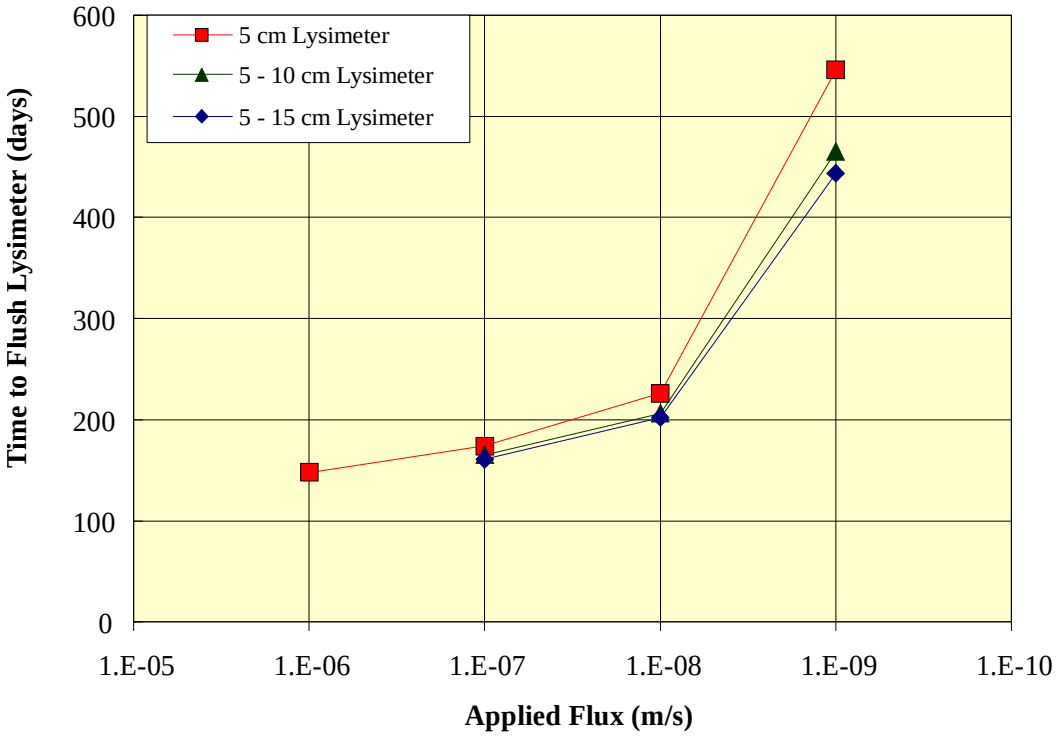

Figure 4.17 - Effect of bell shapes on the time to flush the lysimeter

The effect of varying the saturated hydraulic conductivity of the silica flour produced data that gave a much clearer indication of lysimeter performance. Figure 4.18 displays the results of varying the saturated hydraulic conductivity of the silica flour on the suction error. From the graph it can be seen that as the saturated hydraulic conductivity of the silica flour increases, the error increases.

Figure 4.19 displays the results of the effects of varying the silica flour saturated hydraulic conductivity on the equivalent collection area ratio. This graph shows that the equivalent collection area ratio is highly sensitive to the saturated hydraulic conductivity of the silica flour. As the saturated hydraulic conductivity increased an order of magnitude, the model responded by showing almost an order of magnitude increase in the equivalent collection area ratio. As with previous graphs, the smallest lysimeters had the largest equivalent collection area ratios.

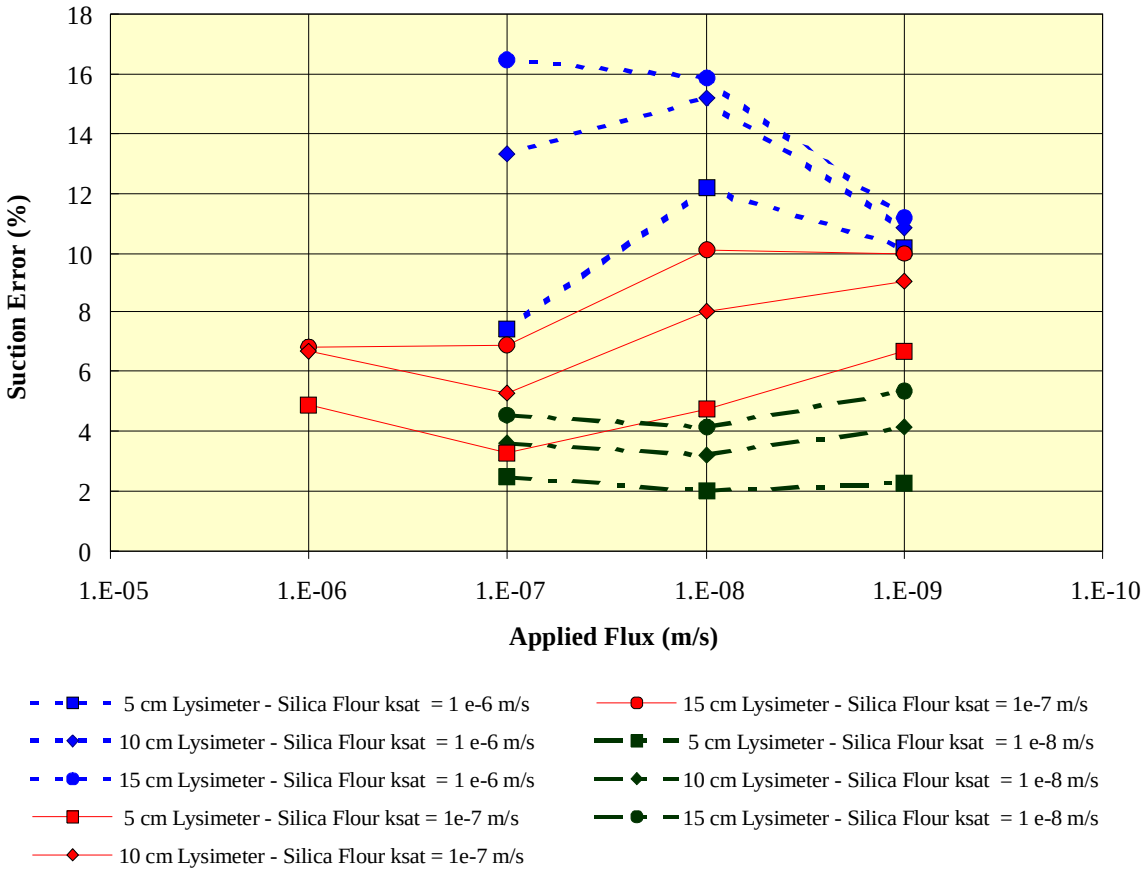

Figure 4.18 - Effect of varying silica flour hydraulic conductivity versus error

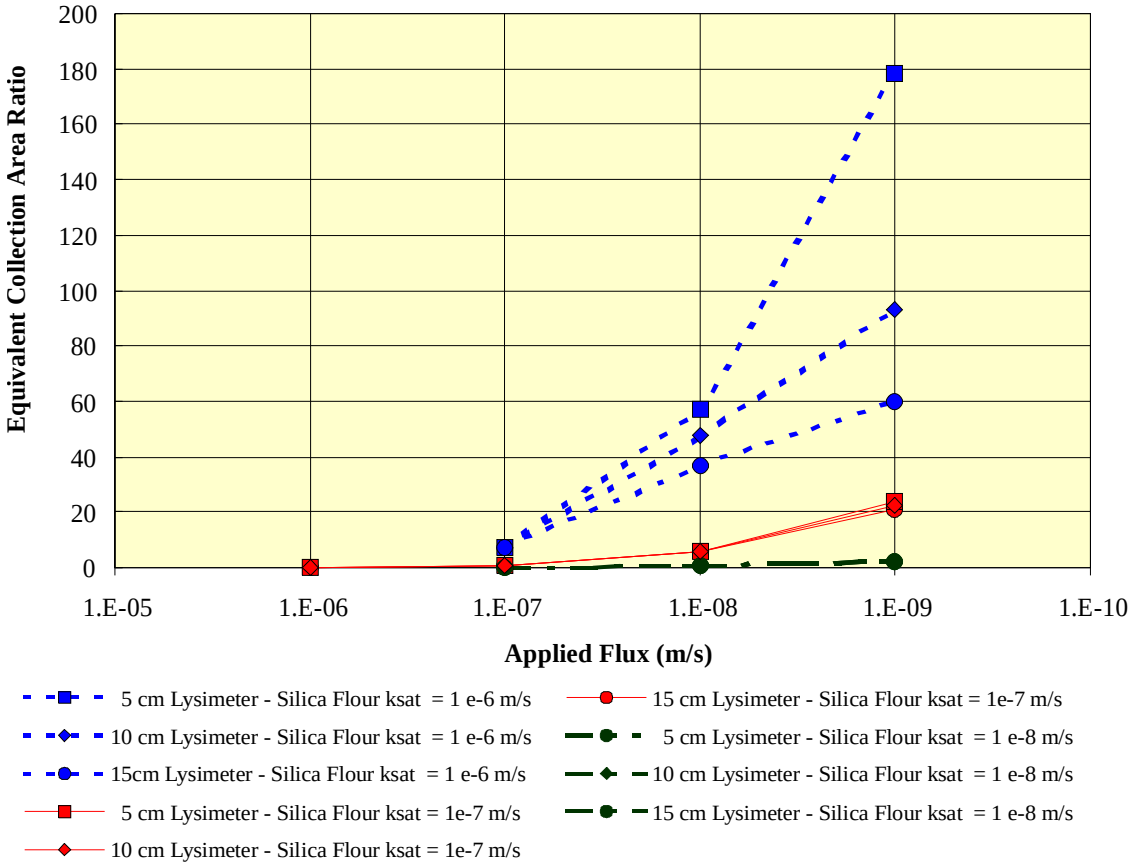

Figure 4.19 - The effect of varying the silica flour ksat on the equivalent collection area ratio

Figure 4.20 displays the effect of varying the saturated hydraulic conductivity on the time to equilibrium. The general trend in this graph is that as the hydraulic conductivity of the waste rock material decreases the longer it takes to come to equilibrium. It might have been expected that there would be larger differences (order of magnitude) between the response times at saturated hydraulic conductivities of 1E-6 and 1E-7 m/s. The lysimeter backfill material remains saturated throughout the drainage and refilling stages. The volume of water that must enter the lysimeter to increase the height of the water table is equal to the volume change due to a change in effective stress in the sample as a result of the altered water table. This is analogous to the process of consolidation. By examining the basic form of the consolidation equation it can be seen that as the hydraulic conductivity decreases by an order of magnitude the time to equilibrium should also by an order of magnitude. However, this assumes that the water

flow into the each sample is identical. This is not the case, as shown in the comparison of the equivalent collection area ratio shown in Figure 4.19.

The effect of the saturated hydraulic conductivity of the silica flour on the time to flush the lysimeter is shown in Figure 4.21. As the hydraulic conductivity of the silica flour decreases the time to equilibrium increases. An order of magnitude change in hydraulic conductivity produces nearly an order of magnitude change in the time to flush the lysimeter.

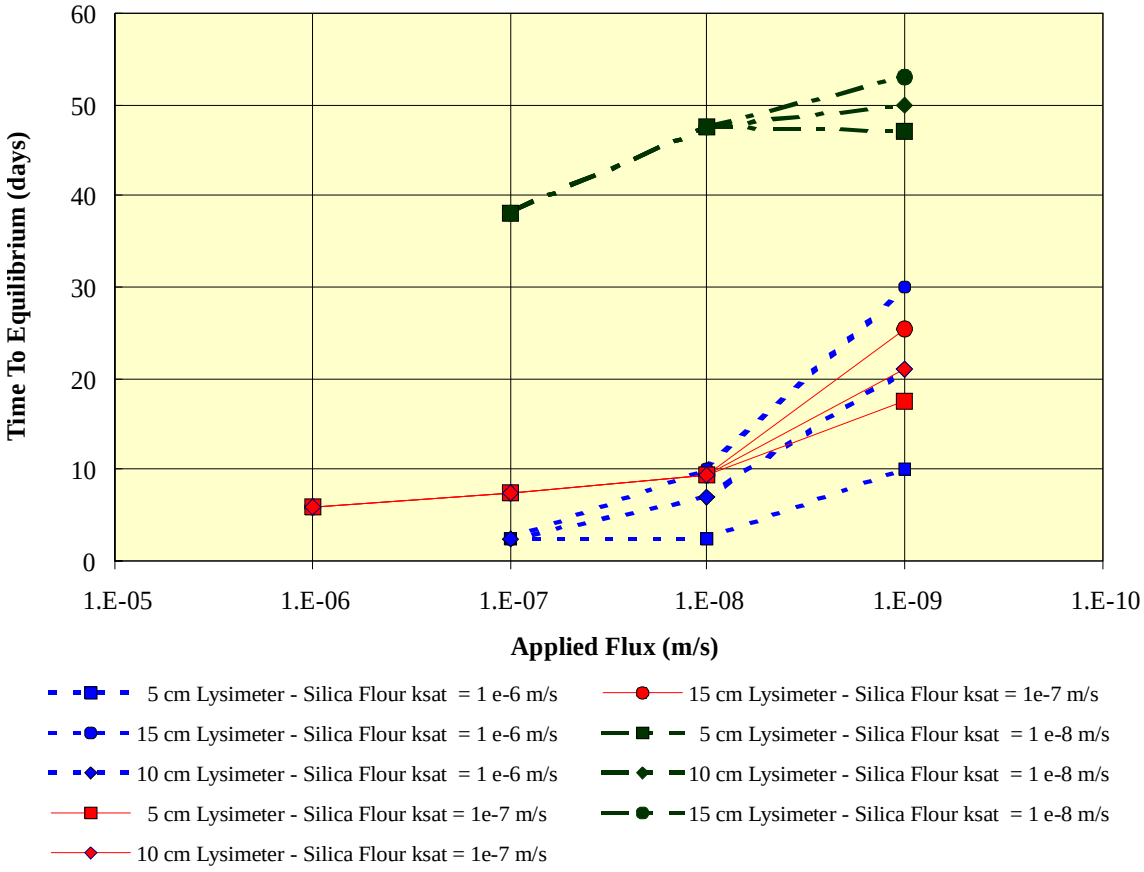

Figure 4.20 - Effect of the saturated hydraulic conductivity on time to equilibrium

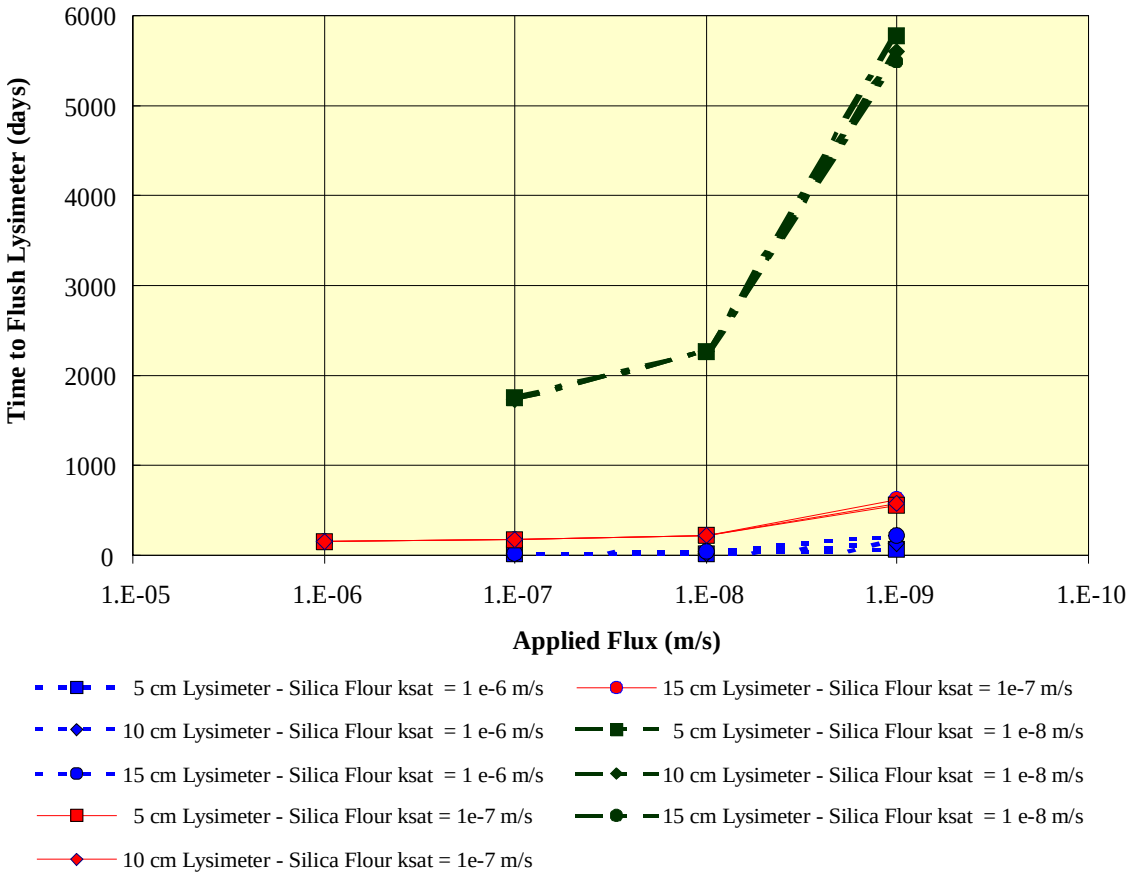

Figure 4.21 - Effect of the saturated hydraulic conductivity on the time to flush the lysimeter

4.5 Prototype Lysimeter Design

The following subsections briefly describe the prototype lysimeter design. In each section, practical considerations are weighed against the theoretical aspects of lysimeter performance as discussed in the previous sections.

4.5.1 Lysimeter Backfill

The ideal lysimeter backfill should have an air entry value higher than the range of expected suction, a high hydraulic conductivity and a low capacity for volume change. It was thought that the maximum suction that would develop in the waste rock was in the order of 25 kPa. Therefore, a material with an air entry value of 30 kPa to 40 kPa was thought to be sufficient. As both suction and saturated hydraulic conductivity are related to grainsize, it follows that choosing a minimum air entry value also limits the

maximum attainable hydraulic conductivity. As grainsize decreases the capacity for volume change generally increases, but, it can be minimized by considering the mineralogy and density of the sample.

A complete thesis could be written on developing the ideal lysimeter backfill by carefully investigation of the material properties described above. However, a readily available silica flour was known to have the desired material properties. Thus, silica flour was chosen as the lysimeter backfill material. Silica flour also has the added advantage of being commercially available. This dramatically decreases the overall cost of the standpipe lysimeter when compared to a lysimeter that is built with a non-commercial grainsize distribution.

4.5.2 Inclusion / Exclusion of Silica Flour Extension

The modelling of the silica flour extension identified that the exclusion of the silica flour extension would decrease the error in the suction measurement. However, the modelling also identified that the equivalent collection area ratios would drop. A third criteria must also be included in this analysis. If the lysimeter does not develop a contact between itself and the surrounding waste rock, suction cannot be measured and a pore water sample cannot be collected. Therefore, although the inclusion of the silica flour extension increases the suction error, it is vital to ensure that a contact is developed between the waste rock and the lysimeter. The increase in the equivalent collection area ratio is an additional benefit.

4.5.3 Lysimeter Size and Bell Shapes

The modelling consistently showed that a smaller diameter lysimeter outperformed larger diameter lysimeters when suction error and equivalent collection area ratios are considered. It could be argued that a pore water sample of a given volume can be collected at a faster rate from the larger lysimeters. However, the time required to flush the porewater in the larger diameter lysimeters is consistently longer than the time required by the small diameter lysimeters. Thus, when the overall sampling time

comprised of both flushing and sampling time is examined, it becomes clear that the smallest diameter lysimeter is the most desirable.

The bell shaped lysimeters modelled in this chapter demonstrated that only marginal increases in the equivalent collection area ratio could be attained through the use of bell shaped lysimeters. The trade off would be an increase in the suction error. When considering constructing and installing a standpipe lysimeter in the field, it can be seen that a straight body section has many advantages over a bell shaped lysimeter. On this basis it was decided that a straight body lysimeter would be used for the prototype.

4.5.4 Prototype Lysimeter Design

The final prototype lysimeter design consisted of a 5 cm diameter lysimeter backfilled with silica flour with a 0.5 m silica flour extension above the top of the lysimeter. The body of the lysimeter can be constructed from polyvinylchloride (PVC) pipe. This design is thought to represent a reasonable balance between theory and practical application. This lysimeter can be constructed of readily available materials. This reduces the overall cost of the lysimeter and allows it to be used as a routine monitoring tool in unsaturated waste rock piles.

CHAPTER 5 LABORATORY PROGRAM

5.1 Introduction

This chapter outlines the test procedures used in the laboratory testing program. This chapter consists of two major sections. The first section describes test methods used to characterize the material properties. The second section describes the procedures used to build the prototype lysimeters.

5.2 Laboratory Program - Material Characterization

The laboratory program consisted of characterizing five different materials. These materials were:

- Silica Flour
- 60% Sand & 40% Silica Flour Mixture
- Cluff Lake Waste Rock
- Simulated Coarse Waste Rock
- Simulated Fine Waste Rock

Silica flour was used as the backfill for the lysimeters. The silica flour is processed silica marketed as SIL-CO-SIL 90 by the U.S. Silica Company of Berkeley Springs, West Virginia. Testing performed on this material included; grainsize analysis, soil-water characteristic curve testing, saturated hydraulic conductivity testing and consolidation testing.

A 60% sand - 40% silica flour mixture was used as the silica flour extension in the coarse waste rock column. There was a concern that the silica flour by itself could wash

away into the coarse waste rock. As a result, sand was added to the silica flour to alter the gradation of the silica flour extension such that the mixture conformed to the grainsize criteria established for filter materials. The sand was purchased locally and is used in sand blasting. Testing on the sand silica mixture consisted of grainsize, soil-water characteristic curve and saturated hydraulic conductivity testing as well as filter tests.

A 1300 kg sample of waste rock was collected from the Dominique-Jeanine Waste Rock Pile at the Cluff Lake Uranium Mine located in northern Saskatchewan. The grainsize of this waste rock sample was measured in the laboratory. This waste rock pile was also the source of waste rock for the prototype waste rock pile constructed by Mr. Craig Nichols as part of his Ph. D. program at the University of British Columbia.

Simulated materials were used to represent the waste rock in the lysimeter prototype. The simulated waste rock materials were a combination of 3 different commercially available materials. The simulated fine waste rock was comprised of 5 parts of a “dirty” pit run gravel and 1 part silica flour. The simulated coarse waste rock was comprised of 1 part of the same “dirty” pit run gravel to 1 part of gravel screened between the ½ and 1 inch sieves. Testing performed on these prepared materials included grainsize and soil-water characteristic curve tests.

The following sections present the test procedures used to characterize the material properties for each material.

5.2.1 Sample Preparation

The silica flour samples were prepared for soil-water characteristic curve, saturated hydraulic conductivity and consolidation testing using the following method. Water was mixed into the silica flour until the percent solids of the mixture was 72% (gravimetric water content ~ 39%). The percent solids is defined as:

$$\% \text{ Solids} = \frac{\text{Mass of Soil}}{\text{Total Mass of Mixture}} \text{ X } 100 \quad \text{..... Eq. 5-1}$$

This volume of water produced a slurried sample, so that it was just workable. Maintaining a high percent solids minimized segregation of the sample during material handling and placement.

To form samples for testing a filter paper was placed on the screen of a 100 mesh sieve. The sample mold was then placed over top of the filter paper. This silica flour mixture was then poured into the sample mold and was allowed to drain for a period of 24 hours. The sample would liquify when vibrated, consequently, the sample was vibrated by striking the edge of the mold, which caused the sample to liquify. The sample was then allowed to consolidate for an additional 24 hrs. During this period the sample was vibrated occasionally. The sample was considered ready when it could no longer be liquified by vibrating the mold.

The sand-silica flour mixture was prepared by adding 3 parts sand and 2 parts silica by mass. The method of sample preparation for the sand and silica flour mixture was identical to that of the silica flour. It was found that a solids content of 82% solids was required to reach a point where the sample was just workable.

5.2.2 Grain Size Analysis

Grain size analysis can be performed using a number of different methods. A mechanical sieve analysis is performed for samples with particles larger than 0.075 mm, a hydrometer analysis can be used for samples that have particles smaller than 0.075 mm. For samples that contain significant portions of both size ranges, both tests can be run to determine the relative proportions of each grain size. The standard method includes both mechanical and hydrometer analysis and is available from ASTM 422-63 (1993). Unless otherwise noted all grain size analyses were performed using ASTM 422-63 (1993).

Testing of the Cluff Lake waste rock sample generally followed the method outlined in ASTM 422-63 (1993). The sample was initially dried. The large cobbles were washed by hand and grouped according to size. All of the wash water was retained. The cobble size particles were sized using square holes cut out of a sheet of plywood.

Dry sieving was initially used to separate out the gravel size particles. This was followed by washing each size range to remove the fines. All of the wash water was retained. The wash water was allowed to settle for a period of at least 24 hrs. The clear fluid on the top was then decanted and discarded. The material that had settled to the bottom was added to the material passing the #4 sieve. The sand sizes were separated by washing them over a sieve. The wash water from this process was retained and then used for the next sieve size. The remaining wash water was slowly decanted over a period of several weeks as the material settled. The remaining fines were dried in the oven. A sample was split out using a riffle splitter and a hydrometer analysis was performed.

5.2.3 Soil-Water Characteristic Curve Test

All of the testing performed to characterize the soil-water characteristic curves of the various materials followed the procedure outlined below. Soil-water characteristic curve testing was performed using tempe cells. Figure 5.1 displays a photograph and schematic drawing of the tempe cells used to measure the soil-water characteristic curve of the soils in the testing program.

The porous ceramic disks were saturated by filling the tempe cells with de-aired water and subjecting the cell to a pressure of 110% of the indicated air entry value of the porous disk for a period of a least one hour.

The silica flour and sand-silica mixture samples were formed in a consolidation ring and placed into the small tempe cells. The waste rock samples were placed directly into the large tempe cells. The waste rock samples were then compacted with 1 blow of a Marshall Hammer over the entire surface area to provide a compaction level comparable to that of the prototype columns. Once the soil samples were placed inside the tempe

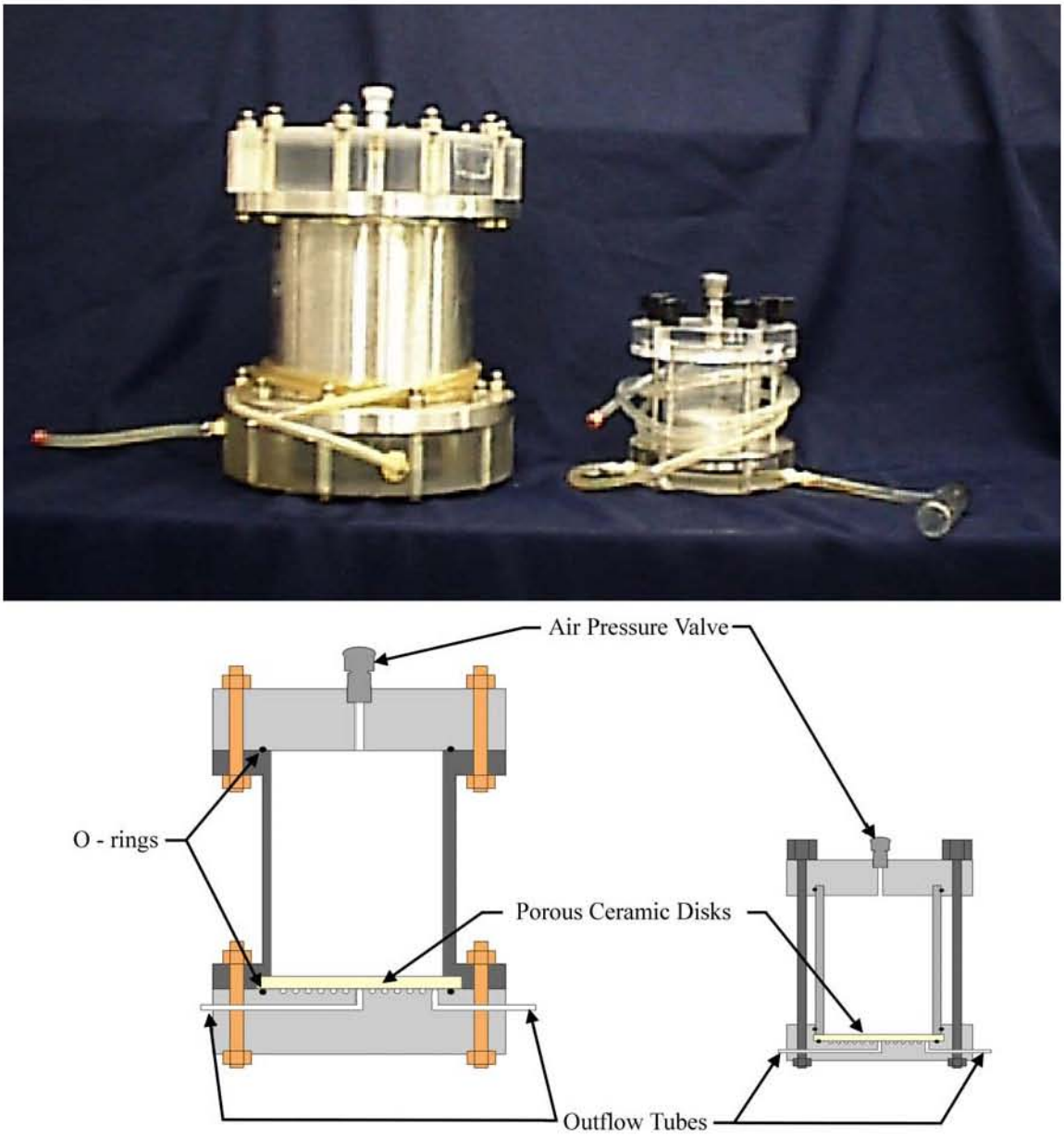

Figure 5.1 - Photographs and schematics of Tempe cells

cells, the sample was saturated from the bottom up by applying a small amount of water pressure to the bottom of the porous disk by elevating the outflow tubes. Saturation was noted when water appeared on the top of the soil sample. The initial weight was then recorded.

During the initial stages of the test, suction was applied to the sample by lowering the outflow tubes. The valve located in the center of the lucite top was left open. The difference between the elevation of the sample and the elevation of the end of the outlet tubes is proportional to the suction in the sample. Water was allowed to drain from the sample until the water pressure head inside the waste rock sample came to equilibrium with the negative pressure head applied at the end of the outflow tubes. The equilibrium condition was monitored by recording the mass of the sample with time. Once the mass became steady the sample was considered to be at equilibrium. The final mass for this suction was then recorded. The outlet tubes were then lowered and this process was repeated.

At suctions greater than 10 kPa it becomes impractical to lower the outlet tubes. The suction in the sample was then applied using the axis translation technique. The axis translation technique involves translating the reference pressure from pore water pressure to pore air pressure. Air pressure is then used to apply a suction to the sample. This technique requires that both the pore-air pressure and pore-water pressure be controlled. Air pressure is controlled through a valve at the top of the cell. The outflow line is kept equal to zero gauge pressure. The suction is then equal to the positive pore air pressure applied. If the air pressure is increased and the pore-water remains equal to zero gauge pressure, the suction in the soil sample will also increase and eventually come in equilibrium with the applied air pressure. Weighing the sample periodically monitors the progress of the sample as it progresses towards equilibrium. Once the sample weight becomes steady, the weight of the sample at the applied suction is recorded. The air pressure is then increased, thus increasing the applied suction and the process is repeated.

5.2.4 Saturated Hydraulic Conductivity Testing

Saturated hydraulic conductivity testing was performed using both the constant head and falling head saturated hydraulic conductivity tests. The testing methods vary in the manner in which the gradient is applied to the sample. The following sections outline the methods used in each test.

5.2.4.1 Constant Head Saturated Hydraulic Conductivity Analysis

Constant head tests were performed on both the silica flour and the sand-silica flour mixture. The constant head test determines the saturated hydraulic conductivity of a sample by applying a constant hydraulic gradient across the length of sample. The hydraulic conductivity of the sample was calculated from measurements of the flow rate using Darcy's Law. Controlling the elevation of the inflow and outflow tubes set the hydraulic gradient. Figure 5.2 displays a photograph of a constant head test. The gradient was determined by dividing the difference in head (h1-h2) by the length of the sample. The quantity of water passing through the sample with time was determined by weighing the amount of water collected in a reservoir. The test was run for a number of different gradients.

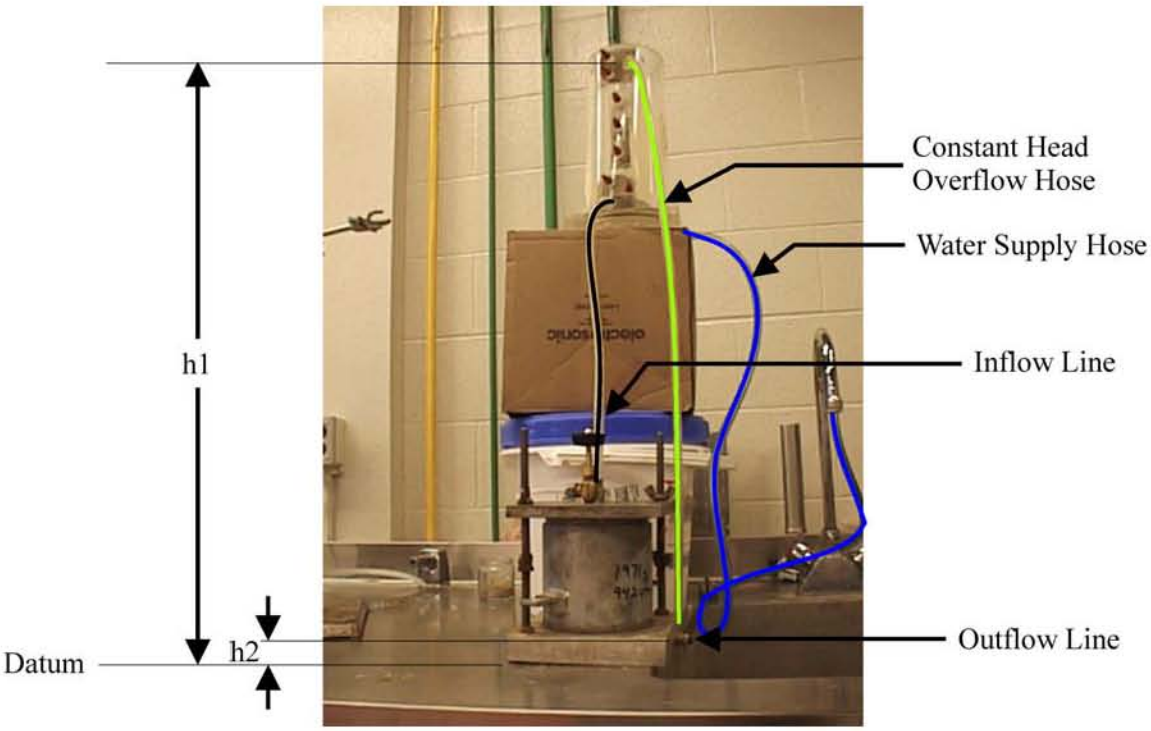

Figure 5.2 - Hydraulic conductivity test - constant head apparatus

5.2.4.2 Falling Head Saturated Hydraulic Conductivity Analysis

This test was used to determine the hydraulic conductivity of the silica flour once it was placed in the lysimeter. The falling head test differs from the constant head test in that the upper head boundary condition is allowed to fall as water is passed through the sample. The lower head boundary condition remains constant. The gradient across the sample is calculated as the average head during a time interval. The flowrate into the sample is calculated from readings the volume of water entering the sample as determined from readings taken from the graduated cylinder with time. As with the constant head test the hydraulic conductivity is calculated using Darcy's Law.

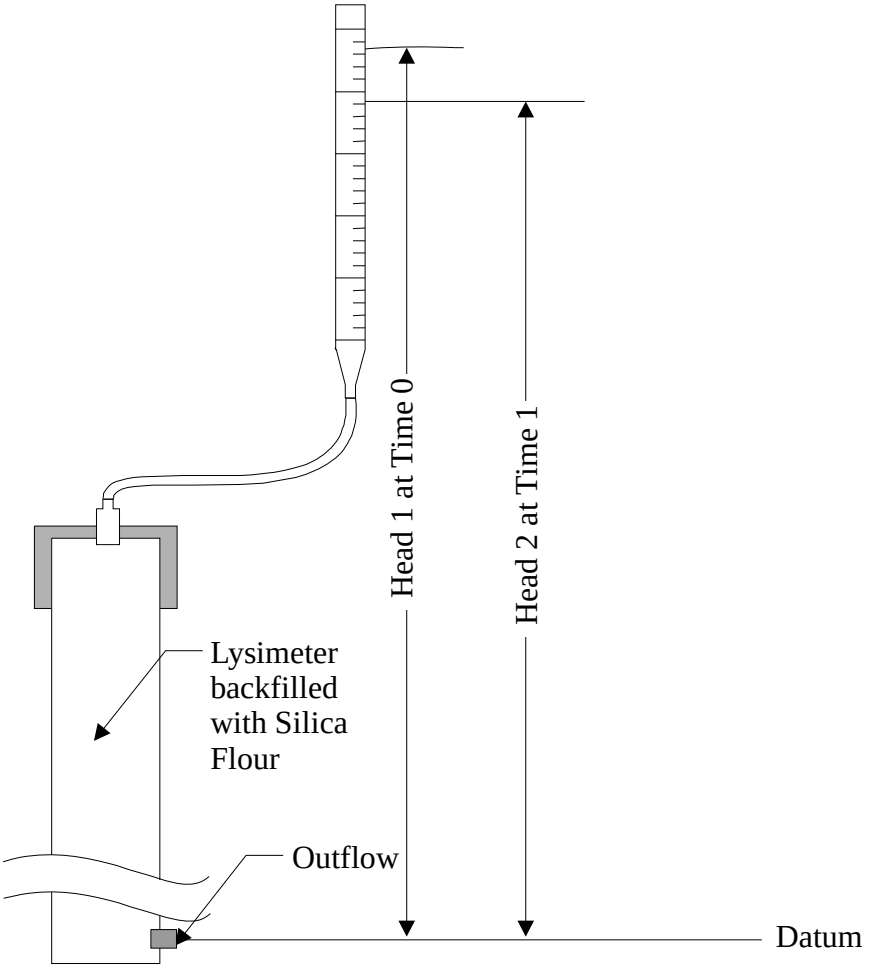

Figure 5.3 - Hydraulic conductivity test - Falling head schematic

5.2.5 Consolidation Test

Consolidation testing was performed on the silica flour sample according to ASTM D2435-96 (1997). Figure 5.4 displays a photograph of the consolidation apparatus used in the testing.

Figure 5.4 - Consolidation apparatus

The data from this test is normally interpreted to determine the coefficient of consolidation (c_v). However, in this case the data collected from the test was used to determine the coefficient of volume change (m_v). The coefficient of consolidation (c_v) is defined by the following equation:

$$c_V = \frac{k}{m_v \rho_w g}$$ ..... Eq. 5-2

where: c_v = Coefficient of consolidation (m^2/s)

k = hydraulic conductivity (m/s)

m_v = Coefficient of volume change (/kPa)

ρ_w = Density of Water (kg/m^3)

g = acceleration due to gravity (m/s^2)

The coefficient of volume change defines the slope of the soil-water characteristic curve prior to the air entry value. Since the lysimeter stays saturated during all phases of operation, the time required to fill the lysimeter is a function of the change in the volume of the silica flour due to changes in effective stress of the silica flour as the water table inside the lysimeter increases or decreases.

The value of the coefficient of volume change can be calculated from consolidation data using the following equation:

$$m_v = \frac{a_v}{1 + e_o}$$ ..... Eq. 5-3

where: a_v = coefficient of compressibility (kPa)

= slope of the void ratio versus overburden pressure plot (arithmetic scale)

e_o = initial void ratio

5.2.6 Filter Testing

There was a concern that the silica flour extension might wash into the coarse waste rock. This would cause a decrease in the equivalent collection area ratio. As a result, filter testing was performed on the 60% sand - 40% silica flour mixture. The purpose of the test was to determine if the silica flour in the mixture would remain in place in the waste rock. The test consisted of placing a layer of coarse waste rock in a constant head permeameter. The sand silica mixture was placed above the waste rock layer. A

constant hydraulic gradient was then applied to the sample. The outflow was collected and analyzed for total suspended solids. The total suspended solids of the outflow were measured with time to determine if the silica flour was migrating out of the sand silica flour mixture.

5.3 Prototype Lysimeter Testing Program

The following sections describe the construction of the prototype lysimeter columns and test methods used during the testing of the standpipe lysimeter.

5.3.1 Testing Program

The test program consisted of two large scale columns to test the performance of the prototype lysimeters in waste rock. The columns differed in the gradation of the waste rock that was placed in them. The two different gradations roughly correspond to the envelope of waste rock gradations as found in the literature. Figure 5.5 displays the grainsize data collected for waste rock in the literature and the envelopes chosen for the fine and coarse waste rock columns. In the actual prototypes, rocks larger than 25 mm were removed, because it was difficult to properly distribute the larger grainsize fractions. Yazdani (1995) studied the effects of removing the coarse fraction (> 8 mm) on the soil-water characteristic curves of waste rock. Yazdani (1995) concluded that the removal of the coarse fraction did not affect the air entry value or residual water content, but that the initial volumetric water content was altered. In the context of this study, the removal of the larger gradations should not affect the suctions produced in the column, but may have increased the available moisture storage within the waste rock column.

Changing the flux applied to the top of the column varied the suction profile within the waste rock columns. The applied fluxes were controlled using peristaltic pumps (at high flow rates) and syringe pumps (at low flowrates). The flow into and out of the waste rock columns was monitored to determine if the columns were at equilibrium. Tensiometers were used to measure the suction profile that developed in the waste rock. These values were compared to the suction measured in the lysimeter. Figure 5.6 shows the setup used to verify suction measurements in the lysimeter.

Flow into the lysimeter was initiated by lowering the water table within the lysimeter by opening a valve at the bottom of the lysimeter. The flowrate with time was then measured. This measurement was then used to calculate the equivalent collection area ratio, time required to collect a 100 ml sample and the time required to flush the lysimeter.

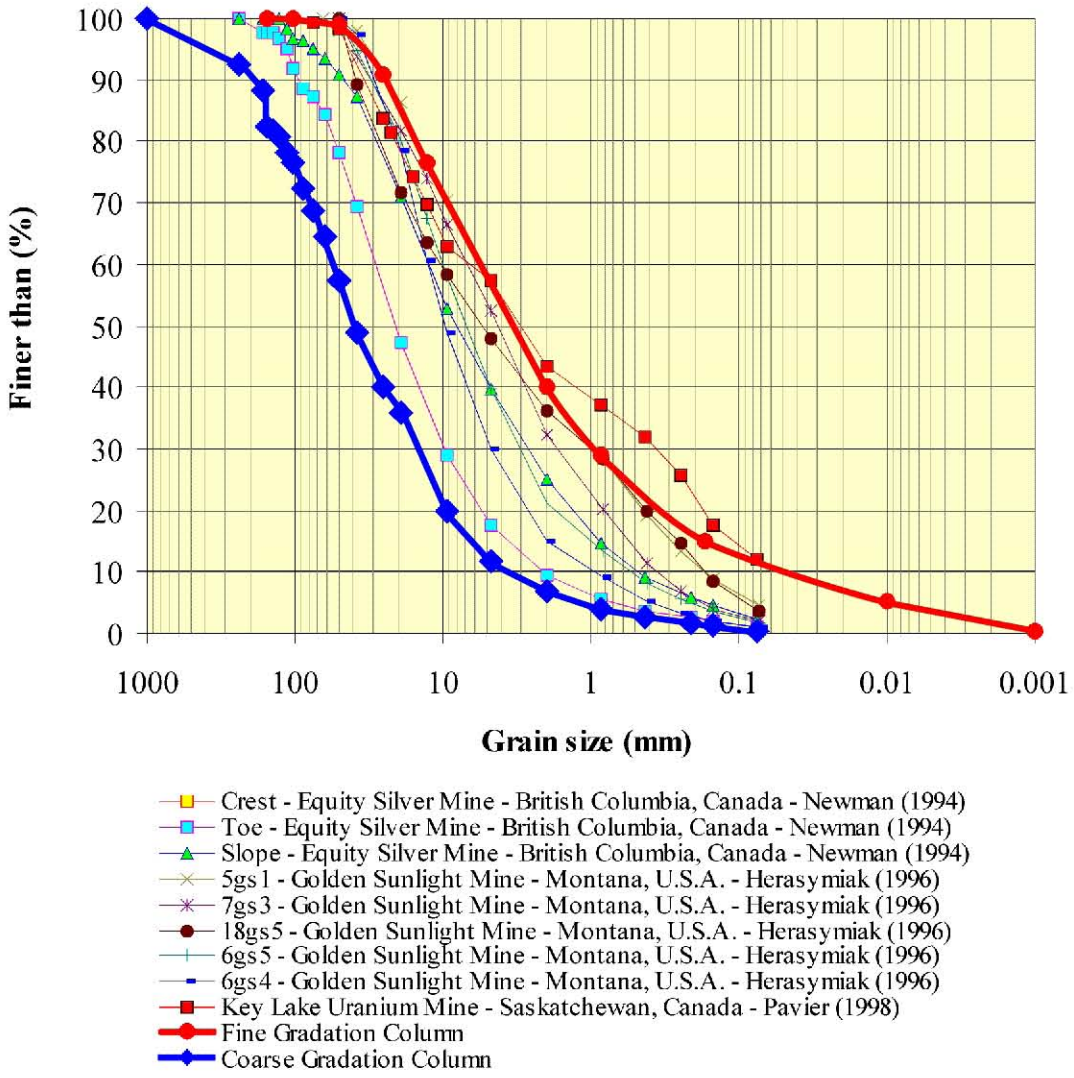

Figure 5.5 - A comparison of grainsize curves for waste rock and those used in the prototype testing columns

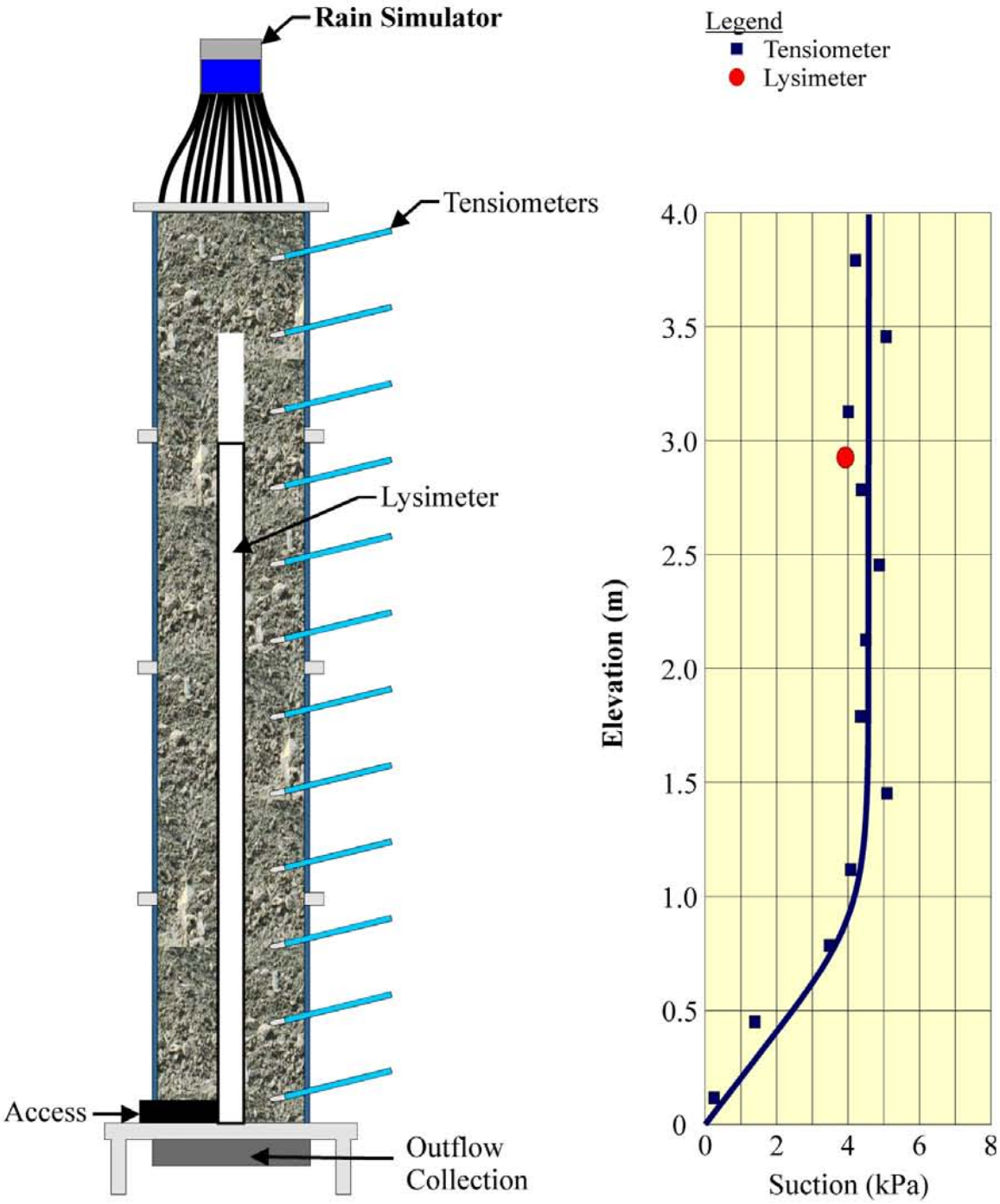

Figure 5.6 - Suction measuring methodology

5.3.2 Prototype Lysimeter Testing Apparatus

The lysimeter testing apparatus was comprised of a number of different parts. For the purposes of illustration these parts have been broken down into the following groups:

- Column
- Rain simulator
- Tensiometers and suction measurement apparatus
- Prototype standpipe lysimeter

5.3.2.1 Column

The column consisted of four 45 gallon drums placed one on top of another. Each drum was approximately 0.55 m in diameter and 0.90 m in height. The drums were held apart using spacers. Each column was supported on an aluminum stand. The aluminum stand had holes drilled through the bottom to allow water to drain out the bottom. A collection pan was also constructed to collect the water that drained through the stand. Storage of water in the pan was minimized by using a pan that sloped to one end. Steel ports measuring 50 mm in diameter were welded into the barrels to provide access for the tensiometers. The ports were spaced as evenly as possible along the length of the column. Figure 5.7 displays some of the details regarding the setup of the column

5.3.2.2 Rain simulator

The rain simulator consisted of a water metering device, a predelivery storage chamber, small diameter hoses to deliver raindrops and a lucite cover which held the hoses in a position such that they distributed the rain equally over the surface of the column.

The water metering devices consisted of peristaltic pumps for flux rates greater than 1E-8 m/s and syringe pumps for flux rates equal to or less than 1E-8 m/s. The peristaltic pump system shown in Figure 5.8 consisted of a controller, a variable speed motor and pump heads. The syringe pump shown in Figure 5.9 was a GDS digital controller produced and marketed by GDS Instruments Ltd. (1991).

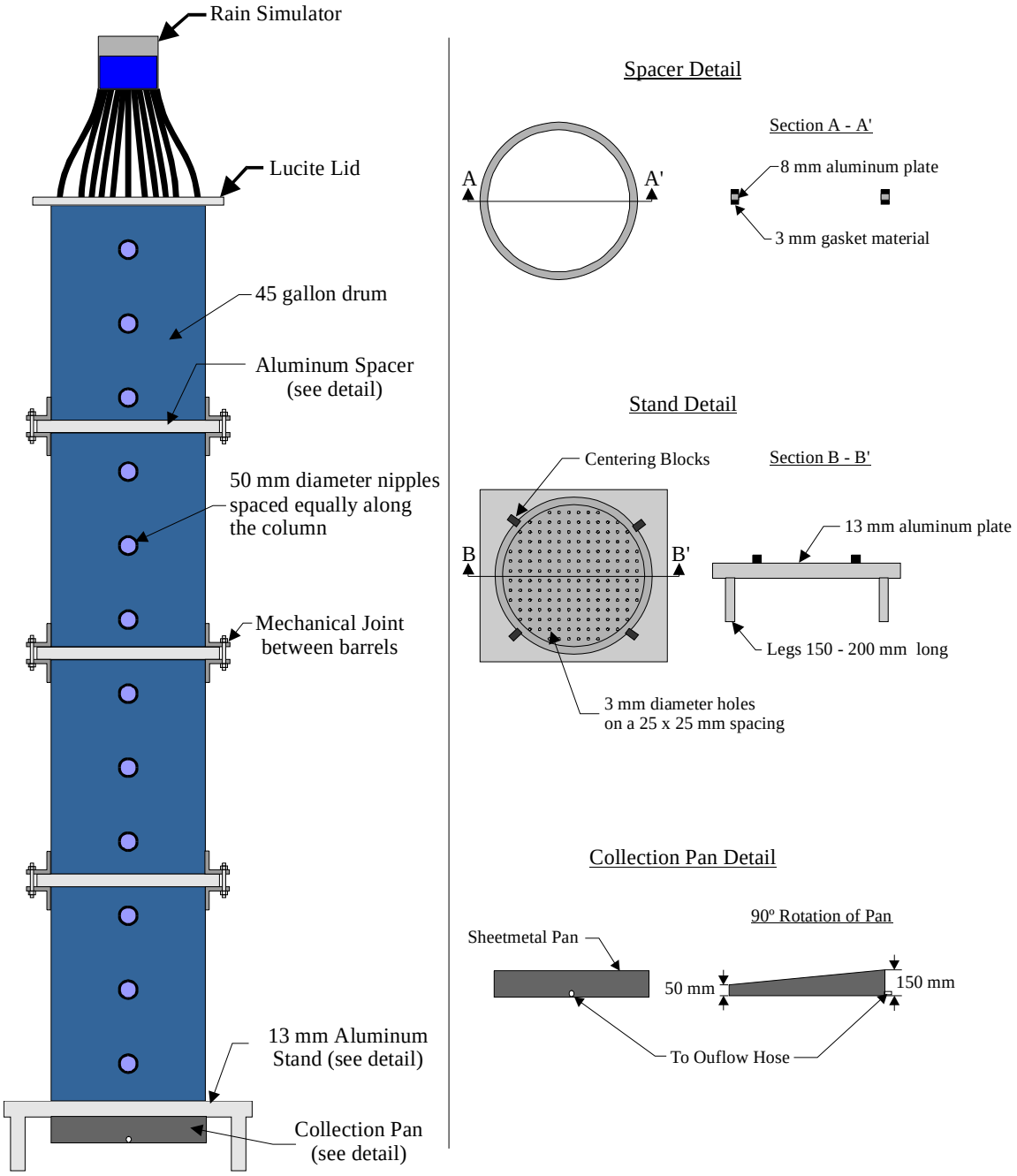

Figure 5.7 - Column construction details

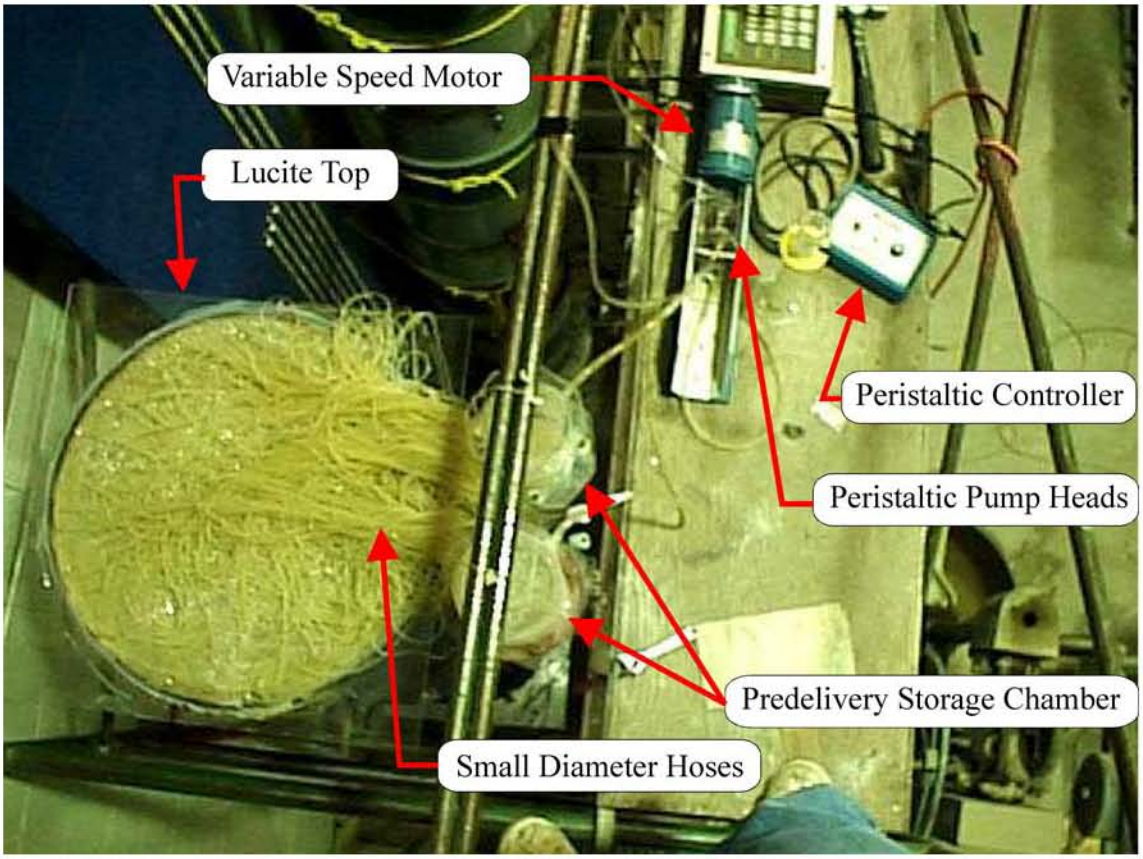

Figure 5.8 - Peristaltic pump system details

The predelivery storage chamber consisted of a lucite chamber. Holes were drilled In the bottom of the chamber to accommodate the small diameter hoses. The hoses were placed in the holes and silicone was used to make a seal between the hose and the lucite. The placement of the predelivery storage chamber was such that the bottom of the chamber was well below the top of the lucite cover on the column. This ensured that water ponded within the chamber, and that all of the hoses transmitted water.

The lucite top was constructed of 4.75 mm lucite plate. Holes were drilled in the plate to accommodate the small diameter hoses. As the experiment progressed the number of hoses was reduced from 288 holes to 8 holes. At high flux rates, 288 holes were used in the lucite cover. At a flux rate of 1E-8 m/s, it was noted that there were air bubbles in some of the hoses. It was feared that at the low flux rates, the water was evaporating through the hoses prior to reaching the column. As a result the number of hoses was decreased.

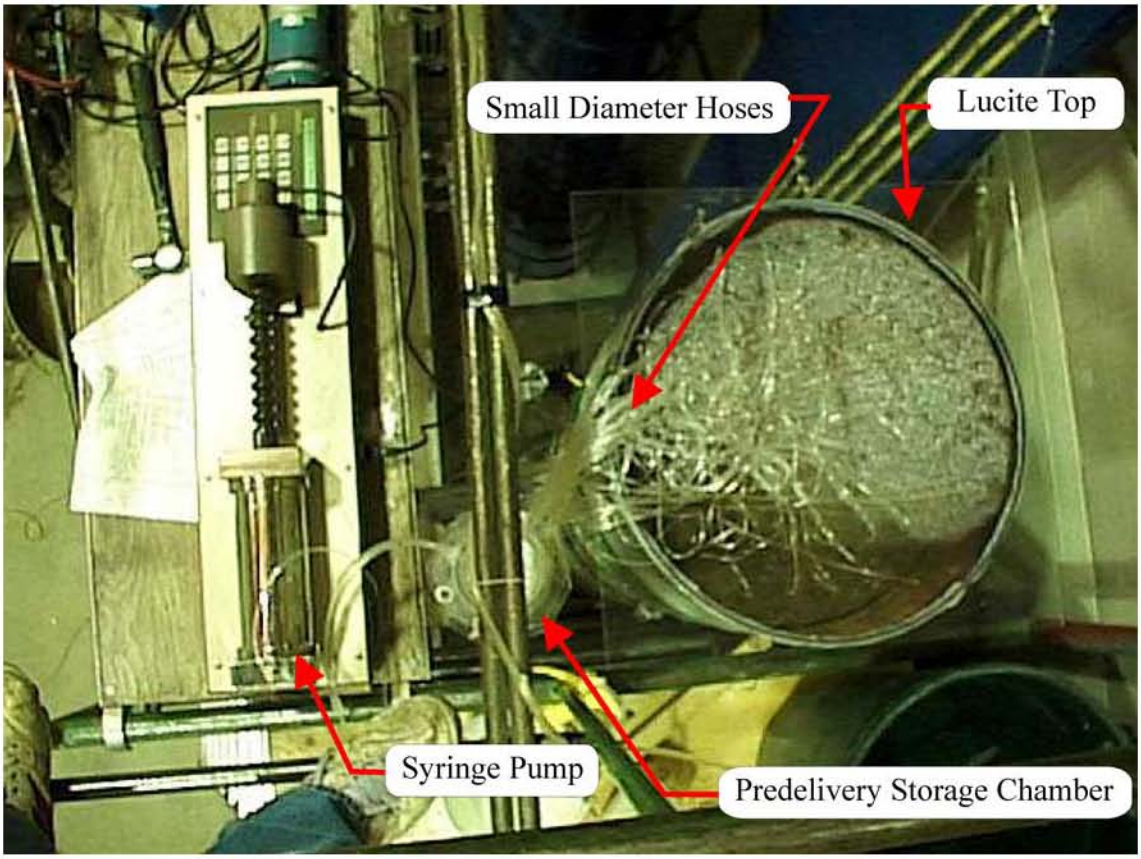

Figure 5.9 - Syringe pump system details

5.3.2.3 Tensiometers and suction measurement apparatus

The tensiometers consisted of a porous ceramic tip and a plastic body. Fittings were attached to the lysimeter such that air bubbles could be removed from the tensiometers and they could be attached to the suction measurement device. Figure 5.10 displays a schematic of the tensiometers used in the laboratory program

To measure suction the tensiometers were connected to a large manometer board via a three-way valve. The valve was hooked up so that either the suction in the tensiometer could be measured or the water level inside the manometer could be increased or decreased. The elevation of the water in the tubes on the manometer board was measured using a tape attached to the board. All elevations were reference from the floor (bottom of the manometer).

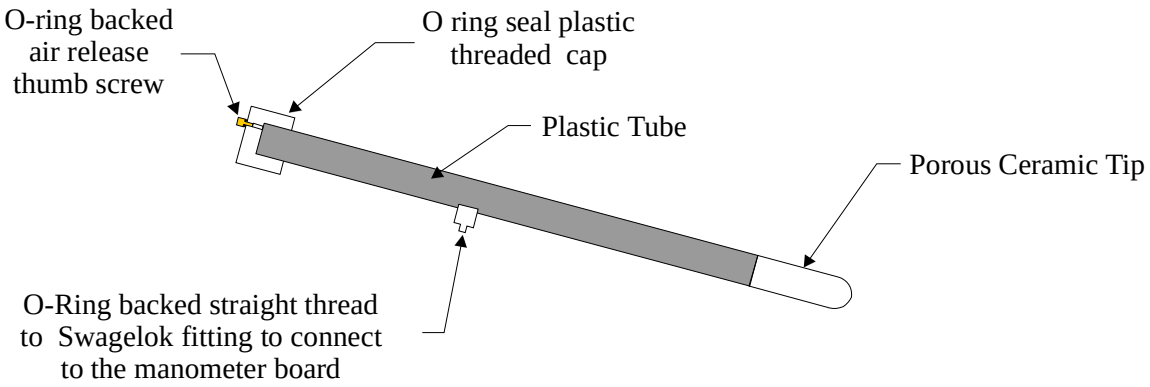

Figure 5.10 - Tensiometer schematic

5.3.2.4 Prototype standpipe lysimeter

The main body of the prototype lysimeter consisted of a 50 mm polyvinylchloride (PVC) pipe backfilled with silica flour. The bottom of the lysimeter contained a porous plastic filter to contain the silica flour and allow water to pass into the storage chamber below. The storage chamber was connected to two hoses. The top hose went to the manometer board to monitor the water level in the lysimeter. The bottom hose was attached to a valve, that when opened, allowed the lysimeter to drain freely. Figure 5.11 displays a schematic diagram of the lysimeter prototype.

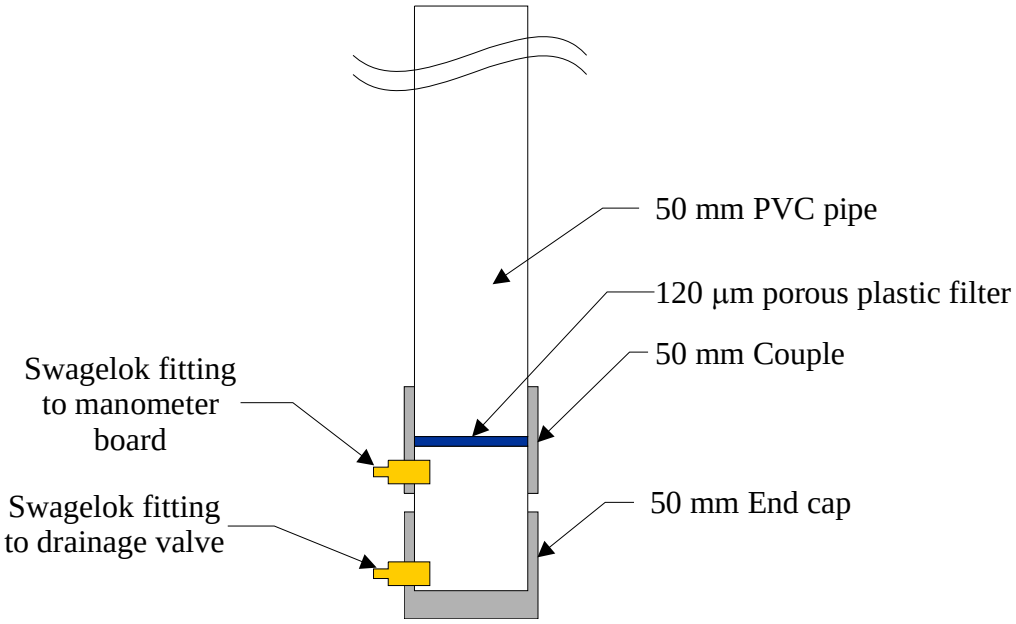

Figure 5.11 - Lysimeter schematic

The porous plastic filter was cut to size from a sheet of porous plastic. The filter was then placed into the couple and silicone was used to secure it in placed. The fittings were then cleaned using a PVC cleaner. The pipes, couples and end caps were then connected using a PVC solvent glue. A liberal amount of the glue was applied to the fittings being connected. The fittings were than pushed together. The process was completed after giving the fittings a twist to ensure that glue covered all of the internal surfaces. The Swagelok fittings were installed by drilling holes in the bottom part of the lysimeter. A tap was then used to make the appropriate threads for the fitting. The hoses extending from these fittings were protected using a piece of 50 mm x 100 mm tube steel. The tube steel was bevelled at the edges such that it fit nicely around the 2" PVC pipe. A piece of plumber's strap was used to secure the PVC pipe to the tube steel. Silicone was used to plug any holes left between the PVC pipe and the tube steel. A hole was also made in the bottom of the first barrel, so that the tube steel could be pushed through it. The barrel and tube steel joint were made water tight by applying silicone. Figure 5.12 displays the tube steel installation.

The silica flour was placed inside the lysimeter in a method analogous to that used to prepare the samples in the material characterization program. The main body of the lysimeter was extended with the use of a coupling and a short piece of pipe. These fittings were attached using silicone around the outsides of the fittings. The silica flour was slurried to 72 % solids and poured into the lysimeter. Silica flour was poured into the lysimeter until the level in the lysimeter extended well above the couple. The silica flour was allowed to settle and drain for a period of approximately 24 hrs. The sample was then vibrated by striking the PVC pipe with a rod, causing the silica flour to liquefy. This process was repeated every couple of hours until the silica flour no longer liquefied. The couple and short extension were then carefully removed.

Figure 5.12 - Bottom of prototype column showing tube steel used to protect hoses

5.3.3 Assembly of the Prototype Lysimeter Testing Apparatus

The assembly of the column progressed from the bottom up and consisted of a number of different operations that are outlined in the following sections. These operations were:

- Preparation and placement of waste rock in the column
- Installation of tensiometers
- Installation of silica flour extension
- Installation of rain simulator

5.3.3.1 Preparation and Placement of Waste Rock

The simulated fine and coarse waste rocks used in the prototype lysimeter testing apparatus are a combination of 3 different materials. The simulated fine waste rock is comprised of 5 parts of a “dirty” pit run gravel to 1 part of silica flour. The simulated

coarse waste rock is comprised of 1 part of the same “dirty” pit run gravel to 1 part of gravel screened between the ½ and 1 inch sieves. The proportions of each material (based on dry weight) was weighed and mixed together to form the simulated waste rock. The mixing was performed using the paddle type mixer shown in Figure 5.13

Figure 5.13 - Paddle type mixer

The waste rock was moisture conditioned to decrease the possibility of channelling through the waste rock due to variations in the initial water content. As a result, the waste rock was moisture conditioned to a water content that was believed to be near its residual water content. This corresponded to a gravimetric water content of 4.5 to 5 percent.

The waste rock was placed in lifts approximately 30 cm thick. The entire surface of each lift was compacted with 1 blow of a Marshall Hammer as shown in Figure 5.14. This nominal level of compaction helped reduce the total settlement in the column. To prevent the material at the top of the lift from becoming a barrier to water flow (due to the formation of a smooth compacted layer at the top), the surface was roughened using a trowel.

5.3.3.2 Installation of Tensiometers

The tensiometers were installed as the level of the waste rock inside the columns rose to the level of the steel ports on the outside of the column. A small channel was dug in the waste rock to accommodate the tensiometer. The middle of the porous ceramic tip was positioned halfway between the wall of the column and the lysimeter. A handful of waste rock material passing the #4 sieve was packed around the porous ceramic tip. This ensured contact between the porous ceramic tip and the surrounding waste rock. Figure 5.15 displays a tensiometer being installed.

Figure 5.14 - Compacting waste rock with a Marshall Hammer

Once the tensiometers were installed in the waste rock, cardboard was wedged into the space between the steel port and the tensiometer. A generous amount of silicone was then used to make a seal between the tensiometer and the steel nipple.

5.3.3.3 Installation of Silica Flour Extension

The silica flour extension in the fine waste rock consisted of only silica flour. The silica flour extension in the coarse waste rock column was constructed with the 60% sand - 40% silica flour mixture. The procedure for placing the two different materials was the same.

Figure 5.15 - Installation of a tensiometer

Prior to the waste rock reaching a height equal to the top of the lysimeter, a pipe extension was placed on the lysimeter. When the waste rock height reached a level equal to 0.5 m above the top of the lysimeter, the silica flour extension was placed. The silica flour was placed by slurrying the silica flour to 72% solids (82% for sand-silica flour mixture) and pouring it into the extension. The extension was then slowly lifted out as the slurry was being poured in. A rod was used to gently tap the slurry down. Once the slurry had reached to the top of the waste rock, it was allowed to settle for a period of 1 hour. As the silica flour consolidated, more silica flour was poured into the hole until it was flush with the waste rock.

5.3.3.4 Installation of Rain Simulator

Once the waste rock within the column reached the top of the last barrel, the lucite cover component of the rain simulator was placed on top. The lucite cover was connected to the column by a bead of silicone placed around the top edge of the last barrel.

CHAPTER 6 PRESENTATION AND DISCUSSSION OF RESULTS

6.1 Introduction

This chapter presents the results of the laboratory testing program. The first section presents the results from laboratory tests used to characterize the materials in the prototype lysimeter. The second section relates directly to the results obtained during testing of the prototype lysimeter design.

6.2 Laboratory Test Results

The results from the laboratory testing program are presented in this section and are grouped according to material type.

6.2.1 Silica Flour

The silica flour was the most extensively tested material in the research program. Figure 6.1 displays the grainsize curve for silica flour. The graph shows that the gradation of the silica flour used in this study closely resembles the silica flour used by Newman (1996).

The soil-water characteristic curve obtained for the silica flour is shown in Figure 6.2, along with the curve obtained by Newman (1996). It can be seen that the two soil-water characteristic curves were very similar. The curve obtained by Newman displayed a higher initial porosity than the silica flour tested in this study. This may be the result of different methods of preparing the sample. The silica flour tested in this study had an air entry value of approximately 30 kPa, while the sample tested by Newman (1996) had an

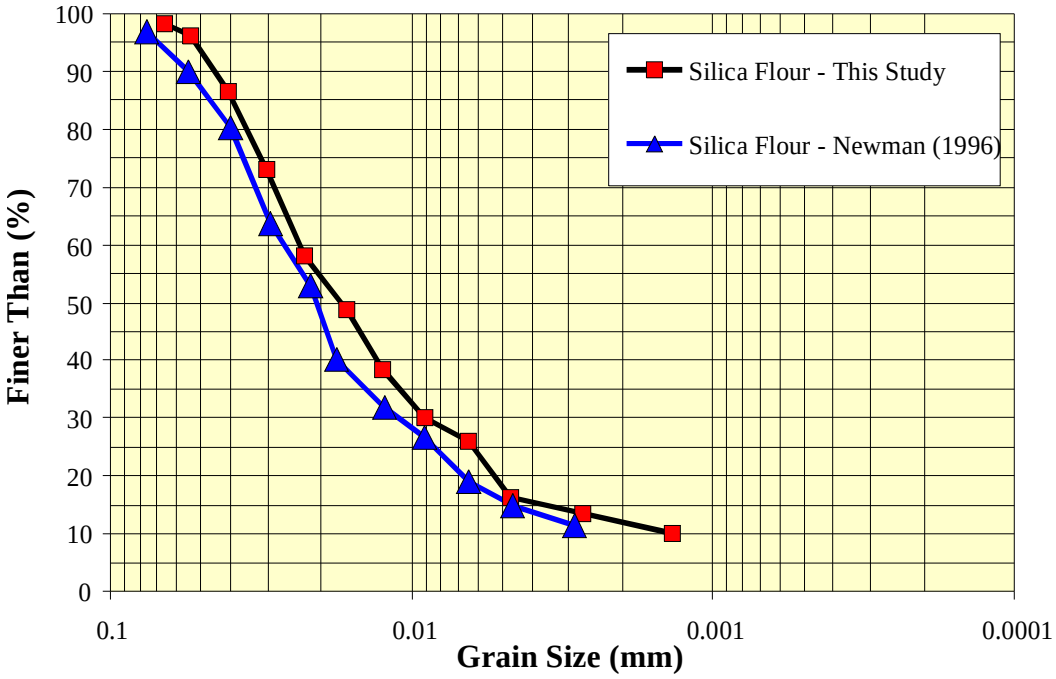

Figure 6.1 - Grainsize of silica flour

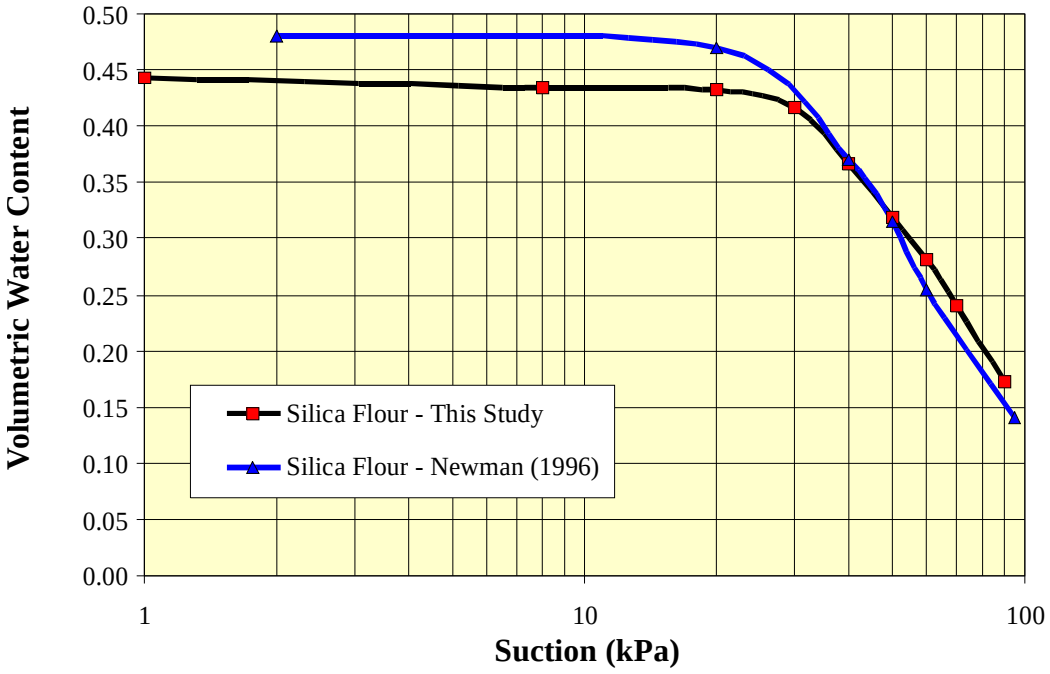

Figure 6.2 - Soil-water characteristic curve of silica flour

air entry value of approximately 25 kPa. This can be explained by the slightly lower initial porosity and finer grain size measured for the silica flour that was used in this study. The two curves display very similar attributes after the air entry value and would likely have comparable suctions at their residual water contents.

The results from the constant head hydraulic conductivity test are shown in Figure 6.3. A linear regression was performed on the data to determine of the slope of the graph. The results of this analysis indicate that the hydraulic conductivity is 1.8 E-7 m/s

The data from the falling head test performed on the lysimeter column is presented in Figure 6.4. The axes of the graph correspond to the form of the equation for the falling head test as put forth by Freeze and Cherry (1979). The equation used was:

$$K = \frac{aL}{At} \ln(\frac{ho}{h}) \quad \text{..... Eq. 6-1}$$

Where: K = saturated hydraulic conductivity (m/s)

a = cross sectional area of the graduated cylinder (m)

L = length of the sample (m)

A = cross sectional area of the sample (m^2)

t = time (s)

ho = Initial height of water in the graduated cylinder (m)

h = height of water in the graduated cylinder at any given time (m)

The falling head test was only run for a limited time with only 6.5% of the excess head being dissipated. The resulting hydraulic conductivity of 1.3 E-7 m/s compares well with the value of 1.8 E-7 m/s recorded in the constant head test.

Newman (1996) also performed saturated hydraulic conductivity tests on silica flour. The results of testing performed by Newman (1996) have been combined with testing from this study and are shown in Figure 6.5. This figure shows the expected trend that as the void ratio decreases the hydraulic conductivity also decreases. However, the order of magnitude decrease in hydraulic conductivity reported by Newman (1996) for a

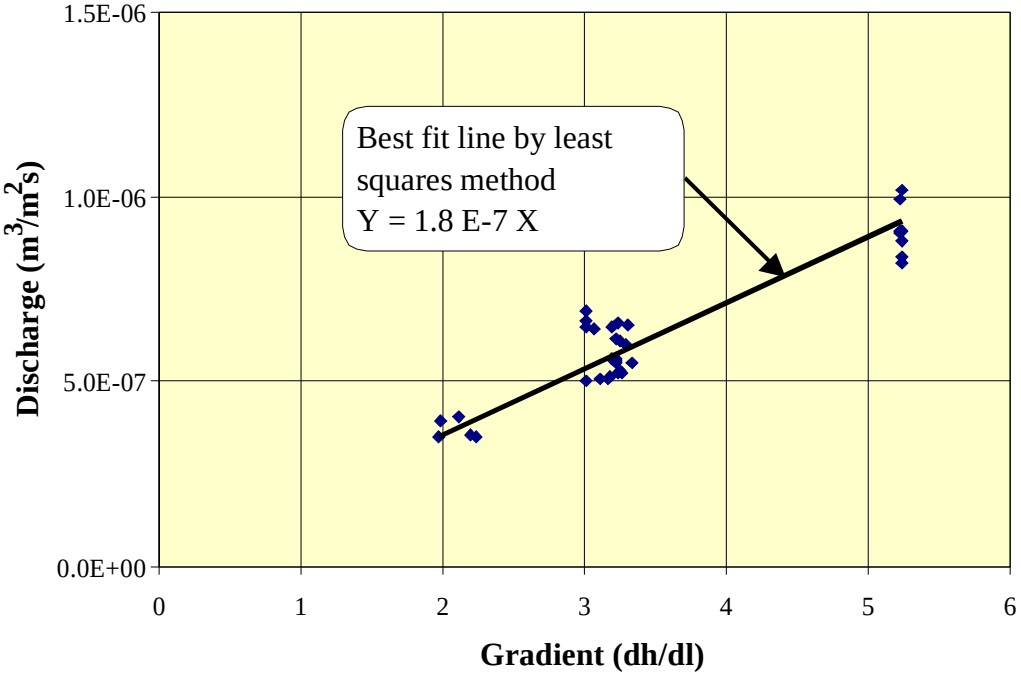

Figure 6.3 - Constant head test results

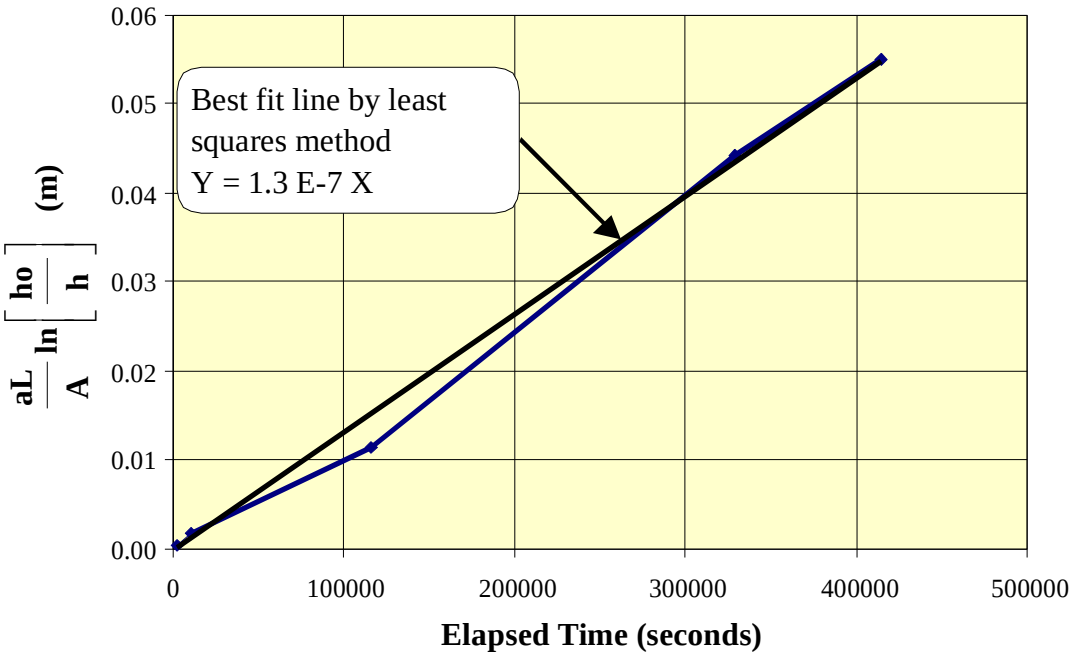

Figure 6.4 - Falling head test results

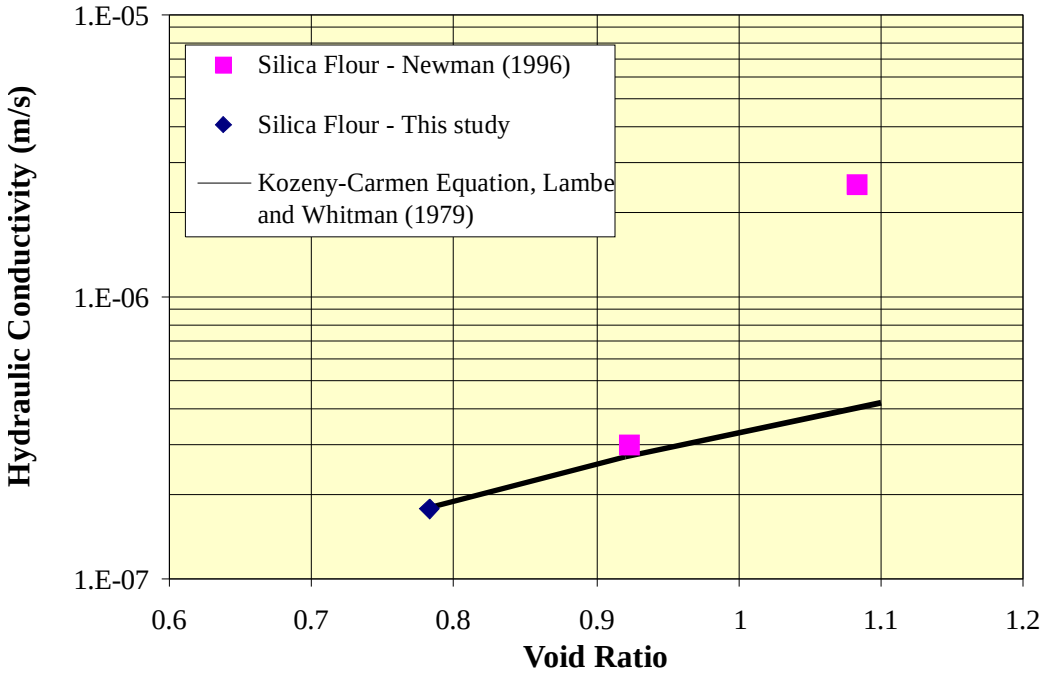

Figure 6.5 - Void ratio versus hydraulic conductivity for silica flour

change in void ratio from 1.08 to 0.92 seems high. A general trend line which corresponds to the Kozeny-Carmen equation described by Lambe and Whitman (1979) was added through the two data points with the lowest void ratio. This trend line would suggest that the slope of hydraulic conductivity and void ratio line should be flatter than that described by the Newman (1996) data for a void ratio of 1.09.

The results of consolidation testing are displayed in Figure 6.6. The data appears reasonable with the exception of the final unloading portion of the curve. It was noted during the last loading increment that silica flour had pushed up between the consolidation ring and the porous disk. It is assumed that caused the uncharacteristic curve shown during the final unloading portion of the graph. As a result, the data from the final unloading has not been used in the analysis.

The values of the coefficient of volume change (m_v) over different loading intervals are shown in Table 6.1. When the lysimeter is placed in the field it will be subjected to some initial overburden stress. Assuming that no other forces influence the stress state of the

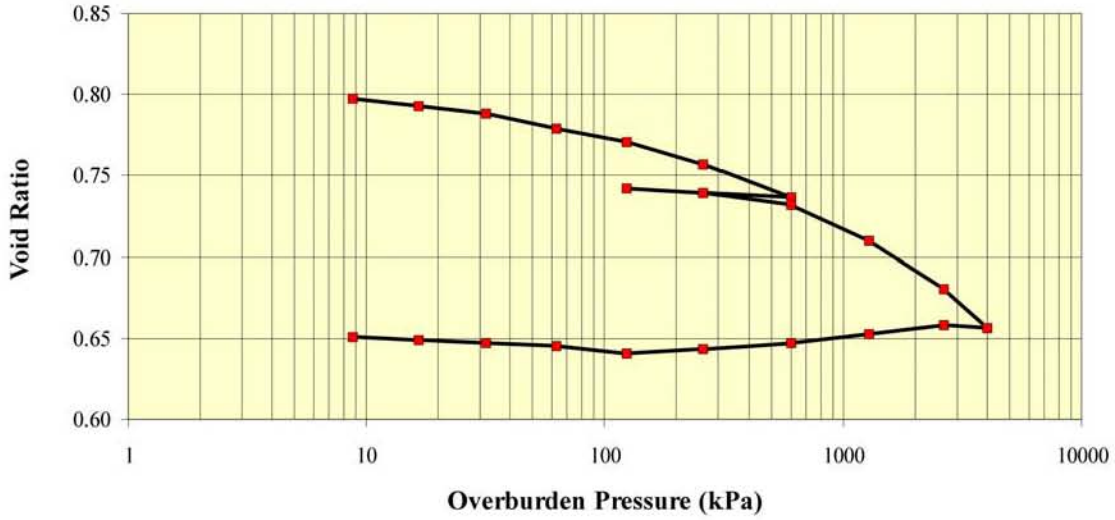

Figure 6.6 - Silica flour consolidation curve

Table 6.1 - Consolidation testing results

Overburden Pressure (kPa)	Void Ratio	av (/kPa)	mv (/kPa)
0	0.801		
8.8	0.797	4.6E-04	2.5E-04
16.5	0.793	5.6E-04	3.1E-04
31.8	0.788	2.9E-04	1.6E-04
62.5	0.779	3.0E-04	1.7E-04
124.0	0.770	1.4E-04	8.0E-05
259.8	0.757	1.0E-04	5.5E-05
599.7	0.737	5.9E-05	3.3E-05
259.8	0.739	7.3E-06	4.0E-06
124.0	0.742	2.2E-05	1.2E-05
259.8	0.739	2.2E-05	1.2E-05
599.7	0.732	2.2E-05	1.2E-05
1278.0	0.710	3.2E-05	1.8E-05
2635.0	0.680	2.2E-05	1.2E-05
3992.8	0.656	1.8E-05	9.7E-06
2635.0	0.658	1.6E-06	8.6E-07
1278.0	0.652	-4.3E-06	-2.4E-06
599.7	0.647	-7.0E-06	-3.9E-06
259.8	0.643	-1.2E-05	-6.9E-06
124.0	0.641	-1.7E-05	-9.4E-06
62.5	0.645	6.3E-05	3.5E-05
31.8	0.647	7.5E-05	4.1E-05
16.5	0.649	1.3E-04	7.3E-05
8.8	0.651	2.1E-04	1.2E-04

lysimeter, the only changes in effective stress would be due to the water table inside the lysimeter rising and falling. As a result, the portion of the curve that most closely resembles the lysimeter in the field is the reloading portion of the curve. The value of the coefficient of volume change for the first reloading cycle as shown Table 6.1 is approximately 1E-5 /kPa. Lambe and Whitman (1979) report values for the constrained secant modulus ($1/m_v$) of 35 to 75 MN/m^2 for a silt material. These values correspond to coefficients of volume change of approximately 1E-5 to 3 E-5 /kPa, which corresponds well with the values determined from this test.

6.2.2 60% Sand, 40% Silica Flour Mixture

The 60% sand, 40% silica flour mixture was used as the silica flour extension in the coarse gradation prototype test column. Figure 6.7 displays the grainsize curve for sand, silica flour and the sand - silica flour mixture. The proportions of the 40% sand to 60% silica flour mixture were based on a "rule of thumb" which suggests that the finest 30% of a mixture controls the soil-water characteristic curve. The soil-water characteristic curve for the sand - silica flour mixture is shown in Figure 6.8. In comparison to the soil-water characteristic curve for the silica flour there are some notable differences. The air entry value of the sand-silica flour mixture is approximately 10 kPa compared to 30 kPa for the silica alone. The effect of having a lower air entry value material in the silica flour extension is that at suctions greater than the air entry value the hydraulic conductivity of the mixture will decrease causing a decrease in the equivalent collection area ratio. Another notable difference in the two soil-water characteristic curves is the differences in the initial porosity. The decrease in porosity in the sand - silica flour mixture results in less water in the lysimeter. As a result, if this material were used as the lysimeter backfill, the time to flush the lysimeter could be reduced by the ratio of the initial porosities. Despite the low air entry value, a review of the data shows promise for future mixes containing a higher percentage of silica flour. The low air entry value indicates that the sand matrix is not entirely full of the silica flour. Adding more silica flour to the mixture would reduce the air entry value and should also reduce the initial porosity as well as decrease the coefficient of volume change. This would result in a better lysimeter performance due to decreased volume change and storage requirements.

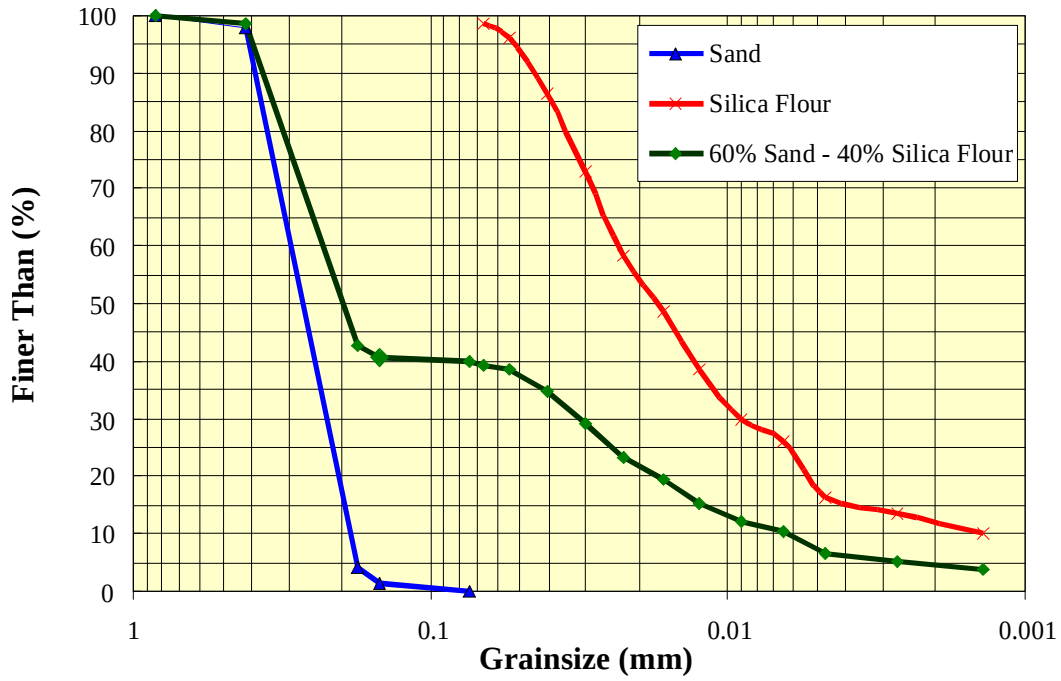

Figure 6.7 - Grain size curve of sand - silica flour mixture

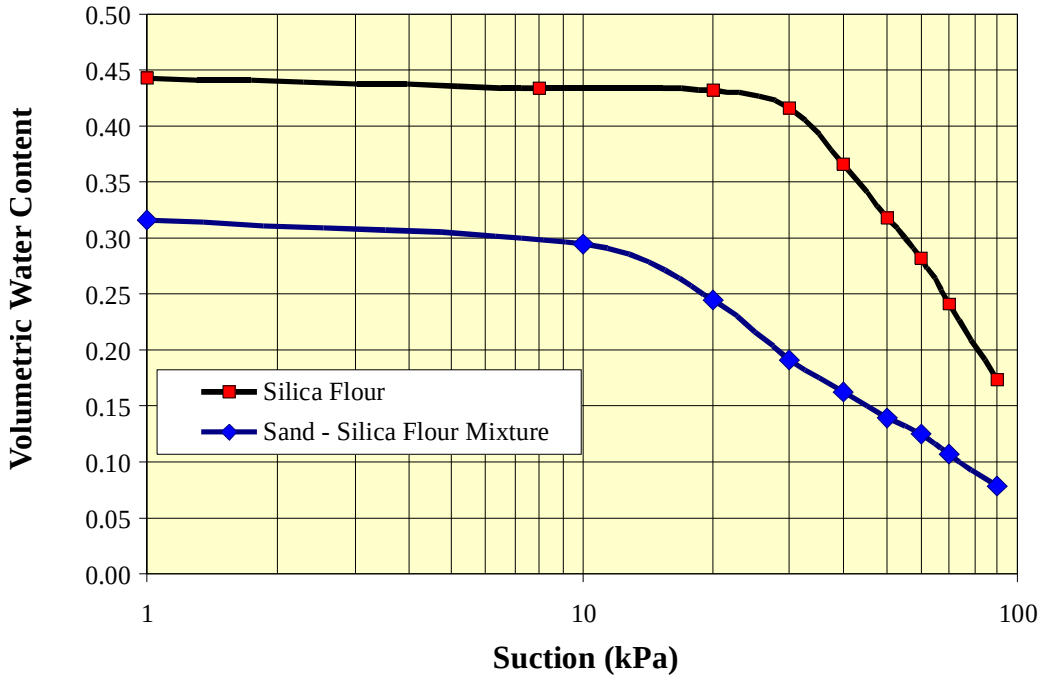

Figure 6.8 - Soil-water characteristic curve for sand-silica flour mixture

The results of the constant head hydraulic conductivity testing are shown in Figure 6.9. As might be anticipated from the results of the soil-water characteristic curve testing, the hydraulic conductivity of the sand-silica flour mixture (9 E-7 m/s) is higher than that of the silica four (1.8 E-7 m/s) by itself.

Filter testing was performed on the sand-silica flour mixture to ensure that the material would not be washed away into the coarse waste rock. The results of this testing are displayed in Figure 6.10. During the initial stage of the test a modest amount of soil was washed out of the test column. This is thought to be primarily a result of flushing out any particles present in the filter. This was followed by a dramatic decrease in the amount of soil lost with time to a level of less than 0.25 g in 29 days. The hydraulic gradient used in this experiment (approximately 3) was higher than that anticipated in the field (approximately 1). The small amount of soil lost during testing using conservative testing parameters indicates that the washing of the sand-silica mixture into the waste rock should not be a problem.

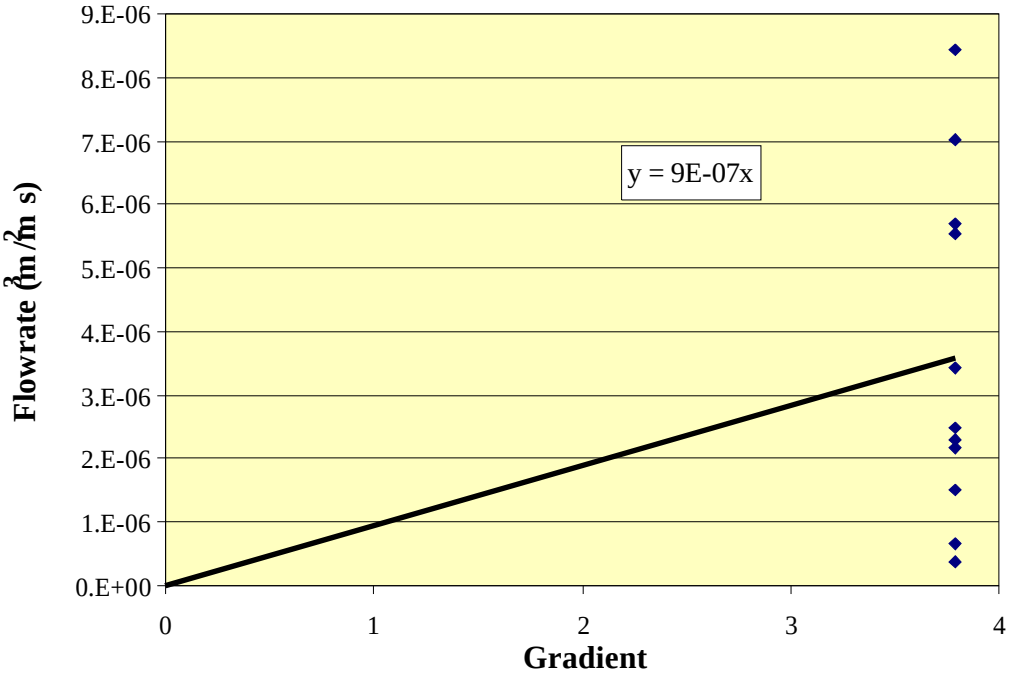

Figure 6.9 - Constant head testing results for sand-silica flour mixture

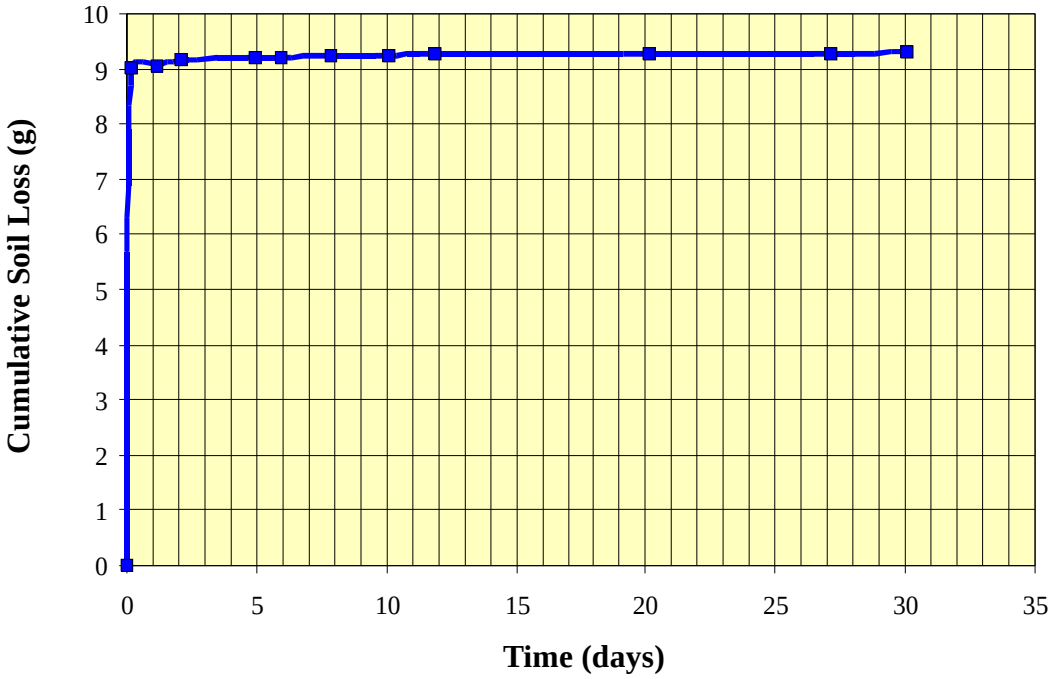

Figure 6.10 - Filter test results of sand-silica flour mixture

6.2.3 Cluff Lake Waste Rock

Figure 6.11 presents the results of the grainsize analysis performed on the Cluff Lake waste rock along with the gradation of the fine and coarse waste rock used in the prototype test columns. It can be seen that the Cluff Lake sample has a gradation that lies within the gradations used to test the prototype.

From the grainsize curve it is possible to classify the waste rock using Herasymiak's (1996) classification of waste rock as shown in Table 2.2. The Cluff Lake sample (% finer than 4.75 mm sieve ≈ 33, % finer than 2 mm sieve ≈ 23) falls into the transition zone between soil like behavior and rock like behavior. This would suggest that the soil-water characteristic curve for the Cluff Lake waste rock should have an air entry value of less 0.1 and a relatively long gradually decreasing water content with increasing suction. Figure 6.12 displays the soil-water characteristic curve for the Cluff Lake sample. It would appear from this graph that the air entry value is approximately 1 kPa. However, one of the limitations of working with coarse grained soils is that the sample must be of a sufficient height to contain all of the particles. As a result, samples

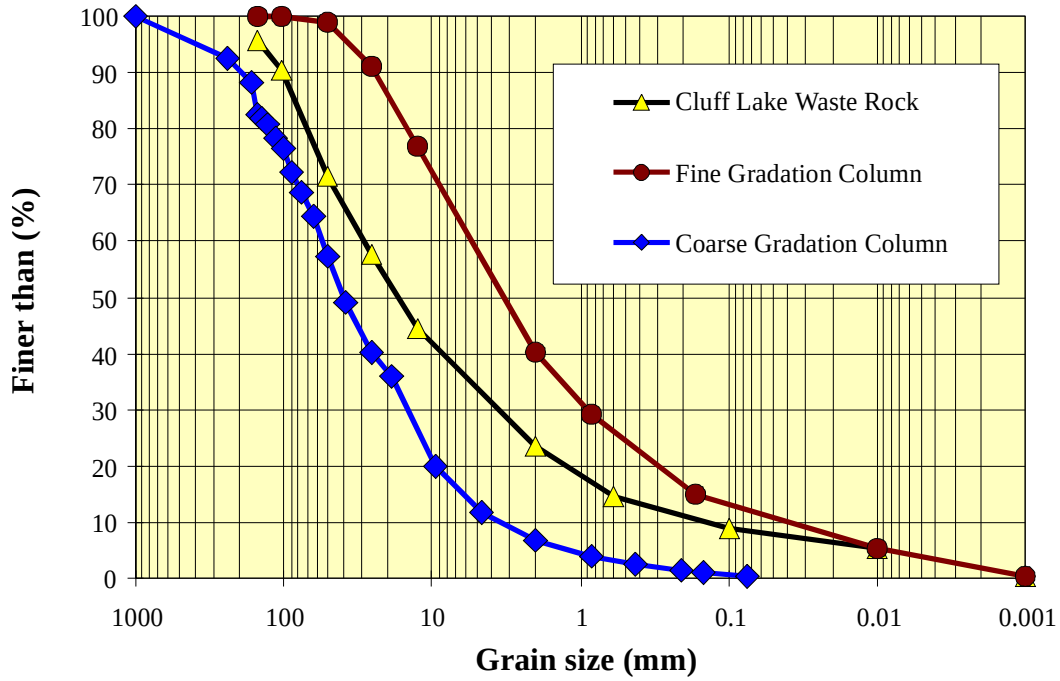

Figure 6.11 - Cluff Lake waste rock gradation

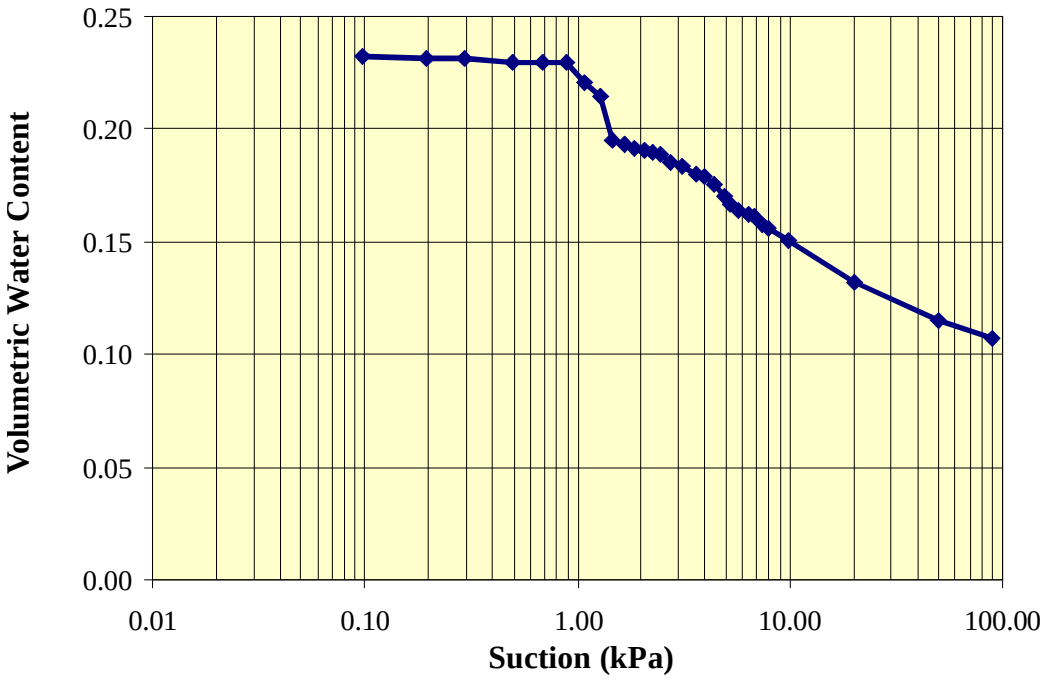

Figure 6.12 - Soil-water characteristic curve for Cluff Lake waste rock

generally have a minimum height of 10 to 15 cm. This can cause a 1 to 1.5 kPa difference in suction from the top to the bottom of the sample under hydrostatic conditions. The value of suction that is recorded, is dependent on the position of the datum used (i.e. top of sample, middle of sample, bottom of sample). As coarse samples generally have a low air entry value (<5 kPa), the choice of the datum has a major impact on the observed air entry value. Herasymiak (1996) chose his datum to be the bottom of the sample. The datum for this testing was the top of the sample. The top was chosen because it reflects a condition where the degree of saturation is equal to 1 at a suction of 0 kPa. If the bottom had been chosen, the degree of saturation would have been much less than 1 at a suction of 0 kPa. The top was used as the datum for all waste rock samples in this study. Considering the difference in the datums used in the two studies, it can be said that this waste rock corresponds well to the transition material described by Herasymiak (1996).

6.2.4 Waste Rock used in Fine Column

The waste rock used in the fine column was the combination of two materials that were predicted to have a combined grainsize that corresponds to the fine edge of the waste rock gradation envelope found in the literature. The predicted grainsize of the fine waste rock column with the plus 25 mm fraction removed is shown in Figure 6.13. The grainsize of the actual column is given by composite sample #1 to #4. These composite samples are the result of combining smaller samples from each mix used in constructing the column. The last batch was the material that was left over from the last mix. As can be seen from this graph, the actual gradation of the fine waste rock used in the column is slightly finer than the predicted grainsize curve. The largest difference (approximately 10%) between the predicted and actual grainsize curves occurred in the fine sand range. This could be due to a number of causes. The “dirty” gravel may have contained slightly more fine sand than the original sample. Alternatively, the mixing process may have broken down the rock so that it contains a slightly higher fine sand content.

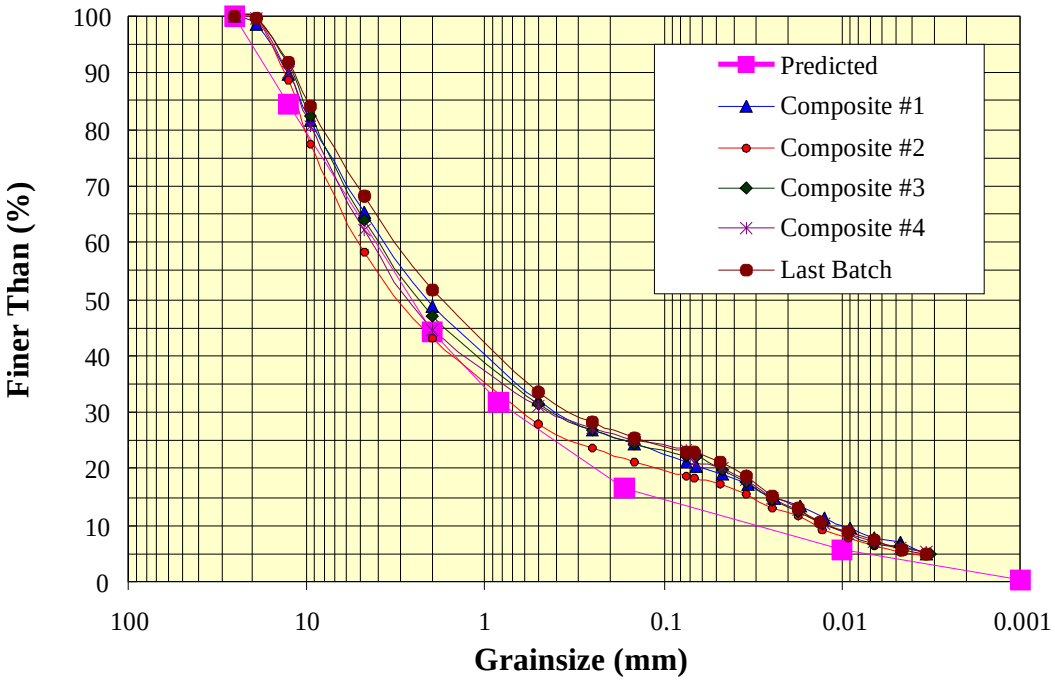

Figure 6.13 - Grainsize of fine column

Two soil-water characteristic curves were generated for the fine column using a single composite sample (a combination of all of the composite samples) and a sample from the last batch. The results of this testing are shown in Figure 6.14. The two samples agree fairly well with one another with air entry values between 1 and 3 kPa. Both samples showed slowly decreasing volumetric water contents as the suction was increased. No well defined residual water content seems to exist at values of suction of less than 100 kPa. With respect to Herasymiak's (1996) classification of waste rock, this waste rock would fall within the soil like category (4.75 mm > 50%, 2 mm > 20%) as shown in Table 2.2. Given the differences in the datums used in the two testing programs, as discussed in section 6.2.3, these soil-water characteristic curves follow the trends for waste rock indicated by Herasymiak.

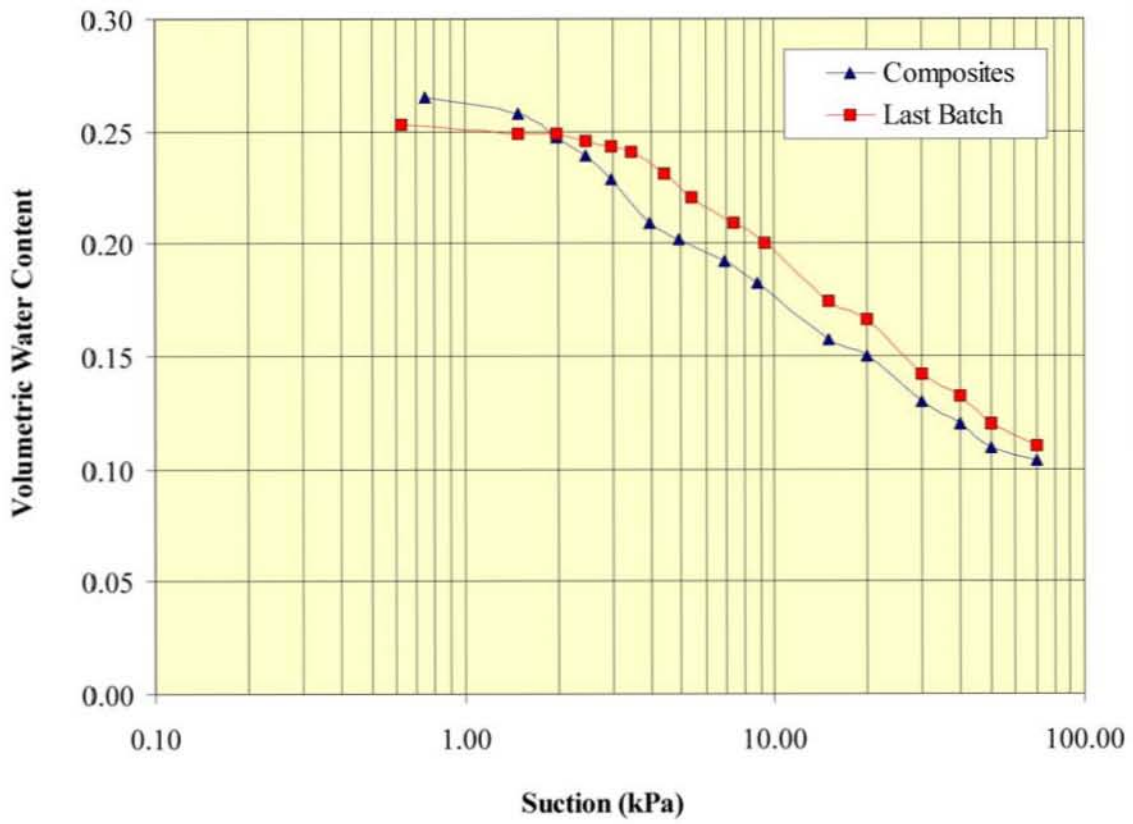

Figure 6.14 - Soil-water characteristic curve results for fine waste rock

6.2.5 Waste Rock used in Coarse Column

The predicted grainsize of the coarse waste rock column, with the plus 25 mm fraction removed, is shown in Figure 6.15. For the coarse column, each mix (excluding the first 2 mixes) used to construct the column was sampled and the results of the grainsize analysis are shown as mix #3 through #12. As with the fine samples, the actual gradation of the coarse waste rock used in the column was slightly finer than the predicted grainsize curve . The largest difference (approximately 5-7%) between the predicted and actual grainsize curves occurred in the fine sand range. The possible reasons for this difference were discussed in the previous section.

Duplicate soil-water characteristic curves were generated for the coarse column from samples that were prepared to the grainsize of the predicted curve. The results of this testing is shown in Figure 6.16. The duplicate samples are in close agreement and have

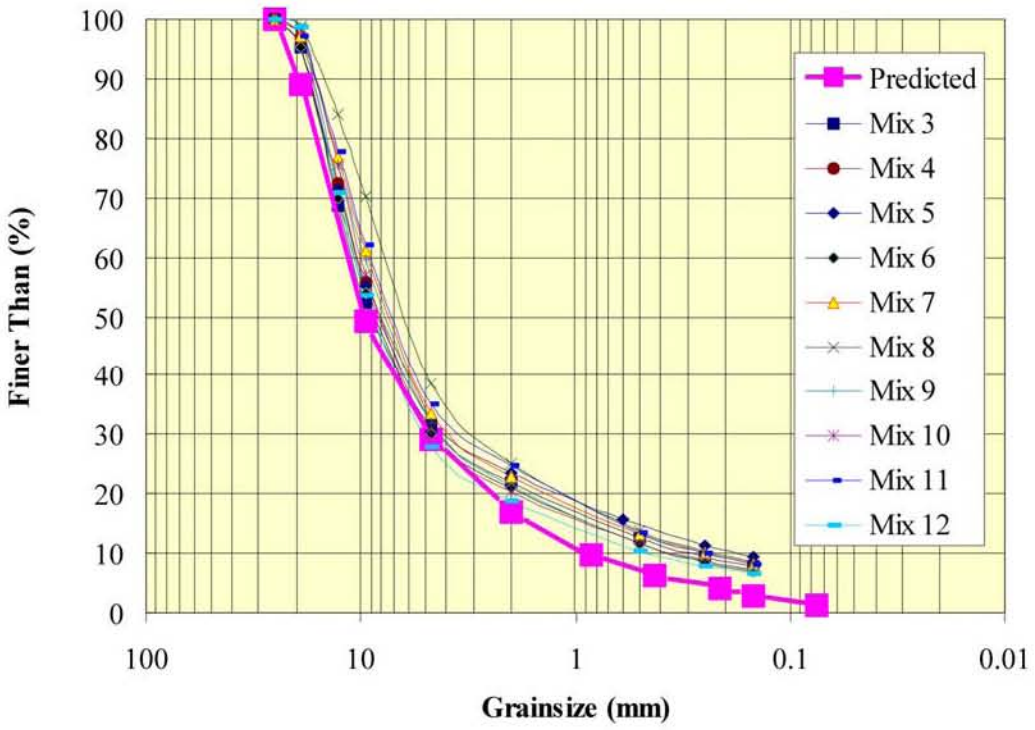

Figure 6.15 - Grainsize analysis of waste rock in coarse column

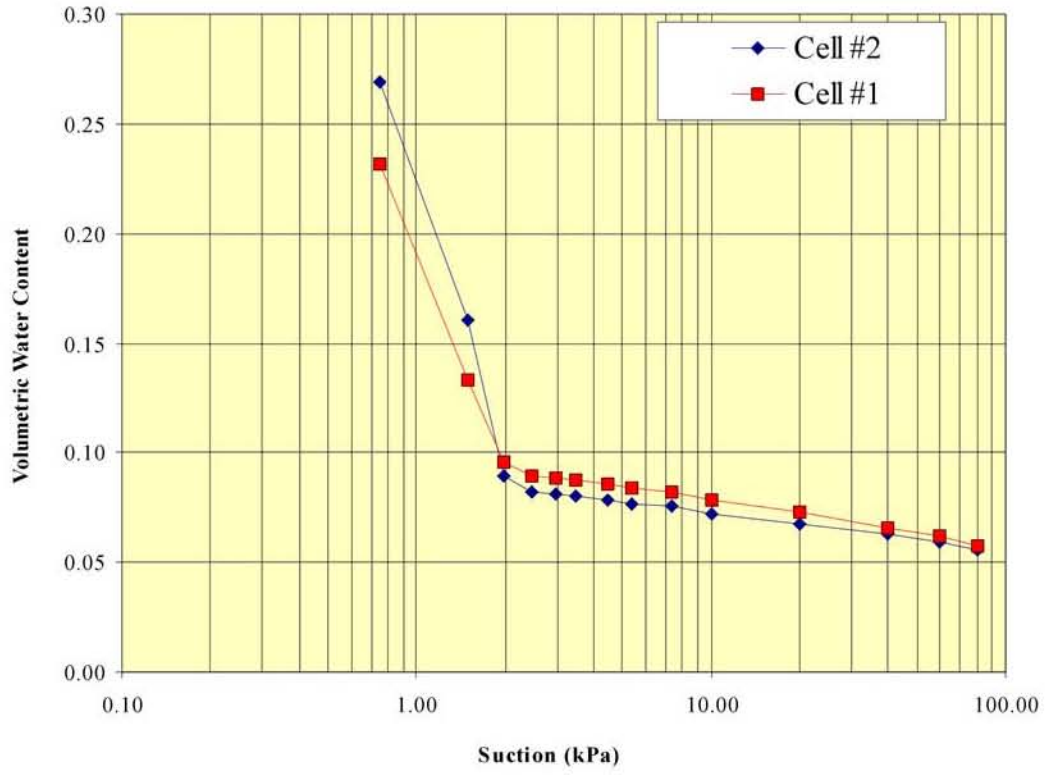

Figure 6.16 - Soil-water characteristic curve results for coarse waste rock

air entry values below 1 kPa. Both samples showed a rapid decrease to their residual volumetric water content at a suction of approximately 2 kPa. With respect to Herasymiak's (1996) classification of waste rock, this waste rock would fall on the border between the rock like and the transition category (4.75 mm = 28 - 35%, 2 mm = 18 - 22%) as shown in Table 2.2. The soil-water characteristic curve, however, indicates that this material belongs to the rock like classification as identified by the steep slope to the residual water content at a suction of approximately 2 kPa.

6.3 Prototype Lysimeter Test Results

The following sections present the results of the testing program for the prototype standpipe lysimeter. This section has been broken into two major subsections. The first subsection presents the results for the fine column and the second subsection presents the results for the coarse column. All of the data collected during column testing is available in Appendix B

6.3.1 Fine Column

The soil suction within the fine column was controlled by varying the applied flux rate. The test results obtained for each of the flux rates are presented in separate sections. These sections will focus primarily on the suction measurements within the column. The approximate flux rates used during the testing of the fine column were 4 E-7 m/s, 8 E-8 m/s, 1 E-8 m/s and 1 E-9 m/s. The final subsection deals with the measurements made during collection of the pore water sample. The focus of this section will be on the equivalent collection area ratios measured in the column under different flux rates.

6.3.1.1 Soil Suction Measurements under a Flux Rate of 4 E-7 m/s

The initial flux rate was chosen to be approximately equal to the saturated hydraulic conductivity of the fine waste rock. The cumulative inflow and outflow from the column are shown in Figure 6.17 . An arbitrary flux of 3 E-6 m/s was initially applied to the top of the column. This flux rate produced ponding on the top of the column during days one through four. As a result, the flux rate was lowered on day four to 3 E-7 m/s. This flux rate allowed the ponded water to dissipate over the next 6 days. A slightly higher flux

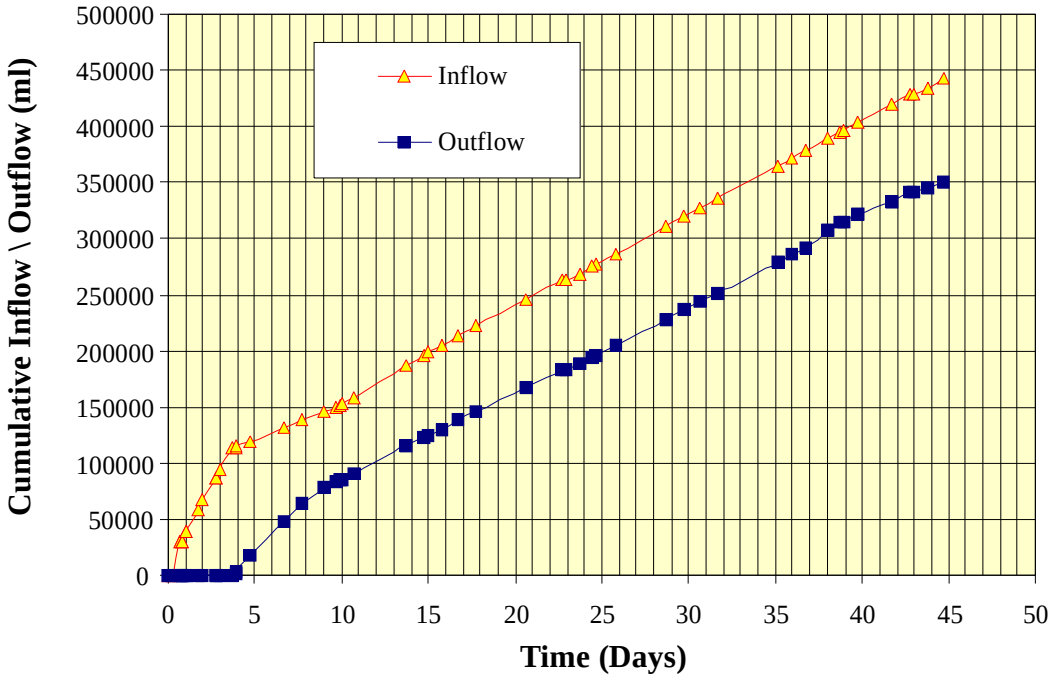

Figure 6.17 - Cumulative flow rates at a flux rate of 4 E-7 m/s

rate of 6 E-7 m/s was attempted around the 10 day mark and resulted in ponding on the column. Consequently, the flux rate was reduced to 4 E-7 m/s. A comparison of the slope of the cumulative outflow plot between time periods four to ten days and from ten days on would suggest that the hydraulic conductivity of the soil is likely closer to 7.7 E-7 m/s. Water droplets falling from the rain simulator on to the top of the column may have washed fines into the soil matrix thereby reducing the hydraulic conductivity at the surface of the column. As all the water must pass through this interface this would reduce the maximum flux that could be applied to the column without ponding. The outflow from the column was approximately equal to the inflow after ten days of the testing, indicating that the column was under steady state conditions.

The pressure profiles recorded by the tensiometers and lysimeter with time are displayed in Figure 6.18. The data plotted on this graph has been selected from the entire data set in order to display the general trends in the soil suction data. Figure 6.19 displays additional data, which is indicative of the entire data set. Figure 6.18 has been plotted starting at the point in time where the flux rate was set to approximately 4 E-7 m/s. At that point in time, the column had been draining under the lower flux rate for a number of days and was almost saturated at a suction of approximately 3 kPa. The suctions

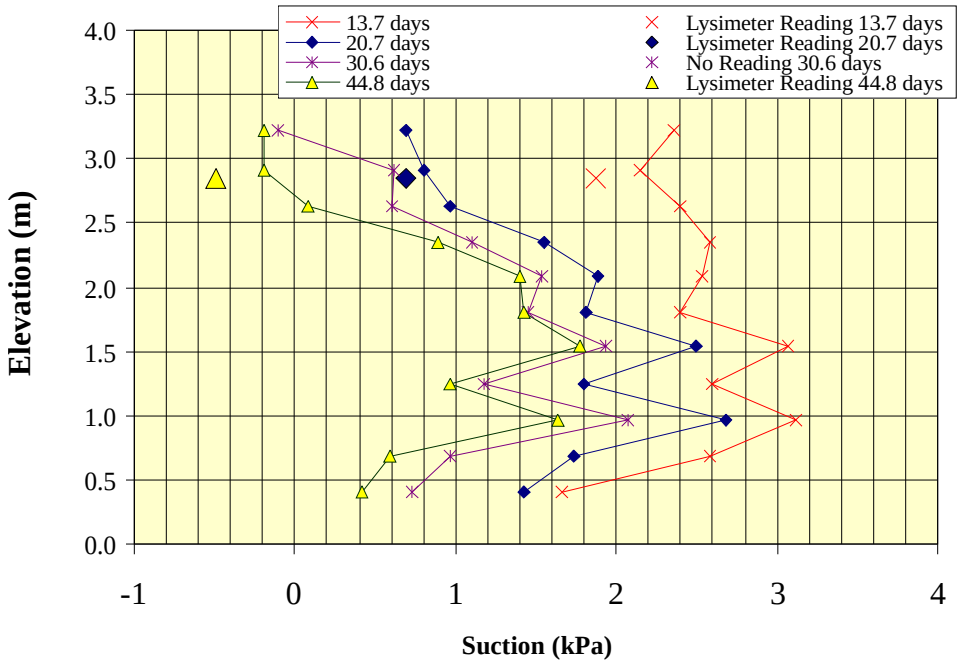

Figure 6.18 - Pressure profiles in the fine column with time at a flux of 4 E-7 m/s

decreased with time as the volumetric water content of the waste rock increases. The final suction measurement at 44.8 days showed a profile which had a suction of 0 kPa at the top and 1.5 kPa near the middle of the column. This variation in suction may be due to heterogeneity in the column. It should be noted that the lysimeter suction measurement always reads slightly lower than the tensiometer suction measurements. This is in agreement with the results of the preliminary modelling. The response time of the lysimeter to changing suctions in the soil compares well to the tensiometer response times.

Figure 6.19 displays all of the data collected at this flux rate for Tensiometers #9 and #10, as well as the lysimeter. The top of the lysimeter was located between Tensiometer #9 and #10. Tensiometer #9 and #10 were located at elevations of 2.633 m and 2.906 m respectively, with the lysimeter being at an elevation of 2.842 m. The daily inflow and outflow rates from the column are illustrated on the secondary y-axis of Figure 6.19.

There appeared to be a slight lag in the response time of the lysimeter to changing suction measurements during the initial 15 days of the test. This may be due to the entire

system coming to steady state conditions under the initial flux rate. The response time of the lysimeter can also be observed after completion of the measurement of the equivalent collection area ratio. During this measurement the lysimeter was drained and the flowrate recorded. The lysimeter returned to values comparable to those of the tensiometers within 6 days after the measurement of equivalent collection area ratio testing. The values of suction measured by the lysimeter were lower than those recorded by the tensiometers. Theoretically, at this flux rate the soil suction measured at Tensiometers #9 and #10 should be the same. The slightly lower readings measured by the lysimeter were in agreement with the results of the preliminary modelling. When the lysimeter was allowed to come to equilibrium, the suctions measured by the lysimeters compared within less than 0.5 kPa of the suctions recorded by the tensiometers.

From the inflow and outflow plot, it can be seen that the outflow becomes slightly erratic towards the end of the testing at this flux rate. This was most likely caused by the growth of biological films at the bottom outlet on the column. The impacts of clogging

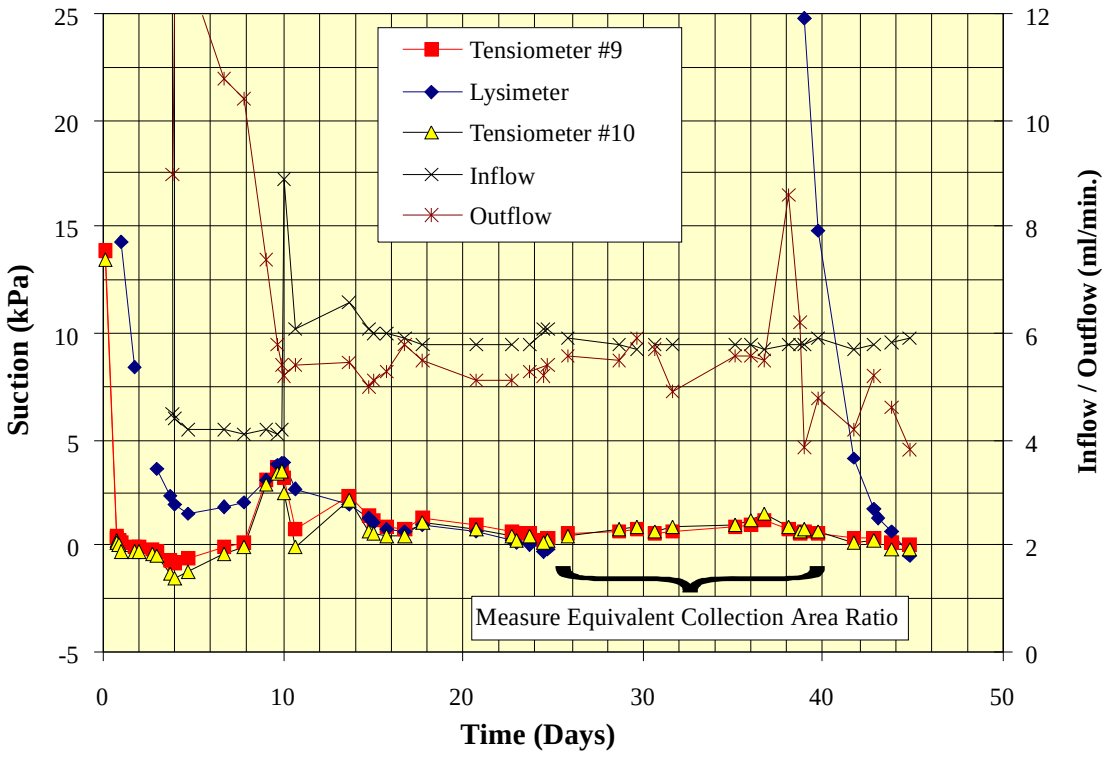

Figure 6.19 - Data collected from fine column at a flux rate of 4 E-7 m/s

at the base on the pressure profiles are more pronounced during the application of the next flux rate.

6.3.1.2 Soil Suction Measurement at a Flux Rate of 8 E-8 m/s

The flux rate of 8 E-8 m/s was the lowest flux rate that could consistently be applied using the peristaltic pump rain simulator setup. The cumulative inflow and outflow of the column at this flux rate is shown in Figure 6.20. The bottom collection pan became clogged with organic material at the beginning of the application of this flux rate,. As a result, the bottom pan was removed and cleaned. Sodium hypochlorite (bleach) was then added to the rain simulator water at a concentration of at least 5 mg/l in order to eliminate any biological growth present in the column. Outflow readings resumed at an elapsed time of 56 days. However, by this time it can be seen that the inflow and outflow to the column had already stabilized indicating that the column was at a steady state condition.

Figure 6.21 displays a graph of pressure profiles at selected time intervals to illustrate the change in the pressure profile as a result of changing the applied flux rate. From this

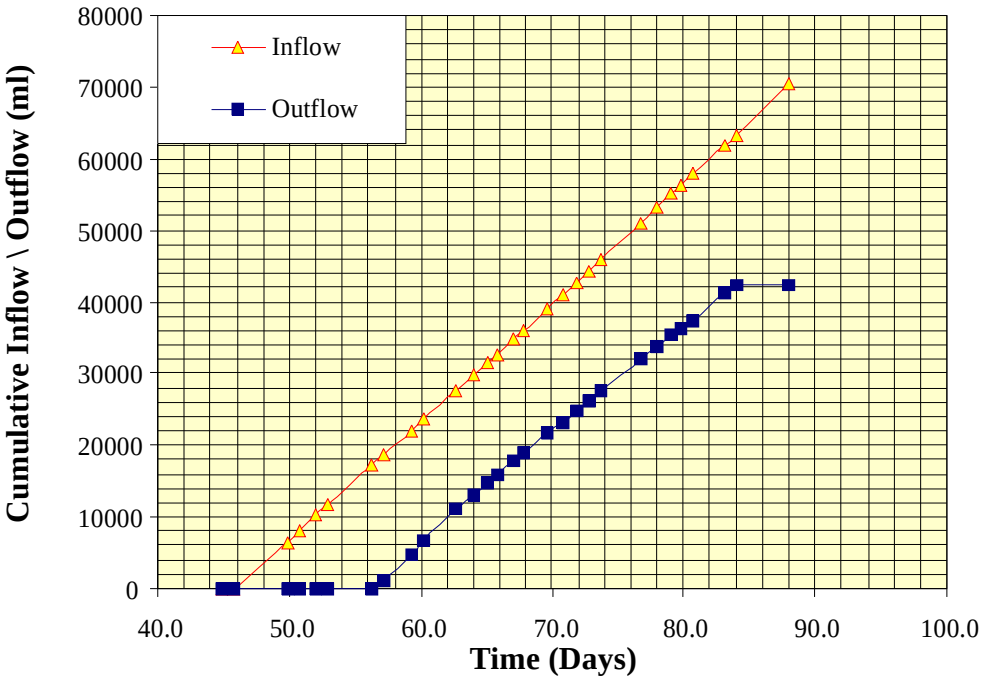

Figure 6.20 - Cumulative flow rates at a flux rate of 8 E-8 m/s

graph it can be seen that the top of the column responded quickly while the middle of the column was slower to respond to the new flux rate. This is typical of the transient response of unsaturated soils moving from a high flux rate to a lower one and will be discussed in more detail in the next chapter.

Tensiometers #6, #11 and #12 experienced problems measuring soil suction during this application rate due to air leaking through fittings into the tensiometer body. This results in the gaps shown in the pressure profiles in Figure 6.21. At the end of this flux rate, these tensiometers were retrofitted with new fittings and brought back into service.

The response of the lysimeters to changes in suction is best illustrated using Figure 6.22. This figure illustrates that the lysimeter suction measurement is similar to that of the tensiometers after approximately 10 days. This is not unreasonable given the amount of water that must be expelled from the lysimeter in comparison to the tensiometers in order to reach equilibrium with the waste rock. It should be noted however, that the lysimeter response time was only 4 days when it was nulled during the measurement of the equivalent collection area ratio. This may be due to a number of reasons. There may be a hydraulic advantage in filling the lysimeter as opposed to emptying the lysimeter by flow into the waste rock. This possibility will be examined further in the next chapter. Another plausible explanation is that the contact between the silica flour and the waste rock materials is better when filling the lysimeter than it is when emptying the lysimeter, due to the increased suction that is applied to the waste rock during filling. This increase in suction would pull water into the void spaces in the waste rock located around the silica flour thus increasing the contact between the two materials. This explanation is consistent with what should be observed due to hysterisis in the soil-water characteristic curve and the associated hydraulic conductivity (these properties are different when the waste rock is drying than when it is wetting). As the waste rock takes on water (the lysimeter is draining) and the hydraulic conductivity of the waste rock would follow the wetting curve. When the waste rock is draining (the lysimeter is filling) the hydraulic conductivity of the waste rock would follow that of the drying curve. The hydraulic conductivity of the wetting curve is lower than the hydraulic conductivity of the drying

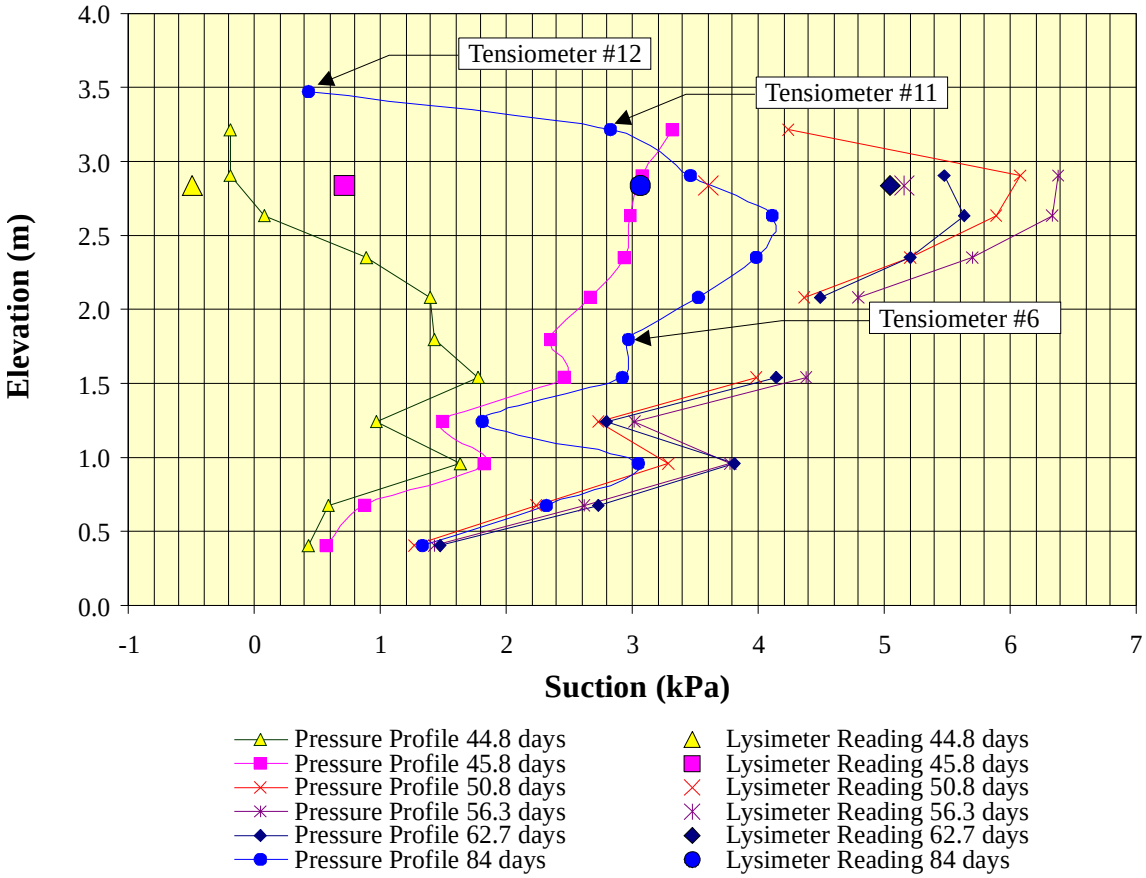

Figure 6.21 - Pressure profiles in the fine column with time at a flux of 8 E-8 m/s

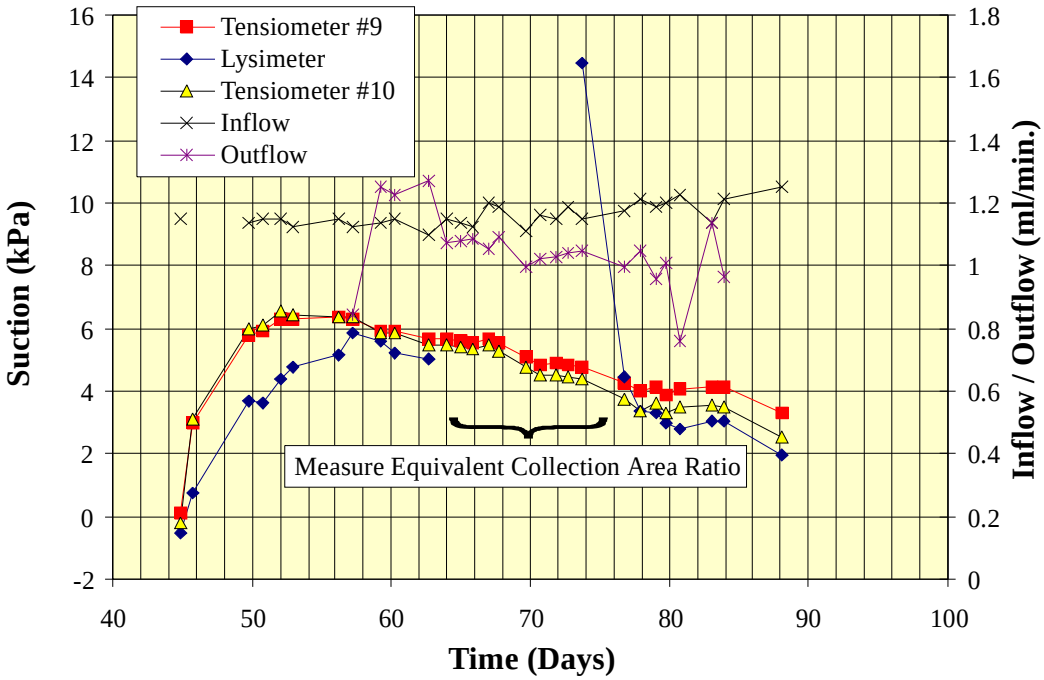

Figure 6.22 - Data collected from fine column at a flux rate of 8 E-8 m/s

curve, which provides a possible explanation why the lysimeter responds faster when filling than when draining. When the lysimeter was allowed the time to come to equilibrium, the suctions that were measured by the lysimeters compared within less than 1 kPa of the suctions recorded by the tensiometers.

Another feature illustrated in Figure 6.22 is the decrease in the measured suction with time. It can be seen that there is a slight increase (approximately 5%) in the inflow rate with time. However, this small increase in flowrate should not cause a 2 kPa shift in suction. The most plausible explanation for this decrease in the suction is linked to the clogging of the bottom pan and the addition of the sodium hypochlorite. From the graph it can be seen that there was a slow gradual decrease in the suctions. This might suggest that the sodium hypochlorite was the cause of the change in the measured suctions. As the biological activity in the column was eliminated, the effects of the organics in the column were removed. This would happen gradually as the sodium hypochlorite was carried by advection and diffusion throughout the entire column, thus, resulting in the slow decrease in the observed suctions.

6.3.1.3 Soil Suction Measurement at a Flux Rate of 1 E-8 m/s

The flux rate 1 E-8 m/s is significant because it represents a flowrate that is approximately equal to the average annual rainfall (30 cm/year). Figure 6.23 displays the cumulative inflow / outflow graph for this flux rate. From the graph it is apparent that the system had not come into equilibrium with respect to inflow and outflow rates. After approximately two months of drainage (88 to 145 days) the outflow rate of the column was about 300 ml per day while 200 ml per day was being applied to the column. As the column moves to increasingly lower outflow rates, the column must drain and release water from storage. This plot illustrates the large amount of time that is required to remove water held in storage within the column at low suctions. Due to time constraints it was not feasible to wait until the column came into equilibrium. As will be seen later in the analysis, although the flowrates in and out of the column are not equal, the suctions within the columns are relatively stable.

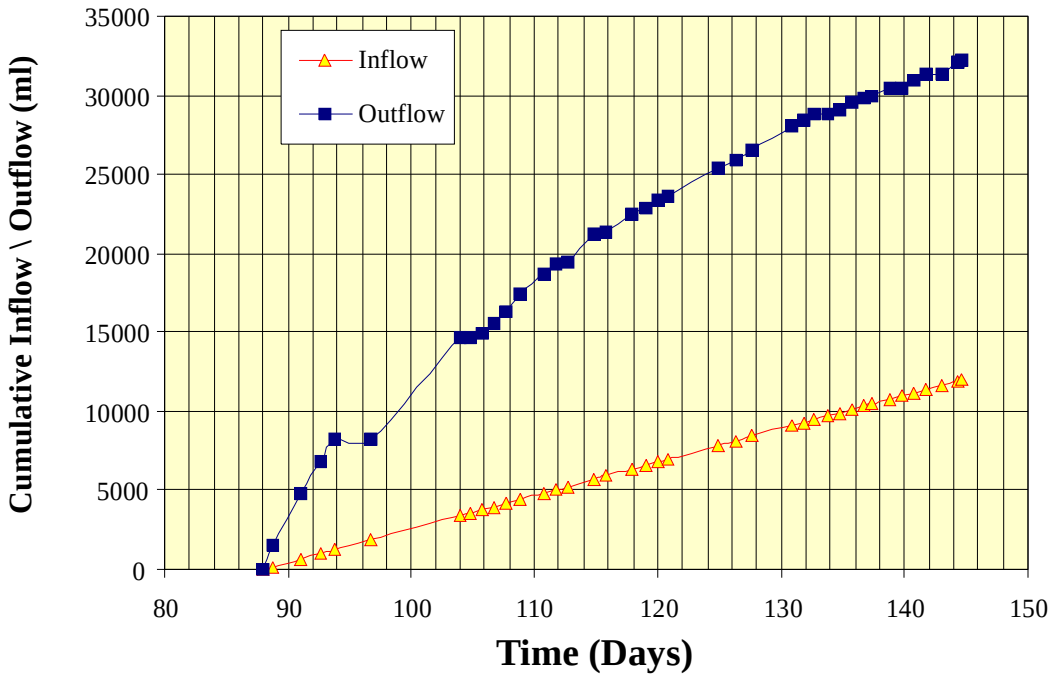

Figure 6.23 - Cumulative flow rates at a flux rate of 1 E-8 m/s

Figure 6.24 displays the pressure profiles generated in the column with time. As with the previous flux rate, it can be seen that the suctions near the top of the column respond the quickest to the change in the flux rate while the middle section is slower to respond.

The lysimeter suction measurement lags behind the tensiometers during the initial stages of the transition from the lower to higher suction. The lysimeter appears to catch up to the tensiometers between 104.8 days and 114.8 days. However, this is the result of nulling the lysimeter as shown in Figure 6.25. As with the previous flux rate, the lysimeter responded much quicker during filling than during emptying. When the lysimeter was allowed the time to come to equilibrium after nulling, the suctions that were measured by the lysimeters compared within less than 2 kPa of the suctions recorded by the tensiometers.

Theoretically, the suctions near the bottom of the column should lie near the hydrostatic line as the required suction is developed. The tensiometers at the bottom of the column appear to have suctions that increase approximately hydrostatically with increasing elevation, however, it is apparent that a line drawn through these points would have a y

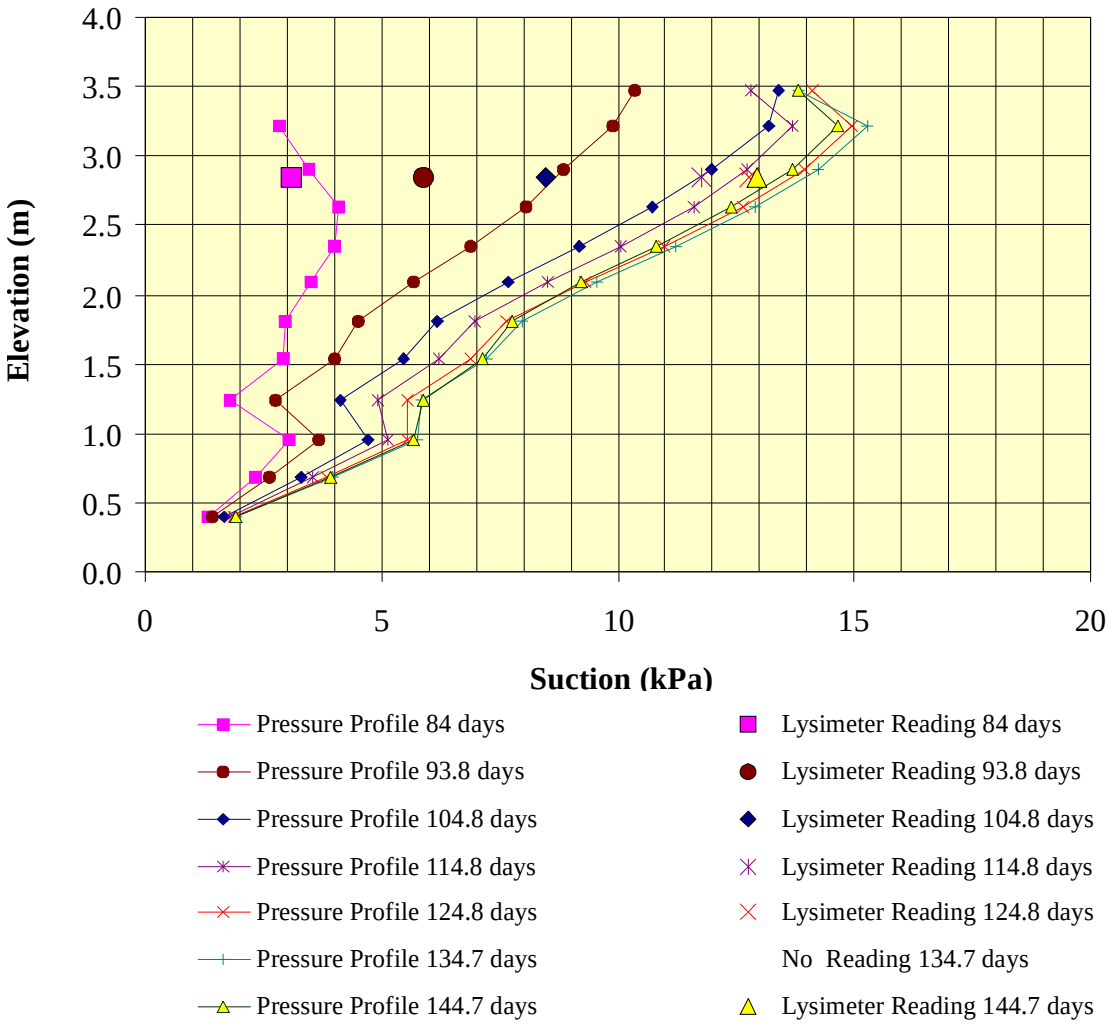

Figure 6.24 - Pressure profiles in the fine column with time at a flux of 1 E-8 m/s

intercept that is above the base of the column. This indicates that the water table within the column lies approximately 0.120m above the bottom of the column. The height of the water table in the column was the amount of head that was required to push the water through the perforated base of the column.

The pressure displayed in Figure 6.25 illustrate that although the flowrates have not come to equilibrium the pressure near the top of the column was relatively stable. The inflow line appears as a straight line due to the fact that the GDS controller is believed to be more accurate than could be measured. Variations in the outflow rate are the result of trying to accurately measure a decreasing flowrate. Several attempts were made to

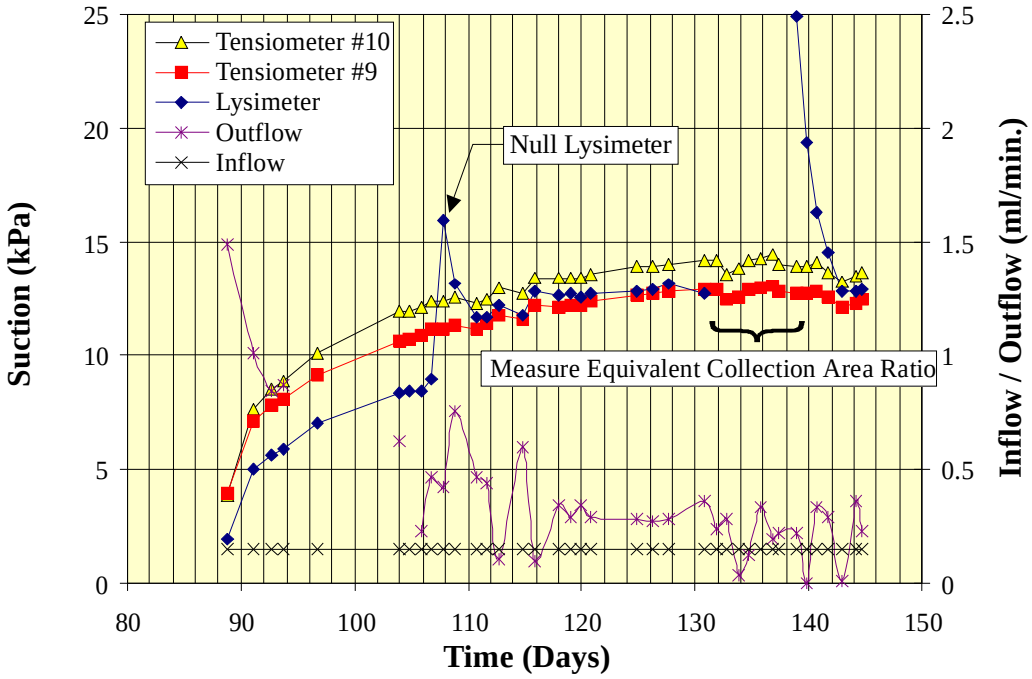

Figure 6.25 - Data collected from fine column at a flux rate of 1 E-8 m/s

improve the apparatus and stabilize the readings, but the data still shows a significant amount of scatter, however, the general trend of the flowrate is clear.

6.3.1.4 Soil Suction Measurement at a Flux Rate of 1 E-9 m/s

The flux rate of 1 E-9 m/s is a flux that represents one tenth of the average annual precipitation. Figure 6.26 displays the cumulative inflow / outflow graph for this flux rate. From the graph it is apparent that the system had not come into equilibrium with respect to inflow and outflow rates. After approximately 101 days of drainage (143 to 244 days) the outflow rate of the column was about 80 ml per day versus the 20 ml per day being applied to the column. As with the previous flux rate this plot illustrates the large amount of time that is required to remove the water held in storage within the column under low suctions.

Figure 6.27 displays the pressure profiles generated in the column with time. As with the previous flux rate, it can be seen that the suctions near the top of the column respond the quickest to the change in the flux rate while the middle section is slower to respond.

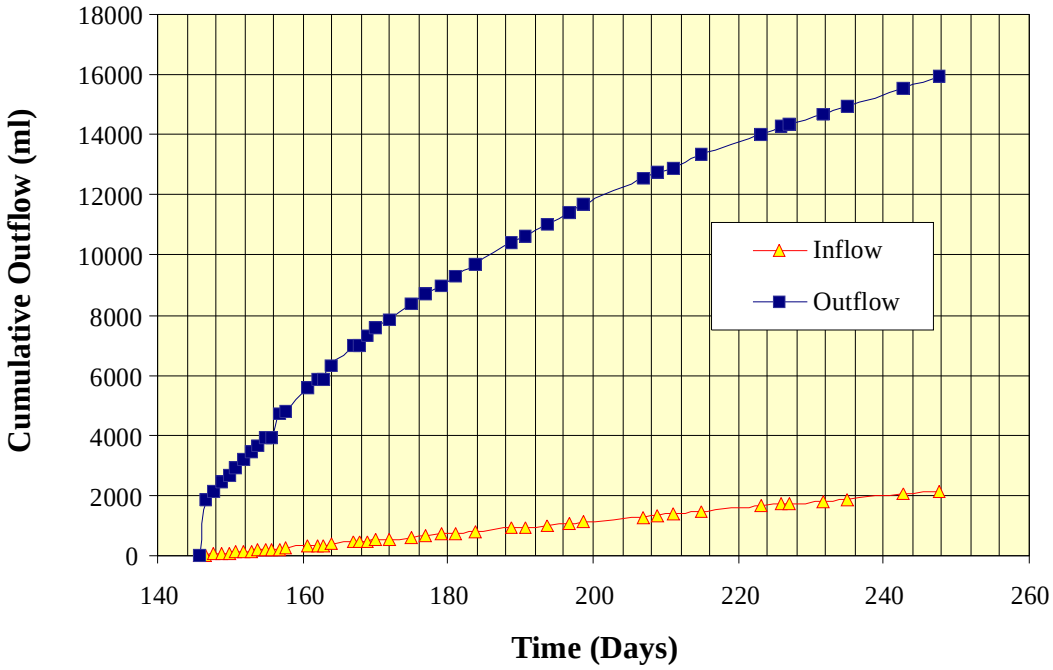

Figure 6.26 - Cumulative flow rates at a flux rate of 1 E-9 m/s

The lysimeter suction measurement lags slightly behind the tensiometers during the initial stages of the transition from the lower to higher suction. However, the time lag does not appear to be as significant as in previous flux rates. This may be due to the slow rate at which the entire column is coming into equilibrium. The lysimeter appears to catch up to the tensiometers by day 235. However, this is the result of nulling the lysimeter during the testing of the equivalent collection area ratio as shown in Figure 6.28. When the lysimeter was allowed the time to come to equilibrium, the suctions that were measured by the lysimeters compared within less than 2 kPa of the suctions recorded by the tensiometers.

As with the previous flux rate, the suctions near the bottom of the column appear to increase hydrostatically with increasing elevation. The y intercept of a line drawn through these points was calculated to be 0.160 m. This indicates that the water table within the column lies 0.160 m above the bottom of the column. This is higher than the previous flux rate possibly indicating that the points used to calculate the line may not have been at the hydrostatic condition causing the decreased y intercept observed.

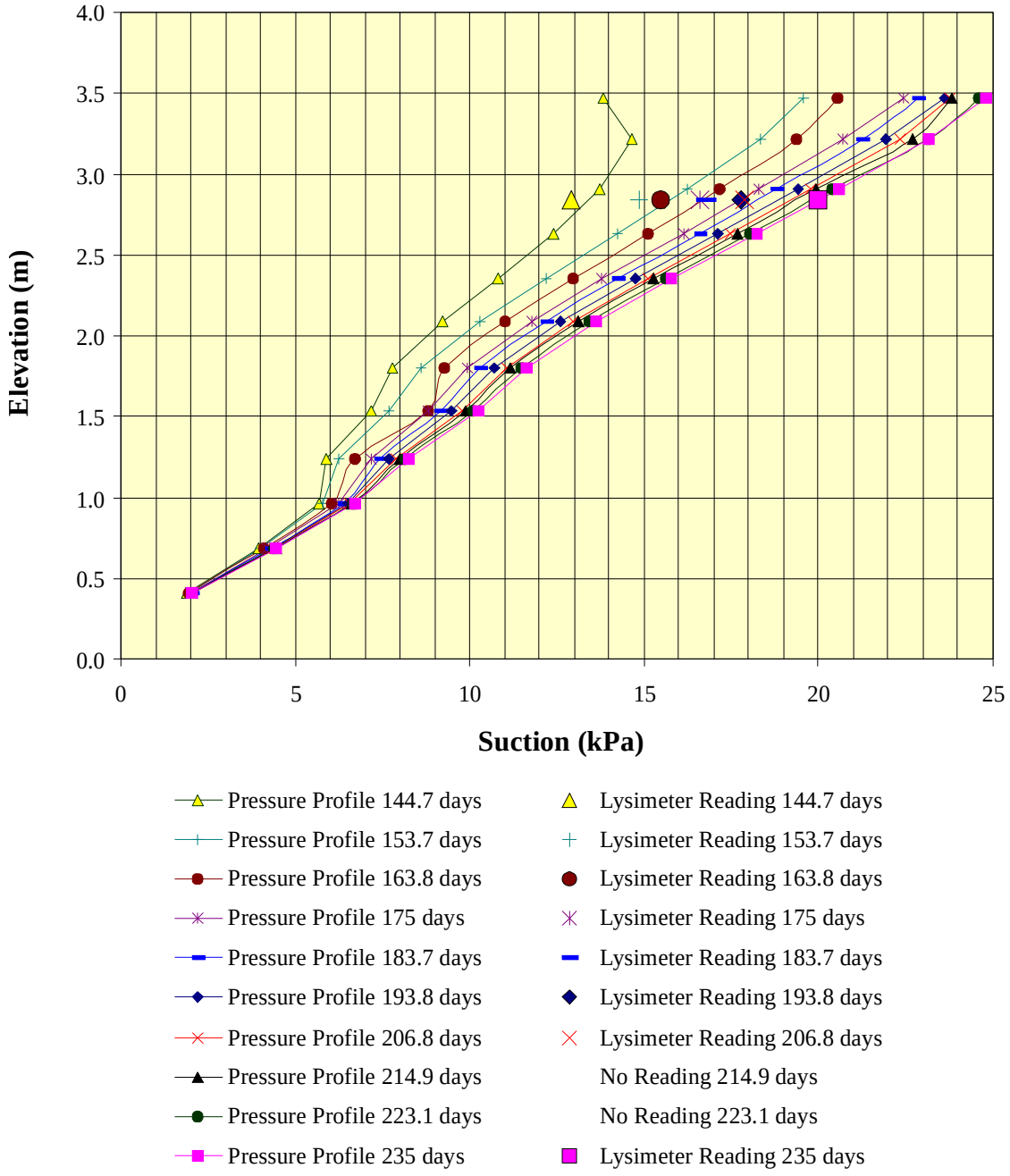

Figure 6.27 - Pressure profiles in the fine column with time at a flux of 1 E-9 m/s

The pressure readings with time shown in Figure 6.28 illustrate that although the flowrates had not come to equilibrium the pressure readings near the top of the column were relatively stable. One notable difference was the difference in suction between Tensiometer #9 and #10. At the high flux rates the difference between the tensiometer

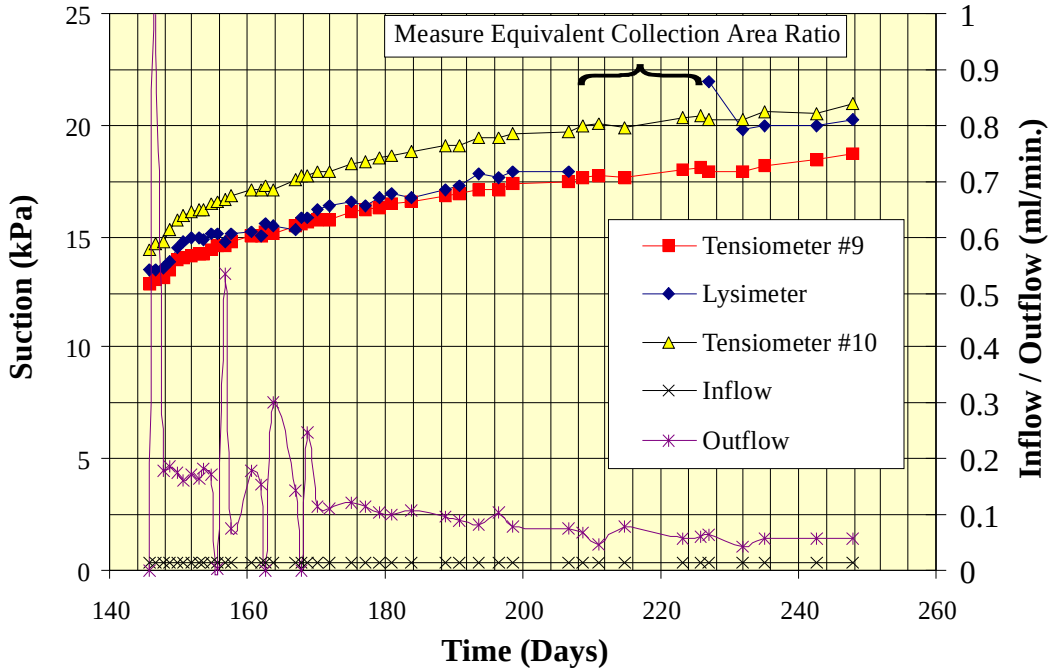

Figure 6.28 - Data collected from fine column at a flux rate of 1 E-9 m/s

suctions was negligible, while under this flux rate the difference was significant. The maximum difference between the recorded suctions as the flux rates decrease will be that associated with the hydrostatic line. The significance of this is in the realization that although the lysimeter suction appeared to stay within the suctions bracketed by the two tensiometers (143 to 204 days), it has not yet come into equilibrium with the soil. The elevation of the lysimeter is much closer to tensiometer #10 than tensiometer #9, as a result, it would be expected that the suction recorded would be closer to that of tensiometer #10. The effect of nulling the tensiometer during the equivalent collection area ratio testing causes the lysimeter suction to return to a value that is closer to that of Tensiometer #10. This indicates that the lysimeter was lagging behind the tensiometers even 60 days after the flux rate was changed. This problem can be mitigated by nulling the lysimeter. This does not pose a problem in field installations as the lysimeter will be nulled periodically during collection of the pore water sample.

6.3.1.5 Collection of a Pore Water Sample in the Fine Column

The equivalent collection area ratio for all flux rates have been tabulated in Table 6.2. As the flux rate decreases the equivalent collection area ratio increases. This is in response to the silica flour becoming the preferential flow path. The volumes collected by the lysimeter only dropped 60 percent even though the flux rate was decreased by 2.5 orders of magnitude. At flux rates higher than the saturated hydraulic conductivity of the silica flour (1.8 E-7 m/s) the equivalent collection area ratio is less than 1 indicating that the waste rock is the preferential flow path. At lower flux rates the equivalent collection area ratio was greater than 1 indicating that the silica flour was the preferential flow path. This was consistent with the results of the preliminary modelling program and the work of Newman (1999).

Table 6.2 - Equivalent collection area ratios for the fine column

Applied Flux Rate (m/s)	Equivalent Collection Area	Collection Volume (ml/day)
4×10^{-7}	0.26	18.9
8×10^{-8}	1.22	16.9
1×10^{-8}	5.51	11.1
1×10^{-9}	13.51	6.4

Figure 6.29 displays the same data plotted on a semi-log plot. As the flux changes the hydraulic conductivity of the waste rock changes while the hydraulic conductivity of the silica flour stays the same. This causes the waste rock to be the preferential flow path at fluxes higher than the saturated hydraulic conductivity of the silica flour. At fluxes lower than the saturated hydraulic conductivity of the silica flour, the silica flour was the preferential flow path. This is shown in the Figure 6.29 as a break in the curve at a flux rate of approximately 1 E-7 m/s.

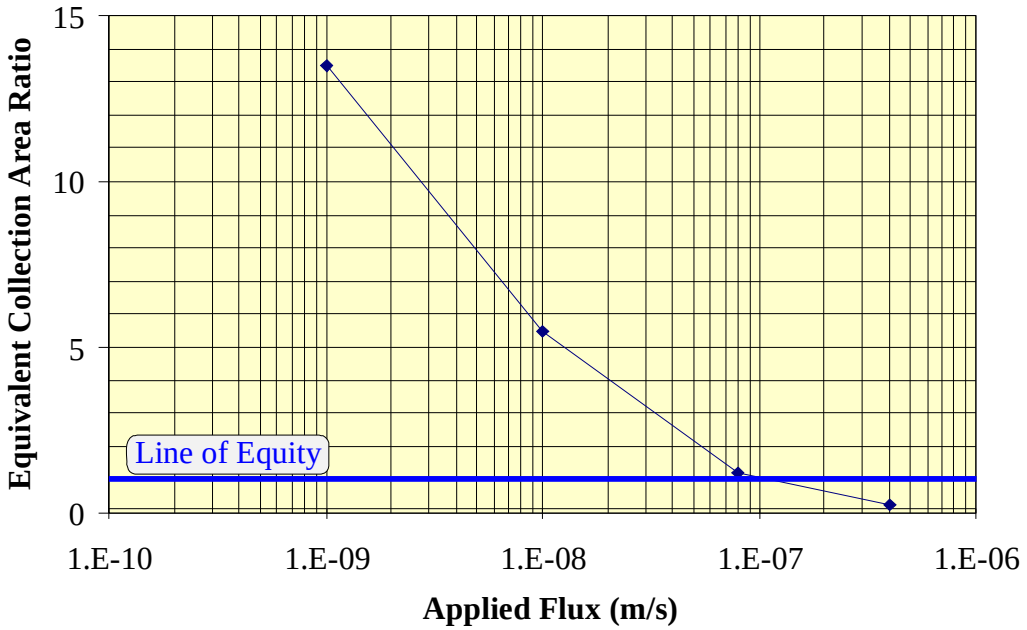

Figure 6.29 - Equivalent collection area ratio for the fine column

6.3.2 Coarse Column

The coarse waste rock remained at or near its residual volumetric water for all of the flux rates used during the testing. Changing the applied flux rate produced very minor changes in the measured soil suctions and there was little or no storage change within the waste rock. The approximate flux rates used during the testing of the coarse column were 5 E-6 m/s, 8 E-8 m/s, 1 E-8 m/s and 1 E-9 m/s. The results of testing of the coarse column will be presented in two subsections. The first subsection will review the suction measurements made within the column at all of the applied flux rates. The final subsection will deal with the measurements made during collection of the pore water sample.

6.3.2.1 Soil Suction Measurement at all Flux Rates

Figure 6.30 displays the cumulative inflow / outflow graph for all flux rates tested on the coarse column. Cumulative inflows and outflows for the flux rate of 5 E-6 m/s were plotted on the primary y - axis, while the other flux rates have been plotted on the secondary y axis. From the graph it is apparent that the system responded rapidly to changes in the flux rate. At these flux rates, the column was at or near its residual

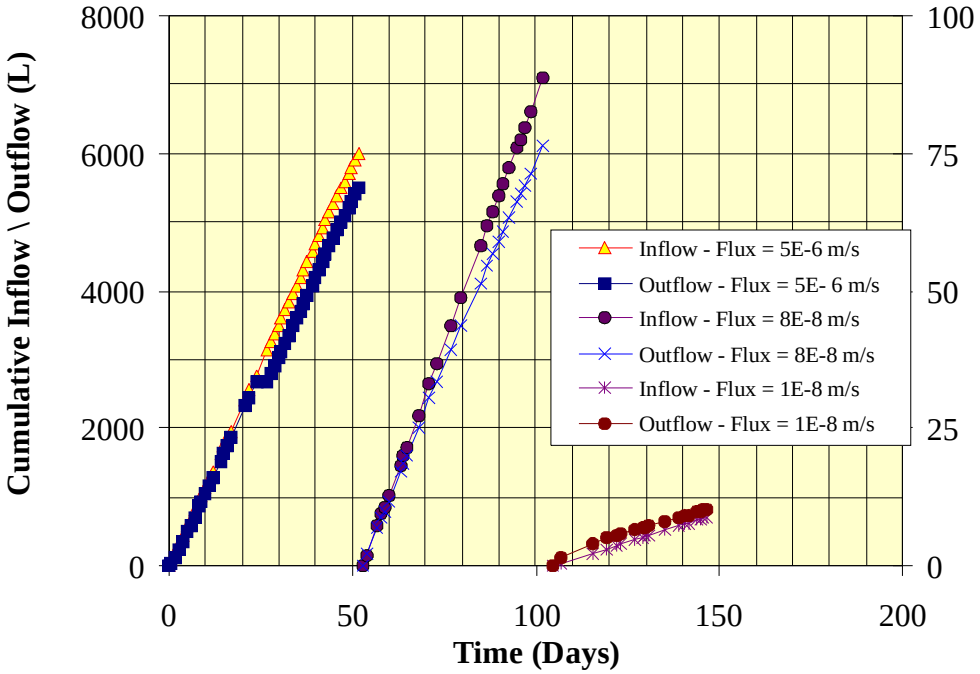

Figure 6.30 - Cumulative flow rates for all flux rates

volumetric water content and as a result there was little or no change in storage associated with a change in flux rate. Therefore, the steady state condition was reached once the water in the column has had the time to drain out of the column.

At a flux rate of 5 E-6 m/s the cumulative inflow and outflow lines fall almost on top of one another. There is a noticeable jog in the outflow graph at an elapsed time of about 25 days. This jog was the result of the rain simulator running out of water, and the outflow rate slowing down. The inflow graph was not corrected because it was unknown at what time it ran out of water.

For the flux rate of 8 E-8 m/s the graph of cumulative inflow and outflow plot as straight lines indicating that the system was at a steady state condition. However, the lines diverge slightly, indicating that either there was a leak in the column or that there was a problem with the outflow measuring system. No leaks were apparent in the column and the method of measurement of the outflow system was to record the outflow rate over a

short period of time on a daily basis. It is possible that there were fluctuations in the flowrate exiting the column, causing the divergence in the lines.

At a flux rate of 1 E-8 m/s the cumulative inflow and outflow lines became parallel quite quickly. There was a small but noticeable bump near the start of the application of this flux rate which might indicate that there was a change in storage of the column. However, it is suspected that this was the result of the water from the previous column being purged from the system. This is reasonable, as it would take some finite amount of time for the water to clear the column after a change in the flux rate.

Figure 6.31 displays pressure profiles with time under the different flux rates. It can be seen that over the entire test there was little or no change in suction. The majority of the column displays a variation in suction of less than 0.2 kPa. The two exceptions are Tensiometer #2 and #12. These tensiometers recorded higher suctions and are thought to be the result of placement procedures. During the placement of tensiometers material screened through the #4 sieve was placed around the lysimeter to ensure contact with the waste rock. It is possible that too much of the screened material was placed at these locations. In these cases the suction measured may be influenced by the soil-water characteristic curve of the material passing the #4 sieve. This would result in suctions that were higher than those of the surrounding waste rock.

There is no consistent pattern with respect to flux rate and the measured suction. The range of suctions measured for the coarse column is probably approaching the limit of the precision of the suction measuring apparatus. The measurement apparatus consisted of a manometer board. The largest error associated with this apparatus was probably due to variations in the atmospheric air pressure. Increases or decreases in the air pressure would cause fluctuations in the measured suctions.

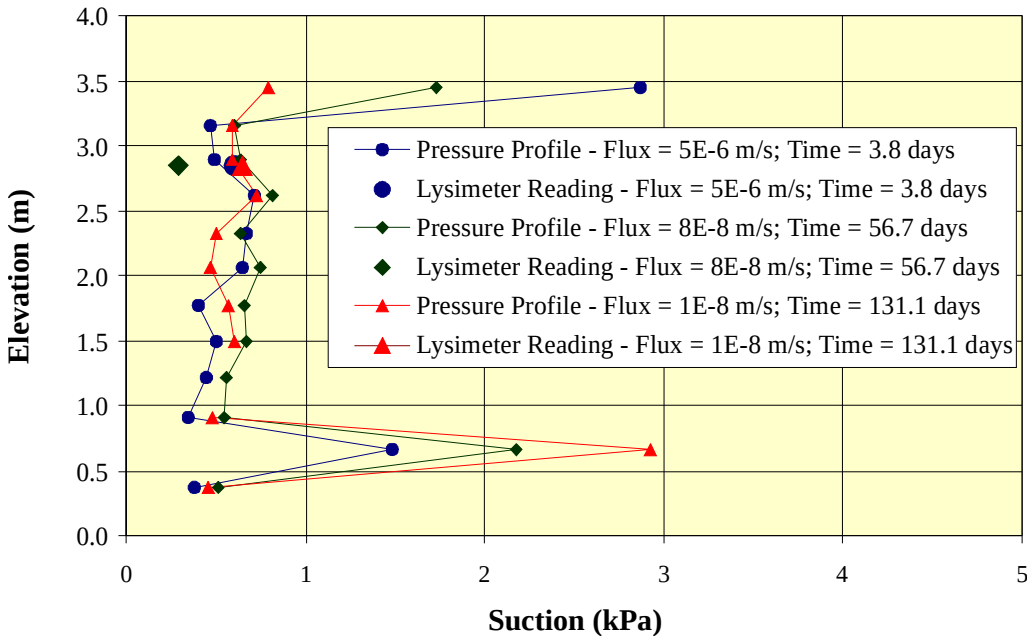

Figure 6.31 - Pressure profiles in the coarse column with time

Figure 6.32 displays a plot of the suction versus time data for Tensiometers #9 and #10 and the lysimeter. The testing of the lysimeter in the coarse column included a component where a pore water sample was taken from a tensiometer located in the silica flour directly above the lysimeter. Figure 6.32 displays the time periods over which testing for the equivalent collection area ratio occurred and when the tensiometer pore water collection testing occurred.

The data collected by the lysimeter was much noisier than the data collected by the tensiometers. This could be due to a number of reasons. The lysimeter was close to saturation and generally reads slightly lower than the tensiometers. As a result, changes in the atmospheric pressure may have a larger impact on the reading. Secondly, at these suctions the water level in the lysimeter is near the top of the lysimeter and edge effects at the lip of the lysimeter may cause fluctuations in the readings. Finally, during much of the testing the lysimeter was being used to collect pore water and as a result, there were no long periods of time at which the stability of the suction reading could be assessed.

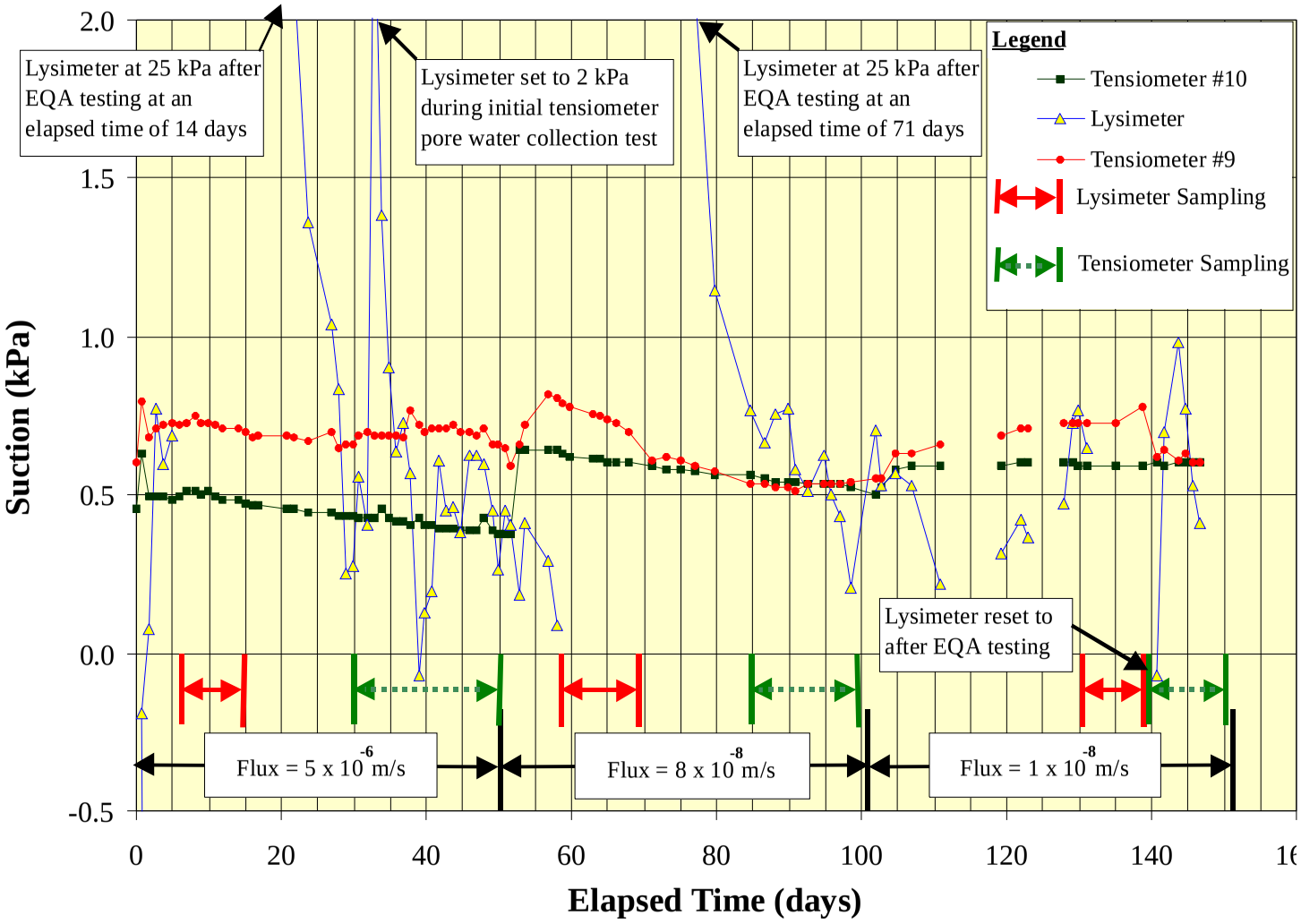

Figure 6.32 - Data collected from coarse column

The lysimeter was nulled a couple of different times after equivalent area testing. The response time of the lysimeter was generally in the order of 14 days. This was slow in comparison to the response times of 6 to 8 days observed in the fine column. The sluggishness of the lysimeter when filling may be due in part to a slight desaturation of the sand silica flour mixture (air entry value of approximately 10 kPa). Some of the recovery time may be due to the time required for the sand silica flour mixture to resaturate. Due to time constraints, the lysimeter was filled up after the equivalent collection area ratio testing at a flux rate of 1 E-8 m/s. Characteristically, the lysimeter was slow to respond when trying to empty the lysimeter and the lysimeter was reset to a suction of approximately 0.5 kPa. The suctions measured by the lysimeters were within 1 kPa of the suctions recorded by the tensiometers. The precision of the suction measurement appears to be in the order of 0.2 kPa

6.3.2.2 Collection of a Pore Water Sample in the Coarse Column

Pore water samples were collected using two different methods. The first involved the standard method used to calculate the equivalent collection area ratio. The second involved removing a pore water sample using a tensiometer located in the silica flour above the tensiometer.

Table 6.3 displays the results of the testing performed to determine the equivalent collection area ratio of the lysimeter in the coarse waste rock column. As in the fine column, at flux rates greater than the saturated hydraulic conductivity of the silica flour the equivalent collection area ratios are less than 1. At fluxes less than the saturated hydraulic conductivity of the silica flour the equivalent collection area ratios are greater than 1. It should be noted that the tensiometer located directly above the lysimeter could have partially blocked some of the flow in the lysimeter resulting in slightly lower equivalent collection area ratios than in the fine column

Table 6.3 - Equivalent collection area ratios for the coarse column

Applied Flux Rate (m/s)	Equivalent Collection Area	Collection Volume (ml/day)
5×10^{-6}	0.01	10.0
8×10^{-8}	0.71	8.6
1×10^{-8}	5.08	7.9

Figure 6.33 displays the data plotted on a semi-log plot. The data collected for the fine column displays the same trend that was shown in the coarse column. The fact that the lines are similar suggests that the equivalent collection area ratio is dependent on the silica flour rather than the waste rock. If the columns had exactly the same gradient, it would be expected that these lines would be the same.

Figure 6.34 displays the results of the pore water sampling using a tensiometer. In this method the outflow tube of the tensiometer was lowered to heights that produced suctions in the tensiometer of 2, 4 and 6 kPa greater than the insitu suction measurement. The flowrate out of the tensiometer was then recorded. This method eliminates the need to pass all of the flow through the entire lysimeter and allows a fresh pore water sample

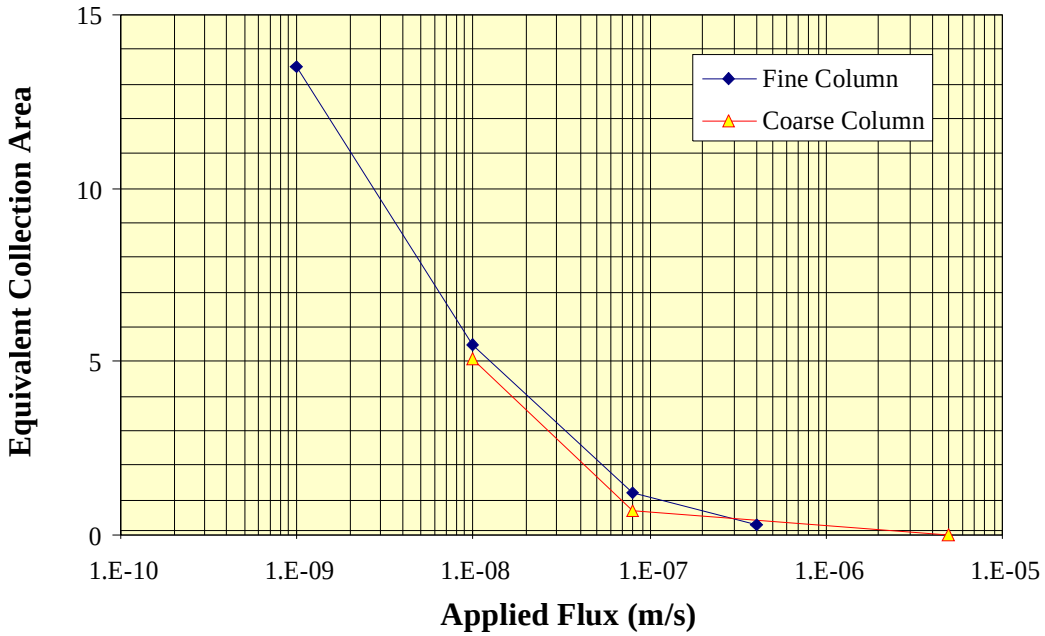

Figure 6.33 - Equivalent collection area ratios for the coarse column

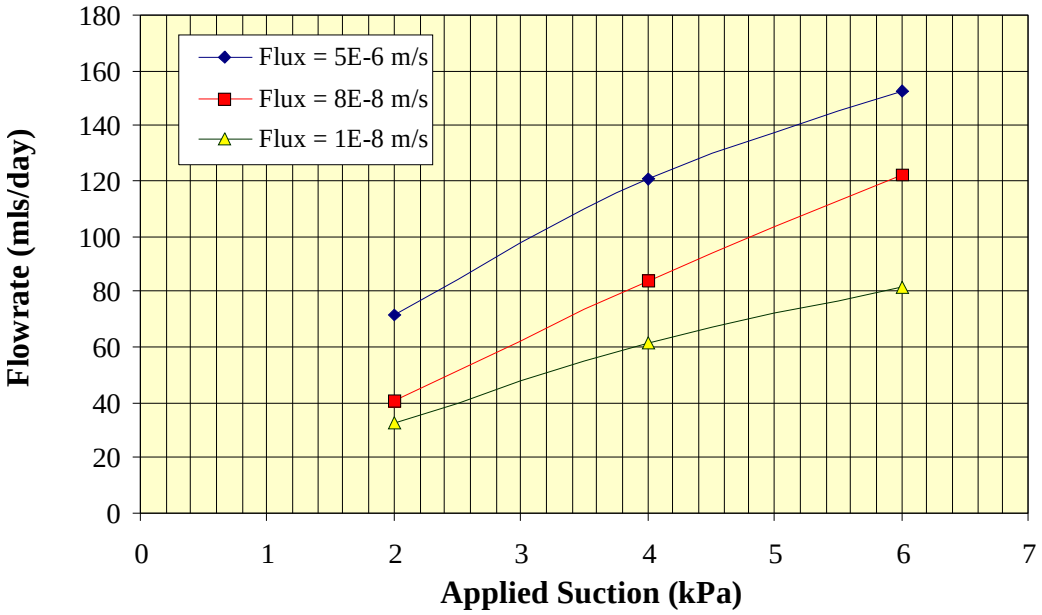

Figure 6.34 - Results of tensiometer sampling of pore water

to be obtained directly. The flowrates recorded out of the tensiometer were substantially higher than those recorded by the lysimeter. This is due to the higher gradient that was applied. In the lysimeter the maximum gradient that can be applied is one. In the tensiometer the gradients (gradients across the tensiometer cup ranged from approximately 3 to 9 at suctions of 2 kPa to 6 kPa respectively) were larger than 1, resulting in more pore fluid being extracted.

Different flux rates produced variations in the flowrate recorded in the tensiometer. As the applied flux decreased 3.5 orders of magnitude, the flowrate into the tensiometer only decreased approximately 50 per cent. For all flux rates the suction in the waste rock column remained relatively constant. This indicates that the gradients around the tensiometer remained relatively constant. As the applied flux rate decreases, the hydraulic conductivity of the waste rock would also decrease. Thus, it would be expected that an order of magnitude shift in the hydraulic conductivity would produce an order of magnitude change in the tensiometer flowrate. This was not observed in the tensiometer. The only reasonable explanation is that as the hydraulic conductivity decreases the area from which the tensiometer collects water increases. This explanation

is consistent with the silica flour around the tensiometer becoming a preferential flow path as shown in the results of the modelling of the equivalent collection area ratio.

The line produced at different suctions for a given flowrate appear slightly curved. This may be due to the fact that water moves in response to hydraulic head. Hydraulic head is comprised of two components, namely elevation and pressure head. In the case of the tensiometer, the elevation stays constant while the suction increases. As a result, it would be expected that the initial part of the line would appear as a curve and would straighten out as the suction increases and the suction component of hydraulic head dominates the equation.

6.4 Summary of the Prototype Lysimeter Testing Results

The lysimeter was able to measure suctions within both the fine and coarse waste rock. For suction values less than 10 kPa the lysimeter was able to measure suctions to within 1 kPa of the suctions measured by the tensiometers. For suction values less than 20 Kpa the suction measurement was within 2 kPa. This suggests a suction error in the order of 10%. At suctions lower than 1 kPa, the suction error may be higher as a result of reaching the limit of measurement precision of the lysimeter. These results are consistent with the results of the preliminary modelling program.

The lysimeter was able to collect a pore water sample at all flux rates. For the fine column, the collection rate varied from 18.9 to 6.4 ml/s over a flux range of 4 E-7 m/s to 1 E-9 m/s respectively. For the coarse column, the collection rate varied from 10 ml/day to 7.9 ml/day over a flux range of 5 E-6 m/s to 1 E-8 m/s respectively. In both cases, as the flux rate dropped below the saturated hydraulic conductivity of the silica flour the column showed significant increases in the equivalent collection area ratio. This indicates that the silica flour became the preferential flow path. This is significant in the coarse column as it demonstrates that even very coarse materials respond to small changes in applied suction.

The tensiometer was found to be an efficient method of removing a pore water sample. The tensiometer produced 4 to greater than 10 times the collection rate of the lysimeter, dependant on the applied suction. This is due in part to the increased gradient across the tensiometer ceramic and no restriction with respect to the hydraulic conductivity of the tensiometer tube (water filled). As a result, the tensiometer should be able to produce a fresh pore water sample much faster than the lysimeter due to the increased collection rates and the decreased water storage requirements in comparison to the lysimeter. If a tensiometer were incorporated into the lysimeter design for the purpose of pore water collection it would greatly increase the efficiency of the suction measurement response time and collection of a pore water sample. However, the operational disadvantages of the tensiometer, such as purging entrapped air, would have to be addressed.

CHAPTER 7 ANALYSIS

7.1 Introduction

In this chapter, the performance of the prototype standpipe lysimeter was compared to the theoretical performance predicted by a numerical model. The purpose of the numerical modelling was to verify the general trends observed in the prototype standpipe lysimeter testing. Detailed calibration and verification of the model was not attempted. The numerical modelling was performed using the same modelling parameters as described in Chapter 4 with two exceptions. The first exception was that the soil-water characteristic curves and hydraulic conductivity functions used in the model were generated from data measured in the laboratory and the lysimeter prototype. The second exception was that the dimensions of the numerical model were changed to reflect the actual size of the components used in the prototypes.

7.2 Soil-water Characteristic Curves and Hydraulic Conductivity Functions

The soil-water characteristic curve tests performed as part of the laboratory program were interpreted prior to being used in the numerical model. The interpretation included reviewing the slope of the soil-water characteristic curves at suctions less than the air entry value and interpreting data generated from multiple samples.

The slope of the soil-water characteristic curve prior to the air entry value is the coefficient of volume change (m_v). This slope is important in the numerical modelling of the lysimeter because it affects the time that it will take for the lysimeter to come into equilibrium with the surrounding waste rock after the lysimeter has been drained. The

coefficient of volume change for the silica flour was measured to be 1 E-5 /kPa. The coefficients of volume change for the waste rock materials and the sand silica flour mixture should be smaller than the coefficient of volume change for the silica flour. In the modelling of the waste rock column a higher coefficient of volume change in the sand silica flour mixture will produce conservative modelling results of the performance of the lysimeter. Thus it was assumed that the coefficient of volume change for the silica sand mixture was equal to that of the silica flour. With respect to the waste rock materials the coefficient of volume change will have a very minimal effect on the numerical model. As a result, the coefficient of volume change for the waste rock materials was also assumed to be equal to that of the silica flour.

The hydraulic conductivity functions for each material were calculated using the data from the soil-water characteristic curves. The hydraulic conductivity functions were calculated using three different formulations; Fredlund and Xing (1994), Brooks and Corey (1964) and Van Genuchten (1980). All of these formulations calculate a relative hydraulic conductivity function. The actual hydraulic conductivity function is obtained by multiplying the relative hydraulic conductivity function by the saturated hydraulic conductivity. The source of the saturated hydraulic conductivity value for each material will be identified during the discussion of the hydraulic conductivity function. The data generated from the waste rock columns provided a unique opportunity to compare the calculated hydraulic conductivity functions with measured values

The soil-water characteristic curve for the silica flour used in the numerical model is shown in Figure 7.1. The slope of the soil-water characteristic curve at suctions less than the air entry value was adjusted so that it was equal to the coefficient of volume change. The data was interpreted from the initial volumetric water content reading at a suction of 0 kPa. For positive pressures (not shown on this logarithmic plot), the volumetric water content was increased with increasing pressure consistent with the coefficient of volume change.

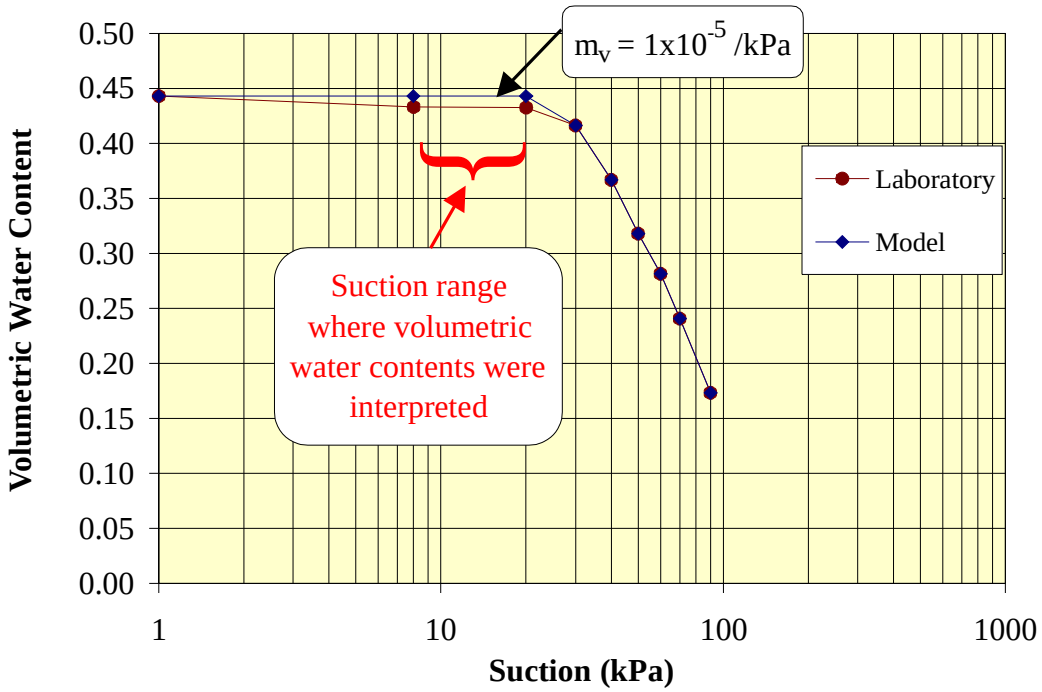

Figure 7.1 - Interpreted soil-water characteristic curve of silica flour

Figure 7.2 displays the hydraulic conductivity functions generated for the silica flour. The saturated hydraulic conductivity of 2 E-7 m/s was determined during the laboratory program. From this figure, it can be seen that the hydraulic conductivity functions generated by the formulations proposed by Brooks and Corey (1964) and Van Genuchten (1980) are similar. The hydraulic conductivity function generated using the Fredlund and Xing (1994) formulation differs from the other curves in that the hydraulic conductivity starts dropping off prior to the other two curves and proceeds at a flatter slope than the other two formulations. The hydraulic conductivity function calculated using the Van Genuchten formulation was arbitrarily chosen for use in the numerical model.

Figure 7.3 displays the soil-water characteristic curve of the sand-silica flour mixture used in the numerical model. Like the silica flour, adjustments were made to the volumetric water contents at values of suction less than the air entry value so that the slope corresponded to the coefficient of volume change.

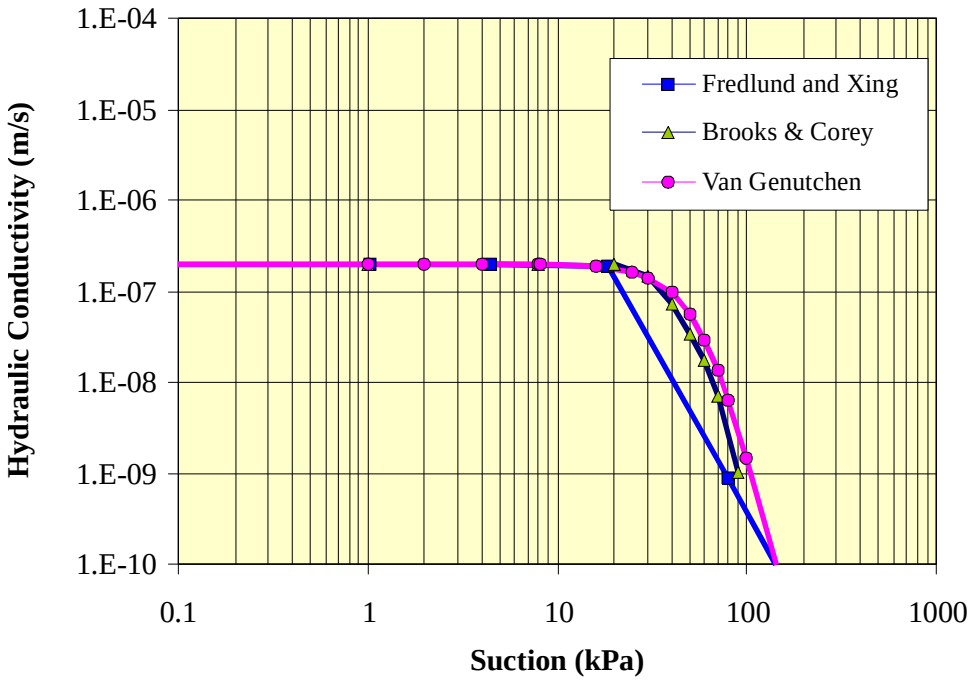

Figure 7.2 - Hydraulic conductivity functions of silica flour

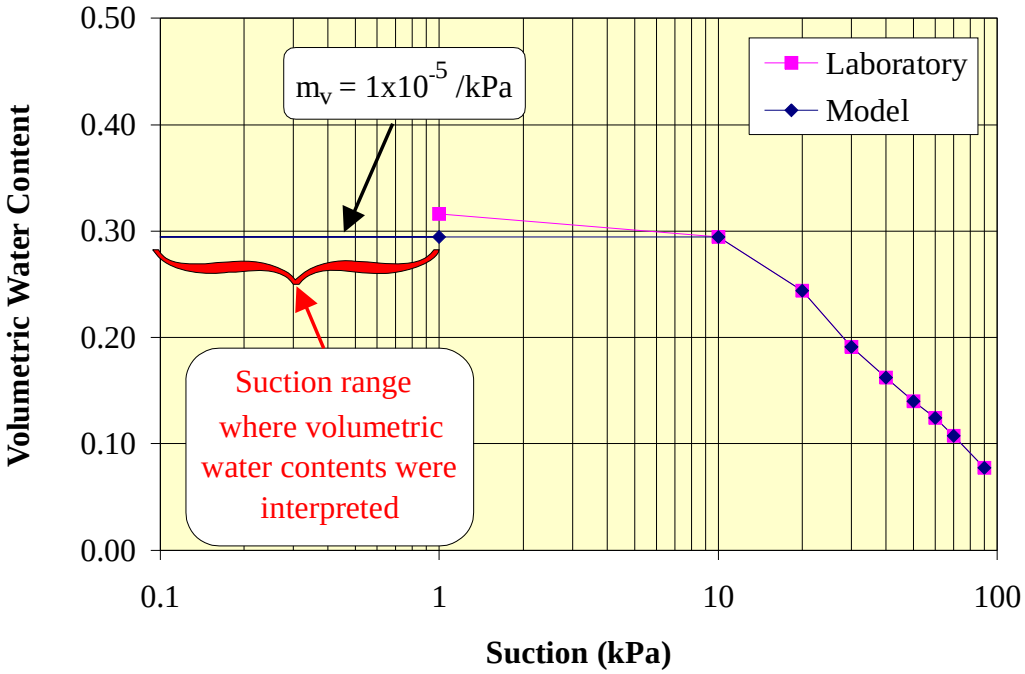

Figure 7.3 - Soil-water characteristic curve of the sand-silica flour mixture

Figure 7.4 displays the hydraulic conductivity functions generated for the sand-silica flour mixture. The saturated hydraulic conductivity of 9 E-7 m/s was determined during the laboratory program. This figure displays the same general trends exhibited in the silica flour with one exception. The initial drop in the hydraulic conductivity as predicted calculated using the Brooks and Corey (1964) and Van Genuchten (1980) formulations are different. This may be due to the curve fitting exercise used in the Van Genuchten formulation. The hydraulic conductivity function calculated using the Van Genuchten formulation was used in the numerical model.

The soil-water characteristic curve used for the fine waste rock column is shown in Figure 7.5. The soil-water characteristic curve used in the model was the result of averaging the data from the duplicate tests of the soil-water characteristic curves. The initial average volumetric water content at a suction of 0 kPa was assumed to be correct and a slope equal to the coefficient of volume change was interpreted from this point. A gentle bend was added to the line so that it matched up with the data from the test at the

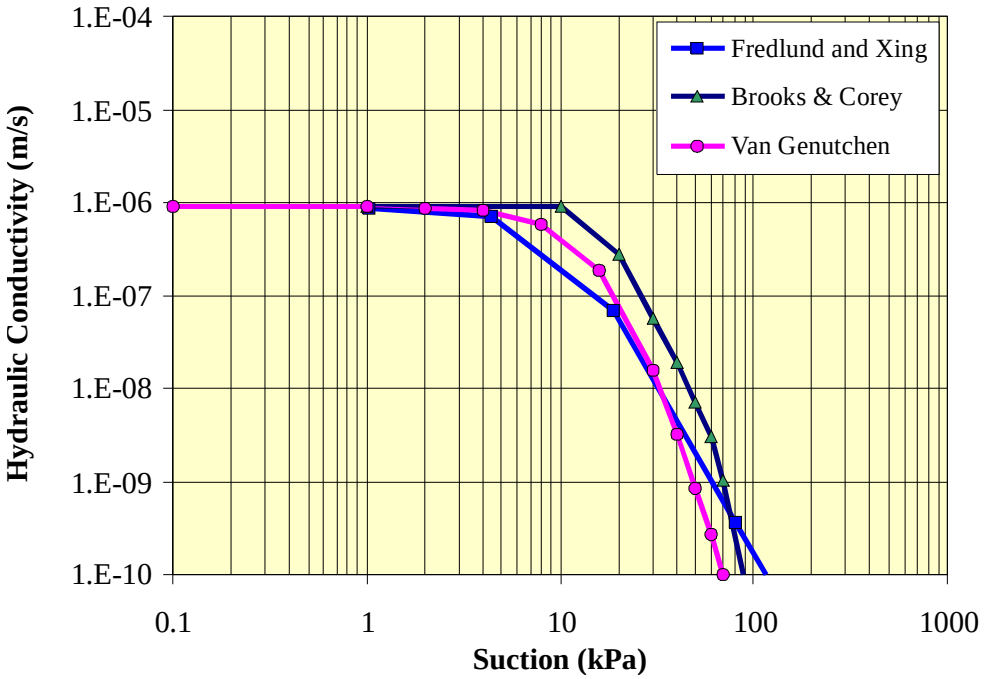

Figure 7.4 - Calculated hydraulic conductivity functions of the sand-silica flour mixture

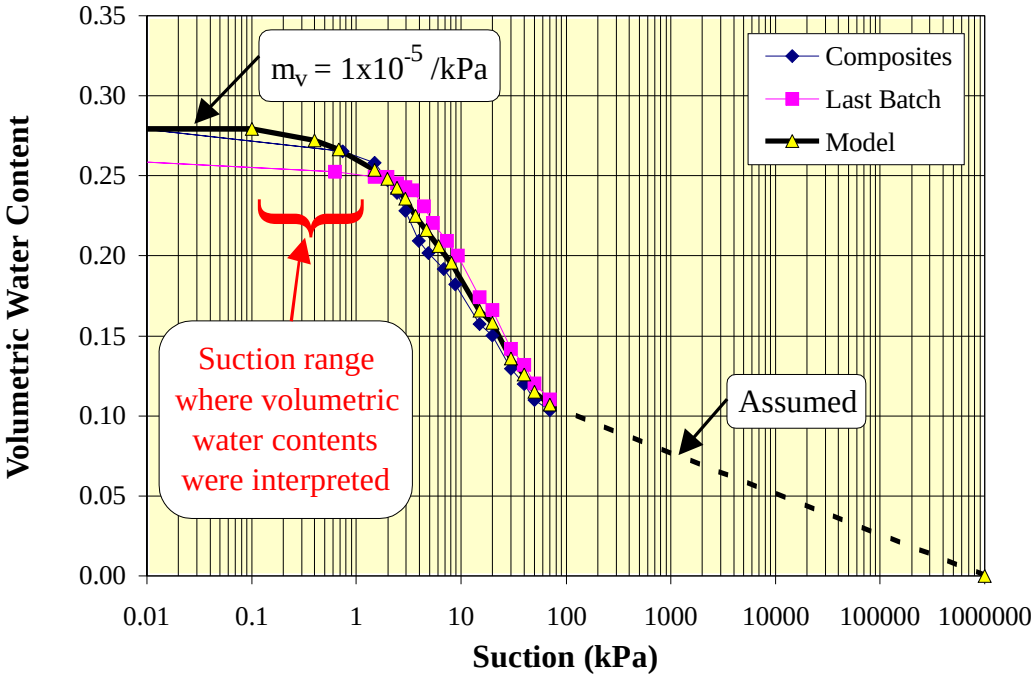

Figure 7.5 - Interpreted soil-water characteristic curve of the fine waste rock column

air entry value. The value of the coefficient of volume change for the waste rock is likely less than that of the silica flour. However, in the case of the waste rock it is unlikely that this portion of the curve will be significant during the modelling, because the suctions that will be generated are greater than the air entry value.

The hydraulic conductivity functions of the fine waste rock are shown in Figure 7.6. The saturated hydraulic conductivity was estimated at 5 E-7 m/s from the data generated from the column testing. All of the hydraulic conductivity functions show a break in the hydraulic conductivity near a suction of 1 kPa followed by a straight line function on the log-log plot in the hydraulic conductivity. The Fredlund & Xing (1994) formulation displayed the flattest slope while the Van Genuchten (1980) formulation showed the steepest slope.

Data from the column was used to generate a hydraulic conductivity curve to compare against the calculated curves. The data was compiled by breaking the column into

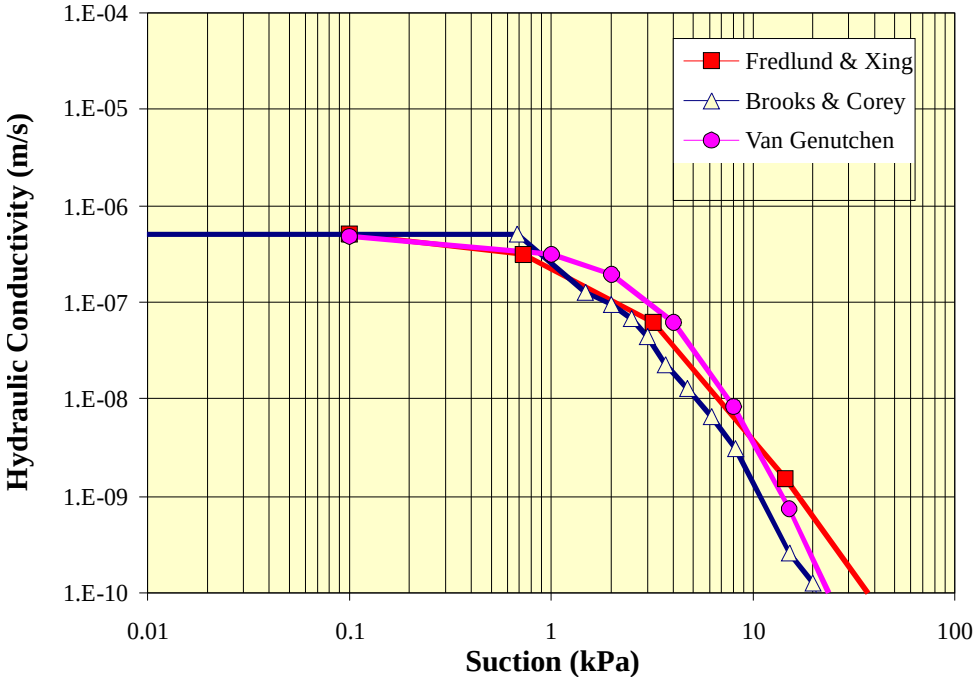

Figure 7.6 - Calculated hydraulic conductivity functions of the fine waste rock

discrete soil layers. These layers corresponded to the soil in between each set of tensiometers. The suction and hydraulic head at the top and bottom of each layer was known. The hydraulic conductivity of the layer could be calculated knowing the flowrate. The actual flowrate was unknown, but should lie between the flux being applied at the top (inflow) and the flux being collected out the bottom of the column (outflow). The data from the column was broken into two different groups for presentation and analysis purposes. The first group consisted of the soil layers in the bottom half of the column and the second group consisted of soil layers in the top half of the column.

Figure 7.7 displays the hydraulic conductivity and suction data collected for the bottom half of the column based on the flowrates out of the bottom of the column (outflow). Similarly, Figure 7.8 displays the same data set, but with hydraulic conductivities based on the flux into the column (inflow). Because the data for tensiometers near the bottom of the column are being used, it would be expected that the calculations shown in Figure 7.8 is a better representation of a hydraulic conductivity envelope, which should contain the actual hydraulic conductivity function.

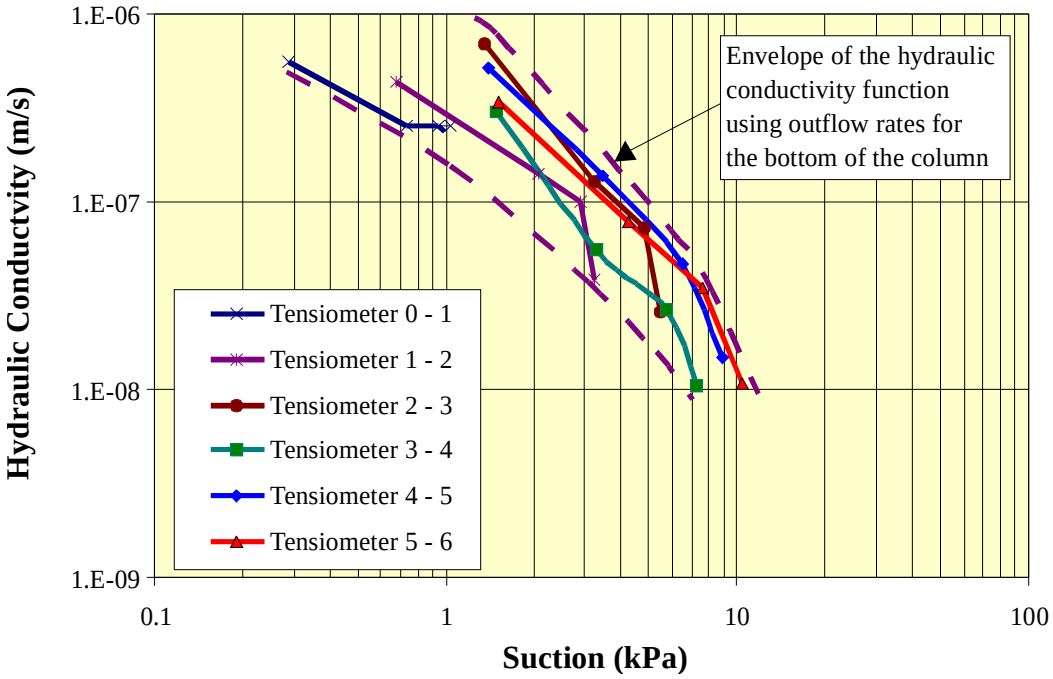

Figure 7.7 - Calculated hydraulic conductivity of the fine waste rock based on outflow rates for the bottom half of the column

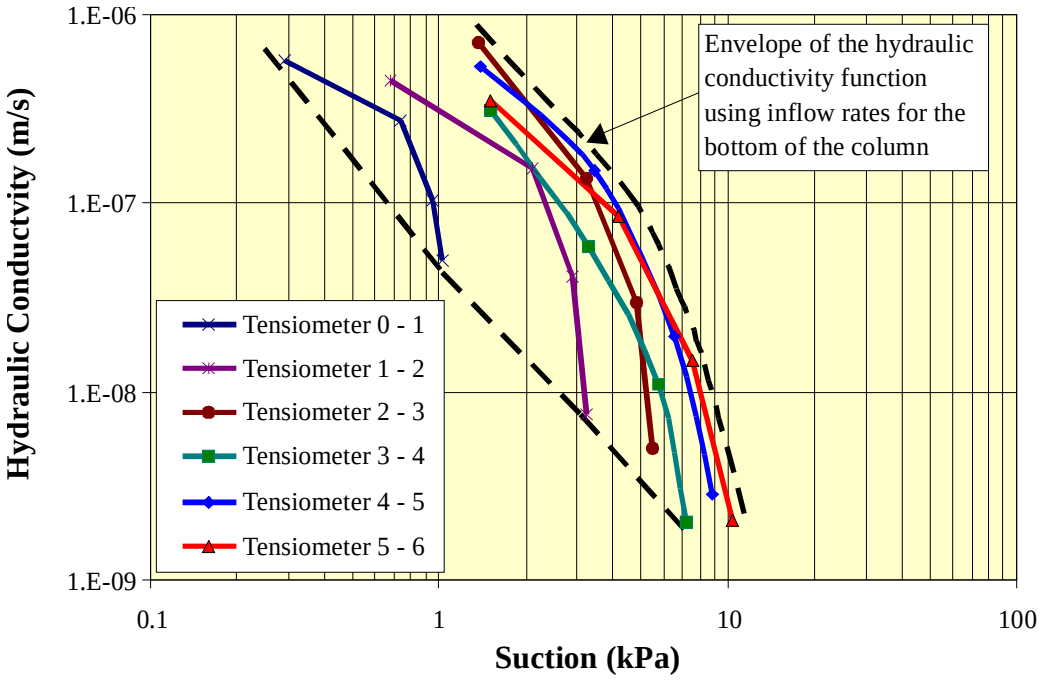

Figure 7.8 - Calculated hydraulic conductivity of the fine waste rock based on inflow rates from the bottom half of the column

A similar analysis was performed on the top half of the column. The results are shown in Figure 7.9 and Figure 7.10. The top half of the column would be expected to have flowrates closer to the inflow rate. Therefore, it was felt that the hydraulic conductivity envelope developed in Figure 7.10 is more likely to contain the correct hydraulic conductivity functions for the waste rock.

Figure 7.11 is a graph that combines the hydraulic conductivity and suction envelopes for the top (based on inflow) and bottom (based on outflow) of the column. The actual hydraulic conductivity of the column is likely to fall within the area that is shared by both of these envelopes as highlighted on the figure.

The top of the column has the largest amount of time to come into equilibrium with the new applied flux rate as the rest of the column must first transmit all of the water released from storage from the soil above it prior to it reaching a state condition. This results in the top of the column responding faster than the rest of the column to changes in the applied flux rate. As a result the data that is gathered from the top of the column

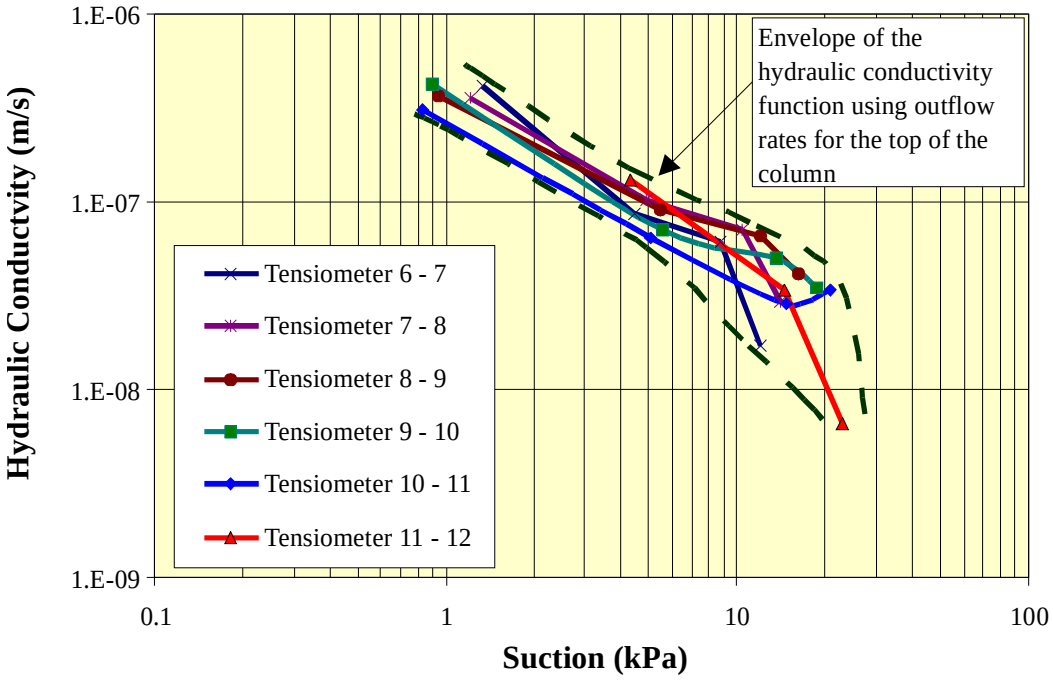

Figure 7.9 - Calculated hydraulic conductivity of the fine waste rock based on outflow rates from the top half of the column

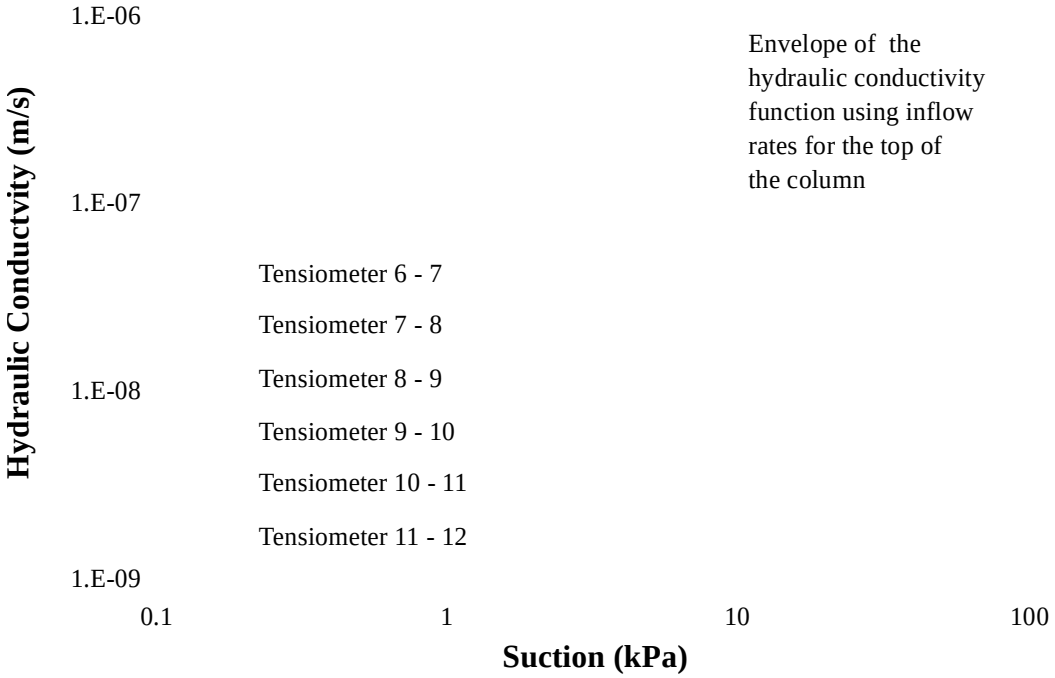

Figure 7.10 - Calculated hydraulic conductivity of fine waste rock based on inflow rates from the top half of the column

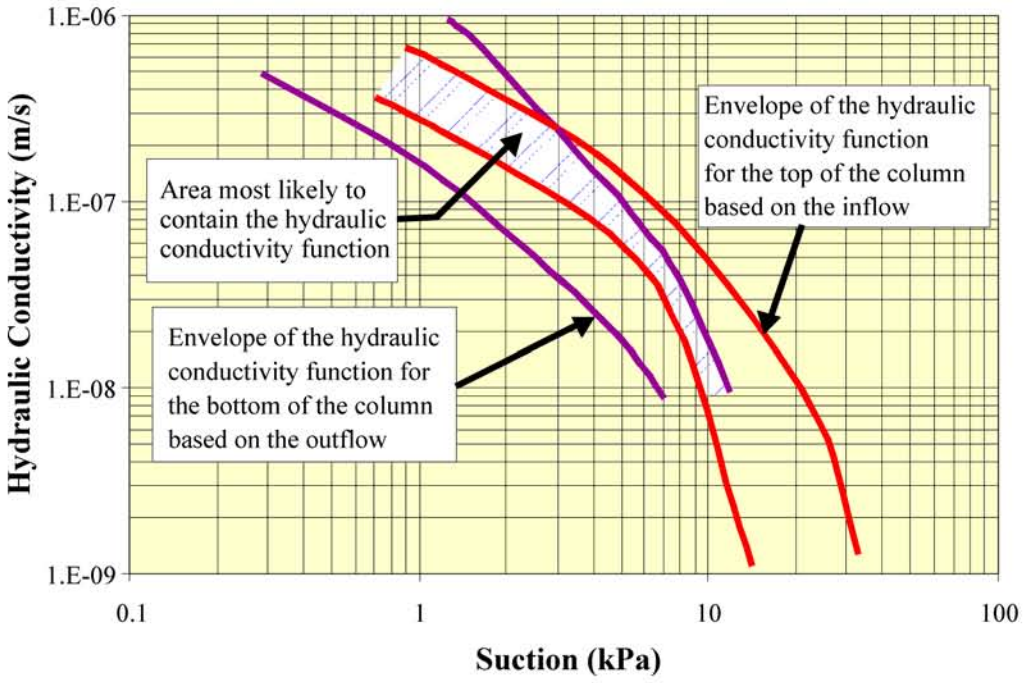

Figure 7.11 - Area most likely to contain the hydraulic conductivity function of the fine waste rock based on inflow and outflow rates of the column

is most likely to represent the actual hydraulic conductivity function. Figure 7.12 displays the maximum suctions observed at the top of the column at a given flux rate. It can be seen that this curve falls within the hydraulic conductivity envelopes suggested by data from the rest of the column. This curve will be used as the hydraulic conductivity function in the numerical model

Figure 7.13 provides a comparison of the calculated hydraulic conductivity functions and the one generated from the column data. The curve from the column takes longer to become a straight line than the calculated curves. The final slope of the column curve has a similar shape to that of the Van Genuchten formulation.

Figure 7.14 displays one of the possible soil-water characteristic curves for the coarse waste rock column. This soil-water characteristic curve was the result of averaging the data from two measured soil-water characteristic curves. The initial average volumetric water content at a suction of 0 kPa was assumed to be correct and a slope equal to the

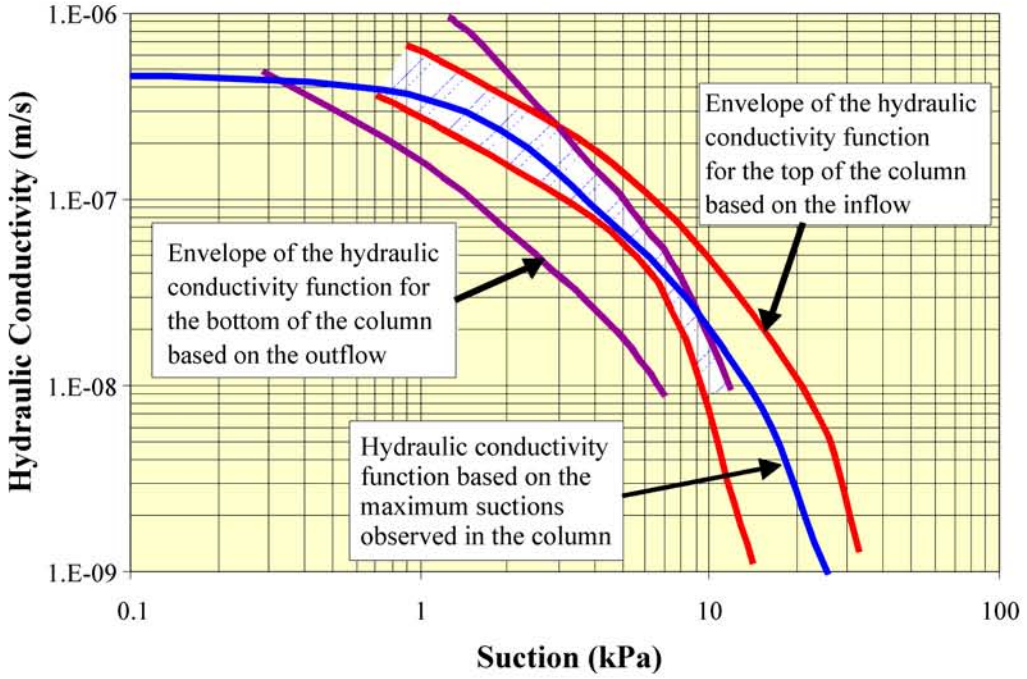

Figure 7.12 - Hydraulic conductivity function of the fine waste rock based on the maximum suctions observed in the column in comparison to the area most likely to contain the hydraulic conductivity function

Figure 7.13 provides a comparison of the calculated hydraulic conductivity functions and the one generated from the column data. The curve from the column takes longer to become a straight line than the calculated curves. The final slope of the column curve has a similar shape to that of the Van Genuchten formulation.

Figure 7.14 displays one of the possible soil-water characteristic curves for the coarse waste rock column. This soil-water characteristic curve was the result of averaging the data from two measured soil-water characteristic curves. The initial average volumetric water content at a suction of 0 kPa was assumed to be correct and a slope equal to the coefficient of volume change was interpreted from this point. A gentle bend was added to the line so that it matched up with the data from the test at the air entry value. As with the fine waste rock, it is unlikely that the portion of the curve at suctions lower than the air entry value will be significant during the modelling, because the suctions that will be generated in the column were greater than the air entry value.

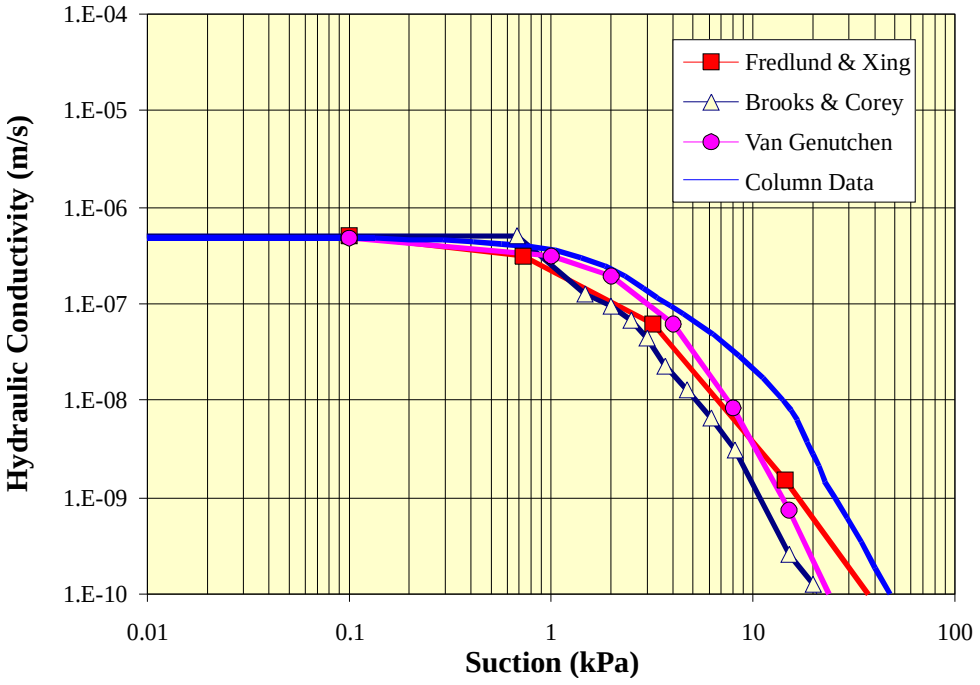

Figure 7.13 - Comparison of hydraulic conductivity functions generated from the soil-water characteristic curves and the hydraulic conductivity functions observed in the fine waste rock column

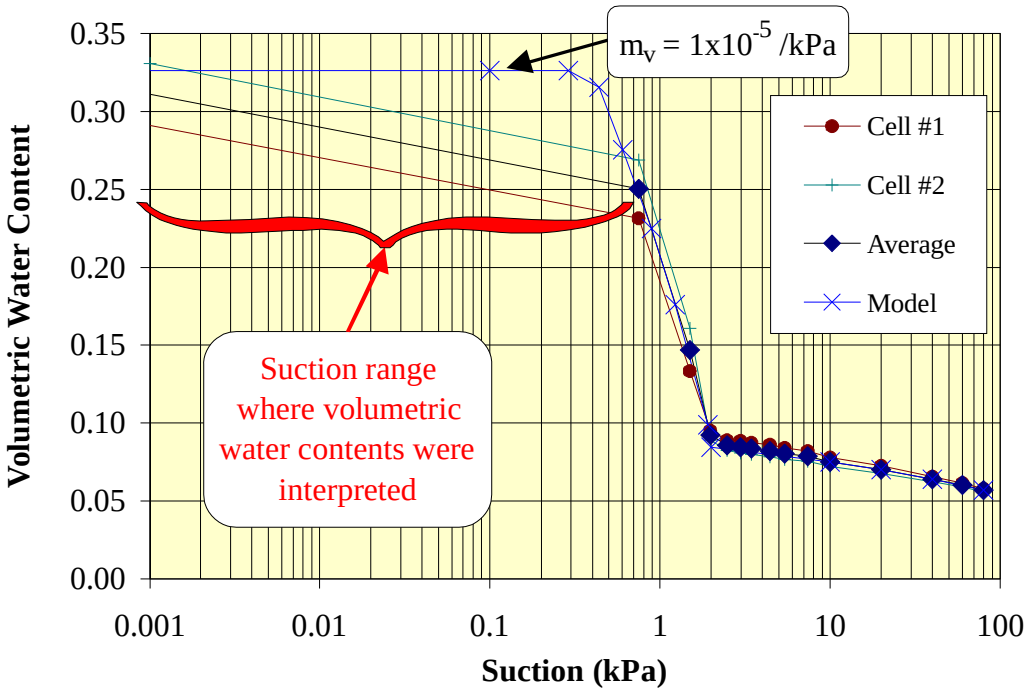

Figure 7.14 - Interpreted soil-water characteristic curve of the coarse waste rock column

There was one notable difference between the soil-water characteristic curve and the data generated from the column. The suction that corresponded to the residual water content in the soil-water characteristic curve was approximately 2 kPa. In comparison the maximum suction observed in the column was approximately 0.7 kPa. The suction observed in the column would be expected to correspond to a suction either in the transition zone of the soil-water characteristic curve or at the residual water content. This observed difference may be the result of the choice of datums during the soil-water characteristic curve testing. Figure 7.15 displays a number of different soil-water characteristic curves based on taking the datum at the top, middle and bottom of the apparatus. For datums at the top and middle of the column the soil-water characteristic curve is relatively well defined because there are at least two points between the air entry value and the residual water content, from which the slope of the line can be extrapolated. For a datum at the bottom of the apparatus the slope of the soil-water characteristic curve is not defined, and thus could possibly take on any slope in the transition zone of the soil-water characteristic curve

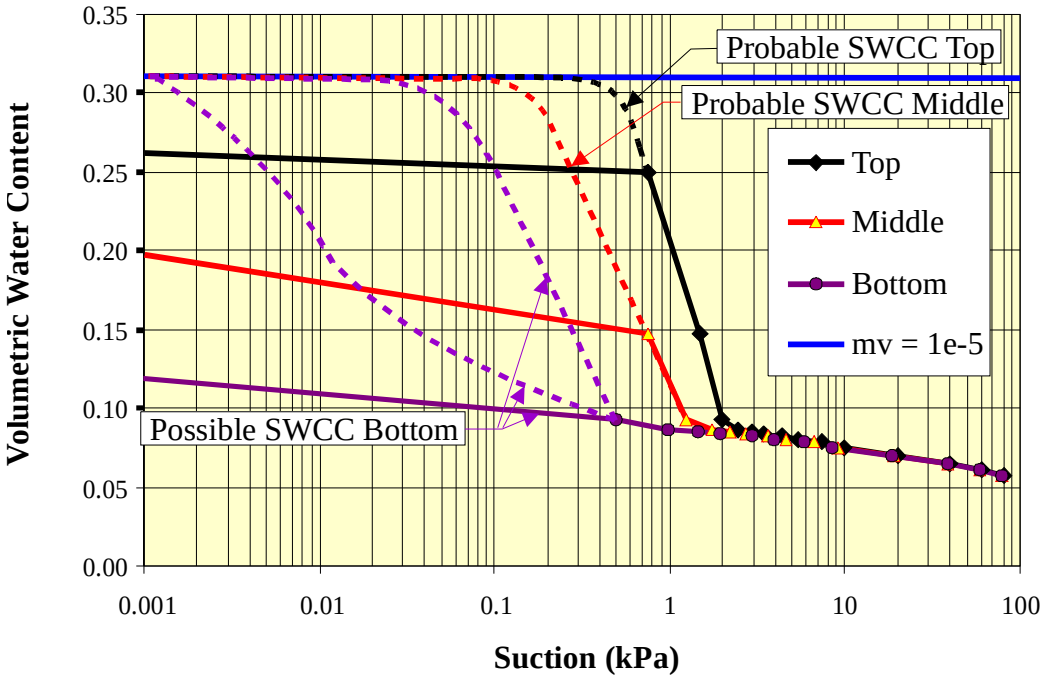

Figure 7.15 - Range of soil-water characteristic curves possible by assuming different datums during the soil water characteristic curve testing of the coarse waste rock

The hydraulic conductivity function generated from data from the column can be used to help justify the correct placement of the soil-water characteristic curve. The following discussion examines the data as if the datum at the top of the sample is correct.

The calculated hydraulic conductivity functions of the coarse waste rock based on a datum that corresponds to the top of the apparatus are shown in Figure 7.16. The saturated hydraulic conductivity was estimated at 5 E-3 m/s using Hazen's technique of estimating the hydraulic conductivity based on grainsize (Freeze and Cherry, 1979). The Fredlund and Xing (1994) curve differed from the other curves in that the location of the break in the curve occurred at a lower suction than the other two curves. The hydraulic conductivity functions all exhibited differing slopes after the air entry value. The Fredlund & Xing (1994) formulation displayed the flattest slope while the Van Genuchten (1980) formulation showed the steepest slope.

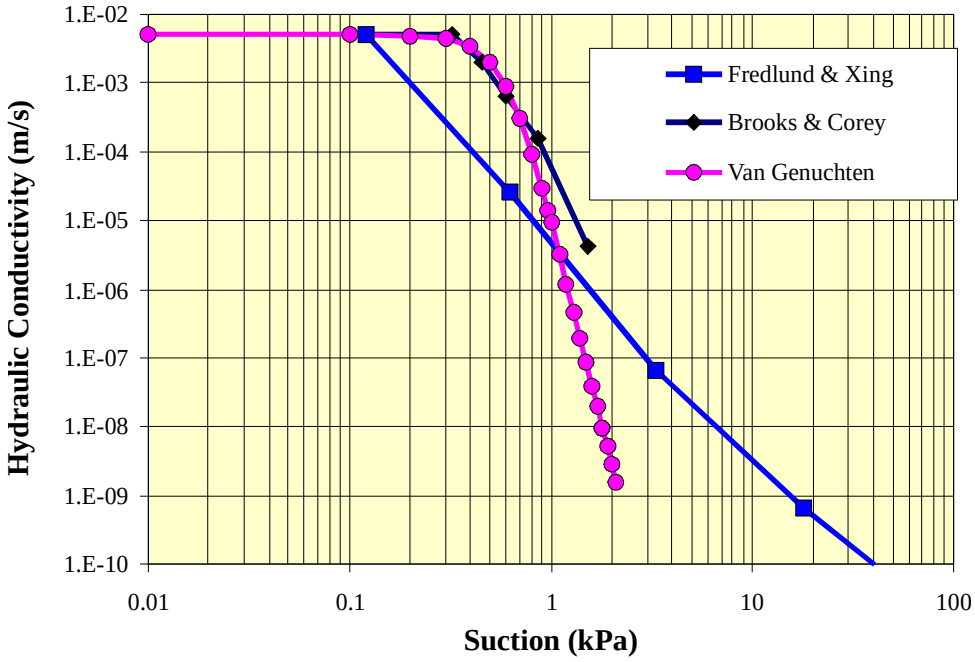

Figure 7.16 - Hydraulic conductivity functions of the coarse waste rock calculated from soil-water characteristic curve data

As with the fine column, data from the coarse column was used to generate hydraulic conductivity curves. The methodology differed from the fine column, since the inflow was approximately equal to the outflow. As a result, the hydraulic conductivity was calculated using a flux that was taken to be the average of the inflow and outflow rates. The results have been grouped into the top and bottom halves of the column for presentation purposes. Figure 7.17 displays the comparison between the hydraulic conductivity curves for the bottom half of the column and the calculated hydraulic conductivity curves. Tensiometer #2 was identified in the previous chapter as yielding higher suctions than the other tensiometers in the column. As a result the readings from the soil layers including this tensiometer should be viewed with some caution.

Figure 7.18 displays the comparison between the hydraulic conductivity curves for the top half of the column and the calculated hydraulic conductivity curves. Tensiometer #12 was also identified in the previous chapter as having anonymously high readings. In both of these graphs it is apparent that most of the data falls within a narrow range. The measured hydraulic conductivity functions display a decrease in the suction values at flux rates lower than 1 E-8 m/s. This is likely due to the precision of the suction

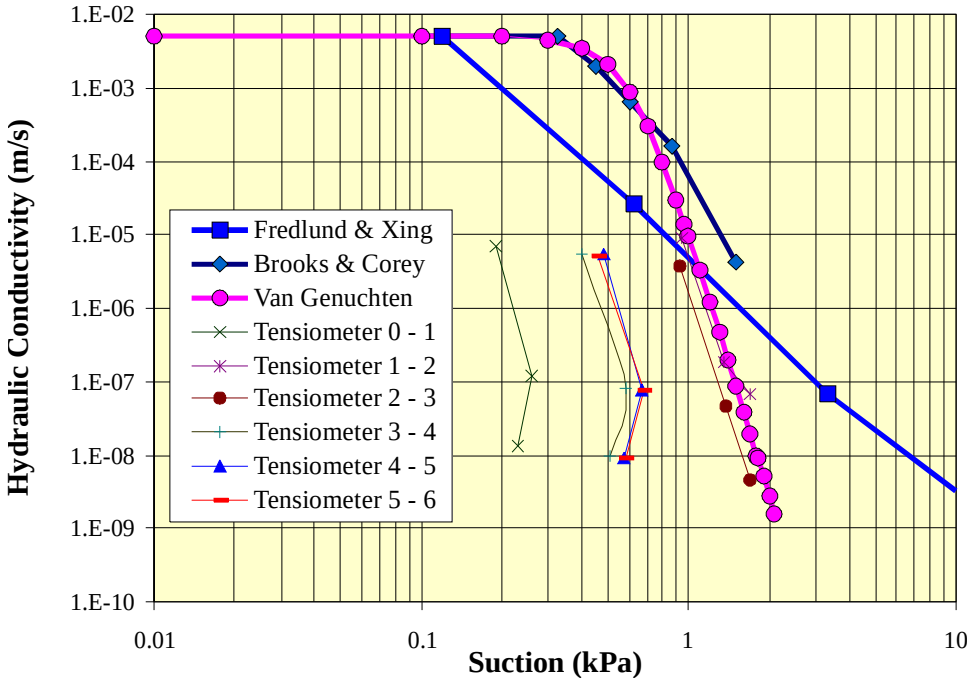

Figure 7.17 - Hydraulic conductivity functions of the coarse waste rock based on flowrates in the bottom half of the column in comparison to the hydraulic conductivity functions calculated from the soil-water characteristic curve data

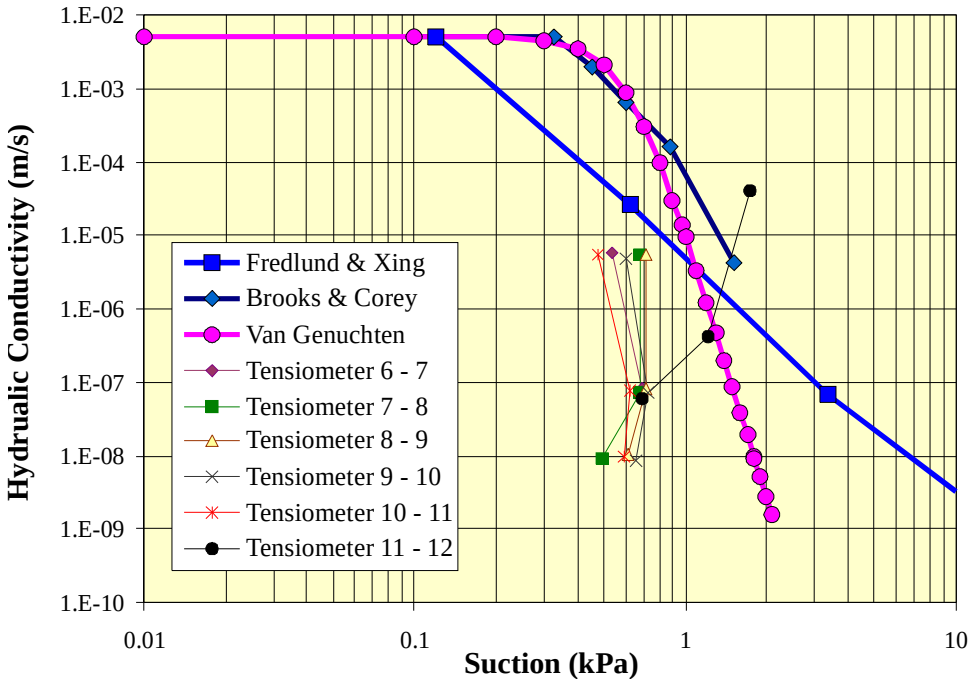

Figure 7.18 - Hydraulic conductivity functions of the coarse waste rock based on flowrates in the top half of the column in comparison to the hydraulic conductivity functions calculated from the soil-water characteristic curve data

measuring device as discussed in Section 6.3.2.1. However, the general trend of the data is still distinguishable. In most cases, the hydraulic conductivity of the waste rock measured in the column parallels or is steeper than the hydraulic conductivity function calculated using the Van Genuchten (1980) formulation. This suggests that the slope of the soil-water characteristic curve in the transition zone must as steep or steeper than the case when the datum is taken at the top. Therefore, the slope of the Van Ganuchten formulation was positioned so that it intercepted the data generated from the column as shown in Figure 7.19. The air entry value of the soil-water characteristic curve was estimated from the point at which this line intersects the saturated hydraulic conductivity (this assumes that the estimated hydraulic conductivity is correct). The air entry value was found to be 0.25 kPa. Knowing the air entry value and that the slope of the transition zone is approximately the same as for a datum at the top of the sample an appropriate soil-water characteristic curve can be constructed.

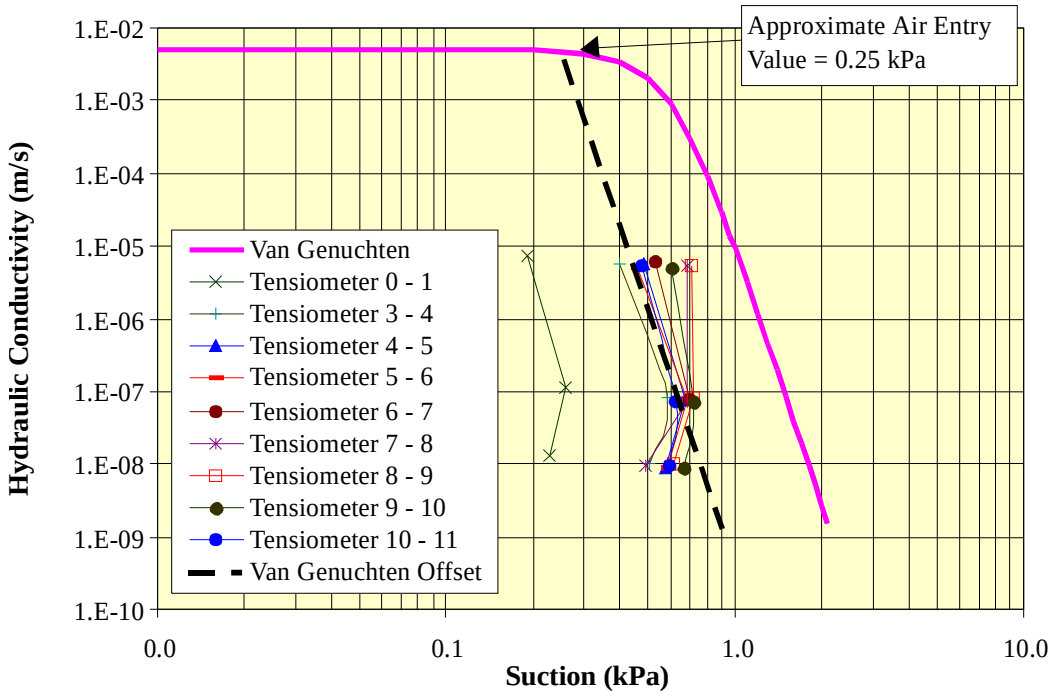

Figure 7.19 - Estimation of the air entry value of the coarse waste rock using a slope offset of the Van Genuchten Formulation

The interpreted soil-water characteristic curve for the coarse waste rock is shown in Figure 7.20. It compares favorably with the soil-water characteristic curve that would have been generated if the middle of the apparatus were chosen as the datum. This soil-water characteristic curve was used in the numerical model. The hydraulic conductivity curve used in the numerical model corresponded to Van Genuchten formulation adjusted to the new soil-water characteristic curve as shown in Figure 7.21.

The preceding discussion has focused on fitting the soil-water characteristic curve and hydraulic conductivity functions to those observed in the column. It should be noted however, that this is not the only possible solution. Two other alternative solutions exist that can also describe the hydraulic conductivity functions observed in the column. The first alternative is that the saturated hydraulic conductivity of the waste rock may be too high. If the saturated hydraulic conductivity of the waste rock was lowered to approximately 5 E-6 m/s (approximately 3 orders of magnitude), the hydraulic conductivity function would occupy roughly the same curve as the interpreted soil-water characteristic curve. However, it is very unlikely that this material would have such a

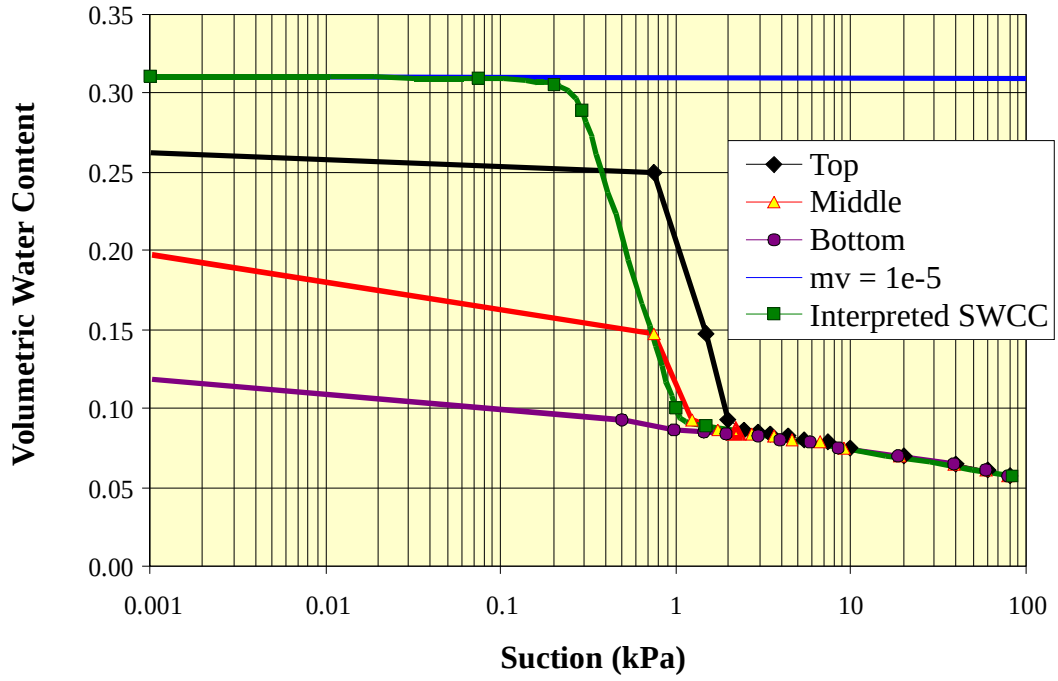

Figure 7.20 - Interpreted soil-water characteristic curve for coarse waste rock based on the estimated air entry value

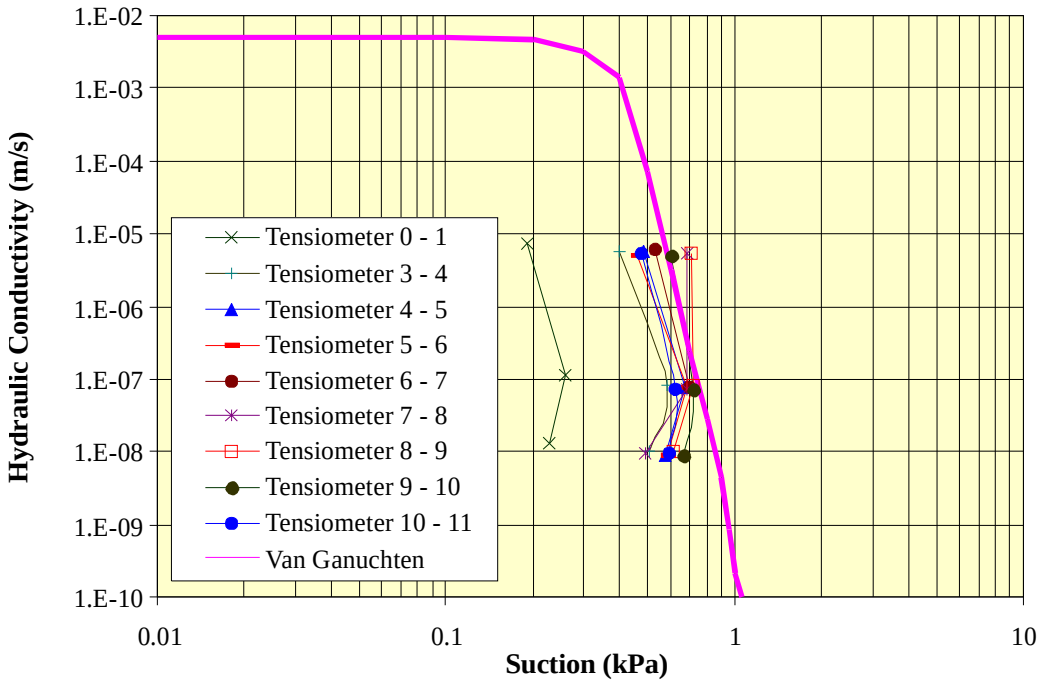

Figure 7.21 - Hydraulic conductivity function based on interpreted soil-water characteristic curve

low hydraulic conductivity. The other alternative is that the column may already be at its residual water content. Referring back to Figure 7.15, it is possible that the entire system could be at or beyond its residual water content. The nature of the hydraulic conductivity function after the residual water content is not well understood. The only possible way to distinguish the most likely scenario is to perform transient modelling using two different soil-water characteristic curves (one which has significant storage in the transition zone, the other at the residual with little or no storage) and compare the differences in the outflow in the models to the outflow of the actual column during changes in the applied flux.

7.3 Fine Column

The following subsections compare the results of numerical modelling and the data obtained from the fine waste rock column. As stated previously, the objective of the numerical modelling is to verify the general trends observed in the column. An intensive calibration and verification of the model was not attempted

7.3.1 Steady State Analysis

The results of the steady state numerical modelling are shown in Figure 7.22 plotted against the data collected from the fine column. The largest difference between the numerical model and the column data occurred at the lowest flux rates (1 E-8 m/s and 1 E-9 m/s). The numerical model displays the results for the steady state case; however the fine column has yet to reach steady state, resulting in the decreased suctions that are observed in the middle of the column. This will be examined in more detail during the transient analysis of the fine column.

The comparison of the modelled to measured equivalent collection area ratio is shown in Figure 7.23. It can be seen that at the high flux rates the equivalent collection area ratio compares well. At lower flux rates there is a pronounced difference in the two curves.

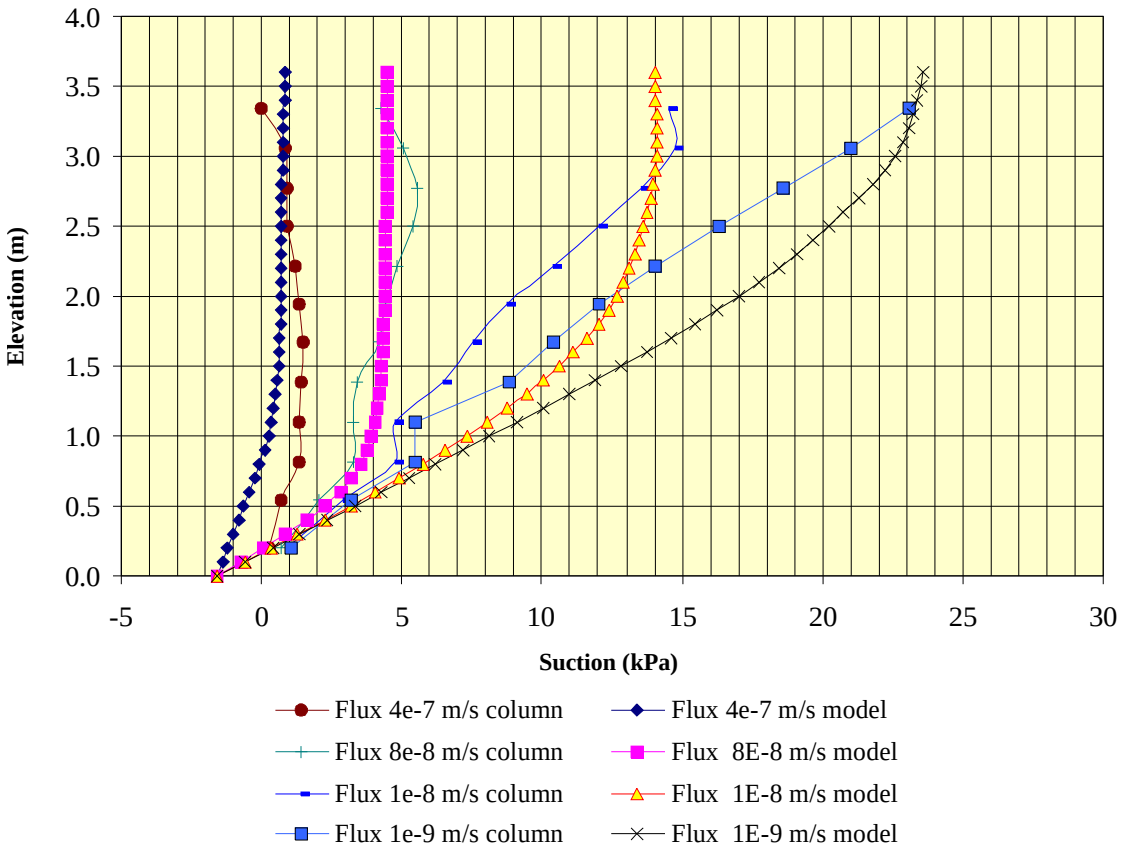

Figure 7.22- A comparison of the of the pressure profiles observed in the column to those calculated in the steady state analysis for the fine column

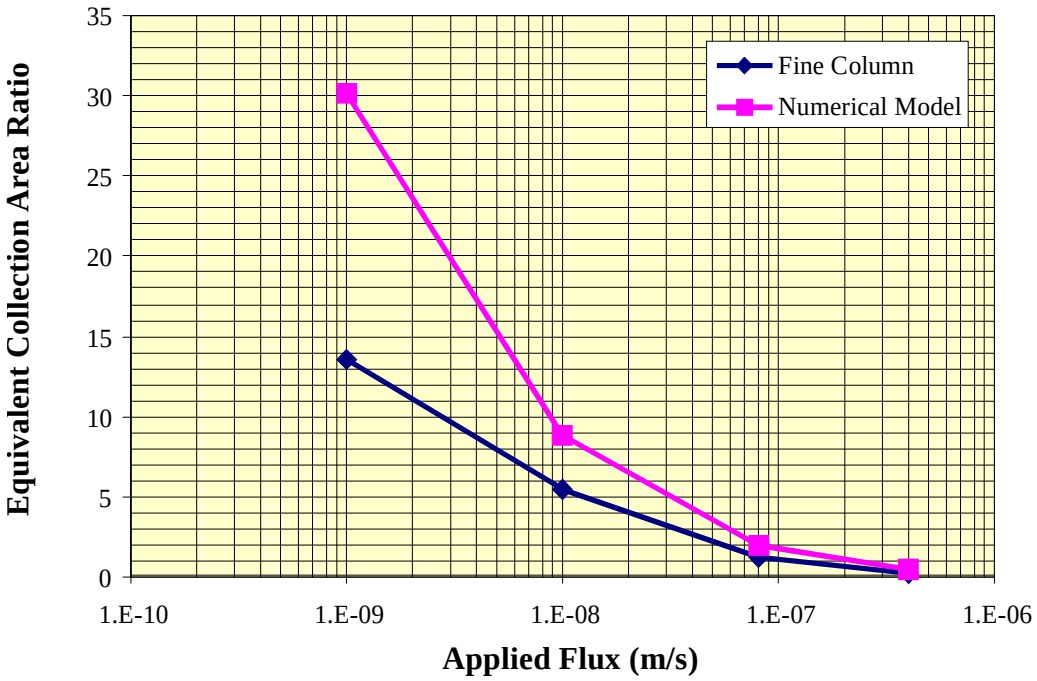

Figure 7.23 - A comparison the equivalent collection area ratio calculated from column data and those calculated by the numerical model

This may be a result of the column not having reached the steady state condition. When the system is at steady state, as is the case in the numerical model, the hydraulic gradient in the waste rock is approximately one. In comparison, the column has not reached the steady state conditions the gradient within the waste rock is significantly smaller than one. As groundwater flow is a function of the hydraulic gradient it would be expected that the model would display a higher equivalent collection area ratio. In addition, the hydraulic conductivity of the column will continue to decrease in the waste rock as the system moves towards the steady state condition. This would cause an increase in the observed equivalent collection area ratio as column comes to a steady state condition. This suggests that a higher equivalent collection area ratio is possible in the field when the lysimeter has been allowed to come to a steady state condition.

7.3.2 Transient Analysis

The following subsections present the result of transient modelling performed on the fine column. The first four subsections have been grouped according to flux rate. The

last subsection deals with the transient response of the lysimeter when filling versus emptying.

7.3.2.1 Initial condition to an applied flux of 4 E-7 m/s

The initial condition imposed on the numerical model consisted of the steady state condition for a flux rate of 1 E-12 m/s. This flux rate was chosen, because it produced a volumetric water content in the waste rock that was comparable to the water content of the material in the column when it was initially placed. The cumulative outflow from the initial condition to a flux rate of 4 E-7 m/s is shown in Figure 7.24. The numerical model displays a similar shaped curve to that measured in the column with the break through of the flux rate occurring at 5 to 10 days. It is important to note that the prototype was subjected to various fluxes until one was found that could be supported by the system. However, it can be seen that both the numerical model and the prototype come into a steady state flow condition after approximately 10 days.

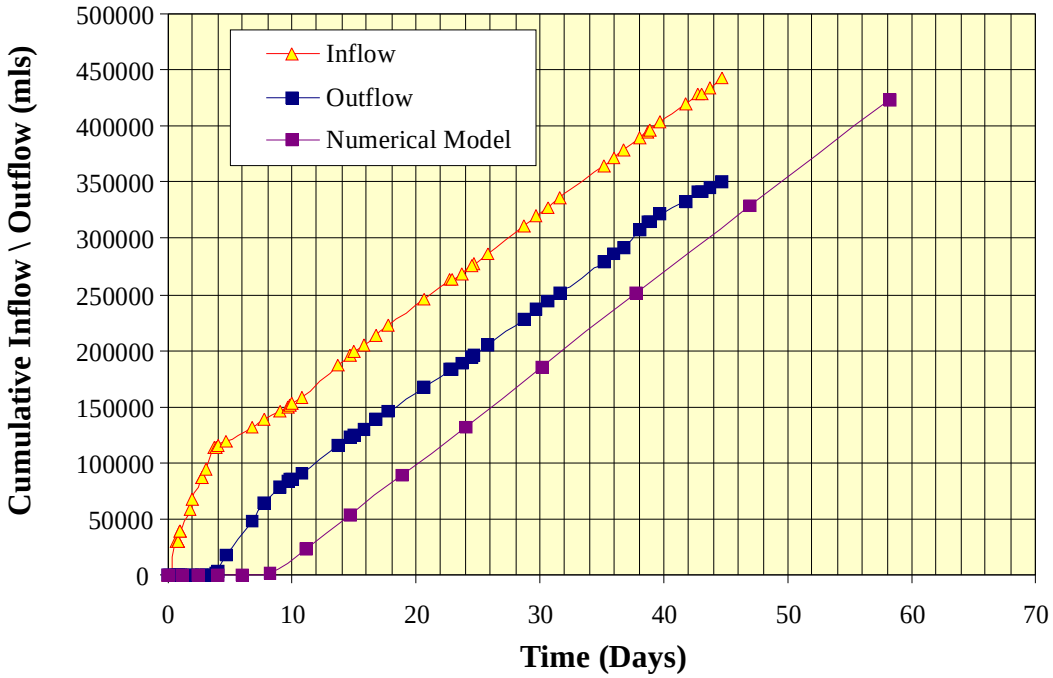

Figure 7.24 - A comparison of the modelled and observed column outflows from the initial condition to the end of the flux rate of 4E-7 m/s

The pressure profiles in the column with time for the numerical model are shown in Figure 7.25. From this graph it can be seen that the system comes to steady pressure readings in 11 days. Data from the column was poor during the initial stages of the testing, because the manometer board could not measure the initial suctions in the column (the water was drawn out of the manometer tubing). As a result the data from the column has not been plotted on this figure.

Figure 7.26 compares the suction generated at an elevation equal to the top of the lysimeter in the numerical model and the data that was collected from the column. The data from the model compares well with the data from the column.

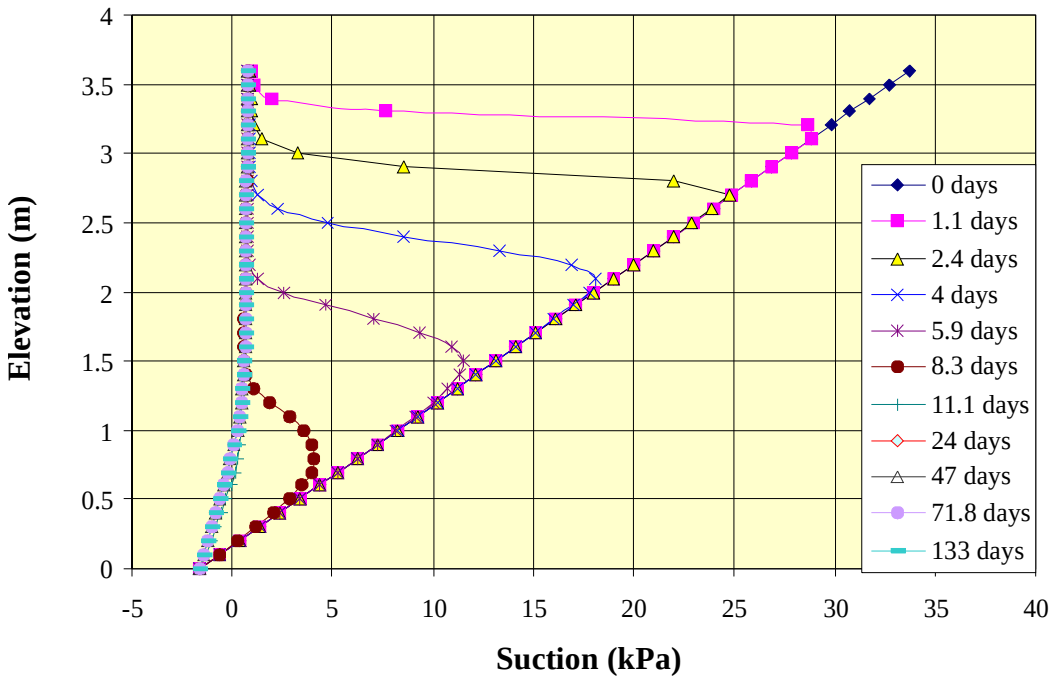

Figure 7.25 - Pressure profiles with time calculated by the numerical model for a change in flux from the initial condition to the end of the constant flux rate of 4E-7 m/s

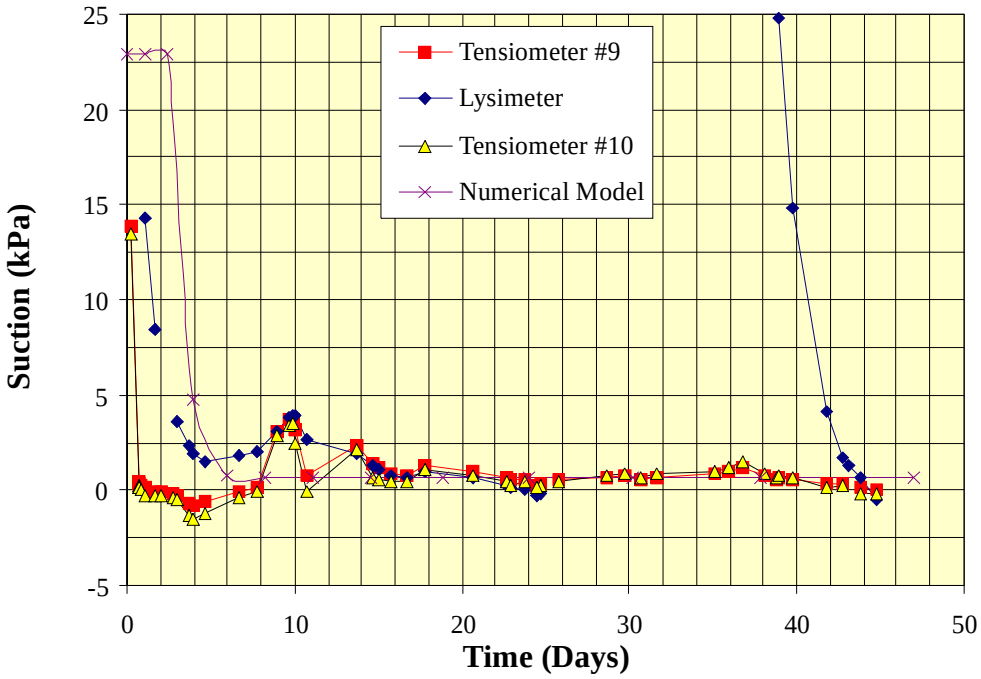

Figure 7.26 - A comparison of the suction values observed in the column and those calculated by the numerical model from the initial condition to the end of the constant flux rate of 4E-7 m/s

7.3.2.2 Flux rate of 4 E-7 m/s to 8 E-8 m/s

The cumulative outflow plot after decreasing the applied flux rate from 4 E-7 m/s to 8 E-8 m/s is shown in Figure 7.27. The outflow out of the column was not recorded as discussed in Section 6.3.1.2. However, it can be seen that once the outflow readings were re-established they show that the column had come to a steady state condition.

Figure 7.28 displays the pressure profiles with time for both the model and the column. The shift in the suction values for the column appears to be slightly faster than that for the model. This might indicate that the hydraulic conductivity of the column was slightly higher than that of the model or that the change in the amount of storage in the system in moving from one flux rate to the other is slightly higher in the model. However, given these small differences it can be said that the model corresponded well with the data observed in the column.

A comparison of the suction measurements near the top of the lysimeter is shown in Figure 7.29. The response times and suction values generated with the numerical model compare well with the measurements made on the column, despite the fact that the suctions decreased with time in the column. The cause of the drop in the suction measurements in the column was discussed in Section 6.3.1.2

7.3.2.3 Flux rate of 8 E-8 m/s to 1 E-8 m/s

Figure 7.30 displays the cumulative outflow for both the numerical model and the fine column. The outflow curves have the same basic shape, however they appear to diverge slightly as the flowrate decreases. This would suggest that the hydraulic conductivity of the column decreases faster than the hydraulic conductivity of the model, such that it takes longer to pass the same amount of water. In comparison to the inflow it can be seen that the column outflow is not at steady state even after 57 days. The numerical model does not appear to be at the steady state condition even after 87 days.

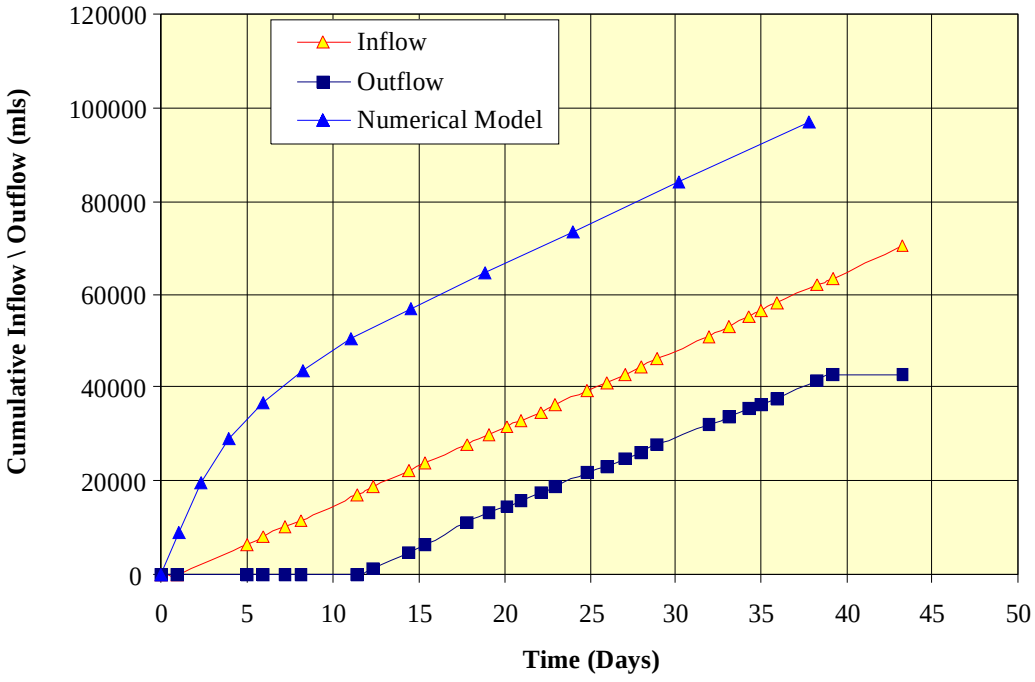

Figure 7.27 - A comparison of the modelled and observed cumulative column outflows from the 4E-7 m/s flux rate to the end of the constant flux rate of 8E-8 m/s

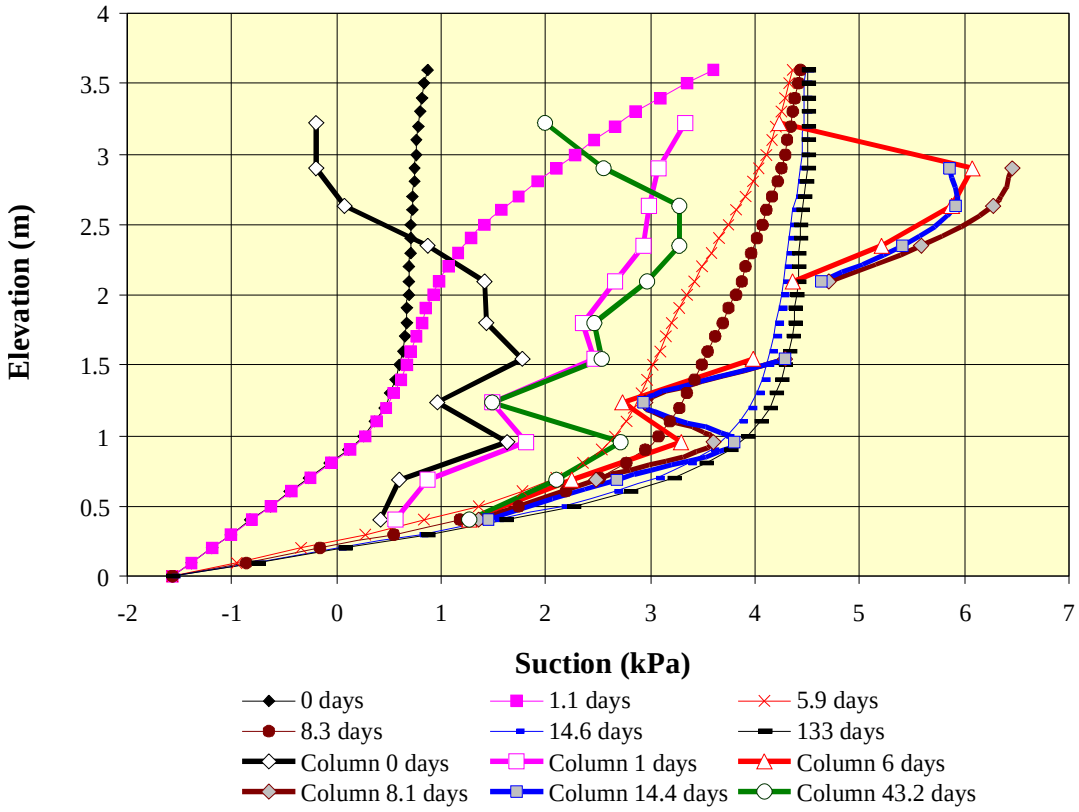

Figure 7.28 - A comparison of the changes in the pressure profile of the column with time calculated by the numerical model and observed in the fine waste rock column for a change in flux from 4E-7 to the end of the constant flux rate of 8E-8 m/s

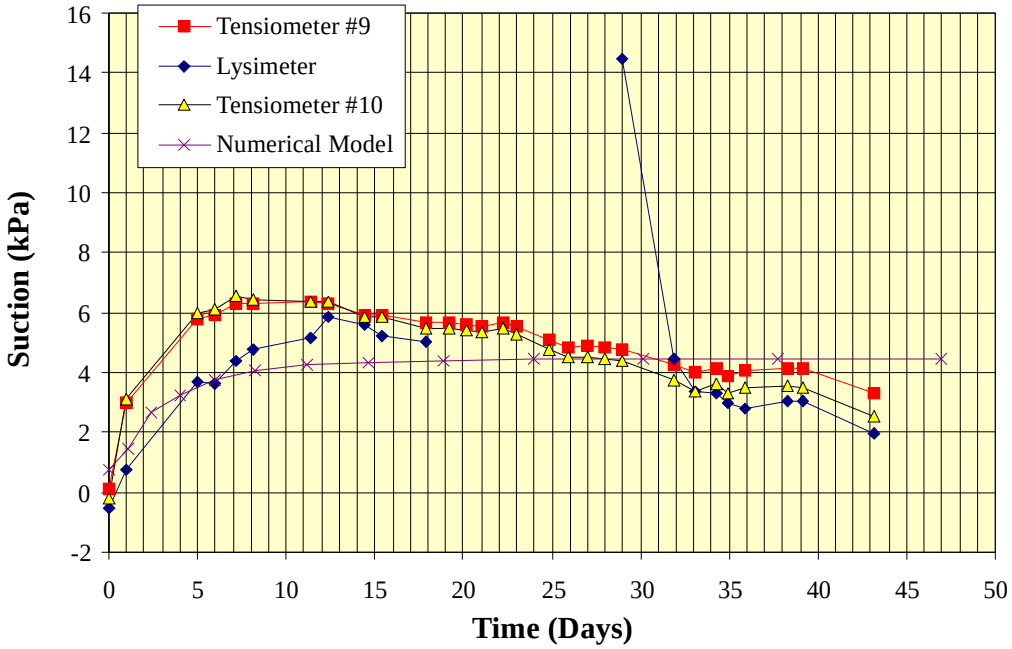

Figure 7.29 - A comparison of the suction values with time observed in the column and those calculated by the numerical model from the flux rate 4E-7 m/s to the end of the constant flux rate of 8E-8 m/s

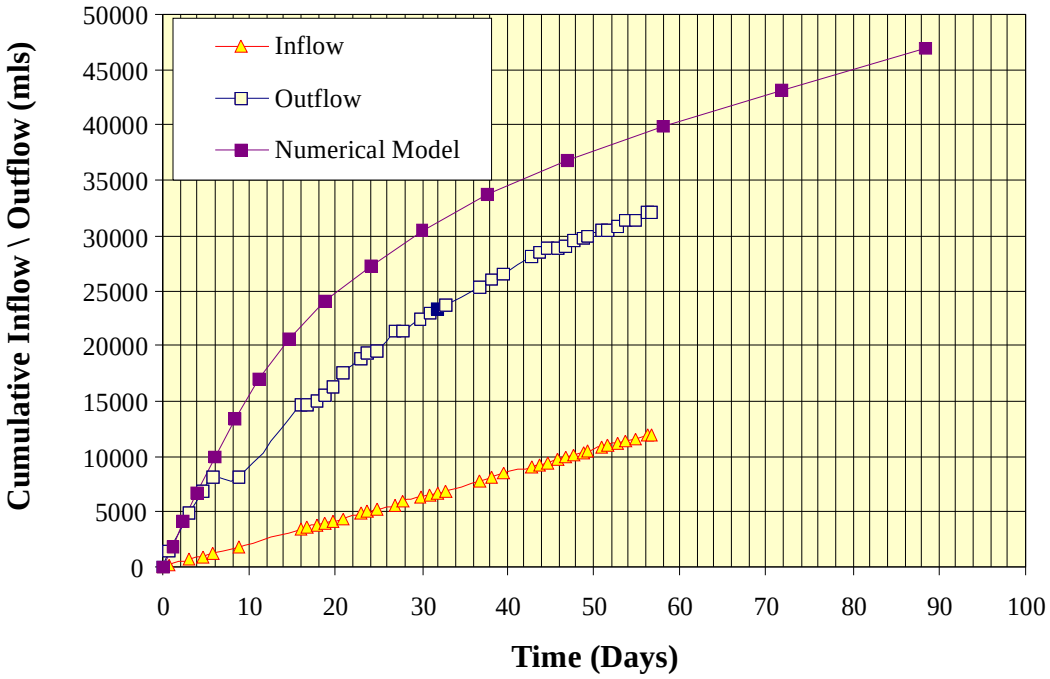

Figure 7.30 - A comparison of the modelled and observed cumulative column outflows from the 8E-8 m/s flux rate to the end of the constant flux rate of 1E-8 m/s

Figure 7.31 displays the pressure profiles with time for both the model and the column. The suction values at the top of both the fine column and model move faster than the middle of the column. The relative change of the suction values at different elevations within the column and the numerical model are similar. However, there was a notable difference between the column and the model in the suction values at the middle of the column. The suction profile of the model has a classical Kisch (1959) solution type of shape, while the middle of the fine column appears more as a straight line. This could be due to heterogeneity in the column. At an elevation of just over 1 m in the fine column there appears to be a break in the pressure profile line after which the pressure profiles appear lower than they should. If a layer located at just above the 1 m level in the column had a slightly lower hydraulic conductivity than the rest of the column it would prevent the rest of the column above from draining, therefore causing lower suctions in the layers above it.

Figure 7.32 displays the pressure profiles at the top of the lysimeter for both the column and the numerical model. The response of the model and column appear similar however

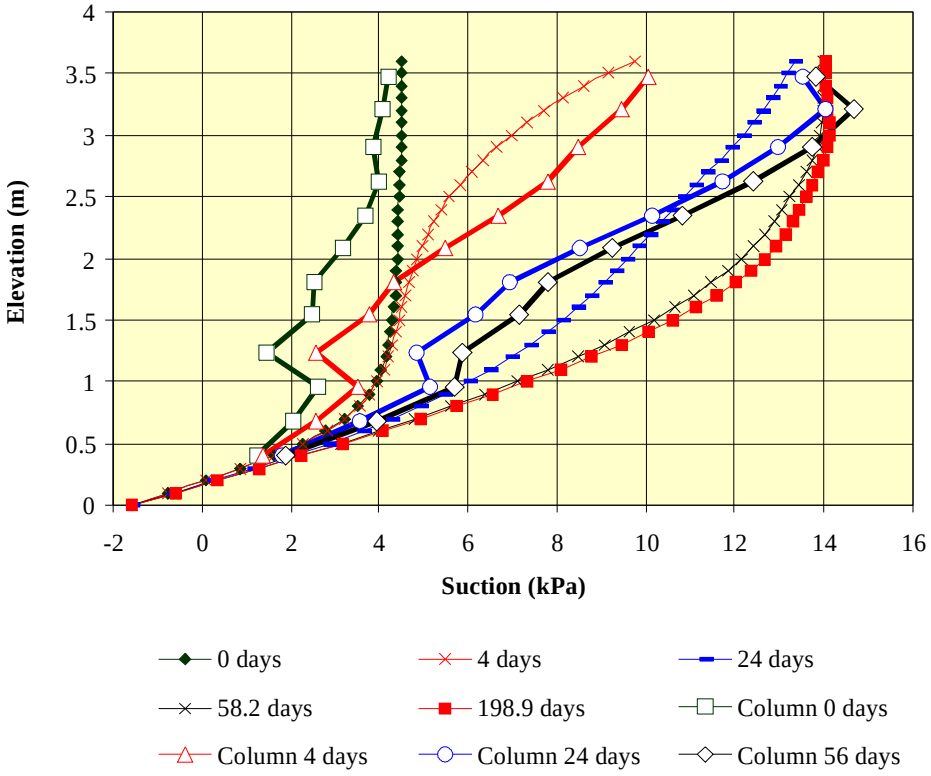

Figure 7.31 - A comparison of the changes in the pressure profile of the column with time calculated by the numerical model and observed in the fine waste rock column for a change in flux from 8E-8 to the end of the constant flux rate of 1E-8 m/s

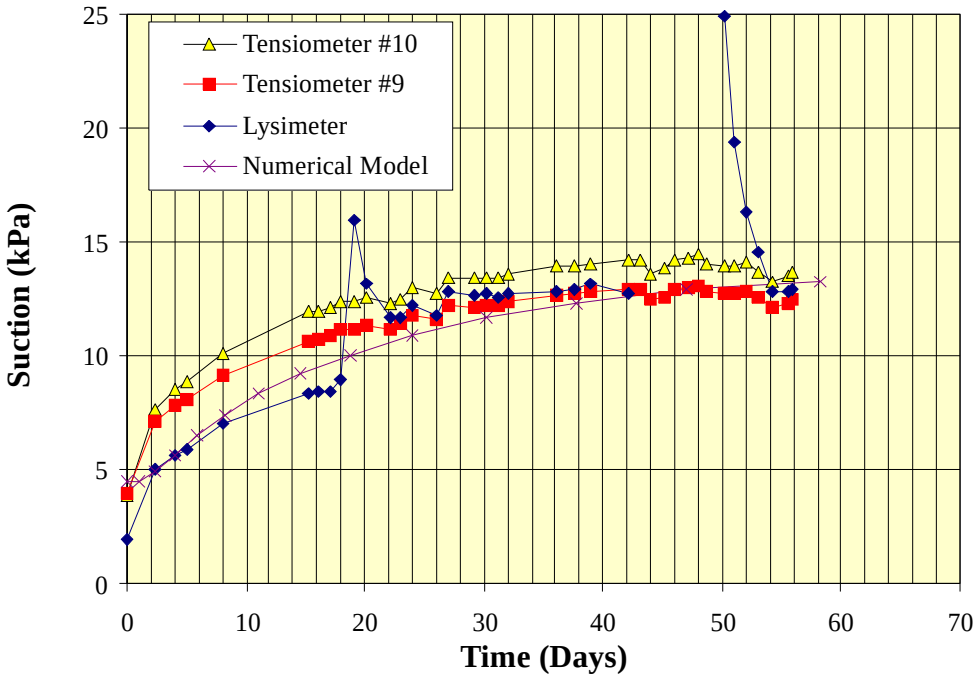

Figure 7.32 - A comparison of the suction values with time observed in the column and those calculated by the numerical model from the flux rate 8E-8 m/s to the end of the constant flux rate of 1E-8 m/s

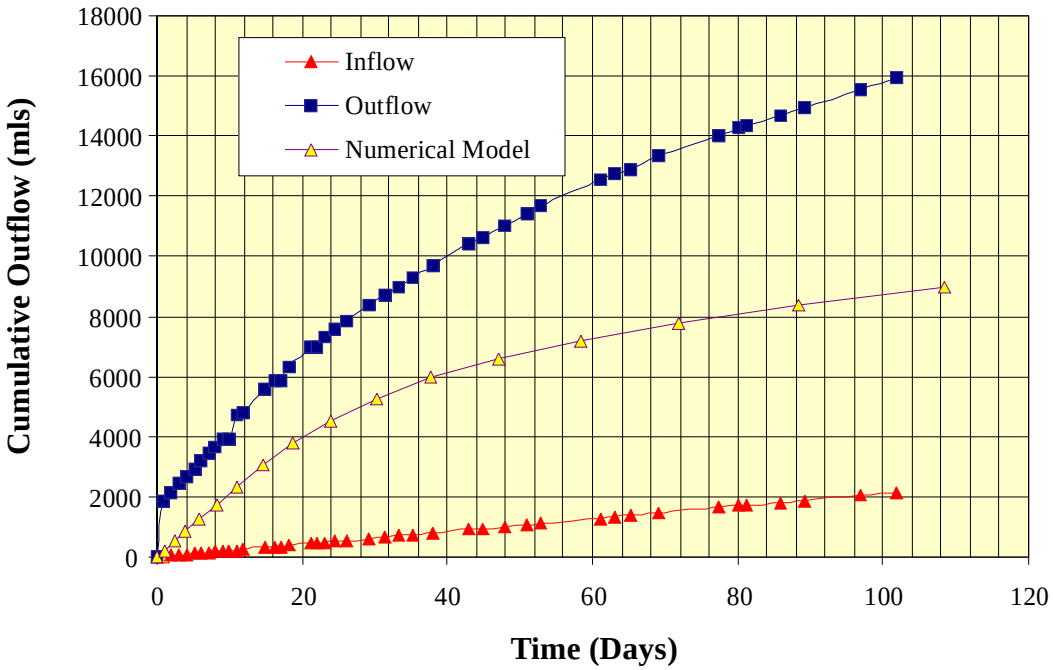

Figure 7.33 - A comparison of the modelled and observed cumulative column outflows from the 1E-8 m/s flux rate to the end of the constant flux rate of 1E-9 m/s

the model appears to lag behind the column slightly. This corresponds with the previous flux rate where the top of the column also responded quicker than the model. This might indicate slight differences in the hydraulic conductivity function or the amount of change of water storage in the system (slightly different soil-water characteristic curves).

7.3.2.4 Flux rate of 1 E-8 m/s to 1 E-9 m/s

The cumulative outflow plot from a flux rate of 1 E-8 m/s to 1 E-9 m/s is shown in Figure 7.33. At first glance, it would appear that the cumulative outflow from the column was much different than that of the model. However, it must be considered that the previous flux rate had not come to the steady state condition. Furthermore, a low hydraulic conductivity layer in the middle of the column would have impeded drainage at the previous flux rate. Thus, the column would have to first remove all of the remaining water held in storage from the previous flux prior to removing the change in water storage due to the change in the flux rate. In both the model and the column it can be seen that even after 100 days the system has not reached a steady state condition.

The pressure profiles with time for both the column and numerical model are shown in Figure 7.34. It shows trends that are similar to those observed during the last flux rate. A comparison between the modelled and column suction values near the lysimeter top is shown in Figure 7.35. Despite the fact that the outflow curves are significantly different, the suctions values reported near the top of the lysimeter in both the model and column compare well.

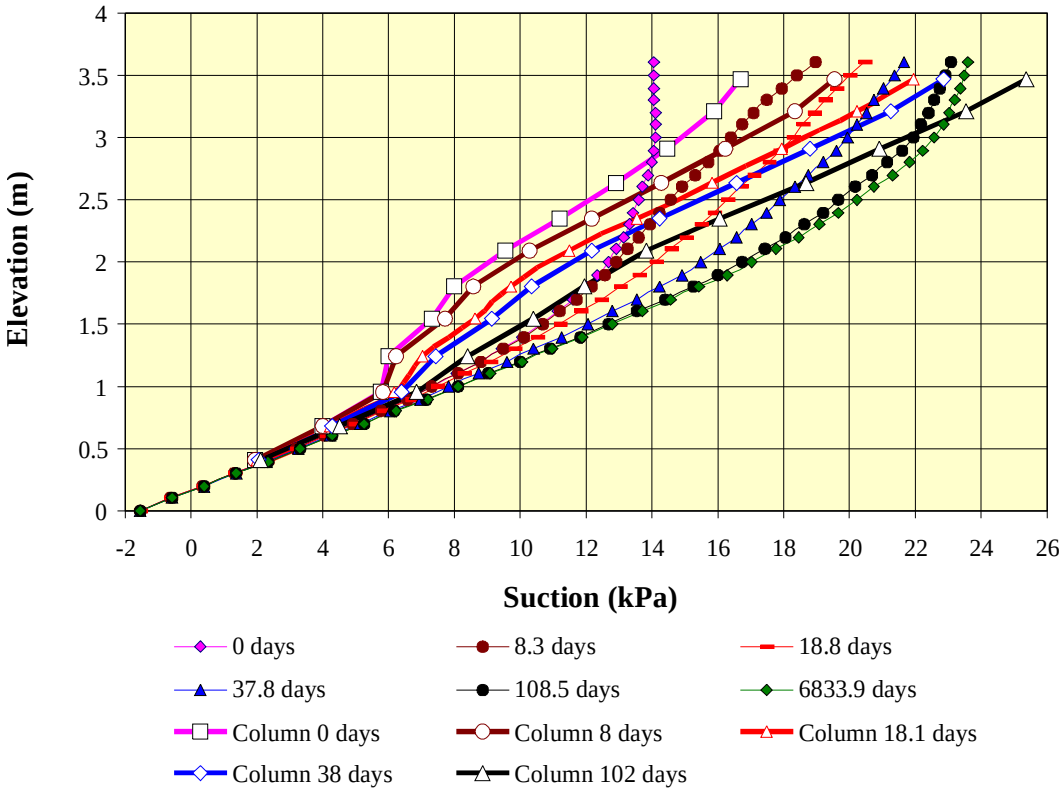

Figure 7.34 - A comparison of the changes in the pressure profile of the column with time calculated by the numerical model and observed in the fine waste rock column for a change in flux from 1E-8 to the end of the constant flux rate of 1E-9 m/s

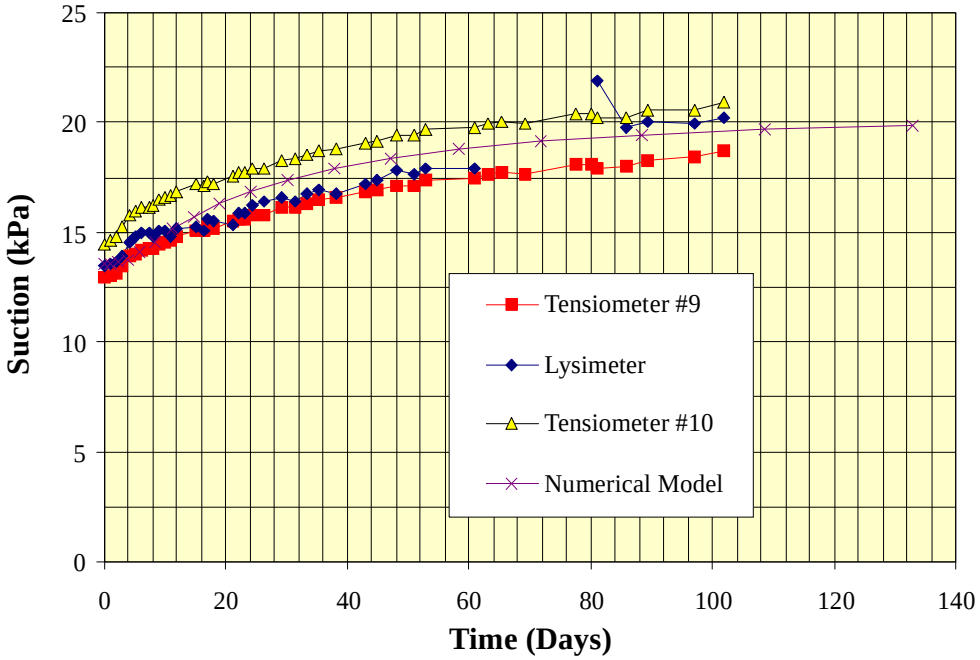

Figure 7.35 - A comparison of the suction values with time observed in the column and those calculated by the numerical model from the flux rate 1E-8 m/s to the end of the constant flux rate of 1E-9 m/s

The Effect of Emptying versus filling the lysimeter on time to equilibrium

Section 6.3 identified that there was an obvious difference between the time that it took for the lysimeter to come to pressure equilibrium with the surrounding waste rock when filling in comparison to when the lysimeter was emptying. A transient analysis was undertaken to determine if the apparent lag when emptying the lysimeter in comparison to filling the lysimeter was the result of the hydraulics of the system. Figure 7.36 displays the results of the transient analysis. It is apparent that there is very little difference in the time to equilibrium for filling versus emptying when hydraulics alone are considered. Therefore, the contact between the silica flour and the waste rock materials must be better when filling the lysimeter than it is when emptying the lysimeter, due to the increased suction that is applied to the waste rock during filling. The increase in suction when filling the lysimeter would pull water into the void spaces in the waste rock located around the silica flour thus increasing the contact between the two materials. Hysterisis in the hydraulic conductivity function of the waste rock may also contribute to the time difference as described in Section 6.3.1.2

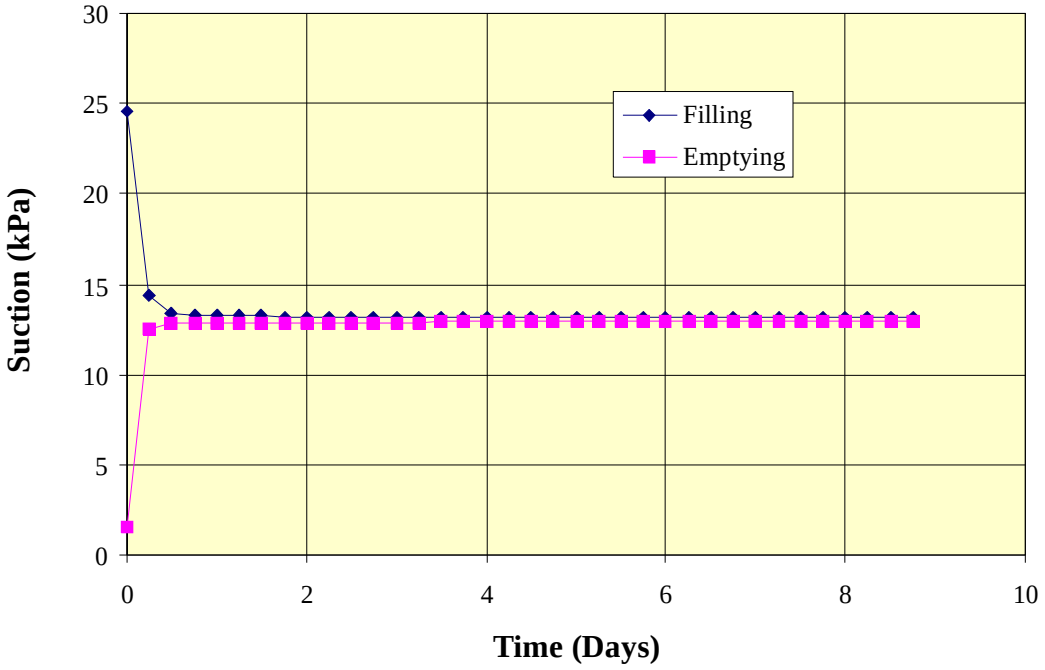

Figure 7.36 - The effect of emptying or filling the lysimeter on the time to return to measuring steady state suction values

7.4 Coarse Column

Numerical modelling of the coarse column could not be achieved due to convergence problems associated with the steep slope of the hydraulic conductivity function. A steady state analysis was performed utilizing the Kisch (1959) solution. Transient analysis of the coarse column by means other than a numerical computer model was not attempted.

7.4.1 Steady State Analysis

The results of the Kisch (1959) solution for the steady state condition for all flux rates are shown in Figure 7.37. The results of the Kisch (1959) solution for coarse waste rock appear as vertical line because the transition zone only extends to approximately 2.5 cm in elevation. The results from the coarse column do not show a clear pattern of increasing suction with a decreasing flux rate as the tensiometers may be within their limits of precision. Assuming that the data from the tensiometers is somewhat representative of the system, it would appear that either the hydraulic conductivity function may be too flat or it could be shifted slightly to the left (lower suctions to produce the same hydraulic conductivity).

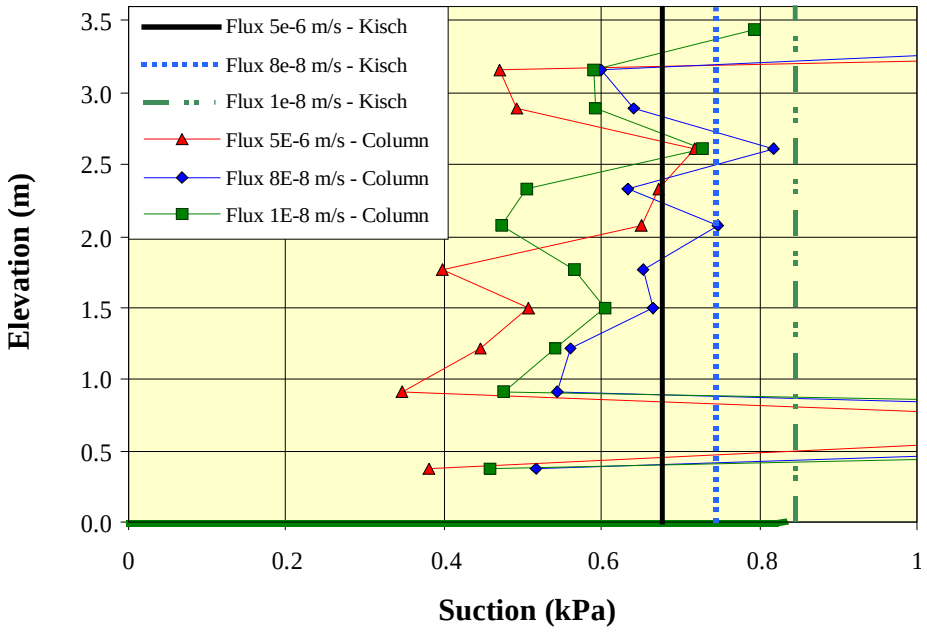

Figure 7.37 - A comparison of the of the pressure profiles observed in the column to those calculated by the Kisch (1959) solution in the coarse column

7.5 Summary of Analysis

The soil-water characteristic curves and hydraulic conductivity curves for both the fine and coarse waste rock were examined. The suctions measured at the top of the fine column were found to be a good representation of the hydraulic conductivity function. In comparison to calculated hydraulic conductivity functions for fine waste rock, the Van Genutchen (1980) formulation was found to be the most similar. The calculated hydraulic conductivity function for the coarse waste rock was found to exhibit higher suctions than those observed in the column at comparable flux rates. Back analysis of the test data revealed two possible rationalizations. The first rationalization was that the difference was a result of the assumed datum (top of soil) during tempe cell testing. The analysis suggested that the middle of the soil in the tempe cell should be used as the datum. The second rationalization is that the coarse column was at or beyond its residual water content where the nature of the hydraulic conductivity function is not well understood. In comparing the measured hydrualic conductivity function to the calculated ones, the Van Genutchen formulation was found to be the most similar.

The steady state modelling of the fine column showed that the measured equivalent collection area ratios were lower those calculated by the numerical model. This may be the result of the column not reaching a steady state condition where the hydraulic gradient is equal to one. In the fine column the hydraulic gradient was less than one. This suggests that the equivalent collection area ratio will improve with time until a steady state condition is reached.

The transient modelling of the fine column suggests that there may have been some heterogeneity in the middle of the column causing the column to display suctions that were lower than those calculated by the numerical model. The lysimeter in the numerical model followed the same trends as those shown in the prototype. The increase in the response time of the lysimeter when filling versus emptying showed that the difference in response times was not a function of the hydraulics of the system. This suggests that hysterisis of the soil-water characteristic curve or better contact when filling was the cause of observed difference in the time for the lysimeter to come to equilibrium.

Numerical modelling of the coarse column was not possible due to convergence problems associated with its steep hydraulic conductivity function. The Kisch (1959) solution was used to compare to the suctions measured in the column. The results of the analysis indicate that although the hydraulic conductivity function of the coarse waste rock was improved through interpretation, the air entry value could still be slightly lower. Unfortunately, the question of whether the coarse waste rock was in the transition or residual stage could not be answered. The solution will have to wait until the appropriate mathematical methods can be discovered to deal with the convergence problems associated with a steeply sloping hydraulic conductivity function.

CHAPTER 8 CONCLUSIONS

The objective of this research program was to design a lysimeter that is capable of measuring soil suction as well as collect a pore water sample for geochemical analysis. This objective was accomplished in a number of steps, which included; identifying key design elements in a preliminary numerical model program, quantifying the material properties of the materials that were used in the construction of the prototype lysimeter, constructing and monitoring two prototype lysimeters and analyzing the results of the prototype lysimeter testing columns.

The conclusions of the preliminary modelling program were:

1. The ideal lysimeter backfill should have an air entry value higher than the range of suctions being measured, a high hydraulic conductivity and a low capacity for volume change. The lysimeter backfill used in the lysimeter prototypes consisted of silica flour, however, the lysimeter performance could be improved by optimizing the material properties of the lysimeter backfill.

2. The modelling of the silica flour extension identified that the exclusion of the silica flour extension would decrease the error in the suction measurement. However, the modelling also identified that the equivalent collection area ratios would drop. A third criteria was also be included in the analysis. If the lysimeter does not develop a contact between itself and the surrounding waste rock, suction cannot be measured and a pore water sample cannot be collected. Therefore, although the inclusion of the silica flour extension increases the suction error, it is vital to ensure that there is a contact developed between waste rock and the lysimeter.

3. The preliminary modelling program consistently showed that smaller diameter lysimeters outperform larger diameter lysimeters when suction error and equivalent collection area ratios are considered

4. The bell shaped lysimeters that were modelled demonstrated that only marginal increases in the equivalent collection area ratio could be attained through the use of bell shaped lysimeters.

5. The standpipe lysimeter will always measure suctions that are slightly lower than the actual suctions in the column. This is due to the small increase in the hydraulic head that must be developed to force the water out of the silica flour and back into the waste rock. For the lysimeter that was used as the prototype, the maximum error that was observed during the preliminary modelling program was less than 8%.

The conclusions of the prototype standpipe lysimeter testing program were:

1. The prototype lysimeter was able to measure suction. The accuracy of the suction measurement was not characterized because there was no suitable absolute reference and it was unclear at what point in time to make the accuracy measurement. In general, for suctions less than 10 kPa the suction measurement was within 1 kPa of the tensiometer measurement, for suctions between 10 and 20 kPa the suction measurement was within 2 kPa of the tensiometer measurement when the column was near a steady state pressure profile and the lysimeter had been nulled. During transient events the lysimeter lagged behind the tensiometers.

2. The prototype lysimeter was able to collect a pore water sample. Pore water samples were collected at all flux rates. The measurement of the equivalent collection area ratio verified that the lysimeter acted as a preferential flow path at fluxes lower than the saturated hydraulic conductivity of the silica flour. This is significant because it allows for the collection of a porewater sample even at very low flux rates.

3. The fact that the equivalent collection area ratio in the coarse waste rock column increased shows that the flow of water in the coarse column responds to small changes in suction. This suggests that the flow of water through coarse waste rock piles can be modelled using models based on the flow of water through a porous medium.

4. Tensiometers when used in conjunction with the preferential flow paths provided by the silica flour can also be used to collect a pore water samples. However, further analysis should be performed to investigate the effect of the elevated gradient on the flow system in the waste rock pile.

The conclusions of the analysis were:

1. The fine waste rock column data displayed the same general trends as the numerical models. Further analysis should be undertaken to verify the cause of the elevated suction values in the middle of the column.

2. An improved method of testing the soil-water characteristic curves of coarse materials should be developed. Specifically, there is a need for a method of correcting the volumetric water contents and suction values obtained at very low suction (less than 1 kPa).

3. A method of modelling coarse grained soils with steep hydraulic conductivity functions should be investigated.

REFERENCES

Aboukhaled, A., Alfaro, A., Smith, M. 1982. Lysimeters. Food and Agr. Org. of the United Nations, FAO Irrig. And Drain. Paper No. 39. 68pp.

ASTM American Society for Testing and Materials. 1993. Designation 422-63 Standard Test Method for Particle Size Analysis of Soils. 1993 Annual Book of ASTM Standards, Philadelphia

ASTM American Society for Testing and Materials. 1997. Designation D-2435-96 Standard Test Method for One-Dimensional Consolidation Properties of Soils. 1997 Book of ASTM Standards, Philadelphia

Barbour, S.L. and Yanful, E.K. 1993. A column study of static nonequilibrium fluid pressures in sand during prolonged drainage. Canadian Geotechnical Journal, 31:299-303

Bews, B.E. and Barbour, S.L. 1997. Numerical Modelling of a 'Multi-Purpose' Lysimeter Design. Internal Report. Dept. of Civil Engineering. University of Saskatchewan.

Bews, B.E., O'Kane, M.A., Wilson, G.W., Williams, D., and Currey, N. 1997a. The Design of a Low Flux Cover System, including Lysimeters, for Acid Generating Waste Rock in Semi-Arid Environments. Proceedings of the 4th International Conference on Acid Rock Drainage (ICARD). Vancouver, B.C. 1997. Vol.2. pp 747-762

Bews, B.E., Barbour, S.L., Wilson, G.W., O'Kane, M.A. 1997b. The Design of Lysimeters for a Low Flux Cover System over Acid Generating Waste Rock. Proceedings 50th Canadian Geotechnical Conference of the Canadian Geotechnical Society. Ottawa, Ont. October 20-22,1997. pp. 26-33.

Bond, W.R. and Rouse, J.V., 1985. Lysimeters Allow Quicker Monitoring of Heap Leaching and Tailings Sites. Mining Engineer (Littleton, Colo) v.37 n.4 pp314-319.

Brooks, R.H. and Corey, A.T. 1964. Hydraulic Properties of Porous Media. Colorado State University (Fort Collins), Hydrology Paper 3

Colman, E.A. and Hamilton, E.L. 1947. The San Dimas Lysimeters: 2.The relative performance of four types of lysimeters. For. Res. Notes no. 47. USDA For.Serv. Calif. For Range Exp. Stn.

Couzens, T.R., 1985. Planning Models:Operating and environmental implications. In design of non-impounding mine waste dumps, M.K. Carter Ed. American

Institute of Mining, Mettalurgical and Petroleum EngineersInc., New York. pp13-20.

Fredlund, D.G. and Rahardjo, H., 1993. H. Soil Mechanics for Unsaturated Soils. John Wiley and Sons Inc. New York, NY.

Fredlund, D.G. and Xing, A. 1994. Equations for the Soil-water Characteristic Curve. Canadian Geotechnical Journal, 31:521-532

Fredlund, D.G., Xing, A and Huang, S. 1994. Predicting the Permeability Function Using the Soil-water Characteristic Curve. Canadian Geotechnical Journal, 31:533-546

Freeze, R.A. and Cherry, J.A., 1979. Groundwater. Prentice Hall, Englewood Cliffs, NJ.

Geoslope Int. 1999. Seep /W users manual.

GDS Instruments Ltd. 1991. The GDS Users Hanbook ver. 1.3.

Gordon, M.E., Huebner, P.M., and Miazga, T.J. 1989. Hydraulic Conductivity of three landfill clay liners. Journal of Geotechnical Engineering. v.118 n8 pp. 1148-1160

Herasymiak, G.M., 1996. Hydrogeology of a Sulphide Waste Rock Dump. M.Sc. Thesis, University of Saskatchewan.

Howell, Terry A., Schneider, A.D., and Jensen, M.E. 1991. History of Lysimeter Design and Use for Evapotranspiration Measurements. Lysimeters for Evapotranspiration and Environmental Measurements Proceedings of the International Symposium on Lysimeters for Evapotranspiration and Environmental Measurements Jul 23-25 1991 1991 Sponsored by : ASCE Irrigation & Drainage Div; ASAE; American Soc of Agronomy; Crop Science Soc of America; Soil Science Soc of America; et al Publ by ASCE New York NY USA p 1-9 ASBN : 0-87262-813-2

Jemison, J.M. and Fox R.H. 1992. Estimation of Zero-Tension Lysimeter Collection Efficiency. Soil Science, v.154 n.2 pp.85-94

Jordan, C.F., 1966. A Simple-Tension Free Lysimeter. Soil Science, v.106 n.3 pp81-86

Kisch, M. 1959., The theory of seepage from clay-blanketed reservoirs. Geotechnique, 9:9-21.

Kohnke, H., Dreibelbis, F.R., and Davidson, J.M. 1940. A survey and discussion of lysimeters and a bibliography on their construction and performance. Misc. Publ. No. 372., U.S. Dept. of Agric., Washington, D.C. 68p.

Koorevaar,P., Melenik, G. and Dirksen, C. 1983. Elements of Soil Physics. New York: Elsevier Science Publishing Company Inc., 228 pp.

Lambe, T.W., Whitman, R.V. 1979.Soil Mechanics SI Version. John Wiley and Sons Inc. New York, NY.

MEND. 1993. SoilCover User's Manual, Version 1.0, Dept. of Civil Engineering, University of Saskatchewan, Saskatoon, Saskatchewan, Canada

McGuire, P.E., Lowery, B., Helmke, P.A. 1992. Potential Sampling Error: Trace metal adsorption on Vacuum Porous Cup Samplers, Soil Science Society of America Journal, v. 56 pp.74-82.

Morin, K.A., Horne, I.A., and Rehiem, D., 1994. High Frequency Monitoring of Toe Seepage from Mine-rock Dumps, BHP Minerals' Island Copper Mine, B.C. In Proc. 3rd Intl. Conf. on the Abatement of Acid Drainage. Pittsburg, PA. April 24-29, v.1, pp. 346-354

Nevada Division of Water Planning, 1998. Water Words Online Dictionary . http://www.state.nv.us/cnr/ndwp/dict-1/WORD_H.htm

Newman, G., 1996 Heat And Mass Transfer In Unsaturated Soils During Freezing. M.Sc. Thesis, , Dept. of Civil Eng., University of Saskatchewan, Saskatoon, Saskatchewan, Canada

Newman, L., 1994. Analysis performed at the University of Saskatchewan, Saskatoon, Saskatchewan, Canada.

Newman, L. 1997. The Hydrogeology of Waste Rock Dumps and a Mechanism for Unsaturated Preferential Flow. Proceedings of the Fourth International Conference on Acid Rock Drainage (ICARD). Vancouver, B.C. v.2 pp551-565

Newman, L., 1999. A Mechanism for Preferential Flow in Vertically Layered, Unsaturated Systems. M.Sc. Thesis, , Dept. of Civil Eng., University of Saskatchewan, Saskatoon, Saskatchewan, Canada

O'Kane, M. 1995. Instrumentation and monitoring of an engineered soil cover system for acid generating mine waste. M.Sc. Thesis, Dept. of Civil Eng., University of Saskatchewan, Saskatoon, Saskatchewan, Canada

Pavier, D. 1998. Personal communication relating to grainsize curves performed on waste rock from Key Lake. University of Saskatchewan, Saskatoon, Canada

Robertson, A.M. and Barton-Bridges, J. 1990. Cost effective method of long term acid mine drainage control from waste rock piles. Proc. GAC-MAC Conference on AMD, Vancouver, B.C.

Saretzky, G.T., 1998. Hydrological Characterization of a Sulphide Waste Rock Dump. M.Sc. Thesis, , Dept. of Civil Eng., University of Saskatchewan, Saskatoon, Saskatchewan, Canada

Smith, L., Lopez, D.L., Beckie, R., Morin, K., Dawson, R. and Price, W., 1995. Hydrogeology of Waste Rock Dumps. Final report to Department of Natural Resources Canada. Contract No.: 23440-4-1317/01-SQ.

Stoicescu, J.T., 1997. Properties of Unsaturated Sand-Bentonite Mixtures used for Liners and Covers. M.Sc. Thesis, University of Saskatchewan.

Stumm, M., and Morgan, J.J., 1981, Aquatic Chemistry: an introduction emphasizing chemical equilibria in natural waters., New York ; Toronto : Wiley.

Taylor, M.J. and Greenwood, R.J., 1985. Classification and surface water controls. In Design of non-impounding mine waste dumps, M.K. Carter Ed. American Institute of Mining, Metallurgical and Petroleum Engineers Inc., New York. pp.1-13

Tyler, D.D. and Thomas G.W. 1977. Lysimeter Measurements of Nitrate and Chloride Losses from Soil Under Conventional and No-tillage Corn. Journal of Environmental Quality, v.6 n1 pp.63-66.

Van Genuchten, M. 1980. A Closed-Form Equation for Predicting the Hydraulic Conductivity of Unsaturated Soils. *Soil Science of America Journal*, 57:26-29.

Whiting. D.L., 1985. Surface and groundwater pollution potential. In design of non-impounding mine waste dumps. Society of Mining Engineers of America Institute of Mining, Metallurgy and Petroleum Engineers Inc. New York, NY, pp91-97

Wickland, B., 1998. Lysimeter Backfill Design. Undergraduate Thesis at the University of Saskatchewan, Saskatoon, SK, Canada.

Wilson, L.G., Everett, L.G. and Cullen, S.J. ed. 1994 .Handbook of Vadose Zone Characterization & Monitoring. Lewis Publishers, Boca Raton, Florida. ISBN: 0-87371-910-8

Yazdani, J. 1995. Soil-water Characterization of Mine Waste Rock Containing Coarse Material. M. Eng. Thesis. University of Saskatchewan

Appendix A - Summary of Preliminary Modelling

Nominal Body size	Applied Flux (m^3/m^2s)	Ksat Waste Rock (m/s)	Ksat Silica Flour (m/s)	Modelled Diameter (m)	Lysimeter Flux section (m^3/s per rad.)	q Area Flux (m/s)	Equivalent Collection Area Ratio	Time to Collect 100 ml Sample (days)	Volume to Flush (m3)	Time to Flush (days)	Time to Flush (years)	Time to Equil. (days)	Lysimeter Suction @ SS (kPa)	Outside Edge Suction @ SS (kPa)	Suction Error (%)
Effect of Varying Fluxes															
5 cm	1.E-06	1.E-05	1.E-07	0.050	2.745E-11	8.782E-08	0.088	6.7	0.0022	148.6	0.42	5 - 7	3.35	3.52	4.87%
10 cm	1.E-06	1.E-05	1.E-07	0.104	1.189E-10	8.793E-08	0.088	1.5	0.0096	148.4	0.42	5 - 7	3.28	3.52	6.72%
15 cm	1.E-06	1.E-05	1.E-07	0.150	2.475E-10	8.801E-08	0.088	0.7	0.0199	148.3	0.42	5 - 7	3.28	3.53	6.83%
5 cm	1.E-07	1.E-05	1.E-07	0.050	2.333E-11	7.465E-08	0.747	7.9	0.0022	174.8	0.49	6.5 - 8.5	6.88	7.12	3.29%
10 cm	1.E-07	1.E-05	1.E-07	0.104	1.011E-10	7.480E-08	0.748	1.8	0.0096	174.5	0.49	6.5 - 8.5	6.74	7.12	5.29%
15 cm	1.E-07	1.E-05	1.E-07	0.150	2.107E-10	7.492E-08	0.749	0.9	0.0199	174.2	0.49	6.5 - 8.5	6.62	7.12	6.92%
5 cm	1.E-08	1.E-05	1.E-07	0.050	1.800E-11	5.759E-08	5.759	10.2	0.0022	226.6	0.64	8.5 - 10.5	11.28	11.84	4.74%
10 cm	1.E-08	1.E-05	1.E-07	0.104	7.817E-11	5.782E-08	5.782	2.4	0.0096	225.7	0.63	8.5 - 10.5	10.89	11.84	8.04%
15 cm	1.E-08	1.E-05	1.E-07	0.150	1.623E-10	5.771E-08	5.771	1.1	0.0199	226.1	0.64	8.5 - 10.5	10.64	11.84	10.08%
5 cm	1.E-09	1.E-05	1.E-07	0.050	7.467E-12	2.389E-08	23.893	24.7	0.0022	546.2	1.53	16.5 - 18.5	20.59	22.06	6.67%
10 cm	1.E-09	1.E-05	1.E-07	0.104	3.069E-11	2.270E-08	22.700	6.0	0.0096	574.9	1.61	20 - 22	20.06	22.06	9.05%
15 cm	1.E-09	1.E-05	1.E-07	0.150	5.831E-11	2.073E-08	20.732	3.2	0.0199	629.4	1.77	24.5 - 26.5	19.86	22.06	9.98%
5 cm	1.E-10	1.E-05	1.E-07	0.050	Draws Water										
10 cm	1.E-10	1.E-05	1.E-07	0.104	Draws Water										
15 cm	1.E-10	1.E-05	1.E-07	0.150	Draws Water										

Nominal Body size	Applied Flux (m^3/m^2s)	Ksat Waste Rock (m/s)	Ksat Silica Flour (m/s)	Modelled Diameter (m)	Lysimeter Flux section (m^3/s per rad.)	q Area Flux (m/s)	Equivalent Collection Area Ratio	Time to Collect 100 ml Sample (days)	Volume to Flush (m3)	Time to Flush (days)	(years)	Time to Equil. (days)	Lysimeter Suction @ SS (kPa)	Outside Edge Suction @ SS (kPa)	Suction Error (%)
Various Waste Rock k sats															
5 cm	1.E-08	1.E-03	1.E-07	0.050	Draws Water										
10 cm	1.E-08	1.E-03	1.E-07	0.104	Draws Water										
15 cm	1.E-08	1.E-03	1.E-07	0.150	Draws Water										
5 cm	1.E-08	1.E-04	1.E-07	0.050	7.058E-12	2.258E-08	2.258	26.1	0.0022	577.8	1.62	14.5 - 16.5	21.56	22.06	2.26%
10 cm	1.E-08	1.E-04	1.E-07	0.104	3.153E-11	2.332E-08	2.332	5.8	0.0096	559.5	1.57	14.5 - 16.5	21.15	22.05	4.10%
15 cm	1.E-08	1.E-04	1.E-07	0.150	6.677E-11	2.374E-08	2.374	2.8	0.0199	549.7	1.54	16.5 - 18.5	20.86	22.05	5.39%
5 cm	1.E-08	1.E-05	1.E-07	0.050	1.800E-11	5.759E-08	5.759	10.2	0.0022	226.6	0.64	8.5 - 10.5	11.28	11.84	4.74%
10 cm	1.E-08	1.E-05	1.E-07	0.104	7.817E-11	5.782E-08	5.782	2.4	0.0096	225.7	0.63	8.5 - 10.5	10.89	11.84	8.04%
15 cm	1.E-08	1.E-05	1.E-07	0.150	1.623E-10	5.771E-08	5.771	1.1	0.0199	226.1	0.64	8.5 - 10.5	10.64	11.84	10.08%
5 cm	1.E-08	1.E-06	1.E-07	0.050	2.335E-11	7.470E-08	7.470	7.9	0.0022	174.7	0.49	6.5 - 8.5	6.55	7.12	7.94%
10 cm	1.E-08	1.E-06	1.E-07	0.104	1.009E-10	7.460E-08	7.460	1.8	0.0096	174.9	0.49	6.5 - 8.5	6.17	7.12	13.30%
15 cm	1.E-08	1.E-06	1.E-07	0.150	2.086E-10	7.415E-08	7.415	0.9	0.0199	176.0	0.49	6.5 - 8.5	5.95	7.12	16.47%

Nominal Body size	Applied Flux (m^3/m^2s)	Ksat Waste Rock (m/s)	Ksat Silica Flour (m/s)	Modelled Diameter (m)	Lysimeter Flux section (m^3/s per rad.)	q Area Flux (m/s)	Equivalent Collection Area Ratio	Time to Collect 100 ml Sample (days)	Volume to Flush (m3)	Time to Flush (days)	Time to Flush (years)	Time to Equil. (days)	Lysimeter Suction @ SS (kPa)	Outside Edge Suction @ SS (kPa)	Suction Error (%)
Various Silica Flour k sats															
5 cm	1.E-07	1.E-05	1.E-06	0.050	2.335E-10	7.471E-07	7.471	0.8	0.0022	17.5	0.05	2 - 3	7.01	7.58	7.45%
10 cm	1.E-07	1.E-05	1.E-06	0.104	1.009E-09	7.462E-07	7.462	0.2	0.0096	17.5	0.05	2 - 3	6.17	7.12	13.34%
15 cm	1.E-07	1.E-05	1.E-06	0.150	2.083E-09	7.406E-07	7.406	0.1	0.0199	17.6	0.05	2 - 3	5.95	7.12	16.47%
5 cm	1.E-08	1.E-05	1.E-06	0.050	1.775E-10	5.680E-07	56.800	1.0	0.0022	23.0	0.06	2 - 3	10.40	11.84	12.15%
10 cm	1.E-08	1.E-05	1.E-06	0.104	6.483E-10	4.795E-07	47.954	0.3	0.0096	27.2	0.08	6 - 8	10.05	11.85	15.16%
15 cm	1.E-08	1.E-05	1.E-06	0.150	1.033E-09	3.674E-07	36.736	0.2	0.0199	35.5	0.10	9 - 11	9.97	11.85	15.84%
5 cm	1.E-09	1.E-05	1.E-06	0.050	5.568E-11	1.782E-07	178.160	3.3	0.0022	73.2	0.21	9 - 11	19.82	22.06	10.15%
10 cm	1.E-09	1.E-05	1.E-06	0.104	1.263E-10	9.338E-08	93.380	1.5	0.0096	139.7	0.39	20 - 22	19.67	22.06	10.85%
15 cm	1.E-09	1.E-05	1.E-06	0.150	1.683E-10	5.983E-08	59.826	1.1	0.0199	218.1	0.61	29 - 31	19.60	22.06	11.17%
5 cm	1.E-07	1.E-05	1.E-08	0.050	2.333E-12	7.467E-09	0.075	78.9	0.0022	1747.7	4.91	36 - 40	6.94	7.12	2.46%
10 cm	1.E-07	1.E-05	1.E-08	0.104	1.012E-11	7.482E-09	0.075	18.2	0.0096	1744.3	4.90	36 - 40	6.87	7.13	3.62%
15 cm	1.E-07	1.E-05	1.E-08	0.150	2.107E-11	7.490E-09	0.075	8.7	0.0199	1742.2	4.89	36 - 40	6.79	7.12	4.55%
5 cm	1.E-08	1.E-05	1.E-08	0.050	1.793E-12	5.736E-09	0.574	102.8	0.0022	2274.9	6.39	45 - 50	11.61	11.84	1.98%
10 cm	1.E-08	1.E-05	1.E-08	0.104	7.784E-12	5.758E-09	0.576	23.7	0.0096	2266.6	6.37	45 - 50	11.46	11.84	3.19%
15 cm	1.E-08	1.E-05	1.E-08	0.150	1.624E-11	5.774E-09	0.577	11.3	0.0199	2260.3	6.35	45 - 50	11.35	11.84	4.14%
5 cm	1.E-09	1.E-05	1.E-08	0.050	7.062E-13	2.260E-09	2.260	260.8	0.0022	5774.6	16.22	45 - 49	21.56	22.05	2.25%
10 cm	1.E-09	1.E-05	1.E-08	0.104	3.155E-12	2.334E-09	2.334	58.4	0.0096	5591.6	15.71	48 -52	21.14	22.05	4.12%
15 cm	1.E-09	1.E-05	1.E-08	0.150	6.677E-12	2.374E-09	2.374	27.6	0.0199	5496.5	15.44	51 -55	20.86	22.05	5.38%

Nominal Body size	Applied Flux (m^3/m^2s)	Ksat Waste Rock (m/s)	Ksat Silica Flour (m/s)	Modelled Diameter (m)	Lysimeter Flux section (m^3/s per rad.)	q Area Flux (m/s)	Equivalent Collection Area Ratio	Time to Collect 100 ml Sample (days)	Volume to Flush (m3)	Time to Flush (days)	Time to Flush (years)	Time to Equil. (days)	Lysimeter Suction @ SS (kPa)	Outside Edge Suction @ SS (kPa)	Suction Error (%)
No Silica Flour															
5 cm	1.E-07	1.E-05	1.E-07	0.050	2.334E-11	7.470E-08	0.747	7.9	0.0022	174.7	0.49	6 - 8	6.88	7.12	3.41%
10 cm	1.E-07	1.E-05	1.E-07	0.104	1.011E-10	7.481E-08	0.748	1.8	0.0096	174.4	0.49	6 - 8	6.74	7.12	5.33%
15 cm	1.E-07	1.E-05	1.E-07	0.150	2.110E-10	7.503E-08	0.750	0.9	0.0199	173.9	0.49	6 - 8	6.59	7.12	7.37%
5 cm	1.E-08	1.E-05	1.E-07	0.050	1.743E-11	5.577E-08	5.577	10.6	0.0022	234.0	0.66	8.5 - 10.5	11.61	11.84	1.98%
10 cm	1.E-08	1.E-05	1.E-07	0.104	7.202E-11	5.327E-08	5.327	2.6	0.0096	245.0	0.69	10 - 12	11.46	11.84	3.22%
15 cm	1.E-08	1.E-05	1.E-07	0.150	1.426E-10	5.072E-08	5.072	1.3	0.0199	257.3	0.72	12.5 - 14	10.95	11.84	7.55%
5 cm	1.E-09	1.E-05	1.E-07	0.050	5.440E-12	1.741E-08	17.408	33.9	0.0022	749.6	2.11	20 - 22	21.82	22.05	1.05%
10 cm	1.E-09	1.E-05	1.E-07	0.104	1.755E-11	1.298E-08	12.984	10.5	0.0096	1005.1	2.82	32 - 34	21.67	22.05	1.71%
15 cm	1.E-09	1.E-05	1.E-07	0.150	2.969E-11	1.056E-08	10.555	6.2	0.0199	1236.3	3.47	40 - 42	21.55	22.04	2.25%
Bell shaped Lysimeters															
5-10 cm	1.E-07	1.E-05	1.E-07	0.050	2.478E-11	7.929E-08	0.793	7.4	0.0022	164.6	0.46	5 - 7	6.75	7.12	5.23%
5-15 cm	1.E-07	1.E-05	1.E-07	0.050	2.521E-11	8.066E-08	0.807	7.3	0.0022	161.8	0.45	5 - 7	6.64	7.12	6.72%
5-10 cm	1.E-08	1.E-05	1.E-07	0.050	1.968E-11	6.297E-08	6.297	9.4	0.0022	207.2	0.58	7 - 9	10.88	11.84	8.10%
5-15 cm	1.E-08	1.E-05	1.E-07	0.050	2.024E-11	6.478E-08	6.478	9.1	0.0022	201.5	0.57	7 - 9	10.66	11.84	10.02%
5-10 cm	1.E-09	1.E-05	1.E-07	0.050	8.784E-12	2.811E-08	28.109	21.0	0.0022	464.2	1.30	13 - 15	20.07	22.06	9.03%
5-15 cm	1.E-09	1.E-05	1.E-07	0.050	9.203E-12	2.945E-08	29.448	20.0	0.0022	443.1	1.24	13 - 15	19.89	22.09	9.96%

Appendix B - Column Data

The data collected from column testing will be presented as a Microsoft Excel 97 spreadsheet on the attached compact disk. The files are located in the Appendix B directory. The file Fine_Column_data.xls presents the raw and reduced data for the fine column while the file Coarse_Column_data.xls presents the data for the coarse column.